Valorisation of watermelon and persimmon fruit residues to obtain compounds of interest in food applications

Aprovechamiento de residuos del fruto de sandía y caqui para la obtención de compuestos de interés en aplicaciones alimentarias

DOCTORAL THESIS

Daniel Alexander Méndez Reyes

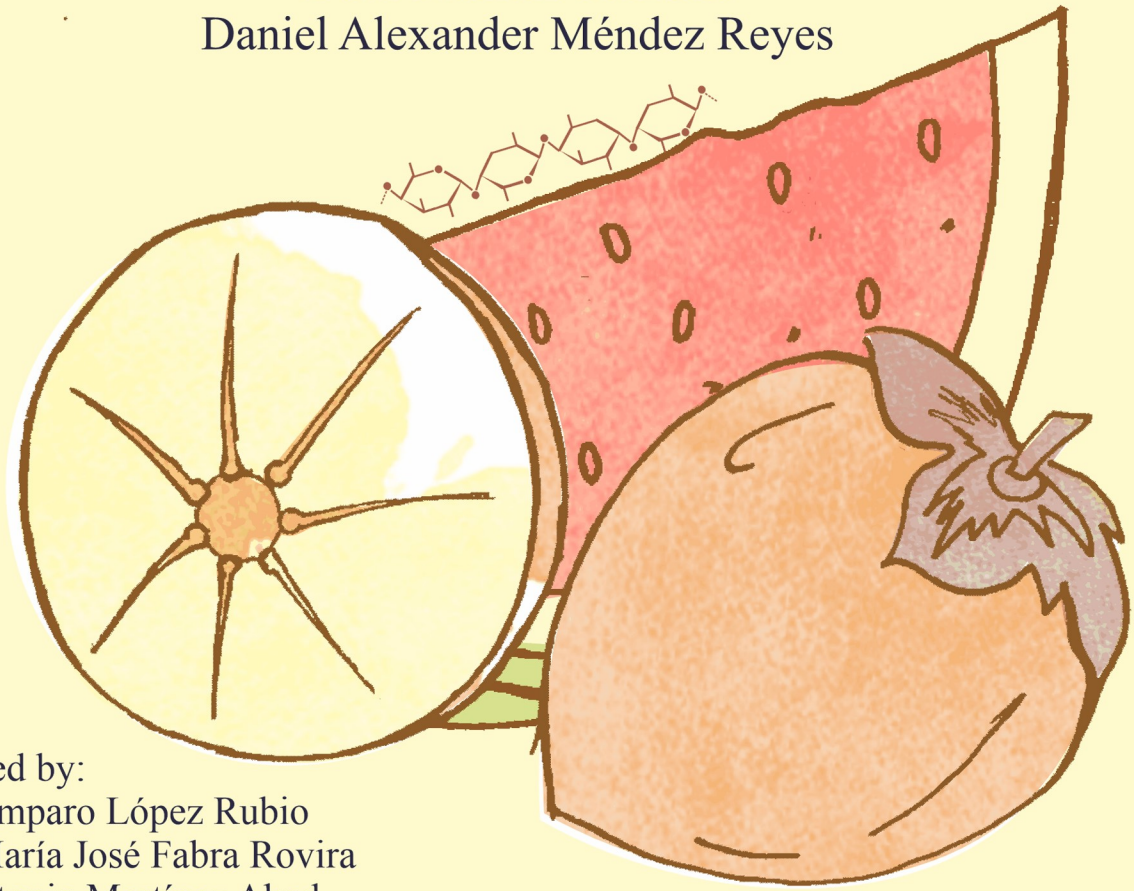

Directed by:
Dra. Amparo López Rubio
Dra. María José Fabra Rovira
Dr. Antonio Martínez Abad

Noviembre 2022

UNIVERSITAT POLITÈCNICA DE VALÈNCIA

iata
Instituto de Agroquímica y Tecnología de Alimentos

CSIC
CONSEJO SUPERIOR DE INVESTIGACIONES CIENTÍFICAS

UNIVERSITAT POLITÈCNICA DE VALÈNCIA

Doctoral Thesis

Doctorado en Ciencia, Tecnología y Gestión Alimentaria

Daniel Alexander Méndez Reyes

Valorisation of watermelon and persimmon fruit residues to obtain compounds of interest in food applications

Aprovechamiento de residuos del fruto de sandía y caqui para la obtención de compuestos de interés en aplicaciones alimentarias

iata
Instituto de Agroquímica y Tecnología de Alimentos

Directed by:

Dra. Amparo López Rubio

Dra. María José Fabra Rovira

Dr. Antonio Martínez Abad

November, 2022

A mi familia

Agradecimientos

Definitivamente en esta vida el 20 % es disciplina y el 80 % suerte, y más que afortunado no he podido ser con los directores que me ha tocado cuando emprendí este reto. María José, contar contigo para desarrollar el doctorado ha sido para mí un privilegio, recordar que mientras estaba en pregrado leía tus artículos y luego estar trabajando contigo en un laboratorio ha sido algo insuperable. Además, su acompañamiento en el proceso y la eficiencia que te caracteriza ha sido clave para desarrollar esta tesis. Amparo, siempre te agradeceré la confianza depositada, tu empatía, carisma y esa facilidad para encontrar la forma de solucionar las cosas más complicadas de la forma más sencilla. Gracias por la oportunidad, de tener el criterio y la buena dirección que me has dado durante estos años y de haberme dado la posibilidad de pertenecer a tu grupo de investigación. Antonio, gracias por aportar tu curiosidad innata, tu experiencia y talento en esta tesis, también por adentrarme en el mundo de los polímeros y tener la paciencia, así como perspicacia de enseñarme todo lo que me has brindado hasta ahora. Marta Martínez, por ser mi madrina a la distancia, que con su colaboración en los trabajos desarrollados y su valiosa contribución han concretado mi desarrollo doctoral.

“El primer doctor de la familia”, habrían sido las palabras de mi padre, hace ya tres años que partió y no puedo dejar de sentir agradecimiento por su ejemplo, fortaleza y energía, que de una u otra manera junto con mi madre, me han llevado al punto en el que estoy ahora. Gracias a ellos por la vida que me regalaron, su sacrificio y su disciplina para sacar a sus dos hijos adelante.

A mi hermano, que diferentes que somos, pero con la unión de sangre que tenemos no me dejara ni yo lo dejare fracasar, que el amor por su familia puedan dar apoyo y ejemplo a mis queridas sobrinas, Ana María y Natalia, que tuve la fortuna de verlas recién nacidas antes de partir en esta aventura doctoral. A mi familia que siempre llevo en el corazón.

A mis compañeros del laboratorio Zaida, Isaac, Cynthia, Hylenne, Vera y Laura, cada uno con su luz me han aportado tanto el excelente ambiente laboral que se vive allí, como su compañía, amistad, risas, confidencias, tristezas, alegrías… que han sido mi gasolina cada día de esta etapa de mi vida y que sin ustedes no hubiera disfrutado tanto, ni habría tenido la templanza emocional de afrontar este reto fuera de mi país natal. A ustedes gracias por ser mi familia aquí en España, aunque no se los haya pedido, por el apoyo incondicional y compartir juntos este reto del doctorado.

A toda la gente del IATA, Irene, Gloria, Pepe, Javier, Antonio, Agustín, Lola, Marta, Enrique, a los que se me escapan ahora de la cabeza que han aportado su granito de arena y esfuerzo para desarrollar esta tesis doctoral, sin su ayuda, esta tesis no sería ni la mitad de lo que es. Mil gracias a ustedes.

A los compañeros que pude conocer fuera del laboratorio, Romain, Enric, Alejandro, Patricia, María Inés, hicieron más que grato el tiempo en el que estuve desarrollando la tesis, compartiendo cervezas y risas, cotilleos e ideas trascendentales de la humanidad.

Gracias a ti Theresa Kefer, por dejarte encontrar en esta etapa de mi vida y tener la paciencia en forma de cariño que me has brindado en este tiempo, para soportar los efectos colaterales que por estar pendiente de este trabajo has tenido que pasar a mi lado, que sin ti la carga que hubiera tenido que soportar sería más grande y pesada, pero que con tu apoyo me has ayudado a ser más feliz.

Abstract

The aim of this doctoral thesis was the valorisation of agro-industrial wastes from watermelon (*Citrullus lanatus*) and persimmon (*Diospyros kaki Thunb*.) fruits to obtain high added-value compounds with potential technological applications in the food industry. Specifically, watermelon rind and persimmon discards are envisaged as a promising pectin source, not only because of the economic importance of the crops but also because of the interesting structural features of the extracted pectin and related functional properties. Furthermore, persimmon fruits are known to be a source of bioactive compounds which can be used to design healthier food products.

In the first part of this thesis, a response surface methodology was carried out to evaluate how different process parameters affect the composition, structural features and extraction yield of watermelon rind pectin (WRP). Based on the results, a combination of rheological, microstructural and scattering tools was used to elucidate the emulsion stabilizing mechanism of WRP, which was able to retain high amounts of sunflower oil (>60%), avoiding coalescence and flocculation. Then, the effect of controlled enzymatic debranching, de-esterification and protein removal on WRP composition and molecular structure was evaluated and the potential of the enzymatically-treated pectin for preparing hydrogels with the addition of $CaCl_2$ was deeply analysed in order to understand how pectin structure and extract composition affected gel formation and properties. It was observed that the small arabinogalactan side chains present in the pectin with low degree of esterification, acted as a reinforcement, inducing the formation of more densely packed networks and stronger hydrogels than their less-branched counterparts. An enzymatically-treated WRP with better gelling properties and yield was subsequently used to develop aerogel structures using supercritical CO_2. The formation of a compacted structure during aerogel formation made it a good candidate for drug delivery systems.

In the second part of the thesis, the potential valorisation of persimmon biomass waste through the extraction of bioactive compounds and pectin-rich extracts and the evaluation of their functional properties was studied. A semi-industrially scaled-up polyphenol-rich extract showed an effective antiviral efficiency and it was able to reduce the cellular

ageing and fat content without affecting the development of *C. elegans* model organism. Furthermore, the extraction conditions of functional pectin-polyphenol-based ingredients were optimized and characterized, which composition was dependent on the severity of the extraction conditions. These functional pectin extracts showed high antiviral efficiency, probably enhanced by the higher stability of the polyphenols as pectin complexes. A successful potential application was explored with an edible coating on blueberries.

Resumen

El objetivo de esta tesis doctoral ha sido la valorización de los residuos agroindustriales de los frutos de la sandía (*Citrullus lanatus*) y del caqui (*Diospyros kaki Thunb.*) para obtener compuestos de alto valor añadido con potenciales aplicaciones tecnológicas en la industria alimentaria. En concreto, la corteza de la sandía y los descartes del caqui se contemplan como una prometedora fuente de pectina, no sólo por la importancia económica de los cultivos, sino también por las interesantes características estructurales de la pectina extraída y sus propiedades funcionales. Además, se sabe que los frutos del caqui son una fuente de compuestos bioactivos que pueden utilizarse para diseñar productos alimentarios más saludables.

En la primera parte de esta tesis, se llevó a cabo una metodología de superficie de respuesta para evaluar cómo afectan los diferentes parámetros del proceso a la composición, las características estructurales y el rendimiento de extracción de la pectina de la corteza de la sandía (WRP). A partir de estos resultados, se utilizó una combinación de herramientas reológicas, microestructurales y de dispersión para dilucidar el mecanismo de estabilización de la emulsión de WRP, que fue capaz de retener altas cantidades de aceite de girasol (>60%), evitando la coalescencia y la floculación. A continuación, se evaluó el efecto de la des-ramificación contralada enzimáticamente, la des-esterificación y la eliminación de proteínas, en la composición y la estructura molecular de la WRP, y se analizó en profundidad el potencial de la pectina tratada enzimáticamente para preparar hidrogeles con la adición de $CaCl_2$, con el fin de comprender cómo la estructura de la pectina y la composición del extracto afectaban a la formación y las propiedades del gel. Se observó que las pequeñas cadenas laterales de arabinogalactano presentes en la pectina con bajo grado de esterificación, actuaban como refuerzo, induciendo la formación de redes más densamente empaquetadas y de hidrogeles más fuertes que sus homólogos menos ramificados. La pectina de sandía tratada enzimáticamente y con mejores propiedades de gelificación y rendimiento, se utilizó posteriormente para desarrollar estructuras de aerogeles utilizando secado con CO_2

supercrítico. La formación de una estructura compactada durante la formación del aerogel lo convirtió en un buen candidato como sistemas de liberación de compuestos activos.

En la segunda parte de la tesis, se estudió la potencial valorización de residuos de biomasa de caqui mediante la extracción de compuestos bioactivos y extractos ricos en pectina y la evaluación de sus propiedades funcionales. Un extracto rico en polifenoles obtenido a escala semi-industrial mostró actividad antiviral y fue capaz de reducir el envejecimiento celular y el contenido de grasa sin afectar al desarrollo del organismo modelo *C. elegans*. Además, se optimizaron y caracterizaron las condiciones de extracción de ingredientes funcionales a base de pectina y polifenoles, cuya composición dependió de la severidad de las condiciones de extracción. Estos extractos funcionales de pectina mostraron actividad antiviral, probablemente potenciada por la mayor estabilidad de los polifenoles que forman complejos con la pectina y se exploró, de manera exitosa, su aplicación como recubrimiento comestible en arándanos.

Resum

L'objectiu d'aquesta tesi doctoral va ser la valorització de residus agroindustrials procedents de fruites de síndria (*Citrullus lanatus*) i caqui (*Diospyros kaki Thunb*.) per obtenir compostos d'alt valor afegit amb potencials aplicacions tecnològiques en la indústria alimentària. En concret, l'escorça de síndria i els descarts de caqui es preveuen com una prometedora font de pectina, no només per la importància econòmica dels cultius, sinó també per les interessants característiques estructurals de la pectina extreta i les propietats funcionals relacionades. A més, se sap que les fruites de caqui són una font de compostos bioactius que es poden utilitzar per dissenyar productes alimentaris més saludables.

En la primera part d'aquesta tesi es va dur a terme una metodologia de superfície de resposta per avaluar com els diferents paràmetres de procés afecten la composició, les característiques estructurals i el rendiment d'extracció de la pectina de síndria (WRP). A partir dels resultats, es va utilitzar una combinació d'eines reològiques, microestructurals i de dispersió per dilucidar el mecanisme estabilitzador de l'emulsió de WRP, que va ser capaç de retenir altes quantitats d'oli de gira-sol (>60%), evitant la coalescència i la floculació. A continuació, es va avaluar l'efecte del de-brassament enzimàtic controlat, la des-esterificació i l'eliminació de proteïnes sobre la composició i l'estructura molecular del WRP i es va analitzar profundament el potencial de la pectina tractada enzimàticament per preparar hidrogels amb l'addició de $CaCl_2$ per entendre com l'estructura de la pectina i la composició de l'extracte afectaven la formació i les propietats del gel. Es va observar que les petites cadenes laterals d´arabinogalàctans presents a la pectina amb baix grau d'esterificació, actuaven com a reforç, induint la formació de xarxes més densament empaquetades i hidrogels més forts que els seus homòlegs menys ramificats. Posteriorment es va utilitzar la pectina de l'escorça de síndria tractada enzimàticament amb millors propietats gelificants i rendiment per desenvolupar estructures d'aerogel utilitzant CO_2 supercrític. La formació d'una estructura compactada durant la formació d'aerogels la va convertir en un bon candidat per als sistemes de alliberació de compostos actius.

En la segona part de la tesi es va estudiar la potencial valorització dels residus de biomassa de caqui mitjançant l'extracció de compostos bioactius i extractes rics en pectina i l'avaluació de les seves propietats funcionals. Un extracte obtingut a escala semi-industrialment ric en polifenols va mostrar una activitat antiviral i va ser capaç de reduir l'envelliment cel·lular i el contingut en greixos sense afectar el desenvolupament de l'organisme model de *C. elegans*. A més, es van optimitzar i caracteritzar les condicions d'extracció d'ingredients funcionals a base de pectina-polifenol, la composició de la qual depenia de la gravetat de les condicions d'extracció. Aquests extractes funcionals de pectina van mostrar una alta eficiència antiviral, probablement millorada per la major estabilitat dels polifenols com a complexos de pectina. De manera exitosa, es va explorar una potencial aplicació com a recobriment comestible sobre nabius.

INDEX

Abbreviations

AIR: Alcohol insoluble residue

DA: Degree of acetylation

DE: Degree of esterification

DM: Degree of methoxylation

GalA: Galacturonic Acid

HG: Homogalacturonan

HM: High methoxylated

G': Elastic modulus

G'': Viscous modulus

LM: Low methoxylated

ME: Methyl esterification

MW: Molecular weight

PME: Pectin methyl esterase

RG-I: Rhamnogalacturonan-I

RG-II: Rhamnogalacturonan-II

Rha: Rhamnose

XGA: Xylogalacturonan

WRP: Watermelon rind pectin

I. INTRODUCTION

1.1. From biomass waste to valorised natural ingredients and biomaterials

Food wastes represent an ever-increasing challenge. Considering the steadily increasing population growth implying a greater generation of wastes, the space in treatment facilities and the landfills will be an unmanageable topic in the near future (Esparza et al., 2020). Moreover, societal concern about environmental sustainability has risen significantly over the past decades. Therefore, attention has been paid to the valorisation of wastes from natural resources in order to obtain functional ingredients (Awasthi et al., 2021; Sabater et al., 2022). Many residues from the food supply chain pose serious environmental problems, while having a great valorisation potential due to their inherent composition which can lead to valuable compounds. Among other advantages, valorisation of food by-products may increase the efficiency of the food supply chain, reduce costs, improve food accessibility, reduce waste and increase food security.

Biomass is renewable organic material that comes from plants, such as shrubs, trees, crops, as well as algae, fungi and other living organisms. Frequently, the vegetable and fruit products are catalogued into the same group of waste, considered as fruit and vegetable wastes. In this sense, the wastes generated from these types of sources are mostly allocated to the harvesting and processing stages, while the consumption stage barely renders 10% of the wastes (Gustavsson et al., 2011). Hence, the development of new strategies for characterization and evaluation of by-products, open new alternatives for the producers and further utilization of wastes, according to the different needs for cost and waste reduction during the food supply chain.

Agri-food waste mainly consists of lignocellulosic material (cellulose, hemicelluloses and lignin) from the plant cell wall. The primary cell wall also consists of a significant amount of pectic polysaccharides that provide structural support to the soft tissues of dicotyledons, while hemicelluloses are more abundant in the secondary plant cell walls (Atmodjo et al., 2013; Voragen et al., 2009). In a biorefinery concept, it is desirable that the feedstock can be transformed into biofuels, biochemicals and biomaterials (Adiletta et al., 2020; Brachi

et al., 2017; Tursi, 2019). Waste generated during food production and processing can be considered feedstock for biorefinery processes, as this waste is generated in a more concentrated and less variable form (Pfaltzgraff et al., 2013). Although seasonality is an issue, numerous examples suggest the feasibility of using plant biomass and agri-food waste as feedstock for biorefining regardless of supply and seasonality, as they constitute cheap non-food materials (Clauser et al., 2021; Naik et al., 2010). However, some authors claim that food waste recovery methods within an integrated "zero waste" concept are at an early stage of development. More studies dealing with a broader range of food matrices and industrial by-products are needed to scale-up these methods on an industrial scale (Cristóbal et al., 2018). On the other hand, these by-products are an excellent source of bioactive compounds, such as phenolic compounds (phenolic acid, carotenoids, flavonoids), bioactive proteins (peptide isolate, amino acids), fatty acids, fibres, and so on. For instance, the seeds of fruits are a good source of essential oils, phytochemicals, and phytosterols. Similarly, fruit and vegetable peels contain pectin, valuable fibres, and minerals. These bioactive compounds can be extracted from the by-products using different technologies and can be utilized to develop various valorised products, including functional foods or dietary supplements. Thus, the production of pectin through the combination of green chemistry and biorefinery is a pending challenge for industries in the agri-food sector (Adiletta et al., 2020; Brachi et al., 2017; Sabater et al., 2022).

1.2. Agricultural waste as a potential feedstock for new natural ingredients

1.2.1. Watermelon (*Citrillus lanatus*)

Watermelon (*Citrillus lanatus*) is a member of the cucurbit family (Cucurbitaceae). It is native to Africa and the best average temperature range for watermelon production during the growing season is between 25 and 30 ºC (Zamuz et al., 2021). Watermelon is one of the most cultivated fruits in the world, with China being the main producer with 60 million tonnes followed by Turkey, India and Brazil, and representing a worldwide production of 100 million tonnes in 2019 (FAOSTAT, 2021). Spain produces the non-

negligible quantity of 1.2 million tonnes and is one of the most important non-citric fruit crops in the country. Likewise, Spain is the first exporter of this fruit in Europe (0.8 million tonnes/year), demonstrating the relevant economic importance of this fruit (Hortoinfo, 2021).

Watermelon biomass can be categorized into three main components, which are flesh, seed, and rind. Considering that flesh contributes to approximately 65% of the total weight, the rind and seeds represent a massive amount (approx. 35%) of agro-waste (Campbell, 2006; Chakrabarty et al., 2020; Hasanin & Hashem, 2020). Around 42 million tonnes of watermelon by-products (rind and seeds) are produced by different cottage fruit juice producers, fruit juice processing industries and restaurants, during harvesting, processing and consumption of watermelon (Zia et al., 2021). Considering that ripe watermelon rinds contain around 20% of cellulose, 23% of hemicellulose, 10% of lignin, and 13% of pectin on a dry weight basis, some studies consider that this large amount of pectin, may serve as a potential source of this valuable polysaccharide (Begum et al., 2017; Sari et al., 2018). Some research has already been focused in the valorisation of this waste as a pectin source (Guo et al., 2021; Hartati & Subekti, 2015; Lee & Choo, 2020; Petkowicz et al., 2017). Looking for valorisation alternatives for watermelon rind waste, which is in most cases indiscriminately disposed into the environment thus constituting environmental challenges (Esparza et al., 2020), implies a deeper understanding of the pectin structure and extraction strategies for further valorisation.

1.2.2. Persimmon (*Diospyros kaki Thunb*.)

Persimmon fruit (*Diospyros kaki Thunb.*) is a fruit tree originating from China. Depending on the species, its commercial interest has been applied to different means such as lumbering (*Diospyrus ebenum*), landscaping (*Diospyrus incostans* and *Diospyrus rhombifolia*), tannin extraction (*Diospyrus oleifera*) and fruit production (*Diospyros kaki*) (Kluge & Tessmer, 2018). The tree is a plant of arboreous size belonging to the genus *Diospyros* and the botanical family *Ebenaceae*. Persimmon is a climacteric fruit that regulates its maturation depending on respiration rates and ethylene gas production. In comparison with other climacteric fruits, persimmon fruit is considered to have lower

ethylene and respiration rate. However, its maturation is not prevented and the whole process is thoroughly triggered by human action (Kluge & Tessmer, 2018). The species of persimmon tree (*Diopyros kaki L.*) that produces edible fruit is the most economically important, with a global production of 4.3 million tons in 2019 (FAOSTAT, 2021). The biggest persimmon producers in the world are China, Korea, Japan, Spain and Brazil (Kluge & Tessmer, 2018). Spain is the most important exporter owing to the "Rojo Brillante" variety with registered designation of origin in the Valencian province and a production of 415000 tonnes per year (FAOSTAT, 2021; Martínez-Las Heras et al., 2016). Depending on the region, a specific harvest time exists for each cultivar. For the southern hemisphere countries such as Brazil, New Zealand and Australia, occurs between February and May. In European and Asian countries, it happens in the second semester, between October and December. Its seasonality also represents some challenges regarding the post-harvesting techniques and storage conditions to improve the quality and minimize losses. Immature untreated fruits are severely affected by small physiological changes causing a poor CO_2 diffusion, which results in a low anaerobic respiration rate, reducing acetaldehyde accumulation which in turn causes a decrease in its interactions with soluble tannins, these being responsible for astringency and rejection (Munera et al., 2019). Likewise, demands in terms of fruit appearance, give rise to huge amounts of discarded fruits at different stages of ripeness, which are estimated to be around 15–20% of the fruit harvested and can reach quantities of 9.500 tons discarded fruit a year (data provided by the second grade cooperative ANECOOP). As an important agricultural waste, untreated persimmon contains a lot of pectin and tannins, suggesting that it may be a potential new source of pectin and bioactive ingredients (Asgar et al., 2004; Jiang et al., 2020). However, it is important to highlight that the source and extraction conditions will determine the functional and technological properties of the extracted pectin, as it will be detailed below.

1.3. Valorisation of pectin-rich biomass

1.3.1. Industrial interest of pectin

The market for pectin has significantly grown due to the increasing demand of the food industry and consumers towards healthier texturizing and functional food ingredients (Moslemi, 2021; Muñoz-Almagro, Montilla, et al., 2021). It is believed that pectin will have an interesting trade market in the coming years as compared to some other hydrocolloids because of its positive effect at low quantities, relatively low prices and safety (Moslemi, 2021). Moreover, to satisfy the wishes of consumers, the food industry is looking for low-calorie and low-fat food ingredients. Pectin is broadly used in the food industry to enhance the desired texture in foods and beverages, among other uses. Pectin has the Generally Recognized as Safe (GRAS) designation in the US and is an accepted food additive in the EU, coded E-440. In the last decade, this polysaccharide has been considered an essential ingredient in the production of fruit juices, soy drinks and yogurts, and to stabilise acidic proteins during heating (Muñoz-Almagro, Montilla, et al., 2021).

As result of its diverse and numerous food applications, pectin is considered an attractive investment, being heavily industrialised by companies such as CP Kelco, Cargill, Danisco/Dupont, FMC Biopolymers, Herbstreith & Fox, Naturex/Obipektin, Yantal Andre Pectin, among others.

1.3.2. Novel alternative pectin sources

The main sources of commercial pectin around the world are citrus peels and apple pomace, resulting from citrus and apple processing. Apart from the fruit variety, other factors such as season and agricultural conditions influence properties such as the yield and quality of the pectin extracted (Dranca & Oroian, 2018). Although a more efficient local processing of citrus peel could theoretically sustain the current growing demand for pectin, centralized production make that could be replaced by new alternative sources (Shan, 2016). In this sense, research has explored several alternative sources and extraction methods. The low cost and huge amounts of agro-industrial wastes generated

during the food supply chain is a promising area, to transform this biomass waste material as pectin sources. The possibility of exploiting novel sources to obtain pectin compounds varies depending on several factors including the raw material and the pectin itself. In the case of raw material, aspects such as pectin content, availability, logistics and seasonality. On the other hand, factors related to the pectin comprise the structure, molecular features, chemical composition and rheological properties among others play a key role for new sources of pectin extraction (Reichembach & Petkowicz, 2021).

However, other factors such as logistics can constitute limitations when the material is not accessible in huge quantities in proximity. For instance, bananas and watermelon which are the most produced fruit around the world are mostly consumed at home (FAOSTAT, 2021; Ozcelik & Yavuz-Düzgün, 2016; Singh et al., 2018), although the consumption of packed freshly cut fruits from these fruits is also popular in central and northern Europe, as well as in the Unites States, the logistic factor to gather all the residue for processing is still an issue. By means of traditional acid extraction, these two biomass materials provided pectin with high yield, DE, GalA and MW up to 24% in the AIR fraction (Khamsucharit et al., 2018), 79%, 86%, (Oliveira et al., 2016) and 4×10^4 g/mol, respectively (Maneerat et al., 2017) for banana peel, in the same order for watermelon rind around 20% based on the AIR, 63%, 74% and 4 $\times10^4$ g/mol (Petkowicz et al., 2017). Nevertheless, the gelling capacity has not yet been proven. Other potential sources of pectin correspond to coffee and cacao, mainly produced in developing countries (Borrella et al., 2015). Coffee pulp, obtained from the mechanical removal of skin and pulp from the coffee cherry, is also predominantly found in farms as solid waste (Desai et al., 2020). Cacao shells are typically recollected and processed by hand and the rinds, which remain after the separation of beans and pulp, are usually discarded in the cacao plantation (Gayi & Tsowou, 2017). Both pectins have been extracted from coffee and cacao pod husk with yields of 15% and 10- 11% respectively, showing promising hydrogel structures (G'>G''). Likewise, have shown low DE (41%); (GalA 59%) for cacao pod husk and highly acetylated high DE (57%); (GalA 66%) in the case of coffee pectin. For instance, despite the high degree of acetylation, cacao pod husk was able to form a gel with the addition of high quantities of soluble solids like sucrose with low pH, (Petkowicz et al., 2017;

Vriesmann & Petkowicz, 2013). Another alternative such as orange ponkan peel showed a high DE pectin with demonstrated gelling capacity using sucrose and low pH values (GalA 85%; yield 26%) (Colodel et al., 2018), similar behaviour was reported also for cubiu (*Solanum sessiflorum*) peel (GalA 75%; yield 15%) (Colodel & Petkowicz, 2019) and mango peel (GalA 41%) (Jamsazzadeh Kermani et al., 2015). In the other case, the gelling process by calcium has been achieved for LM pectin extracted from pomegranate peel (GalA up to 69%; yield up to 10%;) (Abid et al., 2017) and cashew apple pomace (GalA 85%; yield 25%;) (Yapo & Koffi, 2014).

Other biomass materials have been described to generate pectin with high yield and GalA contents, such as pectin from sugar beet pulp (yield 23%, GalA 72.4%) (Li et al., 2015) eggplant with reported HM values (GalA >66%; yield 34%) (Kazemi et al., 2019), grapefruit peel (yield 27.34%) (W. Wang et al., 2015), tomato dried peel (yield 32.6%) (Del Valle et al., 2006; Grassino et al., 2016), mango peel (yield 32%, GalA 67%) (do Nascimento Oliveira et al., 2018), carrot pomace (yield 15.6%) (Jafari et al., 2017) and passion fruit (yied 14.60%) (Liew et al., 2016). However, these raw materials are not often accessible. It is the case of eggplant peel which is mostly consumed entirely. Other wastes that could be potential for pectin extraction due to the high amounts produced and high GalA content are cashew pomace, passion fruit rind, tomato and grape pomace waste (Reichembach & Petkowicz, 2021).

1.3.3. Pectin extraction process

Before pectin extraction, pre-treatments such as the removal of solids, blanching, or drying improve the stability of the biomass material in the course of storage and transportation. Likewise, pre-treatments help to inactivate enzymes (PME) and harmful bacteria, that would accelerate the degradation of pectin. In some cases, peels are dried to 10-12% water content to avoid the fermentation process (Chan et al., 2017). The extraction of pectin is a continuous process consisting of the hydrolysis and isolation of pectin from the plant tissue and its dissolution into a solvent (Methacanon et al., 2014). Therefore, for industrial extraction of pectin, aqueous solution buffers, chelating agents, acids, and/or alkalis can be used. Actually, if used consecutively in the above-mentioned

order (from water to base), these different chemical agents may selectively extract pectin with different solubility from the same starting material. However, on a commercial scale, mineral acids such as sulphuric, nitric or hydrochloric are frequently used to extract pectin, since they are cheaper and provide highest yields of pectin usually enriched with GalA units (Chan et al., 2017). Traditional heating extraction requires an acidic pH (1–3), high solid-to-liquid ratio (1:30–1:50), high temperatures (75–100 °C) during a long period (1–5 h) to help pectin dissolution in water (Belkheiri et al., 2021; Chan et al., 2017; Grassino et al., 2018; Kang et al., 2015). The extract containing pectin is separated from the raw materials by filtration or centrifugation, precipitated with an alcohol, washed and dry pressed. The final steps involve complete drying and milling to yield powdered pectin, followed by blending with different production batches to standardize structure and functionality (Chan et al., 2017; May, 1990).

Both the exploration of acid and alkali treatments have largely focused on the optimization of extraction conditions and the elucidation of the resulting primary pectin structure (Colodel et al., 2019; Cui et al., 2020). Considering the structural complexity of pectin, these structural differences attained depending on extraction conditions ultimately impact physicochemical properties such as rheology, emulsifying ability, DE, cation-binding capacity, as well as health promoting effects, such as modelling gut microbiota populations, anti-inflammatory, antiglycation, immunomodulating, antioxidant and anti-proliferation effects, of the obtained pectin (Christiaens et al., 2016; Cui et al., 2021).

Besides conventional chemical extraction methods, there are other promising techniques in maximizing yield and quality, e.g. enzyme-assisted extraction (Idrovo Encalada et al., 2019; Sabater et al., 2018), ultrasound-assisted extraction (Maran & Priya, 2015; J.-S. Yang et al., 2019), microwave-assisted extraction (Lefsih et al., 2017; Maran & Prakash, 2015; J.-S. Yang et al., 2019), use of subcritical fluids (Ma et al., 2020; Pinkowska et al., 2019), or extraction via pulsed electric field (Lal et al., 2021), among others (Fig. 1).

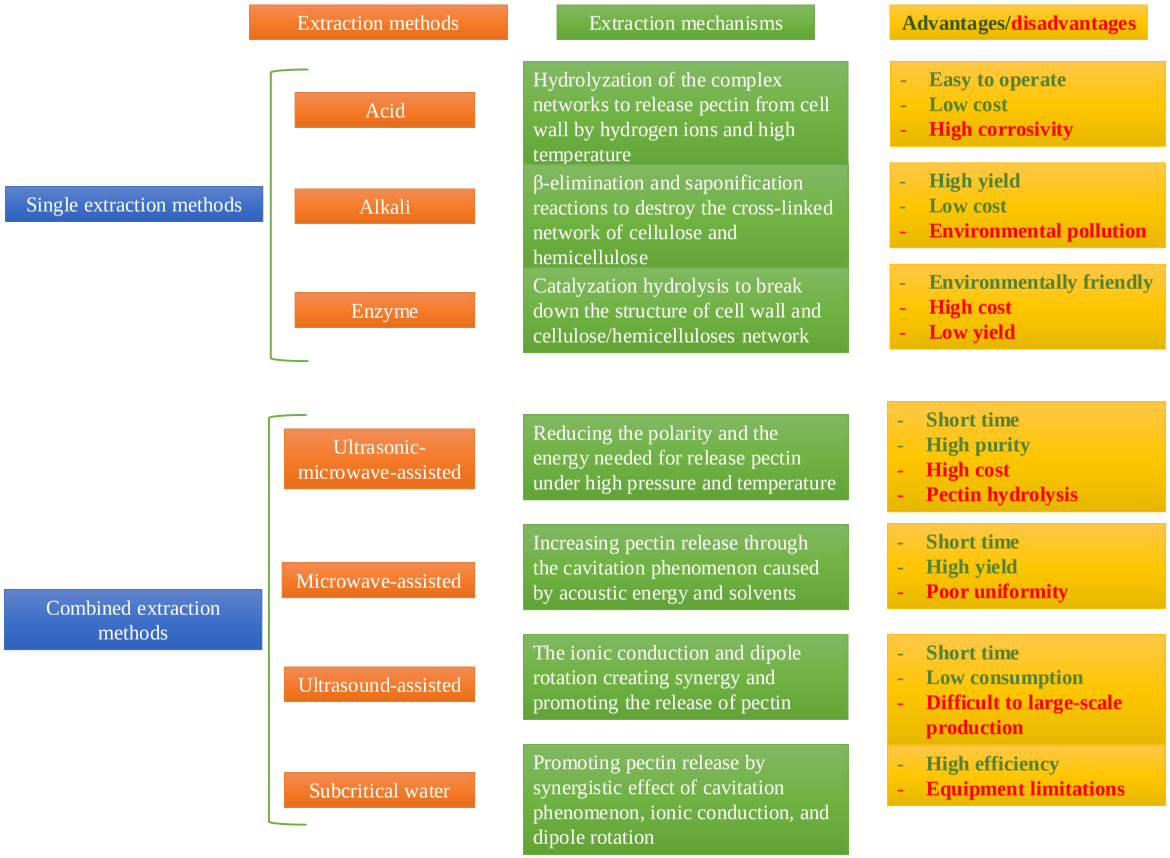

Figure 1. Different methods for extracting pectin from fruits, combined extraction methods refer to the additional process also using the single extraction methods. Adapted with permission of Elsevier from (Cui et al., 2021).

Pectin with different features and yields can be acquired from the same biomass material changing the methodology and factors used for extraction. For instance, in conventional acid extraction, longer extraction times and lower pH values with a high solid:liquid ratio induce a better extraction process and higher yields (Colodel et al., 2018; Pasandide et al., 2017). Harsher conditions (lower pH, longer time, and high temperature) start to degrade the pectin, producing fractions with lower molar mass and DE but higher levels of GalA. This phenomenon is mainly attributed to the hydrolysis attack on pectin side chains that, at the same time, starts a de-esterification process of GalA that occur under these conditions (Abid et al., 2017; Hu et al., 2021; Pereira et al., 2016; C. Wang et al., 2021). Alternatively, various biomass materials (sunflower head, cocoa husk, pistachio green hull, dragon fruit peel, grape pomace, cacao pod husk, jackfruit peel, banana peel, passion fruit rind, pomegranate peel and melon peel) were capable of offering pectin with a wide range of DE. Therefore, it strengthens the idea that extraction factors play a key role in the final pectin structure. However, it is still necessary to investigate if these differences are provoked by a diversity of levels of methyl-esterification in some plants or by the existence of several intermolecular associations, specific fine structures, and configurations, which avoid the pectin from some sources to be less liable to de-esterification (Reichembach & Petkowicz, 2021). In this sense, the importance of investigating the possible variability according to the extraction source is key to valorise different pectin from novel biomass wastes.

1.4. Structure and composition of pectin

Pectin is considered the most complex macromolecule in nature, as it can be composed by 17 different monosaccharides containing more than 20 different linkages (Buggenhout et al., 2009; Ridley et al., 2001; Voragen et al., 2009). It is an essential part in the cell wall structure of plants in early stages of growth during cell expansion, mainly located in the middle lamella (Fig. 2). Present in both primary and secondary plant cell walls, it is abundant in all flowering plants (35%), including fruits and vegetables typically consumed by humans, followed by grasses (2-10%) and other woody tissues (5%) (Voragen et al., 2009). Although specific knowledge on pectin interactions with cellulose and

hemicelluloses remains a scientific challenge (Haas et al., 2020), it is clear that these interactions play an important role in the structure of plant tissue, the cellular adhesion, integrity, rigidity of the cell wall, water absorption and provide a barrier against the external environment (Cui et al., 2021; Dranca & Oroian, 2018; Lara-Espinoza et al., 2018; W. Wang et al., 2018). Likewise, pectin has a significant contribution in the porosity, surface charge, pH, ion balance and even ion transport in the cell wall (McNeil et al., 2003).

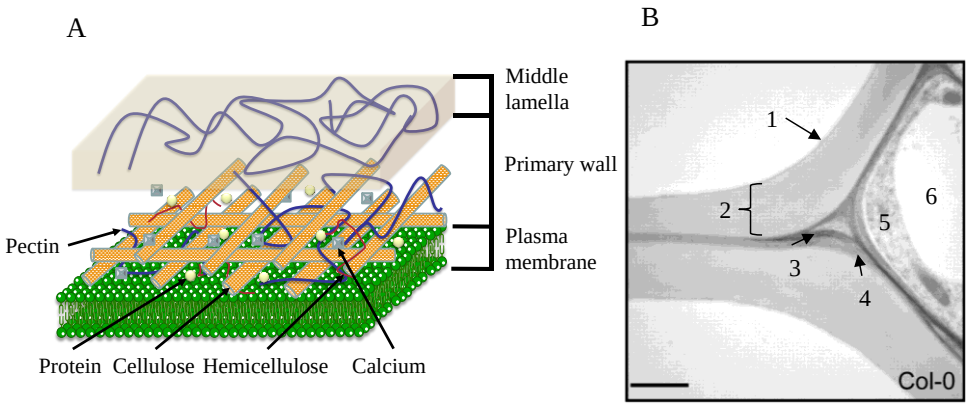

Figure 2. a) Schematic structure of the plant cell wall b) microscopic image of plant cells. Numbers indicate 1) plasma membrane 2) secondary cell wall 3) middle lamella 4) primary cell wall 5) cytosol 6) vacuole (adapted from (Persson et al., 2007) Copyright American Society of Plant Biologists).

1.4.1. Chemical composition

Despite an enormous heterogeneity in the composition, GalA is the main sugar unit in pectin and three major structural patterns are usually recognized throughout the plant kingdom: HG, RG-I, RG-II and XGA.

1.4.1.1. Homogalacturonan (HG)

The most abundant structural pattern is HG, accounting for up to 60% of the total pectin amount (Voragen et al., 2009). This amount can greatly vary depending on the type of

tissue, species, growing stage, environmental conditions, etc. (e.g. 35 and 52 % of uronic acid for tomato and mango, respectively (Muda et al., 1995; Seymour et al., 1990)). HG is a linear polymer consisting of 1,4-linked α-D-GalA units, partially methyl-esterified at C-6 and acetyl-esterified at C-2 or C-3. The pattern and DM and DA again varies depending on the source. HG is produced in the Golgi apparatus with a high DM and later de-esterified by PME in the plant cell wall (Petersen et al., 2008) ME is hypothesized to be tightly regulated by the plant in a developmental and tissue-specific manner (Willats et al., 2001) The HG structure is considered as the linear and smooth region, otherwise, other domains such as RG-I and RG-II, among others, are regarded as hairy or branched regions (Fig. 3) (W. Wang et al., 2018).

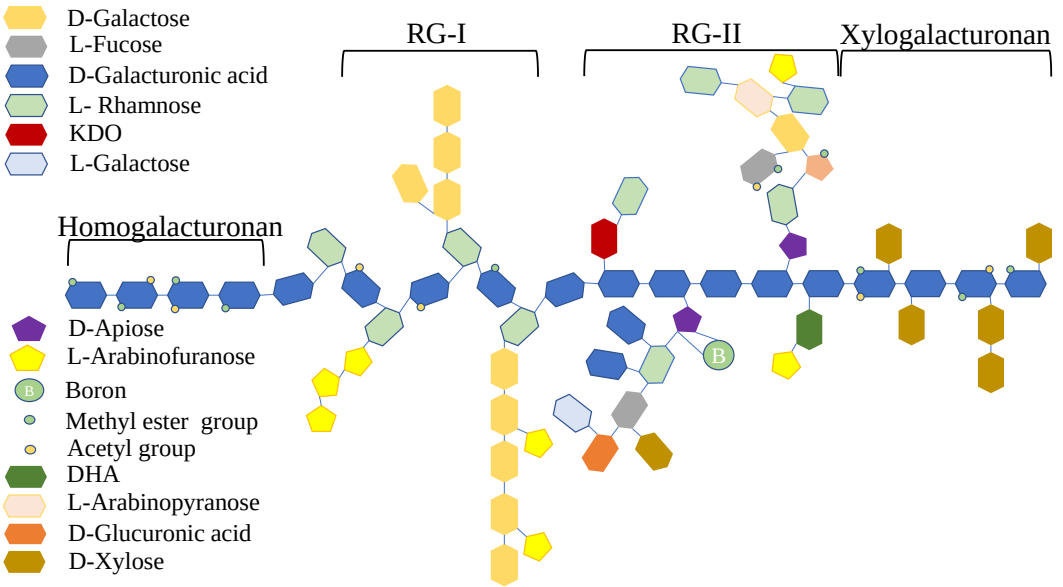

Figure 3. Schematic structure of pectin polysaccharide (Adapted from (Gawkowska et al., 2018; Richard & Hilditch, 2009)).

1.4.1.2. Rhamnogalacturonan-I (RG-I)

RG-I structure consists of a main chain of GalA interrupted by L-rhamnose alternate repeated units, with the configuration (1,4)-α-D-GalA-(1,2)-α-L-Rha, creating the principal backbone of RG-I (Ridley et al., 2001). Some authors reported the length of RG-

I backbone in sugar beet pectin with around 20 residues of this disaccharide (Renard et al., 1995). Likewise, two different configurations with HG have been proposed; one of them, not shown in Fig. 3, alternative to the one explained above, in which HG would be present as a long side chain of RG-I, in most cases covalently connected (Nakamura et al., 2002b; Vincken et al., 2003). This region is scarcely influenced, by ME in the GalA moieties, whereas acetylation does not differ much from GalA residues in HG (C-2/C-3) (Caffall & Mohnen, 2009; Sun et al., 2019). As mentioned before, RG-I belongs to the group domain in pectin considered as "branched" or "hairy region", mainly due to the relatively long and abundant neutral sugar side chains, which can further contribute to the bioactive properties in pectin (W. Wang et al., 2018). These side chains are anchored to C-4, and are typically composed of galactosyl or arabinosyl residues. Both homopolymeric galactan and arabinan can be found, as well as increasingly complex arabinogalactan structures (Lau et al., 1987; Lerouge et al., 1993; Voragen et al., 2009). Arabinogalactan I, as a generally recognized structural example, is composed of a backbone of β-1,4-D-galactopyranosyl residues with attached short chains of α-1.5-arabinose chains at C-3 in the galactose molecule or further β-1,4-D-galactopyranosyl branching sites at C-6 (Gawkowska et al., 2018). The branching degree in the Rha residues varies (20-80%) (Schols et al., 2009) depending on the pectin source, pointing out the importance of the characterization and evaluation of new sources for pectin extraction.

1.4.1.3. Rhamnogalacturonan-II (RG-II)

RG-II is a smaller and less studied pectin component present in higher and lower plants. It has a HG backbone with 4-5 fairly well-defined oligoside side chains containing unusual sugars and quite heterogeneous side chains such as Apio, aceric acid or Kdo (Fig. 3) (Dehors et al., 2019; Ridley et al., 2001).

1.4.1.4. Xylogalacturonan (XGA)

XGA is a region constituted by a HG backbone with xylose residues attached to C-3 (Fig. 3) (Schols et al., 1995, 2009). Depending on the source, the xylosidation can vary, e.g. between 25 and 75% for watermelon and apple, respectively (Schols et al., 2009; Voragen

et al., 2009). Likewise, xylose can be found as a mono-, di- or oligosaccharide side chain of up to seven residues in length in the case of soybean hull pectin (Nakamura et al., 2002a). Although the xylose side chain prevents degradation of the HG backbone by endo-polygalacturonases, in some cases the xylose side chains can be found spaced enough to allow enzymatic breakdown (Mort et al., 2008).

The huge complexity of pectin structure is still in continuous discussion. Moreover, the different complex matrix of each potential source of pectin extraction might allow the discovery of new pectin structures with promising advantages compared to current industrial pectin produced nowadays.

1.4.2. Pectin modifications

The complexity and intrinsic characteristics of pectin polysaccharides allow the tuning and improvement of their properties towards a wide range of applications. Several types of chemical modifications have been achieved using techniques such as chain elongation (grafting and cross-linking), substitution (sulfation, amidation, and thiolation etc.) and depolymerization (β-elimination, mechanical degradation acid or enzymatic hydrolysis) (J. Chen et al., 2015). The most important modification, the DM, DA and degree of amidation, play a key role in the emulsifying capacity and stability, rheology and gelation properties of modified pectins (J. Chen et al., 2015; Renard & Jarvis, 1999). Other chemical modifications are quaternization, sulphation (Martinichen-Herrero et al., 2005; J. Wang et al., 2008) and oxidation, among others (Takei et al., 2010).

Although several products from pectin can be produced by means of chemical modification, enzymatic methods are getting more interest since their environmentally friendly nature, furthermore it allow the selection of a specific region of the polymer for depolymerization under mild conditions, preserving the main structure of pectin (J. Chen et al., 2015). As a result of the well-known complex structure of pectin, the list of different pectin active enzymes can be long. These enzymes usually are divided into two differentiated factions. In the first faction, it is found the enzymes in charge of the depolymerization of the main HG backbone of the pectin. These include pectate lyase,

polygalacturonanase, pectin acetyl esterase, and PME. The second group of enzyme activities is towards the degradation of the "hairy region" composed of RG and related side chains. These include arabinanases, galactanases, arabinofuranosidases, galactosidases, rhamnogalacturonanase, rhamnogalacturonan lyase, rhamnohydrolase, and rhamnogalacturonan galactohydrolases, among others (J. Chen et al., 2015; Funami et al., 2011; Ngouémazong, Kabuye, et al., 2012).

The high complexity of pectin frequently hinders enzymatic degradation. Consequently, treatments with several enzymes acting simultaneously are necessary due to the different type of structural organizations and substitutions. In fact, various pectin enzymes have been demonstrated to act synergistically. Different works are focused on using pectin-modifying enzymes to make controlled changes on the molecular structure of this carbohydrate (removal of methoxyl groups and branched side chains), with the main goal of improving the rheological and gelling properties (Kastner et al., 2019; Ngouémazong et al., 2012; Ralet et al., 2001; Talekar et al., 2020). Another interesting application of enzyme treatments was the study of the effect of protein moieties in the application of sugar beet pectin as an emulsifier (Funami et al., 2011) confirming the key role of the presence of proteins in stabilizing emulsions.

Therefore, pectin-modifying enzymes can be used to tailor compositional and structural properties of new pectin sources, depending on the technological applications within the food industry.

1.5. Main technological applications of pectin in foods

1.5.1. Rheological properties

Pectin is recognized for its interesting technological properties, such as stabilizer, thickener, emulsifier and glazing agent. The rheology of different pectin-rich matrices is influenced by factors such as concentration, sucrose addition, pH, temperature, MW and cation addition, among others (Chan et al., 2017). The evaluation of parameters such as the viscoelastic behaviour, flow properties and viscous characteristics is crucial and offers

an insight on the rheological properties of pectin. It has been demonstrated that dilute solutions of pectin contain homogeneously dispersed pectin molecules that are too far to interact between them and, thus, there is only a slight increase in viscosity due to distortion in the velocity pattern of the liquid by an increased proportion of hydrated molecules (Guimarães et al., 2009). When increasing concentration, the intermolecular distances between the pectin molecules decrease, promoting intermolecular interactions, such as hydrogen bonding. This is also influenced by the DE, favouring electrostatic interactions along and between the pectin chains (Guimarães et al., 2009; Sengkhamparn et al., 2010; Torralbo et al., 2012). At low concentrations (up to 3%), a linear relationship is usually observed between shear stress and shear rate of pectin solutions, indicating Newtonian behaviour, after which a shear thinning behaviour is observed (i.e. a decrease in viscosity with increase in shear rate) (Chan et al., 2017). This transition is dependent on the MW or internal structure of the pectin used (Nascimento et al., 2016; Sousa et al., 2015). Therefore, several factors such as pectin source, fruit maturity and extraction conditions (Yuliarti et al., 2015) will have an impact on the pectin structure and on the intermolecular interactions, such as hydrogen bonds, electrostatic repulsion, hydrophobic association, and Van der Waals forces (Hua et al., 2015). Although increased extraction temperatures imply a reduction in viscosity and higher extraction yields, a compromise exists between efficiency and depolymerisation resulting in shorter chains and consequently in lower viscosity (Carene et al., 2020; do Nascimento Oliveira et al., 2018).

1.5.2. Emulsions

Oil-in-water emulsions are thermodynamically unstable systems, consisting of dispersed oil droplets in a continuous, aqueous phase. Emulsifiers are often added to kinetically stabilize oil-in-water emulsions. In the emulsification process, the emulsifier adsorbs at the surface of the fine droplets, which are created by mechanical homogenization, and protects them from coalescing with neighbouring drops by forming a steric stabilizing layer. Emulsifying capacity and emulsion stability are two parameters used to characterize an emulsion. They are defined, respectively, as the maximum amount of oil that can be

emulsified by a fixed amount of the emulsifying agent and as the rate of phase separation of water and oil during emulsion storage (Dranca & Oroian, 2018).

As mentioned before, the effect of pectin as a stabilizing agent is well-known due to its ability to increase the viscosity of solutions. However, pectin has demonstrated a promising emulsifying effect provoked by its particular surface-active properties. In some cases, the pectin can act as a stabilizer and emulsifier at the same time effects would occur (Schmidt et al., 2015). The DE and protein content in pectin extracts have been detected to be the main factors affecting the droplet size of pectin emulsions. A higher quantity of bound protein has been seen to result in smaller emulsion droplets related to the presence of hydrophobic protein moieties linked to the arabinogalactan parts of pectin while pectin methyl, acetyl, and ferulic acid ester contents provide the ability to being adsorbed at the oil–water interface (Verkempinck et al., 2018). Emulsions produced from pectin with high or low DE have shown smaller droplets than those produced from pectin with medium DE (Schmidt et al., 2015). Likewise, the emulsifying ability of pectin is strongly influenced by its intrinsic molecular features. The MW of pectin is a crucial parameter that affects its conformation in solution and its ability to form a protective layer around oil droplets for a stable emulsion. For instance, low-MW pectin is unable to stabilize the oil/water interface and produce very thin adsorbed layers (Jung & Wicker, 2012; Zhao et al., 2020). On the other hand, pectin with relatively high MW is able to induce a greater number of intermolecular interactions, resulting in higher emulsifying capacities (Ngouémazong et al., 2015). Likewise, the influence of MW is highly related to increase of viscosity of the aqueous continuous phase can reduce oil droplet coalescence and flocculation (Dickinson, 2003). The ability of pectin to increase the viscosity of the aqueous phase is partly caused by its HG domain, and might be dependent on the HG and RG-I (HG/RG-I) ratio (Ngouémazong et al., 2015). As an example, among commercial pectin, those from citrus peel and apple pomace are not considered as effective emulsifying agents as those from sugar beet (Liu et al., 2019). The origin of these different behaviour is mainly attributed to the higher protein and ferulic acid contents in the latter (Siew & Williams, 2008).

1.5.3. Gel formation

Pectin is a natural ionic polysaccharide extensively used in the food and pharmaceutical industries due to its ability to form gels (Braccini & Pérez, 2001). The principle for gelling is the linking of the neighbouring chains of pectin molecules via junction zones to result in a filamentous network. A junction zone is constituted by segments from two or more polymer molecules that are held together and stabilized by hydrogen bonding between the carboxyl and secondary alcohol groups or/and hydrophobic interactions of methoxylated esters groups. The molecular structure, intermolecular forces, and nature of the junction zones determine gelation and, ultimately, the properties of the gel (Ishwarya Padma et al., 2022). The DE, expressing the DE to GalA, plays a main role in the gelation process and is used to classify the type of pectin. HM pectins have DE values greater than 50%, i.e., more than half of the carboxyl groups are in the methyl ester form, and LM pectins, have DE values lower than 50% (Carene et al., 2020). According to the DE, the gelation process changes drastically, as do the interactions and organization of the three-dimensional network (May, 1990). However, other properties such as MW, GalA content, monosaccharide composition, branching degree, protein entanglements, etc, will have an impact in the supramolecular structure and also influence the final physicochemical and gelling properties (Rodsamran & Sothornvit, 2019; Wandee et al., 2019).

1.5.3.1. Gelation process in high methoxylated pectin

Cold gelation of HM pectin consists of an initial heating temperatures higher than 50 °C to achieve dissolution of pectin in water. During heating, hydrophobic interactions are formed between the non-polar methoxylated ester groups in the GalA sugar units (Burey et al., 2008). The junction zones are stabilized by these hydrophobic interactions combined with hydrogen bonds (Fig. 4a). The hydrophobic effects are promoted due to unfavourable interactions between water molecules and the methoxylated ester groups of pectin molecules. Consequently, the methoxylated ester groups stimulate changes in water structure and thereby reduce its entropy (Thakur et al., 1997). Owing to their incompatibility with water, the methoxyl groups are forced to coalesce and reduce their area of interface with water to lessen the effects of the above entropy change. Actual

gelation occurs during the subsequent cooling step, which is favoured with low pH acidic conditions, where the hydrophobic interactions are loosened and replaced by hydrogen bonds between hydrophilic carboxyl (-COOH) groups on the pectin chain and also between the hydroxyl (-OH) groups of neighbouring molecules (Oakenfull & Scott, 1984).

While organic acids are employed to control the pH, soluble solids (mainly sugars like sucrose), are used as the co-solute at concentrations >50% to reduce the water activity, and stabilize the junction zones by promoting the aforementioned hydrophobic interactions. Sugars reduce the hydration capacity of pectin by competing for the available water. Due to their hydrophilicity, sugars bind a significant amount of available water in the system, increasing the proximity between pectin macromolecules and facilitating bond formation (Evageliou et al., 2000; Fraeye et al., 2010). Other co-solutes which can be also employed include sorbitol, ethylene glycol, ethanol, and t-butanol.

Due to this mechanism of gelation, the pattern of ME also influences the gelling properties of HM pectin, referred to as degree of blockiness. In this sense, HM pectin showing a block distribution of methyl esters groups gels faster as compared with those having a random methyl ester distribution (Gamonpilas et al., 2015).

1.5.3.2. Gelation process in low methoxylated pectin

LM pectin forms a gel via a single-step process known as the “ionotropic gelation”, which is independent on temperature, sugar, and acid. Typically, this mechanism involves the cation-mediated gelation (mainly, Ca^{2+}) of negatively charged carboxylate groups ($-COO^-$) available on the backbone of LM pectin, where the divalent metal cations promote chelation between the polyanion-cation and polyanion pairs of carboxylate groups on the adjacent helices of pectin chains (Braccini & Pérez, 2001; Patel et al., 2014; Powell et al., 1982; Ström et al., 2007). The above phenomenon has been described as “ionic molecular association”, and the gelling mechanism of LM pectin is well-known as the “egg box” model (Fig. 4b). The name “egg box” signals the structure of the junction zones formed by the calcium-induced association between chains of HG (Grant et al., 1973; Ventura et al., 2013). An effective calcium bridging is made possible by the relative rigidity of HG

chains (Axelos & Thibault, 1991). The formation of calcium bridges requires a certain amount of dissociated carboxyl groups (COO^-), for which reason pH must be greater than the pKa of pectin. After two pectin chains bind the first Ca^{2+} ion and align in an anti-parallel orientation with respect to each other, they promote an easier binding of the next calcium ion followed by a sequence of binding events. The initial dimer association is strongly stabilized by Van der Waals and hydrogen bonding, in addition to electrostatic interactions (Braccini & Pérez, 2001). As such, the formation of an increased number of "egg box" structures is related to stronger and stiffer gels. The "egg box" model is also applied to explain the gelation process of alginate, another widely used hydrocolloid.

Apart from the cold gelation and ionotropic gelation mechanisms, there are other pectin gelation mechanisms, all of which may coexist depending on the heterogeneity of the pectin structure and other factors related to the gelation process, which are discussed in depth in different reviews (L. Cao et al., 2020; Gawkowska et al., 2018).

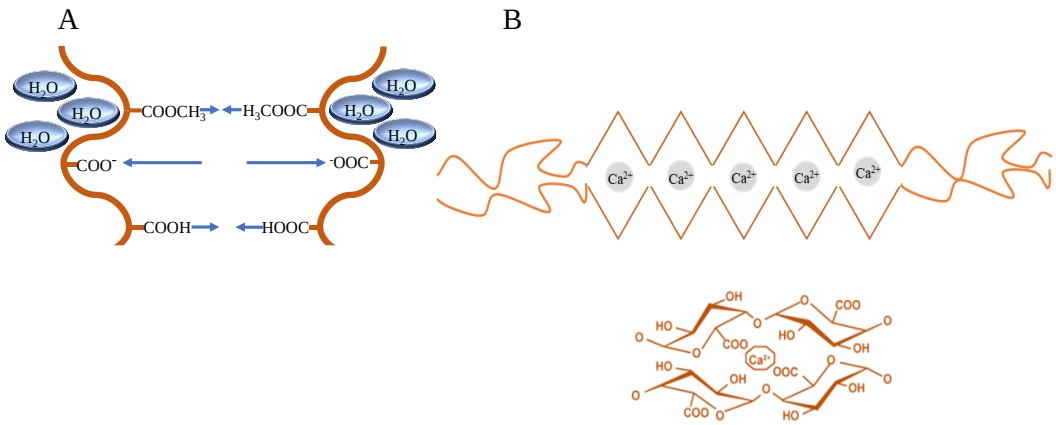

Figure 4. Gelling mechanisms of pectin: A) cold gelation of HM pectin; B) egg-box model of LM pectin (adapted from (Ishwarya Padma et al., 2022)).

1.5.4. Novel applications for pectin gels

A gel is an advanced material consisting of three-dimensional (3D) networks with the ability to incorporate large amounts of water (hydrogel) or other liquids such as oil (oleogel and emulsion gels). The liquid within the 3D gel structure can also be replaced by

air, thus giving rise to special dry materials (generally termed aerogels) with broad number of applications related to their spatial structure and unique properties, including high surface area, porosity, and loading capacity (Abdullah, Zou, et al., 2022; Y. Cao & Mezzenga, 2020).

As mentioned in section 1.5.3., the gelation process is altered by both intrinsic and extrinsic parameters. Intrinsic factors consist of the distribution pattern and the number of free carboxyl groups, branched side chains, source and MW of pectin, on the other hand, extrinsic factors involve ionic strength, calcium concentration, concentration, temperature and pH (Gigli et al., 2009). This capacity has been exploited to produce novel tailored materials, such as emulsion gels, aerogels and biopolymeric films.

1.5.4.1. Emulsion gels

Another advanced application of emulsion structures for replacement of saturated fats is the emulsion gels. Currently, different types of fats are used in the formulation of a great amount of food products, not just for sensory aspects but also for the desired technological properties of a certain product. In this sense, many efforts have been directed in the replacement of saturated fatty acids in food matrices due to the concern related to the effects on consumer's health, which are related to the potential increase of cardiovascular diseases and the incidence of obesity-related disorders (Kwon, 2016; Skelhon et al., 2013). Oil structuring has received considerable interest because it represents a target market for the food industries. The three-dimension network of emulsion gels arises from the supramolecular organization of structuring agents (polymers with gelling capacity in the aqueous phase, called gelator) which entrap liquid oil (oil content ≥ 95%) into a non-flowing condition. Fundamentally, the hydrogel network should provide a framework in which oil is retained and prevented from being released during storage. In addition to these fundamental requirements, an ideal gelator must be food-grade, economically viable, versatile, efficient (be able to structure lipids at relatively low concentrations) and capable of forming structures with similar physical properties (hardness/plasticity at a given temperature, melting point, melting profile) to the corresponding lipid material to be replaced (Co & Marangoni, 2012). From the point of view of ingredient engineering, the

most used gelling polysaccharides are arabic gum, chitosan, pectin, alginate, xanthan gum, carrageenan and carboxymethylcellulose (Devi et al., 2017). However, a few studies have identified the potential of HM pectin as a structuring candidate for emulsion gels due to its ability to adsorb at the oil-water interface while forming a gel in the water phase (Chan et al., 2017; Ishwarya Padma et al., 2022; Schmidt et al., 2017). This is particularly interesting for the preparation of pectin emulsion-gels obtained from new pectin sources since they present practical applications in the food industry providing a solid-like functionality to fat-containing products without compromising textural properties.

1.5.4.2. Aerogels

The name aerogel has long been reserved for materials prepared by supercritical drying, while other porous sol–gel materials produced by evaporation and freeze-drying were referred to as xerogels, (Zhao et al., 2015) and cryogels, respectively. However, it has been better defined as "*a coherent highly porous unique material (solid-state) of low density and high specific surface area, fabricated by the sol-gel method followed by a drying process, comprising three-dimensional networks of interconnected polymers with numerous air-filled pores*" (J. Yang et al., 2019; Zhao et al., 2018). According to the International Union of Pure and Applied Chemistry (IUPAC), "aerogels are non-fluid networks composed of interconnected colloidal particles as dispersed phase in a gas (typically air)". Aerogels can be prepared by replacing the liquid of the gels contained in the three-dimensional network with gas, generating different kinds of porous solid materials with large inner surface area, low weight, low density and high porosity (Abdullah, Liu, et al., 2022).

Traditionally, inorganic materials (silica, titanium, graphene, etc.) are used to make aerogels, and these aerogels are used for non-food applications (Mikkonen et al., 2013). However, concerns about sustainability, biodegradability, and long-term negative impact on the environment have driven researchers to find safe, green alternatives (Ganesan et al., 2018). Biopolymers (polysaccharides, protein, etc.) can be used to develop aerogels for different food and non-food applications due to their non-toxic features. In addition, biopolymers often have a high density of functional surface groups, for example, amino

groups on chitosan or carboxyl groups on pectin or alginate, thus opening up new applications and providing convenient anchoring points for added functionality, for food- and health-related applications such as wound healing or drug delivery.

Aerogel pectins have been explored as carriers of maghemite nanoparticles in the form of bulk cylinders and microspheres with mixtures of apple and citrus pectin, for potential application as magnetic targeting drug delivery vehicles. The results indicated a good performance in the preservation of the material after overall processing (García-González et al., 2012). On the other hand, a first approach was carried out to characterize and evaluate different types of porous pectin aerogels made with citrus pectin, demonstrating the potential of porous pectin matrices for drug delivery purposes (Groult et al., 2021a). A more emphasized investigation of pectin material regarding the importance of gelation bath and DE was performed with citrus pectin aerogels. In this case, the release kinetic of drug loaded theophylline was modelled to identify the main physical mechanism that govern the drug release (Groult et al., 2021b). Moreover, different authors have characterized and evaluated the potential of pectin as an aerogel material with different shapes (monoliths and microspheres) mainly from commercial citrus and apple pectins (Preibisch et al., 2018; Veronovski, Tkalec, Knez, Novak, et al., 2014). Nevertheless, most of these studies are mainly focused on the structural and mechanical properties of the developed aerogels and on the gelation mechanism, ignoring critical factors such as structural, compositional and physicochemical characteristics of the pectin itself, which play a key role in their technological applications. Moreover, due to the emerging interest towards pectin, alternative sources like by-products and agri-food wastes are interesting to be explored in order to provide new structural and potential technological applications.

In addition, aerogels provide the possibility of carrying and protecting bioactive compounds by incorporating them into their structure. The aerogel solid skeleton dictates the chemical affinity of the matrix to the adsorbed molecule and, in the case of drugs, their partition coefficient between the aerogel and the aqueous medium when immersed in body fluids (García-González et al., 2021). Despite of the different potential properties, very few biopolymer aerogels have made the transition to industrial production, presenting a

major challenge in terms of research and development in the coming years (Zhao et al., 2018).

1.5.5. Pectin films and coatings

Nowadays, food packaging is an essential part of the food industry. However, increasing environmental concerns about traditional packaging and growing demands for food quality, promote biodegradable packaging as a prominent alternative on the market to overcome the challenges faced by traditional plastic packaging (Huang et al., 2021; Nastasi et al., 2022). Renewable and biodegradable natural polymeric materials constitute ideal candidates to replace conventional polymers (Otoni et al., 2017). Among this type of biopolymers, pectin-based films from agricultural food waste is a popular trend and it has been widely dealt with in different reviews (Mellinas et al., 2020; Nastasi et al., 2022; Otoni et al., 2017). Edible pectin films and coatings may be used as biopolymer-based materials whose application range can be enhanced with the addition of plant extracts to create new active packaging strategies (Go & Song, 2020; Nìmah et al., 2020; Otoni et al., 2017). Among the methods generally used to produce these films from pectin, the casting method or the application as a coating and wrapping after film formation, are the most common approaches. The plant extract can be incorporated before, during or after dissolution and homogenization of the pectin polymer (Nastasi et al., 2022).

The film forming properties are mainly attributed to the different characteristics of pectin that are directly correlated to the extraction factors and production source (Huang et al., 2021). As in previous applications, factors such as linearity, sugar side chains, GalA content, DE, MW, presence of protein, among others, exert a significant influence on the film forming capabilities and mechanical properties, e.g. higher branched properties reduce the mobility and improve the films compactness (Shafie et al., 2020). In this sense, lower DE showed improvements on the mechanical characteristics of pectin films with a more uniform structure, due to more hydrogen bonds generated by polar groups (Moreira et al., 2013). Pectin films themselves have low values of tensile strength, high hydrophilicity and brittle structure, limiting their applications (Jahromi et al., 2020; Meerasri & Sothornvit, 2020). In order to avoid these non-desirable effects, mixtures with

other polymers and incorporation of plant extracts and active agents such as essential oils, antioxidant or antimicrobial compounds have been performed (Almasi et al., 2020; Lin et al., 2020). For instance, the effect of the addition of phenolic groups from ellagitannins on pectin films, has demonstrated improved hydrophobic properties with the increase of cross-linking zones generated by the hydrogen bonds induced by phenolic compounds (Y. Chen et al., 2020). Thus, the potential to explore mixtures of film-forming pectin solution with other biopolymers or extracts from biomass waste is a promising alternative for greener preservation strategies.

1.6. Miscellaneous applications of bio-functional compounds from biomass residues

In line with waste valorisation, by-products generated through the food chain can also be an excellent source of bioactive compounds, such as phenolic compounds (phenolic acid, carotenoids, flavonoids), bioactive proteins (peptide isolates, amino acids), fatty acids, dietary fibre, and so on. For instance, the fruits are a good source of essential oils, phytochemicals, pectin, valuable fibres, and minerals (Kris-Etherton et al., 2002; Marić et al., 2018; Mena-García et al., 2019; Yahia & Ornelas-Paz, 2009). In particular, persimmon fruit is well-known for its diverse beneficial human health properties, such as anti-tumor, anti-hypercholesterolemic, antioxidant effect, antidiabetic effect, prevention of dyslipidemia, anti-inflammatory, among others. These beneficial effects are mainly attributed to their richness in phenolic compounds, vitamin C and carotenoids (Direito et al., 2021; Matheus et al., 2022). The beneficial implications of these compounds, increase the interest for their obtention and characterization (Veberic et al., 2010). Several investigations have been focused on the comparison of different cultivars, and their effect over sensory and phytochemical composition (J. Chen et al., 2016; Jang et al., 2011; Khokhlov & Plugatar, 2016; Maeda et al., 2018a, 2018b; Qi et al., 2019; Veberic et al., 2010; Yoo et al., 2019). However, there is an increased interest in the valorisation of the discarded persimmon fruit to generate opportunities and create more sustainable systems, including the development of edible film, ethanol production, animal feed, peel powder, emulsifier agent, and enhancer gel properties (Conesa et al., 2019; Hwang et al., 2011;

Jiang et al., 2020; Kawase et al., 2003; Lucas-González et al., 2018; Mamet et al., 2017; Matheus et al., 2021; Muñoz-Almagro, Vendrell-Calatayud, et al., 2021). These different applications, and those that have not yet been explored, highlight the potential valorisation of persimmon discards in terms of the amount of antioxidant compounds and biopolymers that, together with the interactions they may have, play an important role in their application and functionality. Besides nutraceutical properties, natural antioxidants and colour compounds can be a greener alternative for synthetic antioxidants, which could be used in different food or pharmaceutical applications (Altemimi et al., 2017; Kowalska et al., 2017; Trigo et al., 2020).

Currently, the discovery of new, safe, and effective antivirals has become an active focus of research, in the frame of several foodborne outbreaks and the COVID pandemic (L. Chen & Huang, 2018). The advantages of choosing natural products for the development of new antivirals are their chemical diversity, the possibility of active principles acting at different biological targets, and low toxicity (de Godoi et al., 2019; Martinez et al., 2014). Some studies related to the effectiveness of pectin as antiviral compounds have been reported. Pectin from *Inga* spp. fruit showed an antiviral activity against herpes simplex virus type 1 and poliovirus, which was mainly attributed to the sulphated polysaccharides and related to the degree of sulphation, molecular weight, and sugar composition (de Godoi et al., 2019). In a different study, the pectin fraction extracted from *Basella Rubra* L. exhibited antiviral activity against herpes simplex virus type 2 by interfering with absorption and penetration of the virus to host cells (Dong et al., 2011). Another case of successful antiherpetic *in-vitro* activity was with the use of pectin from *Cucumis melo* var. acidulus (Agostinho et al., 2021). Moreover, other bioactive compounds such as tannins, have been widely recognized by its antiviral capacity (Kaczmarek, 2020). That is the case of isolated tannins from mango which shown to inhibit influenza and coxsackie virus (Abdel-Mageed et al., 2014). Likewise, the antiviral activity of persimmon polyphenol extracts from immature green fruit containing 22% of tannins was evaluated on enveloped (influenza virus H3N2, H5N3, herpes simplex virus-1, vesicular stomatitis virus, Sendai virus and Newcastle disease virus) and non-enveloped viruses (poliovirus, coxsackie virus, adenovirus, rotavirus, feline calicivirus and mouse norovirus), demonstrating a

broad range of antiviral efficacy (Ueda et al., 2013). The promising use of persimmon pectin and its high tannin content (dealt with in this thesis work), opens up an opportunity to establish new food technological applications, taking advantage of the polysaccharide-tannin complexes for new bioactive and technological applications.

In summary, the potential for waste valorisation from fruit waste by-products is a vast field of research that remains to be explored. Each type of fruit has unique characteristics and compounds that can determine its use for many industrial applications, making its characterisation and subsequent valorisation relevant. Pectin, a complex carbohydrate with unique characteristics depending on the source and extraction conditions, can be a versatile feedstock to offer properties that are still being investigated today. Likewise, the industrial interest in polyphenolic compounds, for their different benefits and applications in human health, further underlines fruit valorisation. Research on how structural features affect functional and technological properties is ongoing and will remain a hot topic of interest in the coming years. Likewise, the cost-effectiveness of extraction, refining and formulation of these new ingredients of interest should be evaluated in order to allow for these novel food technology applications to come into the market.

References

Abdel-Mageed, W. M., Bayoumi, S. A. H., Chen, C., Vavricka, C. J., Li, L., Malik, A., Dai, H., Song, F., Wang, L., Zhang, J., Gao, G. F., Lv, Y., Liu, L., Liu, X., Sayed, H. M., & Zhang, L. (2014). Benzophenone C-glucosides and gallotannins from mango tree stem bark with broad-spectrum anti-viral activity. *Bioorganic & Medicinal Chemistry*, *22*(7), 2236–2243. https://doi.org/10.1016/J.BMC.2014.02.014

Abdullah, Liu, L., Javed, H. U., & Xiao, J. (2022). Engineering Emulsion Gels as Functional Colloids Emphasizing Food Applications: A Review. *Frontiers in Nutrition*, *0*, 752. https://doi.org/10.3389/FNUT.2022.890188

Abdullah, Zou, Y. C., Farooq, S., Walayat, N., Zhang, H., Faieta, M., Pittia, P., & Huang, Q. (2022). Bio-aerogels: Fabrication, properties and food applications. *Https://Doi.Org/10.1080/10408398.2022.2037504*. https://doi.org/10.1080/10408398.2022.2037504

Abid, M., Cheikhrouhou, S., Renard, C. M. G. C., Bureau, S., Cuvelier, G., Attia, H., & Ayadi, M. A. (2017). Characterization of pectins extracted from pomegranate peel and their gelling properties. *Food Chemistry*, *215*, 318–325. https://doi.org/10.1016/J.FOODCHEM.2016.07.181

Adiletta, G., Brachi, P., Riianova, E., Crescitelli, A., Miccio, M., & Kostryukova, N. (2020). A Simplified Biorefinery Concept for the Valorization of Sugar Beet Pulp: Ecofriendly Isolation of Pectin as a Step Preceding Torrefaction. *Waste and Biomass Valorization*, *11*(6), 2721–2733. https://doi.org/10.1007/S12649-019-00582-4/FIGURES/4

Agostinho, K. F., Rechenchoski, D. Z., Faccin-Galhardi, L. C., De Sousa, A. L. N., Cunha, A. P., Ricardo, N. M. P. S., Linhares, R. E. C., & Nozawa, C. (2021). Cucumis melo pectin as potential candidate to control herpes simplex virus infection. *FEMS Microbiology Letters*, *368*(4), 13. https://doi.org/10.1093/FEMSLE/FNAB013

Almasi, H., Azizi, S., & Amjadi, S. (2020). Development and characterization of pectin films activated by nanoemulsion and Pickering emulsion stabilized marjoram (Origanum majorana L.) essential oil. *Food Hydrocolloids*, *99*, 105338. https://doi.org/10.1016/J.FOODHYD.2019.105338

Altemimi, A., Lakhssassi, N., Baharlouei, A., Watson, D. G., & Lightfoot, D. A. (2017). Phytochemicals: Extraction, Isolation, and Identification of Bioactive Compounds from Plant Extracts. *Plants*, *6*(4). https://doi.org/10.3390/PLANTS6040042

Asgar, M. A., Yamauchi, R., & Kato, K. (2004). Structural features of pectins from fresh and sun-dried Japanese persimmon fruit. *Food Chemistry*, *87*(2), 247–251. https://doi.org/10.1016/j.foodchem.2003.11.016

Atmodjo, M. A., Hao, Z., & Mohnen, D. (2013). Evolving Views of Pectin Biosynthesis. *Http://Dx.Doi.Org/10.1146/Annurev-Arplant-042811-105534*, *64*, 747–779. https://doi.org/10.1146/ANNUREV-ARPLANT-042811-105534

Awasthi, M. K., Ferreira, J. A., Sirohi, R., Sarsaiya, S., Khoshnevisan, B., Baladi, S., Sindhu, R., Binod, P., Pandey, A., Juneja, A., Kumar, D., Zhang, Z., & Taherzadeh, M. J. (2021). A critical review on the development stage of biorefinery systems towards the management of apple processing-derived waste. *Renewable and Sustainable Energy Reviews*, *143*, 110972. https://doi.org/10.1016/J.RSER.2021.110972

Axelos, M. A. V., & Thibault, J. F. (1991). Influence of the substituents of the carboxyl groups and of the rhamnose content on the solution properties and flexibility of pectins. *International Journal of Biological Macromolecules*, *13*(2), 77–82. https://doi.org/10.1016/0141-8130(91)90052-V

Begum, R., Yusof, Y. A., Aziz, M. G., & Uddin, M. B. (2017). Screening of Fruit Wastes as Pectin Source. *Journal of Environmental Science and Natural Resources*, *10*(1), 65–70. https://doi.org/10.3329/JESNR.V10I1.34696

Belkheiri, A., Forouhar, A., Ursu, A. V., Dubessay, P., Pierre, G., Delattre, C., Djelveh, G., Abdelkafi, S., Hamdami, N., & Michaud, P. (2021). Extraction, characterization, and applications of pectins from plant by-products. *Applied Sciences (Switzerland)*, *11*(14). https://doi.org/10.3390/APP11146596

Borrella, I., Mataix, C., & Carrasco-Gallego, R. (2015). Smallholder Farmers in the Speciality Coffee Industry: Opportunities, Constraints and the Businesses that are Making it Possible. *IDS Bulletin*, *46*(3), 29–44. https://doi.org/10.1111/1759-5436.12142

Braccini, I., & Pérez, S. (2001). Molecular basis of Ca2+-induced gelation in alginates and pectins: The egg-box model revisited. *Biomacromolecules*, *2*(4), 1089–1096. https://doi.org/10.1021/BM010008G/ASSET/IMAGES/LARGE/BM010008GF00007.JPEG

Brachi, P., Riianova, E., Miccio, M., Miccio, F., Ruoppolo, G., & Chirone, R. (2017). Valorization of sugar beet pulp via torrefaction with a focus on the effect of the preliminary extraction of pectins. *Energy and Fuels*, *31*(9), 9595–9604. https://doi.org/10.1021/ACS.ENERGYFUELS.7B01766/ASSET/IMAGES/LARGE/EF-2017-01766C_0007.JPEG

Buggenhout, S. Van, Sila, D. N., Duvetter, T., Loey, A. Van, & Hendrickx, M. (2009). Pectins in Processed Fruits and Vegetables: Part III—Texture Engineering. *Comprehensive Reviews in Food Science and Food Safety*, *8*(2), 105–117. https://doi.org/10.1111/J.1541-4337.2009.00072.X

Burey, P., Bhandari, B. R., Howes, T., & Gidley, M. J. (2008). Hydrocolloid gel particles: Formation, characterization, and application. *Critical Reviews in Food Science and Nutrition*, *48*(5), 361–377. https://doi.org/10.1080/10408390701347801

Caffall, K. H., & Mohnen, D. (2009). The structure, function, and biosynthesis of plant cell wall pectic polysaccharides. *Carbohydrate Research*, *344*(14), 1879–1900.

Campbell, M. (2006). *Extraction of Pectin From Watermelon Rind*. Oklahoma State University.

Cao, L., Lu, W., Mata, A., Nishinari, K., & Fang, Y. (2020). Egg-box model-based gelation of alginate and pectin: A review. In *Carbohydrate Polymers* (Vol. 242, p. 116389). Elsevier. https://doi.org/10.1016/j.carbpol.2020.116389

Cao, Y., & Mezzenga, R. (2020). Design principles of food gels. *Nature Food*, *1*(2), 106–118. https://doi.org/10.1038/s43016-019-0009-x

Carene, M., Picot-Allain, N., Ramasawmy, B., & Emmambux, M. N. (2020). *Extraction, Characterisation, and Application of Pectin from Tropical and Sub-Tropical Fruits: A Review*. https://doi.org/10.1080/87559129.2020.1733008

Chakrabarty, N., Mourin, M. M., Islam, N., Haque, A. R., Akter, S., Siddique, A. A., & Sarker, M. (2020). Assessment of the Potential of Watermelon Rind Powder for the Value Addition of Noodles. *Journal of Biosystems Engineering 2020 45:4*, *45*(4), 223–231. https://doi.org/10.1007/S42853-020-00061-Y

Chan, S. Y., Choo, W. S., Young, D. J., & Loh, X. J. (2017). Pectin as a rheology modifier: Origin, structure, commercial production and rheology. *Carbohydrate Polymers*, *161*, 118–139. https://doi.org/10.1016/j.carbpol.2016.12.033

Chen, J., Du, J., Ge, Z., Zhu, W., Nie, R., & Li, C. (2016). Comparison of sensory and compositions of five selected persimmon cultivars (Diospyros kaki L.) and correlations between chemical components and processing characteristics. *Journal of Food Science and Technology*, *53*(3), 1597–1607. https://doi.org/10.1007/s13197-015-2102-y

Chen, J., Liu, W., Liu, C.-M. M., Li, T., Liang, R.-H. H., & Luo, S.-J. J. (2015). Pectin Modifications: A Review. *Critical Reviews in Food Science and Nutrition*, *55*(12), 1684–1698. https://doi.org/10.1080/10408398.2012.718722

Chen, L., & Huang, G. (2018). The antiviral activity of polysaccharides and their derivatives. *International Journal of Biological Macromolecules*, *115*, 77–82. https://doi.org/10.1016/J.IJBIOMAC.2018.04.056

Chen, Y., Xu, L., Wang, Y., Chen, Z., Zhang, M., & Chen, H. (2020). Characterization and functional properties of a pectin/tara gum based edible film with ellagitannins from the unripe fruits of Rubus chingii Hu. *Food Chemistry*, *325*, 126964. https://doi.org/10.1016/J.FOODCHEM.2020.126964

Christiaens, S., Van Buggenhout, S., Houben, K., Jamsazzadeh Kermani, Z., Moelants, K. R. N., Ngouémazong, E. D., Van Loey, A., & Hendrickx, M. E. G. (2016). Process–Structure–Function Relations of Pectin in Food. *Critical Reviews in Food Science and Nutrition*, *56*(6), 1021–1042. https://doi.org/10.1080/10408398.2012.753029

Clauser, N. M., Felissia, F. E., Area, M. C., & Vallejos, M. E. (2021). A framework for the design and analysis of integrated multi-product biorefineries from agricultural and forestry wastes. *Renewable and Sustainable Energy Reviews*, *139*, 110687. https://doi.org/10.1016/J.RSER.2020.110687

Co, E. D., & Marangoni, A. G. (2012). Organogels: An alternative edible oil-structuring method. In *JAOCS, Journal of the American Oil Chemists' Society* (Vol. 89, Issue 5, pp. 749–780). John Wiley & Sons, Ltd. https://doi.org/10.1007/s11746-012-2049-3

Colodel, C., & Petkowicz, C. L. O. (2019). Acid extraction and physicochemical characterization of pectin from cubiu (Solanum sessiliflorum D.) fruit peel. *Food Hydrocolloids*, *86*, 193–200. https://doi.org/10.1016/J.FOODHYD.2018.06.013

Colodel, C., Vriesmann, L. C., & Lucia de Oliveira Petkowicz, C. (2019). Rheological characterization of a pectin extracted from ponkan (Citrus reticulata blanco cv. ponkan) peel. *Food Hydrocolloids*, *94*, 326–332. https://doi.org/10.1016/j.foodhyd.2019.03.025

Colodel, C., Vriesmann, L. C., Teófilo, R. F., & de Oliveira Petkowicz, C. L. (2018). Extraction of pectin from ponkan (Citrus reticulata Blanco cv. Ponkan) peel: Optimization and structural characterization. *International Journal of Biological Macromolecules*, *117*, 385–391. https://doi.org/10.1016/J.IJBIOMAC.2018.05.048

Conesa, C., Laguarda-Miró, N., Fito, P., & Seguí, L. (2019). Evaluation of Persimmon (Diospyros kaki Thunb. cv. Rojo Brillante) Industrial Residue as a Source for Value Added Products. *Waste and Biomass Valorization*, *Idm*, 1–12. https://doi.org/10.1007/s12649-019-00621-0

Cristóbal, J., Caldeira, C., Corrado, S., & Sala, S. (2018). Techno-economic and profitability analysis of food waste biorefineries at European level. *Bioresource Technology*, *259*, 244–252. https://doi.org/10.1016/J.BIORTECH.2018.03.016

Cui, J., Ren, W., Zhao, C., Gao, W., Tian, G., Bao, Y., Lian, Y., & Zheng, J. (2020). The structure–property relationships of acid- and alkali-extracted grapefruit peel pectins. *Carbohydrate Polymers*, *229*, 115524. https://doi.org/10.1016/j.carbpol.2019.115524

Cui, J., Zhao, C., Feng, L., Han, Y., Du, H., Xiao, H., & Zheng, J. (2021). Pectins from fruits: Relationships between extraction methods, structural characteristics, and functional properties. In *Trends in Food Science and Technology* (Vol. 110, pp. 39–54). Elsevier. https://doi.org/10.1016/j.tifs.2021.01.077

de Godoi, A. M., Faccin-Galhardi, L. C., Rechenchoski, D. Z., Arruda, T. B. M. G., Cunha, A. P., de Almeida, R. R., Rodrigues, F. E. A., Ricardo, N. M. P. S., Nozawa, C., & Linhares, R. E. C. (2019). Structural characterization and antiviral activity of pectin isolated from Inga spp. *International Journal of Biological Macromolecules*, *139*, 925–931. https://doi.org/10.1016/J.IJBIOMAC.2019.07.212

Dehors, J., Mareck, A., Kiefer-Meyer, M. C., Menu-Bouaouiche, L., Lehner, A., & Mollet, J. C. (2019). Evolution of cell wall polymers in tip-growing land plant gametophytes: Composition, distribution, functional aspects and their remodeling. In

Frontiers in Plant Science (Vol. 10, p. 441). Frontiers Media S.A. https://doi.org/10.3389/fpls.2019.00441

Del Valle, M., Cámara, M., & Torija, M.-E. (2006). Chemical characterization of tomato pomace. *Journal of the Science of Food and Agriculture*, *86*(8), 1232–1236. https://doi.org/10.1002/jsfa.2474

Desai, N. M., Varun, E., Patil, S., Pimpley, V., & Murthy, P. S. (2020). Environment Pollutants During Coffee Processing and Its Valorization. *Handbook of Environmental Materials Management*, 1–13. https://doi.org/10.1007/978-3-319-58538-3_209-1

Devi, N., Sarmah, M., Khatun, B., & Maji, T. K. (2017). Encapsulation of active ingredients in polysaccharide–protein complex coacervates. *Advances in Colloid and Interface Science*, *239*, 136–145. https://doi.org/10.1016/J.CIS.2016.05.009

Dickinson, E. (2003). Hydrocolloids at interfaces and the influence on the properties of dispersed systems. *Food Hydrocolloids*, *17*(1), 25–39. https://doi.org/10.1016/S0268-005X(01)00120-5

Direito, R., Rocha, J., Sepodes, B., & Eduardo-Figueira, M. (2021). From diospyros kaki L. (persimmon) phytochemical profile and health impact to new product perspectives and waste valorization. *Nutrients*, *13*(9). https://doi.org/10.3390/NU13093283

do Nascimento Oliveira, A., de Almeida Paula, D., Basílio de Oliveira, E., Henriques Saraiva, S., Stringheta, P. C., & Mota Ramos, A. (2018). Optimization of pectin extraction from Ubá mango peel through surface response methodology. *International Journal of Biological Macromolecules*, *113*, 395–402. https://doi.org/10.1016/j.ijbiomac.2018.02.154

Dong, C. X., Hayashi, K., Mizukoshi, Y., Lee, J. B., & Hayashi, T. (2011). Structures of acidic polysaccharides from Basella rubra L. and their antiviral effects.

Carbohydrate Polymers, *84*(3), 1084–1092. https://doi.org/10.1016/J.CARBPOL.2010.12.073

Dranca, F., & Oroian, M. (2018). Extraction, purification and characterization of pectin from alternative sources with potential technological applications. *Food Research International*, *113*(February), 327–350. https://doi.org/10.1016/j.foodres.2018.06.065

Esparza, I., Jiménez-Moreno, N., Bimbela, F., Ancín-Azpilicueta, C., & Gandía, L. M. (2020). Fruit and vegetable waste management: Conventional and emerging approaches. *Journal of Environmental Management*, *265*, 110510. https://doi.org/10.1016/j.jenvman.2020.110510

Evageliou, V., Richardson, R. K., & Morris, E. R. (2000). Effect of pH, sugar type and thermal annealing on high-methoxy pectin gels. *Carbohydrate Polymers*, *42*(3), 245–259. https://doi.org/10.1016/S0144-8617(99)00191-5

FAOSTAT. (2021). *CROPS*. http://www.fao.org/faostat/en/#data/QC/visualize

Fraeye, I., Colle, I., Vandevenne, E., Duvetter, T., Van Buggenhout, S., Moldenaers, P., Van Loey, A., & Hendrickx, M. (2010). Influence of pectin structure on texture of pectin–calcium gels. *Innovative Food Science & Emerging Technologies*, *11*(2), 401–409. https://doi.org/10.1016/J.IFSET.2009.08.015

Funami, T., Nakauma, M., Ishihara, S., Tanaka, R., Inoue, T., & Phillips, G. O. (2011). Structural modifications of sugar beet pectin and the relationship of structure to functionality. *Food Hydrocolloids*, *25*(2), 221–229. https://doi.org/10.1016/j.foodhyd.2009.11.017

Gamonpilas, C., Krongsin, J., Methacanon, P., & Goh, S. M. (2015). Gelation of pomelo (Citrus maxima) pectin as induced by divalent ions or acidification. *Journal of Food Engineering*, *152*, 17–23. https://doi.org/10.1016/J.JFOODENG.2014.11.024

Ganesan, K., Budtova, T., Ratke, L., Gurikov, P., Baudron, V., Preibisch, I., Niemeyer, P., Smirnova, I., & Milow, B. (2018). Review on the production of polysaccharide aerogel particles. *Materials*, *11*(11), 1–37. https://doi.org/10.3390/ma11112144

García-González, C. A., Carenza, E., Zeng, M., Smirnova, I., & Roig, A. (2012). Design of biocompatible magnetic pectin aerogel monoliths and microspheres. *RSC Advances*, *2*(26), 9816–9823. https://doi.org/10.1039/c2ra21500d

García-González, C. A., Sosnik, A., Kalmár, J., de Marco, I., Erkey, C., Concheiro, A., & Alvarez-Lorenzo, C. (2021). Aerogels in drug delivery: From design to application. *Journal of Controlled Release*, *332*, 40–63. https://doi.org/10.1016/J.JCONREL.2021.02.012

Gawkowska, D., Cybulska, J., & Zdunek, A. (2018). Structure-related gelling of pectins and linking with other natural compounds: A review. *Polymers*, *10*(7), 762. https://doi.org/10.3390/polym10070762

Gayi, S. K., & Tsowou, K. (2017). Cocoa Industry: Integrating Small Farmers into the Global Value Chain. *Cocoa Industry*. https://doi.org/10.18356/CFB75B0E-EN

Gigli, J., Garnier, C., & Piazza, L. (2009). Rheological behaviour of low-methoxyl pectin gels over an extended frequency window. *Food Hydrocolloids*, *23*(5), 1406–1412. https://doi.org/10.1016/J.FOODHYD.2008.09.015

Go, E. J., & Song, K. Bin. (2020). Development and Characterization of Citrus Junos Pomace Pectin Films Incorporated With Rambutan (Nephelium Lappaceum) Peel Extract. *Coatings 2020, Vol. 10, Page 714*, *10*(8), 714. https://doi.org/10.3390/COATINGS10080714

Grant, G. T., Morris, E. R., Rees, D. A., Smith, P. J. C., & Thom, D. (1973). Biological interactions between polysaccharides and divalent cations: The egg-box model. *FEBS Letters*, *32*(1), 195–198. https://doi.org/10.1016/0014-5793(73)80770-7

Grassino, A. N., Barba, F. J., Brnčić, M., Lorenzo, J. M., Lucini, L., & Brnčić, S. R. (2018). Analytical tools used for the identification and quantification of pectin extracted from plant food matrices, wastes and by-products: A review. *Food Chemistry*, *266*(May), 47–55. https://doi.org/10.1016/j.foodchem.2018.05.105

Grassino, A. N., Halambek, J., Djaković, S., Rimac Brnčić, S., Dent, M., & Grabarić, Z. (2016). Utilization of tomato peel waste from canning factory as a potential source for pectin production and application as tin corrosion inhibitor. *Food Hydrocolloids*, *52*, 265–274. https://doi.org/10.1016/j.foodhyd.2015.06.020

Groult, S., Buwalda, S., & Budtova, T. (2021a). Pectin hydrogels, aerogels, cryogels and xerogels: Influence of drying on structural and release properties. *European Polymer Journal*, *149*, 110386. https://doi.org/10.1016/J.EURPOLYMJ.2021.110386

Groult, S., Buwalda, S., & Budtova, T. (2021b). Tuning bio-aerogel properties for controlling theophylline delivery. Part 1: Pectin aerogels. *Materials Science and Engineering: C*, *126*, 112148. https://doi.org/10.1016/J.MSEC.2021.112148

Guimarães, G. C., Júnior, M. C. C., & Rojas, E. E. G. (2009). Density and kinematic viscosity of pectin aqueous solution. *Journal of Chemical and Engineering Data*, *54*(2), 662–667. https://doi.org/10.1021/je800305a

Guo, Z., Ge, X., Yang, L., Gou, Q., Han, L., & Yu, Q. li. (2021). Utilization of watermelon peel as a pectin source and the effect of ultrasound treatment on pectin film properties. *LWT*, *147*, 111569. https://doi.org/10.1016/j.lwt.2021.111569

Gustavsson, J., Cederberg, C., & Sonesson, U. (2011). *Global Food Losses and Food Waste*.

Haas, K. T., Wightman, R., Meyerowitz, E. M., & Peaucelle, A. (2020). Pectin homogalacturonan nanofilament expansion drives morphogenesis in plant epidermal cells. *Science*, *367*(6481), 1003–1007. https://doi.org/10.1126/science.aaz5103

Hartati, I., & Subekti, E. (2015). Microwave assisted extraction of watermelon rind pectin. *International Journal of ChemTech Research*, *8*(11), 163–170.

Hasanin, M. S., & Hashem, A. H. (2020). Eco-friendly, economic fungal universal medium from watermelon peel waste. *Journal of Microbiological Methods*, *168*, 105802. https://doi.org/10.1016/j.mimet.2019.105802

Hortoinfo. (2021). *España es el primer exportador mundial de sandía, delante de México, Italia y Marruecos*. https://www.hortoinfo.es/index.php/10460-exportacion-mundial-sandia-210521

Hu, W., Chen, S., Wu, D., Zhu, K., & Ye, X. (2021). Physicochemical and macromolecule properties of RG-I enriched pectin from citrus wastes by manosonication extraction. *International Journal of Biological Macromolecules*, *176*, 332–341. https://doi.org/10.1016/j.ijbiomac.2021.01.216

Hua, X., Wang, K., Yang, R., Kang, J., & Zhang, J. (2015). Rheological properties of natural low-methoxyl pectin extracted from sunflower head. *Food Hydrocolloids*, *44*, 122–128. https://doi.org/10.1016/j.foodhyd.2014.09.026

Huang, J., Hu, Z., Hu, L., Li, G., Yao, Q., & Hu, Y. (2021). Pectin-based active packaging: A critical review on preparation, physical properties and novel application in food preservation. *Trends in Food Science & Technology*, *118*, 167–178. https://doi.org/10.1016/J.TIFS.2021.09.026

Hwang, I.-W. W., Jeong, M. C., & Chung, S. K. (2011). The Physicochemical Properties and the Antioxidant Activities of Persimmon Peel Powders with Different Particle Sizes. *Journal of the Korean Society for Applied Biological Chemistry*, *54*(3), 442–446. https://doi.org/10.3839/jksabc.2011.068

Idrovo Encalada, A. M., Pérez, C. D., Gerschenson, L. N., Rojas, A. M., & Fissore, E. N. (2019). Gelling pectins from carrot leftovers extracted by industrial-enzymes with

ultrasound pretreatment. *LWT*, *111*, 640–646. https://doi.org/10.1016/j.lwt.2019.05.085

Ishwarya Padma, S., Sandhya, R., & Nisha, P. (2022). Advances and prospects in the food applications of pectin hydrogels. *Critical Reviews in Food Science and Nutrition*, *62*(16), 4393–4417. https://doi.org/10.1080/10408398.2021.1875394

Jafari, F., Khodaiyan, F., Kiani, H., & Hosseini, S. S. (2017). Pectin from carrot pomace: Optimization of extraction and physicochemical properties. *Carbohydrate Polymers*, *157*, 1315–1322. https://doi.org/10.1016/j.carbpol.2016.11.013

Jahromi, M., Niakousari, M., Golmakani, M. T., & Mohammadifar, M. A. (2020). Physicochemical and structural characterization of sodium caseinate based film-forming solutions and edible films as affected by high methoxyl pectin. *International Journal of Biological Macromolecules*, *165*, 1949–1959. https://doi.org/10.1016/J.IJBIOMAC.2020.10.057

Jamsazzadeh Kermani, Z., Shpigelman, A., Pham, H. T. T., van Loey, A. M., & Hendrickx, M. E. (2015). Functional properties of citric acid extracted mango peel pectin as related to its chemical structure. *Food Hydrocolloids*, *44*, 424–434. https://doi.org/10.1016/J.FOODHYD.2014.10.018

Jang, I.-C., Oh, W.-G., Ahn, G.-H., Lee, J.-H., & Lee, S.-C. (2011). Antioxidant Activity of 4 Cultivars of Persimmon Fruit. *Food Sci. Biotechnol*, *20*(1), 71–77. https://doi.org/10.1007/s10068-011-0010-0

Jiang, Y., Xu, Y., Li, F., Li, D., & Huang, Q. (2020). Pectin extracted from persimmon peel: A physicochemical characterization and emulsifying properties evaluation. *Food Hydrocolloids*, *101*(September 2019), 105561. https://doi.org/10.1016/j.foodhyd.2019.105561

Jung, J., & Wicker, L. (2012). Laccase mediated conjugation of sugar beet pectin and the effect on emulsion stability. *Food Hydrocolloids*, *28*(1), 168–173. https://doi.org/10.1016/J.FOODHYD.2011.12.021

Kaczmarek, B. (2020). Tannic Acid with Antiviral and Antibacterial Activity as A Promising Component of Biomaterials—A Minireview. *Materials 2020, Vol. 13, Page 3224*, *13*(14), 3224. https://doi.org/10.3390/MA13143224

Kang, J., Hua, X., Yang, R., Chen, Y., & Yang, H. (2015). *Characterization of natural low-methoxyl pectin from sunflower head extracted by sodium citrate and purified by ultrafiltration*. https://doi.org/10.1016/j.foodchem.2015.02.037

Kastner, H., Einhorn-Stoll, U., & Drusch, S. (2019). Influence of enzymatic and acidic demethoxylation on structure formation in sugar containing citrus pectin gels. *Food Hydrocolloids*, *89*, 207–215. https://doi.org/10.1016/j.foodhyd.2018.10.031

Kawase, M., Motohashi, N., Satoh, K., Sakagami, H., Nakashima, H., Tani, S., Shirataki, Y., Kurihara, T., Spengler, G., Wolfard, K., & Molnár, J. (2003). Biological activity of persimmon (Diospyros kaki) peel extracts. *Phytotherapy Research*, *17*(5), 495–500. https://doi.org/10.1002/ptr.1183

Kazemi, M., Khodaiyan, F., & Hosseini, S. S. (2019). Eggplant peel as a high potential source of high methylated pectin: Ultrasonic extraction optimization and characterization. *LWT*, *105*, 182–189. https://doi.org/10.1016/j.lwt.2019.01.060

Khamsucharit, P., Laohaphatanalert, K., Gavinlertvatana, P., Sriroth, K., & Sangseethong, K. (2018). Characterization of pectin extracted from banana peels of different varieties. *Food Science and Biotechnology*, *27*(3), 623–629. https://doi.org/10.1007/s10068-017-0302-0

Khokhlov, S., & Plugatar, Y. (2016). Chemical composition of persimmon cultivars grown in Crimea. *Acta Horticulturae*, *1139*(1139), 677–681. https://doi.org/10.17660/ActaHortic.2016.1139.116

Kluge, R. A., & Tessmer, M. A. (2018). Caqui— Diospyros kaki. In *Exotic Fruits* (pp. 113–119). https://doi.org/10.1016/b978-0-12-803138-4.00016-2

Kowalska, H., Czajkowska, K., Cichowska, J., & Lenart, A. (2017). What's new in biopotential of fruit and vegetable by-products applied in the food processing industry. *Trends in Food Science & Technology*, *67*, 150–159. https://doi.org/10.1016/J.TIFS.2017.06.016

Kris-Etherton, P. M., Hecker, K. D., Bonanome, A., Coval, S. M., Binkoski, A. E., Hilpert, K. F., Griel, A. E., & Etherton, T. D. (2002). Bioactive compounds in foods: their role in the prevention of cardiovascular disease and cancer. *The American Journal of Medicine*, *113*(9), 71–88. https://doi.org/10.1016/S0002-9343(01)00995-0

Kwon, Y. (2016). Effect of trans–fatty acids on lipid metabolism: Mechanisms for their adverse health effects. *Http://Dx.Doi.Org/10.1080/87559129.2015.1075214*, *32*(3), 323–339. https://doi.org/10.1080/87559129.2015.1075214

Lal, A. M. N., Prince, M. V., Kothakota, A., Pandiselvam, R., Thirumdas, R., Mahanti, N. K., & Sreeja, R. (2021). Pulsed electric field combined with microwave-assisted extraction of pectin polysaccharide from jackfruit waste. *Innovative Food Science & Emerging Technologies*, *74*, 102844. https://doi.org/10.1016/J.IFSET.2021.102844

Lara-Espinoza, C., Carvajal-Millán, E., Balandrán-Quintana, R., López-Franco, Y., & Rascón-Chu, A. (2018). Pectin and pectin-based composite materials: Beyond food texture. In *Molecules* (Vol. 23, Issue 4, p. 942). MDPI AG. https://doi.org/10.3390/molecules23040942

Lau, J. M., McNeil, M., Darvill, A. G., & Albersheim, P. (1987). Treatment of rhamnogalacturonan I with lithium in ethylenediamine. *Carbohydrate Research*, *168*(2), 245–274. https://doi.org/10.1016/0008-6215(87)80029-0

Lee, K. Y., & Choo, W. S. (2020). Extraction Optimization and Physicochemical Properties of Pectin from Watermelon (Citrullus lanatus) Rind: Comparison of

Hydrochloric and Citric acid Extraction. *Journal of Nutraceuticals and Food Science*, *5*(1), 1. https://doi.org/10.36648/nutraceuticals.5.1.1

Lefsih, K., Giacomazza, D., Dahmoune, F., Mangione, M. R., Bulone, D., San Biagio, P. L., Passantino, R., Costa, M. A., Guarrasi, V., & Madani, K. (2017). Pectin from Opuntia ficus indica: Optimization of microwave-assisted extraction and preliminary characterization. *Food Chemistry*, *221*, 91–99. https://doi.org/10.1016/j.foodchem.2016.10.073

Lerouge, P., O'Neill, M. A., Darvill, A. G., & Albersheim, P. (1993). Structural characterization of endo-glycanase-generated oligoglycosyl side chains of rhamnogalacturonan I. *Carbohydrate Research*, *243*(2), 359–371. https://doi.org/10.1016/0008-6215(93)87039-U

Li, D. Q., Du, G. M., Jing, W. W., Li, J. F., Yan, J. Y., & Liu, Z. Y. (2015). Combined effects of independent variables on yield and protein content of pectin extracted from sugar beet pulp by citric acid. *Carbohydrate Polymers*, *129*, 108–114. https://doi.org/10.1016/J.CARBPOL.2015.04.058

Liew, S. Q., Chin, N. L., Yusof, Y. A., & Sowndhararajan, K. (2016). Comparison of Acidic and Enzymatic Pectin Extraction from Passion Fruit Peels and Its Gel Properties. *Journal of Food Process Engineering*, *39*(5), 501–511. https://doi.org/10.1111/jfpe.12243

Lin, D., Zheng, Y., Wang, X., Huang, Y., Ni, L., Chen, X., Wu, Z., Huang, C., Yi, Q., Li, J., Qin, W., Zhang, Q., Chen, H., & Wu, D. (2020). Study on physicochemical properties, antioxidant and antimicrobial activity of okara soluble dietary fiber/sodium carboxymethyl cellulose/thyme essential oil active edible composite films incorporated with pectin. *International Journal of Biological Macromolecules*, *165*, 1241–1249. https://doi.org/10.1016/J.IJBIOMAC.2020.10.005

Liu, Z., Pi, F., Guo, X., Guo, X., & Yu, S. (2019). Characterization of the structural and emulsifying properties of sugar beet pectins obtained by sequential extraction. *Food Hydrocolloids*, *88*, 31–42. https://doi.org/10.1016/J.FOODHYD.2018.09.036

Lucas-González, R., Pellegrini, M., Viuda-Martos, M., Pérez-Álvarez, J. Á., & Fernández-López, J. (2018). Persimmon (Diospyros kaki Thunb.) coproducts as a new ingredient in pork liver pâté: influence on quality properties. *International Journal of Food Science and Technology*, 1232–1239. https://doi.org/10.1111/ijfs.14047

Ma, X., Jing, J., Wang, J., Xu, J., & Hu, Z. (2020). Extraction of Low Methoxyl Pectin from Fresh Sunflower Heads by Subcritical Water Extraction. *ACS Omega*, *5*(25), 15095–15104. https://doi.org/10.1021/ACSOMEGA.0C00928/ASSET/IMAGES/MEDIUM/AO0C00928_M005.GIF

Maeda, H., Akagi, T., & Tao, R. (2018a). Quantitative characterization of fruit shape and its differentiation pattern in diverse persimmon (Diospyros kaki) cultivars. *Scientia Horticulturae*, *228*(October 2017), 41–48. https://doi.org/10.1016/j.scienta.2017.10.006

Maeda, H., Akagi, T., & Tao, R. (2018b). Quantitative characterization of fruit shape and its differentiation pattern in diverse persimmon (Diospyros kaki) cultivars. *Scientia Horticulturae*, *228*(5), 41–48. https://doi.org/10.1016/j.scienta.2017.10.006

Mamet, T., Yao, F., Li, K. kai, & Li, C. mei. (2017). Persimmon tannins enhance the gel properties of high and low methoxyl pectin. *LWT*, *86*, 594–602. https://doi.org/10.1016/j.lwt.2017.08.050

Maneerat, N., Tangsuphoom, N., & Nitithamyong, A. (2017). Effect of extraction condition on properties of pectin from banana peels and its function as fat replacer in salad cream. *Journal of Food Science and Technology*, *54*(2), 386–397. https://doi.org/10.1007/s13197-016-2475-6

Maran, J. P., & Prakash, K. A. (2015). Process variables influence on microwave assisted extraction of pectin from waste Carcia papaya L. peel. *International Journal of Biological Macromolecules*, *73*, 202–206. https://doi.org/10.1016/J.IJBIOMAC.2014.11.008

Maran, J. P., & Priya, B. (2015). Ultrasound-assisted extraction of pectin from sisal waste. *Carbohydrate Polymers*, *115*, 732–738. https://doi.org/10.1016/j.carbpol.2014.07.058

Marić, M., Grassino, A. N., Zhu, Z., Barba, F. J., Brnčić, M., & Rimac Brnčić, S. (2018). An overview of the traditional and innovative approaches for pectin extraction from plant food wastes and by-products: Ultrasound-, microwaves-, and enzyme-assisted extraction. *Trends in Food Science and Technology*, *76*(March), 28–37. https://doi.org/10.1016/j.tifs.2018.03.022

Martinez, J. P., Sasse, F., Brönstrup, M., Diez, J., & Meyerhans, A. (2014). Antiviral drug discovery: broad-spectrum drugs from nature. *Natural Product Reports*, *32*(1), 29–48. https://doi.org/10.1039/C4NP00085D

Martínez-Las Heras, R., Amigo-Sánchez, J. C., Heredia, A., Castelló, M. L., & Andrés, A. (2016). Influence of preharvest treatments to reduce the seasonality of persimmon production on color, texture and antioxidant properties during storage. *CYTA - Journal of Food*, *14*(2), 333–339. https://doi.org/10.1080/19476337.2015.1113204

Martinichen-Herrero, J. C., Carbonero, E. R., Gorin, P. A. J., & Iacomini, M. (2005). Anticoagulant and antithrombotic activity of a sulfate obtained from a glucan component of the lichen Parmotrema mantiqueirense Hale. *Carbohydrate Polymers*, *60*(1), 7–13. https://doi.org/10.1016/J.CARBPOL.2004.11.014

Matheus, J. R. V., Andrade, C. J. de, Miyahira, R. F., & Fai, A. E. C. (2022). Persimmon (Diospyros Kaki L.): Chemical Properties, Bioactive Compounds and Potential Use in the Development of New Products–A Review. In *Food Reviews International* (Vol. 38, Issue 4, pp. 384–401). https://doi.org/10.1080/87559129.2020.1733597

Matheus, J. R. V., de Assis, R. M., Correia, T. R., da Costa Marques, M. R., Leite, M. C. A. M., Pelissari, F. M., Miyahira, R. F., & Fai, A. E. C. (2021). Biodegradable and Edible Film Based on Persimmon (Diospyros kaki L.) Used as a Lid for Minimally Processed Vegetables Packaging. *Food and Bioprocess Technology*, *14*(4), 765–779. https://doi.org/10.1007/S11947-021-02595-1/FIGURES/6

May, C. D. (1990). Industrial pectins: Sources, production and applications. *Carbohydrate Polymers*, *12*(1), 79–99. https://doi.org/10.1016/0144-8617(90)90105-2

McNeil, M., Darvill, A. G., Fry, S. C., & Albersheim, P. (2003). STRUCTURE AND FUNCTION OF THE PRIMARY CELL WALLS OF PLANTS. *Https://Doi.Org/10.1146/Annurev.Bi.53.070184.003205*, *53*, 625–663. https://doi.org/10.1146/ANNUREV.BI.53.070184.003205

Meerasri, J., & Sothornvit, R. (2020). Characterization of bioactive film from pectin incorporated with gamma-aminobutyric acid. *International Journal of Biological Macromolecules*, *147*, 1285–1293. https://doi.org/10.1016/J.IJBIOMAC.2019.10.094

Mellinas, C., Ramos, M., Jiménez, A., & Garrigós, M. C. (2020). Recent trends in the use of pectin from agro-waste residues as a natural-based biopolymer for food packaging applications. In *Materials* (Vol. 13, Issue 3, p. 673). MDPI AG. https://doi.org/10.3390/ma13030673

Mena-García, A., Ruiz-Matute, A. I. I., Soria, A. C. C., & Sanz, M. L. L. (2019). Green techniques for extraction of bioactive carbohydrates. *TrAC Trends in Analytical Chemistry*, *119*, 115612.

Methacanon, P., Krongsin, J., & Gamonpilas, C. (2014). Pomelo (Citrus maxima) pectin: Effects of extraction parameters and its properties. *Food Hydrocolloids*, *35*, 383–391. https://doi.org/10.1016/j.foodhyd.2013.06.018

Mikkonen, K. S., Parikka, K., Ghafar, A., & Tenkanen, M. (2013). *Prospects of polysaccharide aerogels as modern advanced food materials*. *34*(2), 124–136.

Moreira, F. K. V., De Camargo, L. A., Marconcini, J. M., & Mattoso, L. H. C. (2013). Nutraceutically inspired pectin-Mg(OH)2 nanocomposites for bioactive packaging applications. *Journal of Agricultural and Food Chemistry*, *61*(29), 7110–7119. https://doi.org/10.1021/JF402110G/SUPPL_FILE/JF402110G_SI_001.PDF

Mort, A., Zheng, Y., Qiu, F., Nimtz, M., & Bell-Eunice, G. (2008). Structure of xylogalacturonan fragments from watermelon cell-wall pectin. Endopolygalacturonase can accommodate a xylosyl residue on the galacturonic acid just following the hydrolysis site. *Carbohydrate Research*, *343*(7), 1212–1221. https://doi.org/10.1016/j.carres.2008.03.021

Moslemi, M. (2021). Reviewing the recent advances in application of pectin for technical and health promotion purposes: From laboratory to market. *Carbohydrate Polymers*, *254*, 117324. https://doi.org/10.1016/J.CARBPOL.2020.117324

Muda, P., Seymour, G. B., Errington, N., & Tucker, G. A. (1995). Compositional changes in cell wall polymers during mango fruit ripening. *Carbohydrate Polymers*, *26*(4), 255–260. https://doi.org/10.1016/0144-8617(95)00028-6

Munera, S., Aleixos, N., Besada, C., Gómez-Sanchis, J., Salvador, A., Cubero, S., Talens, P., & Blasco, J. (2019). Discrimination of astringent and deastringed hard 'Rojo Brillante' persimmon fruit using a sensory threshold by means of hyperspectral imaging. *Journal of Food Engineering*, *263*, 173–180. https://doi.org/10.1016/j.jfoodeng.2019.06.008

Muñoz-Almagro, N., Montilla, A., & Villamiel, M. (2021). Role of pectin in the current trends towards low-glycaemic food consumption. *Food Research International*, *140*, 109851. https://doi.org/10.1016/J.FOODRES.2020.109851

Muñoz-Almagro, N., Vendrell-Calatayud, M., Méndez-Albiñana, P., Moreno, R., Cano, M. P., & Villamiel, M. (2021). Extraction optimization and structural characterization of pectin from persimmon fruit (Diospyros kaki Thunb. var. Rojo brillante). *Carbohydrate Polymers*, *272*, 118411. https://doi.org/10.1016/J.CARBPOL.2021.118411

Naik, S. N., Goud, V. V., Rout, P. K., & Dalai, A. K. (2010). Production of first and second generation biofuels: A comprehensive review. *Renewable and Sustainable Energy Reviews*, *14*(2), 578–597. https://doi.org/10.1016/J.RSER.2009.10.003

Nakamura, A., Furuta, H., Maeda, H., Takao, T., & Nagamatsu, Y. (2002a). Analysis of the molecular construction of xylogalacturonan isolated from soluble soybean polysaccharides. *Bioscience, Biotechnology and Biochemistry*, *66*(5), 1155–1158. https://doi.org/10.1271/bbb.66.1155

Nakamura, A., Furuta, H., Maeda, H., Takao, T., & Nagamatsu, Y. (2002b). Structural studies by stepwise enzymatic degradation of the main backbone of soybean soluble polysaccharides consisting of galacturonan and rhamnogalacturonan. *Bioscience, Biotechnology and Biochemistry*, *66*(6), 1301–1313. https://doi.org/10.1271/bbb.66.1301

Nascimento, G. E. Do, Simas-Tosin, F. F., Iacomini, M., Gorin, P. A. J., & Cordeiro, L. M. C. (2016). Rheological behavior of high methoxyl pectin from the pulp of tamarillo fruit (Solanum betaceum). *Carbohydrate Polymers*, *139*, 125–130. https://doi.org/10.1016/J.CARBPOL.2015.11.067

Nastasi, J. R., Kontogiorgos, V., Daygon, V. D., & Fitzgerald, M. A. (2022). Pectin-based films and coatings with plant extracts as natural preservatives: A systematic review. *Trends in Food Science & Technology*, *120*, 193–211. https://doi.org/10.1016/J.TIFS.2022.01.014

Ngouémazong, D. E., Christiaens, S., Shpigelman, A., van Loey, A., & Hendrickx, M. (2015). The Emulsifying and Emulsion-Stabilizing Properties of Pectin: A Review.

Comprehensive Reviews in Food Science and Food Safety, *14*(6), 705–718. https://doi.org/10.1111/1541-4337.12160

Ngouémazong, D. E., Kabuye, G., Fraeye, I., Cardinaels, R., van Loey, A., Moldenaers, P., & Hendrickx, M. (2012). Effect of debranching on the rheological properties of Ca2+-pectin gels. *Food Hydrocolloids*, *26*(1), 44–53. https://doi.org/10.1016/j.foodhyd.2011.04.009

Nìmah, L., Makhyarini, I., & Normalina. (2020). Musa acuminata L. (Banana) Peel Wastes as Edible Coating Based on Pectin with Addition of Cinnamomum burmannii Extract. *Asian Journal of Chemistry*, *32*(3), 703–705. https://doi.org/10.14233/AJCHEM.2020.22392

Oakenfull, D., & Scott, A. (1984). Hydrophobic Interaction in the Gelation of High Methoxyl Pectins. *Journal of Food Science*, *49*(4), 1093–1098. https://doi.org/10.1111/j.1365-2621.1984.tb10401.x

Oliveira, T. Í. S., Rosa, M. F., Cavalcante, F. L., Pereira, P. H. F., Moates, G. K., Wellner, N., Mazzetto, S. E., Waldron, K. W., & Azeredo, H. M. C. (2016). Optimization of pectin extraction from banana peels with citric acid by using response surface methodology. *Food Chemistry*, *198*, 113–118. https://doi.org/10.1016/j.foodchem.2015.08.080

Otoni, C. G., Avena-Bustillos, R. J., Azeredo, H. M. C., Lorevice, M. V., Moura, M. R., Mattoso, L. H. C., & McHugh, T. H. (2017). Recent Advances on Edible Films Based on Fruits and Vegetables—A Review. *Comprehensive Reviews in Food Science and Food Safety*, *16*(5), 1151–1169. https://doi.org/10.1111/1541-4337.12281

Ozcelik, B., & Yavuz-Düzgün, M. (2016). Watermelon Juice. In *Handbook of Functional Beverages and Human Health* (pp. 577–586). https://doi.org/10.1201/b19490-51

Pasandide, B., Khodaiyan, F., Mousavi, Z. E., & Hosseini, S. S. (2017). Optimization of aqueous pectin extraction from Citrus medica peel. *Carbohydrate Polymers*, *178*, 27–33. https://doi.org/10.1016/j.carbpol.2017.08.098

Patel, A. R., Cludts, N., Sintang, M. D. Bin, Lesaffer, A., & Dewettinck, K. (2014). Edible oleogels based on water soluble food polymers: Preparation, characterization and potential application. *Food and Function*, *5*(11), 2833–2841. https://doi.org/10.1039/c4fo00624k

Pereira, P. H. F., Oliveira, T. Í. S., Rosa, M. F., Cavalcante, F. L., Moates, G. K., Wellner, N., Waldron, K. W., & Azeredo, H. M. C. (2016). Pectin extraction from pomegranate peels with citric acid. *International Journal of Biological Macromolecules*, *88*, 373–379. https://doi.org/10.1016/j.ijbiomac.2016.03.074

Persson, S., Caffall, K. H., Freshour, G., Hilley, M. T., Bauer, S., Poindexter, P., Hahn, M. G., Mohnen, D., & Somerville, C. (2007). The Arabidopsis irregular xylem8 Mutant Is Deficient in Glucuronoxylan and Homogalacturonan, Which Are Essential for Secondary Cell Wall Integrity. *The Plant Cell*, *19*(1), 237–255. https://doi.org/10.1105/TPC.106.047720

Petersen, B. O., Meier, S., Duus, J., & Clausen, M. H. (2008). Structural characterization of homogalacturonan by NMR spectroscopy—assignment of reference compounds. *Carbohydrate Research*, *343*(16), 2830–2833. https://doi.org/10.1016/J.CARRES.2008.08.016

Petkowicz, C. L. O., Vriesmann, L. C., & Williams, P. A. (2017). Pectins from food waste: Extraction, characterization and properties of watermelon rind pectin. *Food Hydrocolloids*, *65*, 57–67. https://doi.org/10.1016/j.foodhyd.2016.10.040

Pfaltzgraff, L. A., de Bruyn, M., Cooper, E. C., Budarin, V., & Clark, J. H. (2013). Food waste biomass: a resource for high-value chemicals. *Green Chemistry*, *15*(2), 307–314. https://doi.org/10.1039/C2GC36978H

Pinkowska, H., Krzywonos, M., Wolak, P., & Złocinska, A. (2019). Pectin and Neutral Monosaccharides Production during the Simultaneous Hydrothermal Extraction of Waste Biomass from Refining of Sugar—Optimization with the Use of Doehlert Design. *Molecules 2019, Vol. 24, Page 472*, *24*(3), 472. https://doi.org/10.3390/MOLECULES24030472

Powell, D. A., Morris, E. R., Gidley, M. J., & Rees, D. A. (1982). Conformations and interactions of pectins: II. Influence of residue sequence on chain association in calcium pectate gels. *Journal of Molecular Biology*, *155*(4), 517–531. https://doi.org/10.1016/0022-2836(82)90485-5

Preibisch, I., Niemeyer, P., Yusufoglu, Y., Gurikov, P., Milow, B., & Smirnova, I. (2018). Polysaccharide-based aerogel bead production via jet cutting method. *Materials*, *11*(8). https://doi.org/10.3390/ma11081287

Qi, Y., Liu, X., Zhang, Q., Wu, H., Yan, D., Liu, Y., Zhu, X., Ren, X., & Yang, Y. (2019). Carotenoid accumulation and gene expression in fruit skins of three differently colored persimmon cultivars during fruit growth and ripening. *Scientia Horticulturae*, *248*(January), 282–290. https://doi.org/10.1016/j.scienta.2018.12.042

Ralet, M.-C., Dronnet, V., Buchholt, H. C., & Thibault, J.-F. (2001). Enzymatically and chemically de-esterified lime pectins: characterisation, polyelectrolyte behaviour and calcium binding properties. *Carbohydrate Research*, *336*(2), 117–125. https://doi.org/10.1016/S0008-6215(01)00248-8

Reichembach, L. H., & Petkowicz, C. L. O. (2021). Pectins from alternative sources and uses beyond sweets and jellies: An overview. *Food Hydrocolloids*, *118*, 106824. https://doi.org/10.1016/j.foodhyd.2021.106824

Renard, C. M. G. C., Crépeau, M. J., & Thibault, J. F. (1995). Structure of the repeating units in the rhamnogalacturonic backbone of apple, beet and citrus pectins. *Carbohydrate Research*, *275*(1), 155–165. https://doi.org/10.1016/0008-6215(95)00140-O

Renard, C. M. G. C., & Jarvis, M. C. (1999). Acetylation and methylation of homogalacturonans 1: Optimisation of the reaction and characterisation of the products. *Carbohydrate Polymers*, *39*(3), 201–207. https://doi.org/10.1016/S0144-8617(99)00006-5

Richard, P., & Hilditch, S. (2009). d-Galacturonic acid catabolism in microorganisms and its biotechnological relevance. *Applied Microbiology and Biotechnology 2009 82:4*, *82*(4), 597–604. https://doi.org/10.1007/S00253-009-1870-6

Ridley, B. L., O'Neill, M. A., & Mohnen, D. (2001). Pectins: structure, biosynthesis, and oligogalacturonide-related signaling. *Phytochemistry*, *57*(6), 929–967. https://doi.org/10.1016/S0031-9422(01)00113-3

Rodsamran, P., & Sothornvit, R. (2019). Microwave heating extraction of pectin from lime peel: Characterization and properties compared with the conventional heating method. *Food Chemistry*, *278*(November 2018), 364–372. https://doi.org/10.1016/j.foodchem.2018.11.067

Sabater, C., Corzo, N., Olano, A., & Montilla, A. (2018). Enzymatic extraction of pectin from artichoke (Cynara scolymus L.) by-products using Celluclast®1.5L. *Carbohydrate Polymers*, *190*, 43–49. https://doi.org/10.1016/J.CARBPOL.2018.02.055

Sabater, C., Villamiel, M., & Montilla, A. (2022). Integral use of pectin-rich by-products in a biorefinery context: A holistic approach. *Food Hydrocolloids*, *128*, 107564. https://doi.org/10.1016/J.FOODHYD.2022.107564

Sari, A. M., Ishartani, D., & Dewanty, P. S. (2018). Effects of microwave power and irradiation time on pectin extraction from watermelon rinds (Citrullus lanatus) with acetic acid using microwave assisted extraction method. *IOP Conference Series: Earth and Environmental Science*, *102*(1), 012085. https://doi.org/10.1088/1755-1315/102/1/012085

Schmidt, U. S., Schmidt, K., Kurz, T., Endreß, H. U., & Schuchmann, H. P. (2015). Pectins of different origin and their performance in forming andstabilizing oil-in-water-emulsions. *Food Hydrocolloids*, *46*, 59–66. https://doi.org/10.1016/j.foodhyd.2014.12.012

Schmidt, U. S., Schütz, L., & Schuchmann, H. P. (2017). Interfacial and emulsifying properties of citrus pectin: Interaction of pH, ionic strength and degree of esterification. *Food Hydrocolloids*, *62*, 288–298. https://doi.org/10.1016/j.foodhyd.2016.08.016

Schols, H. A., Bakx, E. J., Schipper, D., & Voragen, A. G. J. (1995). A xylogalacturonan subunit present in the modified hairy regions of apple pectin. *Carbohydrate Research*, *279*(C), 265–279. https://doi.org/10.1016/0008-6215(95)00287-1

Schols, H. A., Visser, R. G. F., & Voragen, A. G. J. (2009). Pectins and Pectinases. In H. A. Schols, R. G. F. Visser, & A. G. J. Voragen (Eds.), *Pectins and Pectinases*. Wageningen Academic Publishers. https://doi.org/10.3920/978-90-8686-677-9

Sengkhamparn, N., Sagis, L. M. C., de Vries, R., Schols, H. A., Sajjaanantakul, T., & Voragen, A. G. J. (2010). Physicochemical properties of pectins from okra (Abelmoschus esculentus (L.) Moench). *Food Hydrocolloids*, *24*(1), 35–41. https://doi.org/10.1016/J.FOODHYD.2009.07.007

Seymour, G. B., Colquhoun, I. J., Dupont, M. S., Parsley, K. R., & R. Selvendran, R. (1990). Composition and structural features of cell wall polysaccharides from tomato fruits. *Phytochemistry*, *29*(3), 725–731. https://doi.org/10.1016/0031-9422(90)80008-5

Shafie, M. H., Yusof, R., Samsudin, D., & Gan, C. Y. (2020). Averrhoa bilimbi pectin-based edible films: Effects of the linearity and branching of the pectin on the physicochemical, mechanical, and barrier properties of the films. *International Journal of Biological Macromolecules*, *163*, 1276–1282. https://doi.org/10.1016/J.IJBIOMAC.2020.07.109

Shan, Y. (2016). Comprehensive Utilization of Citrus By-Products. In *Comprehensive Utilization of Citrus By-Products*. Elsevier Inc. https://doi.org/10.1016/C2015-0-05660-X

Siew, C. K., & Williams, P. A. (2008). Role of protein and ferulic acid in the emulsification properties of sugar beet pectin. *Journal of Agricultural and Food Chemistry*, *56*(11), 4164–4171.

Singh, R., Gosewade, S., Ravinder Singh, C., & Kaushik, R. (2018). Bananas as underutilized fruit having huge potential as raw materials for food and non-food processing industries: A brief review. *~ 574 ~ The Pharma Innovation Journal*, *7*(6), 574–580.

Skelhon, T. S., Olsson, P. K. A., Morgan, A. R., & Bon, S. A. F. (2013). High internal phase agar hydrogel dispersions in cocoa butter and chocolate as a route towards reducing fat content. *Food & Function*, *4*(9), 1314–1321. https://doi.org/10.1039/C3FO60122F

Sousa, A. G., Nielsen, H. L., Armagan, I., Larsen, J., & Sørensen, S. O. (2015). The impact of rhamnogalacturonan-I side chain monosaccharides on the rheological properties of citrus pectin. *Food Hydrocolloids*, *47*, 130–139. https://doi.org/10.1016/j.foodhyd.2015.01.013

Ström, A., Ribelles, P., Lundin, L., Norton, I., Morris, E. R., & Williams, M. A. K. (2007). Influence of pectin fine structure on the mechanical properties of calcium-pectin and acid-pectin gels. *Biomacromolecules*, *8*(9), 2668–2674. https://doi.org/10.1021/bm070192r

Sun, L., Ropartz, D., Cui, L., Shi, H., Ralet, M. C., & Zhou, Y. (2019). Structural characterization of rhamnogalacturonan domains from Panax ginseng C. A. Meyer. *Carbohydrate Polymers*, *203*, 119–127. https://doi.org/10.1016/J.CARBPOL.2018.09.045

Takei, T., Sato, M., Ijima, H., & Kawakami, K. (2010). In situ gellable oxidized citrus pectin for localized delivery of anticancer drugs and prevention of homotypic cancer cell aaggregation. *Biomacromolecules*, *11*(12), 3525–3530. https://doi.org/10.1021/BM1010068/ASSET/IMAGES/LARGE/BM-2010-010068_0004.JPEG

Talekar, S., Vijayraghavan, R., Arora, A., & Patti, A. F. (2020). Greener production of low methoxyl pectin via recyclable enzymatic de-esterification using pectin methylesterase cross-linked enzyme aggregates captured from citrus peels. *Food Hydrocolloids*, *108*, 105786. https://doi.org/10.1016/j.foodhyd.2020.105786

Thakur, B. R., Singh, R. K., & Handa, A. K. (1997). Chemistry and Uses of Pectin - A Review. In *Critical Reviews in Food Science and Nutrition* (Vol. 37, Issue 1, pp. 47–73). Taylor & Francis Group. https://doi.org/10.1080/10408399709527767

Torralbo, D. F., Batista, K. A., Di-Medeiros, M. C. B., & Fernandes, K. F. (2012). Extraction and partial characterization of Solanum lycocarpum pectin. *Food Hydrocolloids*, *27*(2), 378–383. https://doi.org/10.1016/J.FOODHYD.2011.10.012

Trigo, J. P., Alexandre, E. M. C., Saraiva, J. A., & Pintado, M. E. (2020). High value-added compounds from fruit and vegetable by-products - Characterization, bioactivities, and application in the development of novel food products. *Critical Reviews in Food Science and Nutrition*, *60*(8), 1388–1416. https://doi.org/10.1080/10408398.2019.1572588

Tursi, A. (2019). A review on biomass: importance, chemistry, classification, and conversion. *Biofuel Research Journal*, *6*(2), 962–979. https://doi.org/10.18331/BRJ2019.6.2.3

Ueda, K., Kawabata, R., Irie, T., Nakai, Y., Tohya, Y., & Sakaguchi, T. (2013). Inactivation of Pathogenic Viruses by Plant-Derived Tannins: Strong Effects of Extracts from Persimmon (Diospyros kaki) on a Broad Range of Viruses. *PLOS ONE*, *8*(1), e55343. https://doi.org/10.1371/JOURNAL.PONE.0055343

Veberic, R., Jurhar, J., Mikulic-Petkovsek, M., Stampar, F., & Schmitzer, V. (2010). Comparative study of primary and secondary metabolites in 11 cultivars of persimmon fruit (Diospyros kaki L.). *Food Chemistry*, *119*(2), 477–483. https://doi.org/10.1016/J.FOODCHEM.2009.06.044

Ventura, I., Jammal, J., & Bianco-Peled, H. (2013). Insights into the nanostructure of low-methoxyl pectin-calcium gels. *Carbohydrate Polymers*, *97*(2), 650–658. https://doi.org/10.1016/j.carbpol.2013.05.055

Verkempinck, S. H. E., Kyomugasho, C., Salvia-Trujillo, L., Denis, S., Bourgeois, M., van Loey, A. M., Hendrickx, M. E., & Grauwet, T. (2018). Emulsion stabilizing properties of citrus pectin and its interactions with conventional emulsifiers in oil-in-water emulsions. *Food Hydrocolloids*, *85*, 144–157. https://doi.org/10.1016/j.foodhyd.2018.07.014

Veronovski, A., Tkalec, G., Knez, Z., Novak, Z., Veronovski, A., Tkalec, G., Knez, Z., & Novak, Z. (2014). Characterisation of biodegradable pectin aerogels and their potential use as drug carriers. *Carbohydrate Polymers*, *113*, 272–278. https://doi.org/10.1016/j.carbpol.2014.06.054

Vincken, J. P., Schols, H. A., Oomen, R. J. F. J., McCann, M. C., Ulvskov, P., Voragen, A. G. J., & Visser, R. G. F. (2003). If homogalacturonan were a side chain of rhamnogalacturonan I. Implications for cell wall architecture. *Plant Physiology*, *132*(4), 1781–1789. https://doi.org/10.1104/pp.103.022350

Voragen, A. G. J. J., Coenen, G.-J. J., Verhoef, R. P., & Schols, H. A. (2009). Pectin, a versatile polysaccharide present in plant cell walls. *Structural Chemistry*, *20*(2), 263–275. https://doi.org/10.1007/s11224-009-9442-z

Vriesmann, L. C., & Petkowicz, C. L. O. (2013). Highly acetylated pectin from cacao pod husks (Theobroma cacao L.) forms gel. *Food Hydrocolloids*, *33*(1), 58–65. https://doi.org/10.1016/J.FOODHYD.2013.02.010

Wandee, Y., Uttapap, D., & Mischnick, P. (2019). Yield and structural composition of pomelo peel pectins extracted under acidic and alkaline conditions. *Food Hydrocolloids*, *87*, 237–244. https://doi.org/10.1016/j.foodhyd.2018.08.017

Wang, C., Qiu, W. Y., Chen, T. T., & Yan, J. K. (2021). Effects of structural and conformational characteristics of citrus pectin on its functional properties. *Food Chemistry*, *339*(September 2020), 128064. https://doi.org/10.1016/j.foodchem.2020.128064

Wang, J., Zhang, Q., Zhang, Z., & Li, Z. (2008). Antioxidant activity of sulfated polysaccharide fractions extracted from Laminaria japonica. *International Journal of Biological Macromolecules*, *42*(2), 127–132. https://doi.org/10.1016/J.IJBIOMAC.2007.10.003

Wang, W., Chen, W., Zou, M., Lv, R., Wang, D., Hou, F., Feng, H., Ma, X., Zhong, J., Ding, T., Ye, X., & Liu, D. (2018). Applications of power ultrasound in oriented modification and degradation of pectin: A review. *Journal of Food Engineering*, *234*, 98–107. https://doi.org/10.1016/j.jfoodeng.2018.04.016

Wang, W., Ma, X., Xu, Y., Cao, Y., Jiang, Z., Ding, T., Ye, X., & Liu, D. (2015). Ultrasound-assisted heating extraction of pectin from grapefruit peel: Optimization and comparison with the conventional method. *Food Chemistry*, *178*, 106–114. https://doi.org/10.1016/J.FOODCHEM.2015.01.080

Willats, W. G. T., McCartney, L., & Knox, J. P. (2001). In-situ analysis of pectic polysaccharides in seed mucilage and at the root surface of Arabidopsis thaliana. *Planta 2001 213:1*, *213*(1), 37–44. https://doi.org/10.1007/S004250000481

Yahia, E. M., & Ornelas-Paz, J. de J. (2009). Chemistry, Stability, and Biological Actions of Carotenoids. In *Fruit and Vegetable Phytochemicals: Chemistry, Nutritional Value, and Stability* (pp. 177–222). https://doi.org/10.1002/9780813809397.ch7

Yang, J., Li, Y., Zheng, Y., Xu, Y., Zheng, Z., Chen, X., & Liu, W. (2019). Versatile Aerogels for Sensors. *Small*, *15*(41), 1902826. https://doi.org/10.1002/SMLL.201902826

Yang, J.-S., Mu, T.-H., & Ma, M.-M. (2019). Optimization of ultrasound-microwave assisted acid extraction of pectin from potato pulp by response surface methodology and its characterization. *Food Chemistry*, *289*, 351–359. https://doi.org/10.1016/J.FOODCHEM.2019.03.027

Yapo, B. M., & Koffi, K. L. (2014). Extraction and characterization of highly gelling low methoxy pectin from cashew apple pomace. *Foods*, *3*(1), 1–12. https://doi.org/10.3390/foods3010001

Yoo, S. K., Kim, J. M., Park, S. K., Kang, J. Y., Han, H. J., Park, H. W., Kim, C. W., Lee, U., & Heo, H. J. (2019). Chemical compositions of different cultivars of astringent persimmon (Diospyros kaki Thunb.) and the effects of maturity. *Korean Journal of Food Science and Technology*, *51*(3), 248–257. https://doi.org/10.9721/KJFST.2019.51.3.248

Yuliarti, O., Matia-Merino, L., Goh, K. K. T., Mawson, J., Williams, M. A. K., & Brennan, C. (2015). Characterization of gold kiwifruit pectin from fruit of different maturities and extraction methods. *Food Chemistry*, *166*, 479–485. https://doi.org/10.1016/J.FOODCHEM.2014.06.055

Zamuz, S., Munekata, P. E. S., Gullón, B., Rocchetti, G., Montesano, D., & Lorenzo, J. M. (2021). Citrullus lanatus as source of bioactive components: An up-to-date review. In *Trends in Food Science and Technology* (Vol. 111, pp. 208–222). Elsevier. https://doi.org/10.1016/j.tifs.2021.03.002

Zhao, S., Malfait, W. J., Guerrero-Alburquerque, N., Koebel, M. M., & Nyström, G. (2018). Biopolymer Aerogels and Foams: Chemistry, Properties, and Applications. *Angewandte Chemie International Edition*, *57*(26), 7580–7608. https://doi.org/10.1002/ANIE.201709014

Zhao, S., Manic, M. S., Ruiz-Gonzalez, F., & Koebel, M. M. (2015). Aerogels. *The Sol-Gel Handbook*, *1–3*, 519–574. https://doi.org/10.1002/9783527670819.CH17

Zhao, S., Ren, W., Gao, W., Tian, G., Zhao, C., Bao, Y., Cui, J., Lian, Y., & Zheng, J. (2020). Effect of mesoscopic structure of citrus pectin on its emulsifying properties: Compactness is more important than size. *Journal of Colloid and Interface Science*, *570*, 80–88. https://doi.org/10.1016/J.JCIS.2020.02.113

Zia, S., Khan, M. R., Shabbir, M. A., & Aadil, R. M. (2021). An update on functional, nutraceutical and industrial applications of watermelon by-products: A comprehensive review. *Trends in Food Science & Technology*, *114*, 275–291. https://doi.org/10.1016/J.TIFS.2021.05.039

II. OBJECTIVES

Objectives

The general objective of the present doctoral thesis was the valorisation of watermelon rinds (*Citrullus lanatus*) and rejected persimmon (*Diospyros kaki Thunb.*) fruits, for obtaining pectin and bioactive extracts of interest for food-related applications.

To achieve this general objective, the following specific objectives were set:

- To **optimize the extraction conditions of pectin from watermelon rinds and persimmon** discards and understand the effect of different factors on the structure-functional relationships.
- To deeply **characterize the physicochemical and technological properties** of the **pectin extracts.**
- To **optimize the extraction conditions of polyphenolic-rich extracts from persimmon discards,** characterize their **functional and bioactive properties** and understand the effect of the extraction conditions on these properties.
- To **evaluate potential technological applications** of watermelon and persimmon pectin in the food area.

These specific objectives were materialized in 7 individual case studies, which have been structured in 2 chapters in this thesis.

Chapter 1. Valorisation of watermelon rind pectin

1.1. Modelling the extraction of pectin towards the valorisation of watermelon rind waste.
1.2. Understanding the different emulsification mechanisms of pectin: Comparison between watermelon rind and two commercial pectin sources.
1.3. Tailoring structural, rheological and gelling properties of watermelon rind pectin by enzymatic treatments.
1.4. Pectin-based aerogel particles for drug delivery: effect of pectin composition on aerogel structure and release properties.

Chapter 2. Valorisation of persimmon fruits.

1.1. Bioactive extracts from persimmon waste: Influence of extraction conditions and ripeness.
1.2. Influence of the extraction conditions on the carbohydrate and phenolic composition of functional pectin from persimmon waste streams.
1.3. Sustainable bioactive pectin-based films to improve fruit safety via a circular economy approach.

III. RESULTS

Results

This section includes the results from 7 individual case studies, which have been structured in 2 chapters:

Chapter I. Valorisation of watermelon rind pectin

1.1. Modelling the Extraction of Pectin towards the Valorisation of Watermelon Rind Waste.

1.2. Understanding the different emulsification mechanisms of pectin: Comparison between watermelon rind and two commercial pectin sources.

1.3. Tailoring structural, rheological and gelling properties of watermelon rind pectin by enzymatic treatments.

1.4. Pectin-based aerogel particles for drug delivery: effect of pectin composition on aerogel structure and release properties.

Chapter II. Valorisation of persimmon fruits.

2.1. Bioactive extracts from persimmon waste: Influence of extraction conditions and ripeness.

2.2. Influence of the extraction conditions on the carbohydrate and phenolic composition of functional pectin from persimmon waste streams.

2.3. Sustainable bioactive pectin-based films to improve fruit safety via a circular economy approach.

Thesis flow chart

Chapter 1.

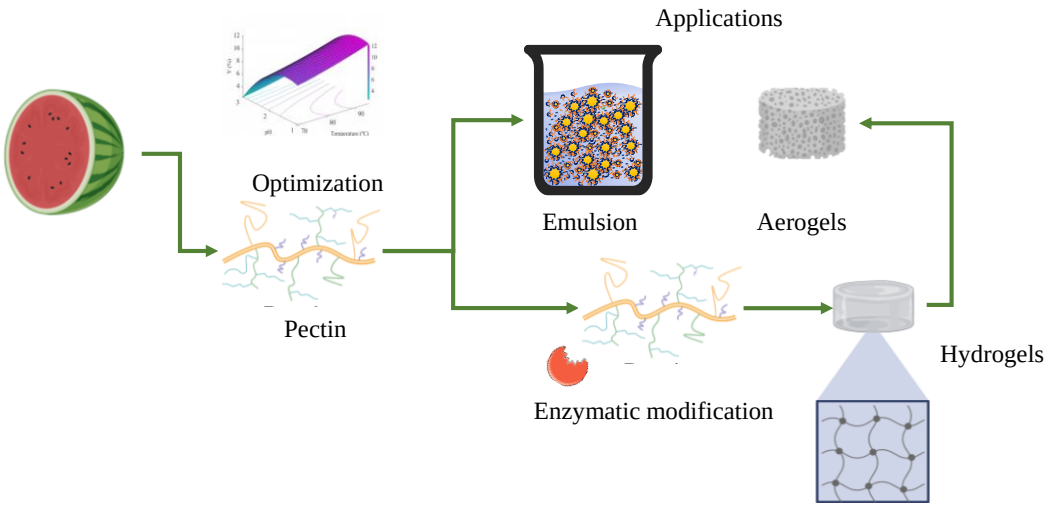

Chapter 2.

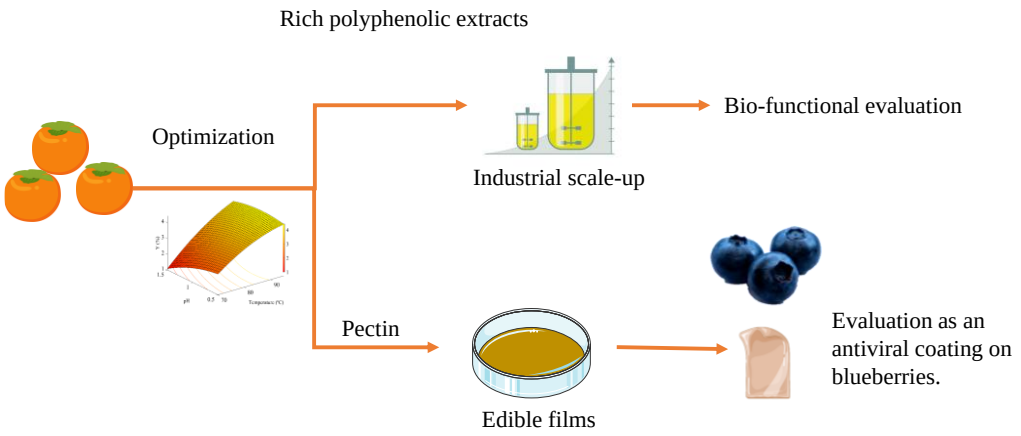

CHAPTER I

VALORISATION OF WATERMELON RIND PECTIN

3.1.1. Modelling the Extraction of Pectin towards the Valorisation of Watermelon Rind Waste

3.1.2. Understanding the different emulsification mechanisms of pectin: Comparison between watermelon rind and two commercial pectin sources.

3.1.3. Tailoring structural, rheological and gelling properties of watermelon rind pectin by enzymatic treatments.

3.1.4. Pectin-based aerogel particles for drug delivery: effect of pectin composition on aerogel structure and release properties.

INTRODUCTION TO CHAPTER 1

Valorisation comprehends the search for new and valuable compounds from biomass waste and their transformation into value-added products. Watermelon residues, such as the rind, are produced worldwide in high amounts and offer the opportunity to obtain different potential exploitable compounds on a large scale. In this regard, pectin, a highly demanded polysaccharide widely used in different industries for its various technological applications, attracted our attention due to its abundance in this waste stream. However, the complex nature of the plant cell wall, the type of extraction process and extraction conditions, influence the final composition and potential technological properties (thickening, viscosity, gelling properties, prebiotic potential, emulsifying properties, or suitability to form oleogels and aerogels, among others). In this sense, knowledge and control of the extraction parameters affecting the desired functionalities is recommendable to improve the final value and promote cost-effectiveness of the products. Likewise, pectin modification can also play a key role in tuning and increasing the range of valorisation strategies, according to market demands.

In the first work, a compositional characterization of the raw material to evaluate potential candidate carbohydrates was carried out. Then, a Box-Behnken experimental design was implemented to investigate how different acid extraction conditions affected the fine composition, chemistry and structure of watermelon rind pectin (WRP).

The interesting structural features of WRP led to the second work, in which its functionality as an emulsifier was tested and compared with two commercial pectin samples (a citrus pectin and an apple pectin). Emulsions prepared at different pectin and oil concentrations were stored, and then the creaming index and oil droplet average sizes within the emulsion were evaluated. Rheological and textural analysis to interpret the interaction between pectin and oil was also assessed. Finally, the microstructure and molecular organization was characterized by SAXS and confocal microscopy. Altogether the results contributed to propose different emulsification mechanisms in all three pectins, depending on the specific structural and compositional features.

Seeking the optimization of the typical thickening/gelling technological application of pectin, the third work includes the development of new modified pectins through enzymatic treatment. Two pectin types with defined structural features, developed according to the mathematical models developed in the first work, were evaluated. Enzymatic treatments aimed at removing the branching sides and/or reduce the degree of esterification to improve the gelation properties. The results evidenced a synergistic effect among the different enzymatic treatments and particular gelling interactions according to the final pectin composition.

The last work consisted in the evaluation of one of the enzymatically modified watermelon rind pectin samples from the previous work (specifically the one with better gelling properties), to produce aerogels as potential drug carrier materials. WRP aerogels were compared with three different commercial pectin aerogels with a low degree of esterification. The study included the characterization of the pectin powder and pectin solutions. Then, hydrogel beads were produced by the dripping method and dried with supercritical CO_2. Finally, an impregnation process and release study was performed using vanillin as a drug model.

3.1.1

MODELLING THE EXTRACTION OF PECTIN TOWARDS THE VALORISATION OF WATERMELON RIND WASTE

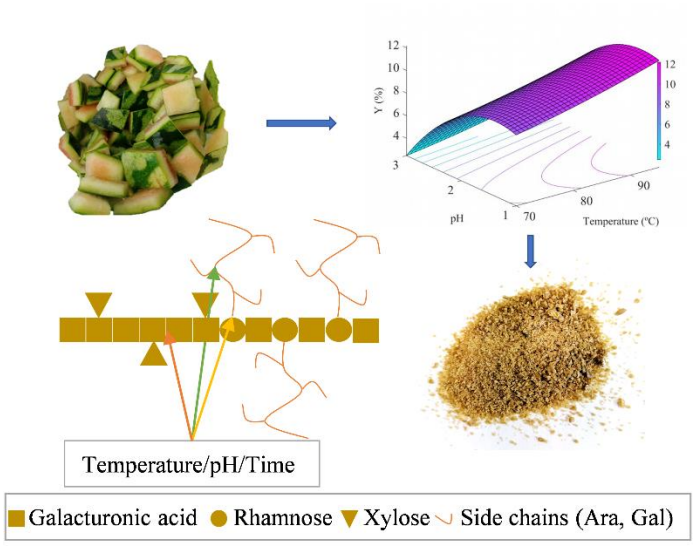

This section is an adapted version of the following published research article:

Méndez, D. A., Fabra, M. J., Gómez-Mascaraque, L., López-Rubio, A., & Martínez-Abad, A. (2021). Modelling the Extraction of Pectin towards the Valorisation of Watermelon Rind Waste. *Foods*, *10*(4), 738.

---

1 Abstract

Watermelon is the second largest fruit crop worldwide, with great potential to valorise its rind waste. An experimental design was used to model how extraction parameters (temperature, pH, and time) impact on the efficiency of the process, purity, esterification degree, monosaccharide composition and molar mass of watermelon rind pectin (WRP), with an insight on changes in their structural properties (linearity, branching degree, extraction severity). The models for all responses were accurately fitted (R^2 >90%, lack of fit $p \geq 0.05$) and experimentally validated. At optimum yield conditions, WRP yield (13.4%), purity (540 µg/g galacturonic acid) and molar mass (106.1 kDa) was comparable to traditional pectin sources, but showed a higher branching degree with longer galactan side chains and a higher protein interaction. Harsher conditions (pH 1) generated purer homogalacturonan fractions with average molar masses (80 kDa) at the expense of yield, while mild extraction conditions (pH≥2) produced highly branched entangled pectin structures. This study underlines novel compositional features in WRP and the possibility of producing novel customized pectin ingredients with a wider potential application scope depending on the targeted structure.

2 Introduction

Around 60% of the total food waste is attributed to agricultural, post-harvesting, processing or distribution, causing significant losses for producers as well as food security and environmental concerns (FAO, 2019). Watermelon (*Citrullus lanatus*) is a fruit with a great economic importance, being the second world's largest fruit crop, with a global production of approximately 103 million tonnes in 2018 (FAOSTAT, 2021). Watermelon rind (WR), which constitutes approximately 30% of the whole fruit, is most often dumped arbitrarily into the environment, raising environmental concerns (Hartati & Subekti, 2015). The valorisation of this waste is limited due the lack of knowledge on possible conversion strategies of potential valuable compounds (Dranca & Oroian, 2018; Gómez et al., 2014).

Pectin is a complex cell wall polysaccharide from plant sources, consisting mainly of homogalacturonan (HG), rhamnogalacturonan-I (RG-I) and minor rhamnogalacturonan-II

(RG-II) and xylogalacturonan (XGA) regions. HG is a homopolymer consisting of α-(1-4)-linked-D-galacturonic acid units (GalA) which can be naturally methylesterified at the C-6 carboxyl group (Dranca & Oroian, 2018). The degree of esterification (DE) governs much of the properties in pectin, where high methoxy (HM) pectin (DE 50–80%) form gels at low pH (2.5-3.5) or in the presence of high amounts of soluble solids such as sucrose (55%) and low methoxy (LM) pectin (DE <50%) can form gels in the presence of divalent cations, and is also more resistant to a wider range of pH than HM pectin (Wai et al., 2009). Rhamnogalacturonan-I (RG-I) is generally composed of a backbone of the repeating disaccharide [→2)- α-L-rhamnopyranose-(1→4)- α-D-GalA-(1→/], sometimes substituted at the O-4 position of the rhamnose residue with neutral sugar side chains of galactose, arabinose, of varying length and composition, producing the so-called "hairy" region with RG-II (Schols et al., 2009).

Pectin has been recognized for its numerous uses as a technological adjuvant in the food industry, as its different structures may lead to different gelling, stabilization, emulsifying properties or sustained release functionalities in complex food matrices (Müller-Maatsch et al., 2016; Wusigale et al., 2020). These properties differ depending on the complexity of the pectin structure, which in turn depend on the source and the extraction parameters. For instance, the presence of branching structures and their entanglement cause an increasing shear rate dependence of viscosity (Methacanon et al., 2014; Ngouémazong, Kabuye, et al., 2012). Also, intermolecular forces and the nature of junction zones at which the polymer molecules are cross-linked, improves the maintenance of network together to form gels with components like divalent cations (Ngouémazong, Kabuye, et al., 2012). Apart from their technological value, the interest in pectins associated with human health benefits has been recently increasing, linked to the effect against diverticular disorders, diabetes, regulation of serum cholesterol and glucose levels, immunological and anticancer properties, also ultimately related to compositional and structural features in pectin (Wusigale et al., 2020; Yapo, 2011).

Currently, sugar beet pulp, citrus albedo and apple pomace are the most common sources used for pectin extraction (Dranca & Oroian, 2018; Pasandide et al., 2017). However, due

to the high demand in the global market and growing interest in valorising side streams to obtain pectins with diverse functional properties, research attention has been given to the composition and extraction from other non-commercial sources, such as broccoli, tomato, carrots (Houben et al., 2011), onion hulls, sour cabbage, sour cucumber, endive roots or pumpkin waste, among many others (Dranca & Oroian, 2018; Müller-Maatsch et al., 2016). The interest in pectin extraction from WR was originally evaluated by Campbell, (2006), who investigated the effect of pH, solid to liquid ratio and different enzyme treatments, amongst others, in pectin yield, degree of methoxylation and galacturonic acid degree. Subsequently, the use of a weak organic and strong acids (Lee & Choo, 2020; Rasheed, 2008) or the effect of microwave-assisted extraction on pectin yields has also been explored (Hartati & Subekti, 2015; Prakash Maran et al., 2014), although previous works did not include a proper pectin characterization. Petkowicz et al., (2017) demonstrated the functional properties of WR pectin using conventional acid extraction, but the structural and functional characterization corresponded to a specific extraction condition (0.1N nitric acid, boiling under reflux during 1h using a solid-liquid ratio of 1:25 (w/v)). There is thus, a lack of information about pectin in WR and how the extraction parameters affect its composition and structure, information of great interest as it will ultimately affect its potential industrial uses.

This study contributes to expand this knowledge with a more comprehensive characterization of WRP, including response surface methodologies to relate how different process parameters (pH, temperature and time) affect these compositional and structural features, optimize process efficiency (pectin yield and purity) to critically discuss valorisation strategies for this waste.

3 Materials and methods

3.1 Sample preparation

Fresh commercial state watermelon (*Citrullus lanatus*) fruits were kindly supplied by Anecoop S. Coop. during the summer season of 2019 from Almeria, Spain. The fruits were processed removing the red part of the fruit and keeping the white rinds, which were

chopped in pieces of 0.5 - 2.5 cm and immersed in 4 volumes of distilled water for 10 min with gentle agitation. After that, the water was drained, and the rinds were freeze-dried. The dried material was milled in liquid nitrogen using an A11 Basic IKA mill (IKA, Staufen, Germany) and stored in desiccators at 0% humidity until used. Citrus and apple pectin (CP and AP, respectively) were used for comparative purposes (Sigma-Aldrich). phenol red (ACS grade), sodium hydroxide (pharma grade) were supplied by Sigma-Aldrich (Stenheim, Germany). Acetone (99%) was from WVR chemicals. N-hexane (>95% purity) and ethanol (96% (v/v), USP grade) were purchased from Panreac Applichem (Darmstadt, Germany). Analytical standards: D-(+)-Galactose CAS:59-23-4, D-(+)-Galacturonic Acid monohydrate CAS:91510-62-2, L-Rhamnose monohydrate CAS: 10030-85-0, D-Glucoronic Acid (GalA) CAS:6556-12-3, D-(+)-Mannose (Man) CAS: 3458-28-4, D-(+)-Glucose (Glu) CAS: 50-99-7, D-(-)-Fructose (Fru) CAS: 57-48-7, L-(-)-Fucose (Fuc) CAS: 2438-80-4, D-(+)-Xylose (Xyl) CAS:58-86-6, L-(+)-Arabinose (Ara) CAS: 5328-37-0 were purchased from (Sigma-Aldrich).

3.2 Proximate analysis

A proximate analysis was made to the watermelon rind. Moisture was determined according to approved method 935.29 (AOAC, 1996). Protein determination was carried out by the Dumas combustion method according to ISO/TS, 16634–2 (2016) and a nitrogen conversion factor of 5.35 (Fujihara et al., 2001). Lipid was measured after Soxhlet extraction according to Somashekar et al., (2001). Ash content was determined according to the standard method TAPPI T211 om-07. Carbohydrates were calculated as the sum of all sugar constituents following the method described in section 2.6. All analyses were done in triplicate.

3.3 Experimental design

The individual and interactive effects of process variables (temperature (70-95 °C, X_1), time (30-90 min; X_2) and pH (1-3; X_3)) over pectin extracted from WR were evaluated. A Box–Behnken response surface experimental design (BBD) with three factors at three levels (Table 1) was chosen, the upper and lower values were selected based on previous literature

(Marić et al., 2018). The experiments were developed in a randomized order with an empirical second-order regression polynomial mathematical model, which exhibits the relationship between response and independent variables. Fifteen experiments were generated with three replications at the centre points (Cep). The generation of the experimental design, analysis of variance (ANOVA), quality of fit (coefficient of determination (R^2)), lack of fit and yield optimization were attained using the software Statgraphics® Centurion, version XVIII (Manugistic, Inc., Rockville, MD, USA). After optimization, validation experiments in triplicate were performed under optimal conditions and compared with predicted values from the models.

3.4 Pectin extraction

Pectin extractions were made with a solid-liquid ratio of 1:20 (w/v) in acidic aqueous solutions, adjusting the pH with a 1 M HCl solution, then heated on a hotplate with magnetic stirring for the selected time. After that, the pectin-based solution was first filtered with a muslin cloth, followed by vacuum filtration using Whatman filter paper n° 4 at 60 °C. The pectin-based solution was mixed with 96% (v/v) ethanol at a ratio of 1:2 (v/v) and left overnight in the freezer. The coagulated pectin was centrifuged at (23450 g for 20 min) and washed with 96% (v/v) ethanol and acetone in consecutive washing cycles, in order to remove water and low molecular weight or polar compounds. The wet pectin was left to dry at 60 °C in a hot air oven until constant weight, then grounded and stored in a desiccator until further analysis. Pectin yield (Y%) was calculated from the following equation:

$$Y(\%) = \frac{m_0}{m} \times 100 \qquad \text{(Eq. 1)}$$

Where m_0 (g) is the weight of dry pectin and m (g) is the weight of dry watermelon rind powder.

Table 1. Box–Behnken experimental design (BBD), coded levels and actual values (in parentheses) of the variables: extraction temperature (X_1, °C); time (X_2, min); pH (X_3). The responses considered were the yield (Y), degree of esterification (DE), anhydrouronic acid content (AUA) and methoxyl content (MeO).

	Independent variables			**Experimental values**			
Run	**X_1 (°C)**	**X_2 (min)**	**X_3 (pH)**	**Y(%)**	**DE (%)**	**AUA(%)**	**MeO (%)**
1	-1 (70)	0 (60)	-1 (1)	6.88	65.47	59.54	6.87
2	+1 (95)	-1 (30)	0 (2)	10.72	75.30	56.92	7.55
3	-1 (70)	+1 (90)	0 (2)	7.55	76.65	55.56	7.51
4	0 (82.5)	-1 (30)	+1 (3)	2.45	87.28	43.22	6.66
5	+1 (95)	0 (60)	-1 (1)	9.95	52.48	69.08	6.39
6	-1 (70)	0 (60)	+1 (3)	2.03	81.04	33.48	4.78
7	0 (82.5)	-1 (30)	-1 (1)	8.50	62.97	66.96	7.43
8	+1 (95)	0 (60)	+1 (3)	4.44	88.25	49.70	7.73
9	+1 (95)	+1 (90)	0 (2)	12.19	76.08	57.29	7.68
10	0 (82.5)	+1 (90)	-1 (1)	10.81	58.98	66.44	6.90
11	-1 (70)	-1 (30)	0 (2)	6.92	76.85	53.60	7.26
12	0 (82.5)	+1 (90)	+1 (3)	3.44	89.05	47.91	7.03
13	0 (82.5)	0 (60)	0 (2)	8.61	78.52	61.32	8.48
14	0 (82.5)	0 (60)	0 (2)	8.04	80.88	63.16	9.00
15	0 (82.5)	0 (60)	0 (2)	7.80	80.83	54.85	7.80
OP	95	90	1.36	13.4	61.62	66.42	6.76
AP	-	-	-	-	77.18	62.17	9.00
CP	-	-	-	-	55.19	69.62	6.78

Y: yield; DE: degree of esterification; MeO: methoxyl content; AUA: anhydrouronic acid content.

3.5 Determination of pectin composition with titrimetric methods.

Methoxyl content (MeO%), anhydrouronic acid (AUA%) and degree of esterification (DE) of extracted pectins were measured according to the method described by Grassino, Brnčić,

et al., (2016). Pectin samples of 0.05 g were weighed and wetted with 0.5 mL of ethanol (96%) and dissolved in 10 mL of a 10% (w/v) sodium chloride solution overnight with magnetic stirring. Two drops of phenol red were added to the dissolved pectin as indicator and the solution was titrated with 0.1 M NaOH. Then, 25 mL of 0.25 M NaOH was added and mixed vigorously to de-esterify pectin and left at room temperature for 30 min. Next, a volume of 25 mL of standardized 0.25 M HCl was added to neutralize NaOH and titrated again with 0.1 M NaOH until colour change. The determinations were performed in triplicate and citrus and apple pectin were used as references.

3.6 Monosaccharide composition

The sugar composition of the extracts was determined after acidic methanolysis as previously described (Martínez-Abad et al., 2018). Freeze-dried samples (1 mg) were incubated with 1 mL of 2 M HCl in dry methanol for 5 h at 100 °C. Samples were then neutralized with pyridine, dried under a stream of air, and further hydrolysed with 2 M trifluoroacetic acid (TFA) at 120 °C for 1 h. The samples were again dried under a stream of air and re-suspended in 1mL milliQ water, filtered (0.22 µm pore size) and injected. The monosaccharides were analysed using high performance anion exchange chromatography with pulsed amperometric detection (HPAEC-PAD) with a ICS-3000 system (Dionex) equipped with a CarboPac PA1 column (4 × 250 mm, Dionex). 10 µl of sample was injected and eluted at a flow rate of 1 mL $min^{-1,}$ and 30°C. Neutral sugars were eluted in water for 16 min with post-column addition of 0.5 mL min^{-1} of 300mM sodium hydroxide after a preconditioning isocratic step with 260mM sodium hydroxide and 68mM sodium acetate (7min) and 5 min equilibration time in water prior to injection. Uronic acids were eluted in the same run with a gradient to 250mM sodium acetate and 250mM sodium hydroxide over 15 additional minutes. Control samples of known concentrations (0-100mg/L; detection limit 0.1mg/L) of mixtures of glucose (Glc), fucose (Fuc), rhamnose (Rha), galactose (Gal), arabinose (Ara), xylose (Xyl), mannose (Man), galacturonic acid (GalA) and glucuronic acid (GlcA) were used for calibration, as prepared from 10mg/mL stock solutions (kept at -20°C until use) and treated analogously. Due to the high lability of fructose (Fru) during methanolysis, the free Fru and Glc were measured using a sucrose, D-fructose and D-

glucose (K-SUFRG) Assay Kit (Megazyme, Bray, Ireland), according to the manufacturer's instructions. All measurements were carried out in triplicate.

3.7 FTIR

FTIR measurements were recorded in transmission mode in a controlled chamber at 21 °C and dry air in order to avoid humidity and CO_2 using a Cary 630 FTIR spectrometer (Agilent, USA). The spectra were taken at 4 cm^{-1} resolution in a wavelength range of 400–4000 cm^{-1} and averaging a minimum of 32 scans. The acquired Spectra were processed using Origin pro 2019 software (OriginLab Corporation, Northampton, MA, USA).

3.8 High performance size exclusion chromatography (HPSEC)

The molar mass (MM) of the pectin extracts was estimated by HPSEC following a previously described method with slight modifications (Gómez-Mascaraque et al., 2019). The HPLC system was equipped with a Waters 2695 separation module, a Waters 2414 refractive index detector (Waters, USA). 0.1 M NaCl (aq.) was used as the mobile phase (Muñoz-Almagro et al., 2018). The samples (1 mg/mL) were dissolved in the mobile phase under magnetic stirring at 40 °C, filtered through 0.8 μm pore syringe filters and injected into an OHpak SB-806 HQ (8 mm x 300 mm) SEC column (Shodex, Japan) equilibrated at 40 °C. The injection volume was 20 μL and the flow rate was 0.5 mL/min. Calibration was performed using P-82 pullulan standards (Shodex, Japan). A deconvolution analysis was made to estimate polydispersity index (PDI). The data were processed and the peaks deconvoluted using Origin pro 2019 software (OriginLab Corporation, Northampton, MA, USA).

4 Results and discussions

4.1 Proximate analysis

The composition of watermelon rind (WR) was first analysed in order to assess its valorisation potential and evaluate the extraction efficiency of different components compared to the starting material. The moisture content of fresh WR (93.3%) was in

agreement with similar studies (Sanwiriya & Suleiman, 2019). Ash content was slightly lower than previously reported values (Al-Sayed & Ahmed, 2013; Sanwiriya & Suleiman, 2019), while protein content was slightly higher (Table 2). These differences might arise from different degrees of ripeness, specific cultivar used, crop condition or method of analysis employed (Al-Sayed & Ahmed, 2013; Sanwiriya & Suleiman, 2019). The main carbohydrate constituents in WR were pectin, cellulose and free sugars (Fru and Glc). Pectin, as the sum of GalA, Rha, Gal, Ara and Fuc, accounted for around 35%, which is higher than previously reported values of 13% (Campbell, 2006), 19-21% (Al-Sayed & Ahmed, 2013). Although GalA content is an internationally recognized indicator for pectin content, other pectins structural neutral sugars, such as the contribution of arabinogalactan can highly differ between pectin sources. These differences are actually very significant in WRP, with >10wt% galactose in the starting material. Pectin composition was therefore mainly ascribed to galacturonan and galactan, with minor fractions of arabinan. The low Rha to Galactose content, suggests longer branching side chains in RG compared to other pectin sources (Houben et al., 2011; Levigne et al., 2002). This could be actually positive, as quality criteria of pectin are ascribed to its rheological properties, linked not only to increased homogalacturonan yield but also reported to be increased with abundance of galactan side chains (Grassino, Halambek, et al., 2016; Mikshina et al., 2017).

Table 2. Composition of watermelon rind.

Proximate analysis	Content (dry basis wt(%))[a]	Monosaccharide composition (μg/mg dry basis)[b]	
Ash	2.55(0.17)	GalA	167.1(7.58)
Fats	1.05(0.15)	Rha	9.2(0.31)
Protein	17.23(0.11)	Gal	111(4.39)
Carbohydrates	83.9(3.45)	Ara	17.1(1.56)
of which		Fuc	11.7(0.29)
Pectin[c]	31.61(1.4)	Xyl	38.8(8.85)
Free sugars[d]	19.47(0.58)	Man	9.6(2.19)
Cellulose[e]	14.28(1.4)	Glu	354.93(45.4)
Others[f]	14.21	Fru	120.2(4.20)

[a] Based on lyophilized WR.
[b] Monosaccharide composition determined by HPAEC-PAD.
[c] Considered as the sum of GalA, Rha, Gal, Ara and Fuc.
[d] Measured with D-fructose and D-glucose (K-SUFRG) Assay Kit.
[e] Estimated as the difference between methanolysis and Saeman hydrolysis detected Glc (Saeman, 1945).
[f] Other sugars not included in the previous groups. Values in brackets correspond to standard deviation.

4.2 Model design and statistical analysis

The solid-liquid ratio (SLR) is an important factor on pectin yield during extraction, some authors reporting the proportional increase of pectin yield with the decrease of solid-liquid ratio, due to higher content surface area between particles and solvent (Pasandide et al., 2018). However, a significant difference on yield for SLR higher than 1:30 (w/v) has not been reported for pectin extraction (Korish, 2015; Pasandide et al., 2018; Prakash Maran et al., 2014). In this study 1:20 (w/v) was selected and fixed for all the treatments developed, based on the good results on pectin yield and purity from watermelon and other fruits (Campbell, 2006; Petkowicz et al., 2017; Prakash Maran et al., 2014; Rodsamran & Sothornvit, 2019), while minimizing solvent use.

Second order polynomial equations including interactive and quadratic terms were employed to generate mathematical models to detect the optimum extraction conditions and express the relationship between process variables and responses. Response variables, all

main significant effects and fitting parameters are shown in Table 3 and all equations are available in suppl. Table S1. The responses evaluated were selected based on the functionality they may confer to pectin. Yield is crucial as a value of extraction efficiency, while degree of esterification (DE), methoxyl content (MeO) and molar mass (MM) are related to thickening, gelling and other rheological properties (Petkowicz et al., 2017). Anhydrouronic acid (AUA) is recognized as a quality factor for pectin extraction, 65% being recommended for food or pharmaceutical additives (Khamsucharit et al., 2018). Moreover, the main carbohydrate constituents of pectin (GalA, Gal, Ara and Rha), were also selected to have an insight on structural changes and due to their influence on the functional properties of pectin (Mao et al., 2019) (Table 3).

Table 3. Main effects of process parameters ((X_1, °C); (X_2, min); (X_3, pH)) and their combinations on the different responses and goodness of fit for the models.

Responses	**Main effects ($p \leq 0.05$)**	**Lack of fit ($p \geq 0.05$)**	**R^2**
Y(%)	X_3, X_3^2, X_1	0.18	97.91
DE(%)	$X_3, X_1X_3, X_3^2, X_1^2$	0.63	99.55
MeO(%)	X_3^2, X_1X_3, X_1^2	0.72	90.24
AUA(%)	X_3	0.54	92.62
MM (kDa)	$X_1, X_3^2, X_1^2, X_2, X_1X_3, X_1X_2, X_2^2$	0.72	99.31
GalA (µg/mg)	X_1, X_3	0.08	94.19
Ara (µg/mg)	$X_3, X_1, X_2, X_1X_3, X_2^2, X_3^2$	0.31	99.60
Xyl (µg/mg)	$X_3, X_1X_2, X_1X_3, X_2X_3, X_3^2$	0.22	98.26
Rha (µg/mg)	X_1, X_3	0.11	95.16
Gal(µg/mg)	X_3	-	65.76

Y: yield; DE: degree of esterification; MeO: methoxyl content; AUA: anhydrouronic acid content; MM: molar mass.

4.3 Effect of extraction parameters on WRP composition and its structural features

4.3.1 Yield

The pectin yields from the different extractions were between 2.1% and 12.2% (Table 1). High yields were thus attained despite starting from a freeze-dried WR sample, which usually hinders wettability, consequently decreasing the pectin yield (Petkowicz et al., 2017). The high yields obtained can be in fact compared to conventional industrial processes of pectin extraction from citrus, apple and sugar beet pectin (25-30, 4.2-19.8, and 15-30%, respectively) (Dranca & Oroian, 2018) and non-conventional pectin sources such as durian rind (2.3-9.3%) (Wai et al., 2009), pumpkin waste (7.4%), passion fruit (10-12.6%), banana peel (9%) or carrot pomace (5-15.2%) (Dranca & Oroian, 2018), or even recent WRP extraction using hydrochloric acid (Lee & Choo, 2020). This evidences a promising potential of WR waste as an alternative cost-effective source of pectin.

The model generated, with a lack of fit test p-value ≥ 0.05, R^2 (97.91), clearly shows a good correlation between the response and the independent variables. Based on the equation parameters (Table 3) and as observed in the 3D-surface plot (Figure S1a), it is evident that extractions conducted at low pH (1-2) have the highest influence on yield, followed by temperature (X_1, *p=0.0012*, X_3, *p=0.0001*). Interestingly, treatment time did not have a significant effect over pectin yield (*p=0.051*).

The positive effect of a low pH is due to hydrolytic attack over the plant cell wall, releasing soluble pectin components (Methacanon et al., 2014). Nevertheless, pH values lower than 1.35 coupled with high temperatures actually reduced yields, as can be noticed for the harshest condition (95 °C, 90 min, pH 1, 9.5%; Table 1). This might be explained by the degradation of polymeric pectin into small molar mass pectin for which the efficiency of alcohol precipitation is reduced (Korish, 2015; Lefsih et al., 2017). On the other hand, increasing pH values above 1.35 gradually decreased the yield due to the inherent recalcitrance and cross-linked character of pectin components within the complex cell wall architecture (Korish, 2015), and aggregation of very high molar mass components slowing down pectin release (Jafari et al., 2017; Moorthy et al., 2015).

The results also indicated that the yield of pectin increased with the effect of high temperature and low pH (Figure S1a, Table 1), probably due to increased solubility of pectin and diffusivity of the solvent into the plant tissue with increasing temperature (Pasandide et al., 2018). Since time did not have a significant effect on yield (*p=0.051*), 30 min was put forward as an effective extraction time to attain relatively high yields.

4.3.2 Pectin esterification.

A quadratic polynomial regression was seen to properly fit the experimental data for DE and MeO, since the lack-of-fit test was insignificant for each of the three parameters. Likewise, R^2 values obtained were all above 90%, pointing out a high reliability of the models. Factors which had a significant influence over both DE and MeO were, as with the yield, the pH, extraction temperature and their interactions (X_3 X_1) (Table 3), in agreement with similar studies on honey dew and sugar beet (Denman & Morris, 2015; Levigne et al., 2002).

The combination of high temperature, long extraction times and a very low pH reduced the DE (Table 1, Figure S1b) due to hydrolytic de-esterification of the HG chains (Jafari et al., 2017; Wai et al., 2009), but still producing HM pectins in all cases, in agreement with WRP extracted at different conditions (Lee & Choo, 2020; Petkowicz et al., 2017). Reported values for the DE vary depending on the type of hydrolytic extraction (e.g. enzymatic vs. acid catalysed or severity of acid extraction), ranging between 38-46% (Campbell, 2006). Although DE and MeO are based on the same titration, the calculation of the DE indicates the ratio of esterified versus non-esterified acid groups regardless of the purity in HG in the sample. A decreased yield of HG (if DE is constant) would thus only affect the MeO. The MeO content in WRP was between 4.8-7.9%, the higher values being similar to those present in commercial AP and CP (7.3 and 9.2% respectively). The lowest degree of MeO (4.7%) was obtained when pectin was extracted at pH 3, for 60 min, at 70 °C (Table 1), because these mild conditions reduced the efficiency of HG extraction (GalA content 199.7 µg/mg; Table 4). On the contrary, the harshest conditions (pH 1, 90 min, at 95 °C) improved HG yield (GalA 672.5 µg/mg; yield 9.95%) but showed also low MeO value, (Table 1; Figure S1c) and the lowest DE (52.48%), again indicating extensive de-esterification (Jafari

et al., 2017; Wai et al., 2009). Other authors have reported MeO values of 5.8-7.6% for tomato peel waste when using an ammonium oxalate buffer (Grassino, Halambek, et al., 2016), and values of 2.2-6.2% for different apple pomace cultivars (Kumar & Chauhan, 2010).

Table 4. Experimental values for neutral sugar (Rha, Ara, Gal, and Xyl) and galacturonic acid (GalA) composition of pectins extracted according to Box-Behnken experimental design.

Run	Fuc (µg/mg)	Rha (µg/mg)	Ara (µg/mg)	Gal (µg/mg)	Xyl (µg/mg)	GalA (µg/mg)
1	3.44(0.21)^{ab}	15.71(0.69)^{f}	9.09(0.65)^{g}	248.49(12.46)^{a}	0(0)^{i}	357.72(15)^{ef}
2	3.35(0.32)^{abc}	17.36(1.77)^{ef}	22.44(2.38^{e}	190.9(20.32)^{bc}	0.46(0.8)^{hi}	442.08(51.95)^{d}
3	3.3(0.3)^{abcd}	16.67(1.13)^{f}	31.49(2.5^{d}	162.4(12.14)^{de}	0.96(0.84)^{ghi}	339.07(30.11)^{f}
4	2.93(0.15)^{bcde}	7.45(0.83)^{ij}	47.31(2.49^{b}	113.02(7.68)^{g}	4.75(0.49)^{b}	254.07(17.53)^{g}
5	1.83(0.19)^{f}	24.65(1.3)^{a}	0(0^{i}	139.04(9.67)^{ef}	2(0.22)^{def}	615.84(54.75)^{a}
6	2.84(0.24)^{cde}	5.67(0.41)^{j}	59.9(4.11)^{a}	121.71(8.44)^{fg}	4.61(0.19)^{b}	199.72(10.97)^{g}
7	3.34(0.12)^{abc}	23.76(0.63)^{ab}	5.71(0.2)^{h}	252.28(7.76)^{a}	0.97(0.85)^{gh}	522.44(3.52)^{bc}
8	2.94(0.3)^{bcde}	10.43(0.88)^{h}	30.4(2.65)^{d}	106.42(12.9)^{gh}	2.32(0.29)^{cd}	368.86(34.65)^{ef}
9	3.33(0.28)^{abc}	19.23(1.54)^{de}	18.65(1.31)^{f}	203.7(18.28)^{b}	1.01(0.87)^{gh}	451.38(39.38)^{d}
10	2.57(0.3)^{e}	22.95(1.97)^{abc}	1.7(1.47)^{i}	211.81(18.38)^{b}	1.05(0.92)^{fgh}	517.28(31.78)^{bc}
11	2.6(0.05)^{e}	13.23(0.19)^{g}	37.64(0.55)^{c}	88.43(1.37)^{h}	2.06(0.06)^{de}	340.74(18.56)^{ef}
12	2.78(0.19)^{de}	8.7(0.67)^{hi}	38.73(2.74)^{c}	109.9(11.78)^{gh}	3.07(0.51)^{c}	333.7(36.41)^{f}
Cep[a]	3.54(0.11)^{a}	16.7(1.32)^{f}	32.82(2.44)^{d}	176.57(12.4)^{cd}	1.52(0.53)^{efg}	386.74(36.4)^{e}
OP[b]	2.51(0.99)^{e}	21.19(0.85)^{cd}	2.26(0.06)^{i}	204.95(5)^{b}	1.9(0.17)^{defg}	540.34(37.02^{b}
AP	1.65(0)^{f}	24.19(0.96)^{ab}	18.47(0.58)^{f}	49.44(1.68)^{i}	14.15(0.76)^{a}	481.97(17.89)^{cd}
CP	0.57(0.21)^{g}	22.27(0.53)^{bc}	19.46(0.71)^{ef}	35.18(1.59)^{i}	3.14(0.1)^{c}	565.91(22.27)^{ab}

[a]Cep. central points.
[b]pectin obtained at optimum yield conditions.
Values in brackets correspond to standard deviation. Means followed by different letters in the same column (a–j) are significantly different ($p \leq 0.05$). Glc, Fru, Man, Fuc and GlcA were not detected or only in trace amounts (<0.5 µg/mg).

4.4 Constituent sugar composition

A quantitative sugar analysis was carried out in order to elucidate the composition of pectin extracted with each treatment condition. Moreover, different sugar ratios (R) were also calculated for each run based on previous literature, as to have an insight on how the

extraction parameters affect the structural complexity of the pectin (Denman & Morris, 2015; Houben et al., 2011; Ognyanov et al., 2018). Table S2 in Suppl. Material summarizes ratios associated with the contribution of branching and its length (RB), the linearity of pectin (RL), the severity of the extraction (RS), or the overall rhamnogalacturonan contribution (RG). The main sugar components were GalA, Gal, Ara, Rha, Xyl and Fuc, in accordance with findings from other authors for carrot or watermelon (Ngouémazong, Kabuye, et al., 2012; Petkowicz et al., 2017). Man, Glc, GlcA and Fru were not detected or only present in trace amounts (≤0.5 μg/mg). The lack of free sugars in the extracts indicates successful removal of non-pectin components (Houben et al., 2011). The contribution of all the models generated for these sugar constituents (GalA, Fuc, Rha, Ara, and Xyl) was significant with R^2 >0.9 (Table 3) and no significant lack of fit, evidencing a very good accuracy of the mathematical models, except for Gal.

4.4.1 Galacturonic acid and homogalacturonan contribution.

The most important sugar constituent in pectin is GalA, being crucial for the thickening or gelling properties. This feature is routinely evaluated for pectin quality as AUA through simple titration, given the lack of significant amounts of any other acid groups in pectin. In this work, both the AUA and the GalA content were compared and introduced in the models (Table 3, Eq. S.6). AUA values were slightly higher than the respective GalA values, fact which may be attributed to the presence of other organic acids or traces of mineral acid from the treatments. The main factors that positively influenced their content were temperature (*p=0.0032*) followed by pH, (*p=0.0009*), the GalA content and AUA varying between 254-615 μg/mg and 33.5-69.1%, respectively (Table 1, Table 4). The mildest conditions showed the lowest AUA and GalA values. This value is consistent with the low MeO, as noted above, supporting the presence of non-pectin components or pectin other than HG or RG. On the contrary, the harshest conditions resulted in high AUA values and higher linearity, as in commercial citrus and apple pectin (see RL ratio in Table S2). The higher purity of HG under these conditions comes at the expense of a slight decrease in the overall yield, as commented on above. Comparable values of AUA were found for dragon fruit 45.2-52.4% (Ismail et al., 2012), apple pomace pectin 70.5% (Kumar & Chauhan, 2010) and tomato peel waste 39.6-52.9% (Grassino, Halambek, et al., 2016; Müller-Maatsch et al., 2016).

4.4.2 Rhamnogalacturonan content

Rha is mainly ascribed to the RG backbone of intercalating [→2)-α -L-Rha-(1→4)- α-D-GalA-(1→/] and its content was, therefore, similarly affected as the GalA content. Temperature (*p=0.017*) and pH (*p=0.0002)* produced a significant increase at harsh conditions, the overall values ranging from 5.6 to 24.6 (µg/mg) (Figure S2b). While Rha contents seems relatively low compared to traditional pectin sources (apple (AP) or citrus pectin (CP) sources, see Table 4), the ratio Rha to GalA is not that different from AP or CP. The lower relative abundance of Rha is a result of higher amounts of Gal and Ara compared to Rha, indicating the presence of longer sugar side chains in RG, as evidenced by high RB ratio (which refers to the side chain length) values compared to AP or CP (cf. Table S2 in Supplementary Material). This evidences that the differences between WR and traditional pectin relies in the composition and extent of the RG rather than in the abundance of RG regions through the pectin backbone. These RB values are also higher than for other alternative pectin sources (3.4-6.3) (Denman & Morris, 2015). Although the traditional "true" gel formation is governed by interaction between HG main chains, the presence of long galactan side chains instead of short-branched RGI regions has been reported to have a positive effect over polymer gelation (Mikshina et al., 2017; Ngouémazong, Kabuye, et al., 2012). In any case, the relative broad range of the branching degree depending on the extraction conditions (RB values 5.6 to 32.0) might be an advantage, as the gelling of pectin could take place either through the long arabinogalactan branched chains (Mikshina et al., 2017; Ngouémazong, Kabuye, et al., 2012), or through the more linear non-methylesterified galacturonic acid chains (Ngouémazong, Tengweh, et al., 2012).

4.4.3 Arabinogalactan, galactan and arabinan content

Ara content in WRP was significantly affected by pH, temperature, time, and the interaction between temperature and pH (Table 3). Its contents were in a range from 0 to 59.9 µg/mg. Pectin extracted at pH 1 showed a significantly lower Ara concentration than that obtained at less aggressive pH 2-3 (see surface plot in Figure S2e in the Supplementary Material),

and a complete degradation of the Ara moieties was observed with the harshest conditions, as indicated by the total Ara content (Table 4), as well as by the different severity factors (RS, Table S2). This is explained by the acid lability, the greatest among all detected sugars, of arabinofuranosyl units (Denman & Morris, 2015). Immunostimulating, anticancer and strong prebiotic activities have been ascribed to the Ara and Gal branching moieties in pectin (Babbar et al., 2016; Yapo, 2011). The good fitting to the model and the correlation to the extraction parameters points out its suitability to target changes in the functional properties of the pectins obtained, fostering the hydrolytic debranching of arabinan and arabinogalactan molecules. The presence of these long-branched chains in pectins has also been correlated with improved emulsifying capacity (Methacanon et al., 2014).

Gal was the most abundant neutral sugar found in all pectin extracts, its concentration ranging from 88.4 to 252.8 μg/mg (Figure S2(d)). Compared with commercial CP and AP, higher amounts were present in most extraction runs indicating a high and long distribution of Gal side chains through WRP, as commented on above and evident from the high values of the RB ratio, related to average size of the branching side chains (see Table S2 in Supplementary Material). Gal content showed nevertheless a low fitting accuracy to the experimental data, and no explicit tendency towards specific conditions was observed. A possible explanation would be the presence of both soluble galactans, not bound to the pectin backbone and easily extracted at mild conditions, as well as of galactans more tightly bound to it. This would explain the presence of significant quantities both at mild or relatively harsh conditions. The only parameter that had an almost significant effect was pH ($p=0.079$), (Eq. S.10 in the Supplementary Material), as Gal readily degraded at very harsh conditions. This is evidenced when looking at the ratio of GalA to Gal, which steadily increased with increasing aggressive conditions, suggesting the presence of galactans not directly linked to the pectin backbone at very mild conditions, mixed galactan and RGI at the centre points, and gradual degradation of Gal at the harshest conditions (Table 4).

4.4.4 Other pectin components

The detection of Xyl suggests the presence of xylogalacturonan regions in pectin, also found in previous studies for watermelon fruit pectin, citrus pectin and carrot pectin (Houben et

al., 2011). An overall low Xyl content was found on all extracts (0-5.39 µg/mg), its content being mainly affected by pH, increasing when pectin was extracted at high pH (Table 4). The mild conditions would foster the preferential extraction of these easier extractable regions at the expense of low yields. However, when harsher conditions (combined low pH and high temperatures) were used (see surface plot in Figure S2a), Xyl content increased again, possibly due to the extraction of some Xyl containing non-pectic polysaccharides, such as xyloglucan (Schols et al., 2009).

Although fucose was not selected for modelling due to its very minor contents (1.8-3.5 µg/mg), it suggests the presence of a small proportion of RG-II (Ognyanov et al., 2018). The highest concentration of Fuc was found at the centre points (Table 4). Its decrease at harsh conditions is probably related to degradation, while the reduced presence at mild conditions is probably related to the low pectin yields, fucose being closely bound to the RG-II regions on the main backbone.

4.5 FTIR

The FTIR spectrum of reference pectins (AP and CP) and two exemplary samples extracts at mild and harsh extraction conditions are presented in Figure 1. The band at 3289 cm^{-1} is mainly ascribed to the hydroxyl groups stretching of water molecules (O-H) in pectin (Lefsih et al., 2017), while the vibrational bands in the range 2850–2919 cm^{-1} can be attributed to the C-H of CH, CH_2 and CH_3 groups (Pasandide et al., 2017). The band at 1746 cm^{-1} is associated to the vibration of the esterified carbonyl group C=O and the band at 1625 cm^{-1} to the free carboxylic groups COO^-, with another one of weaker symmetric vibrating at 1428 cm^{-1} (Pasandide et al., 2017). Both peaks are widely used with regards to the evaluation of the degree of esterification in pectins, which can be estimated as the ratio between the peak area of the band corresponding to the carboxylate esterified group and the sum of both mentioned bands, among other calculation methods (Koh et al., 2018; Kyomugasho et al., 2015). However, for the present samples, peaks related to protein were identified by the weak amide II band at ~1526 cm^{-1} (Chen et al., 2016). Moreover, the broad band centred around 3300 cm^{-1}, also contains contributions from the amide N-H stretching (3540 ~ 3125 cm^{-1}), which causes a sharpening of this band and further evidences the

presence of proteins in the extracts. This causes the vibration band of amide I (~1655 cm^{-1}) to overlap with the bands of interest for DE calculation, and the estimation was not viable (Kyomugasho et al., 2015). A greater protein content is observed at mild extraction conditions compared to harsher conditions giving higher yields or to commercial pectins (CP, AP; Figure 1). Protein content from WRP extracted under optimum conditions to maximize yield (OP; section 3.7) was indeed much higher compared to reference CP and AP pectin (8.9, 2.2 and 1.7% d.w., respectively). This points towards probable protein interaction with AG side chains in the highly branched structures, as suggested previously (Karnik et al., 2016) Although these findings could imply a lower purity of pectin for conventional uses, the presence of small amounts of protein may promote the formation of pectin complexes with interesting emulsifying properties (Chen et al., 2016; Funami et al., 2007). Although further purification treatments to remove proteins is an option, the presence of protein could constitute a valuable factor for WRP extracts with higher versatility for diverse applications. The two strong absorption bands at 1006 and 1079 cm^{-1} are attributed to the glycosidic linkage (C-O and C-C stretching bond) and is typical for backbone vibrations of pectin (Kacuráková et al., 2000; Pasandide et al., 2017). The band at 1077 cm^{-1} can be attributed to neutral Ara-based glycans or RG regions (Kacuráková et al., 2000) and is especially patent noted at less severe (Figure 1) extraction conditions, in agreement with compositional data (Table 4) and RS values (Table S2 in Supplementary Material).

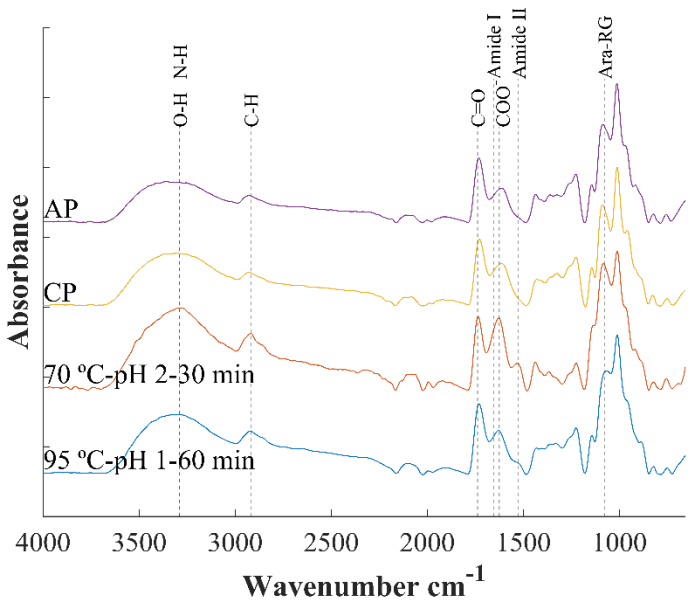

Figure 1. FT-IR spectra of WRP extracted at softer (▬) and harsh (▬) conditions in comparison with commercial apple pectin (AP) and citrus pectin (CP).

4.6 Molar mass distribution

HPSEC was used to study and obtain information about the size and distribution of molar mass (MM) from the different WRP extracts at different conditions, including the WRP sample at the optimized conditions (OP; see section 3.7) and reference pectins (CP and AP) for comparison purposes (Figure 2). The MM distribution of the extracts showed three main peaks, which were different in polydispersity, distribution and signal intensity, mainly depending on temperature and pH (data available in Table S3 of Supplementary Material). Control pectins (AP, CP) showed one single peak, although AP had a broader MM distribution than CP (PDI of 8.9 and 2.0, respectively; Table S3; Figure 2). Likewise, harsh treatments displayed similar MM distribution as in reference pectins (PDI 4.0), associated with higher homogeneity and purity of these pectins. A peak in the low molecular weight region (around 5.9 kDa) was especially patent at either pH 3 or low extraction temperatures, suggesting the preferential extraction of loose or less recalcitrant pectin small fragments (Figure 2, Table S2).

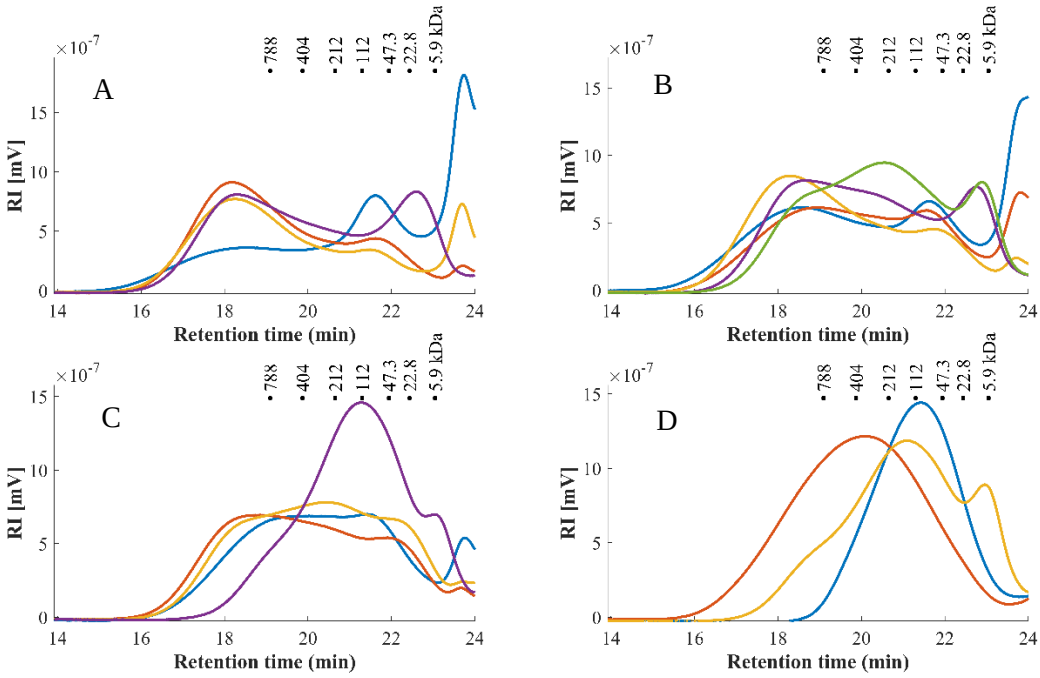

Figure 2. MM distribution of the pectin extractions from WR studied. (A) 70 °C treatment runs: 6 (▬), 3 (▬), 11 (▬), 1 (▬). (B) 82.5 °C treatment runs: 4 (▬), 12 (▬), 13 (▬), 7 (▬), 10(▬). (C) 95 °C treatment runs: 8 (▬), 2(▬), 9 (▬), 5 (▬). (D) citrus pectin (▬), apple pectin (▬) and optimum point condition pectin (▬). For interpretation of the numbers listed, please refer to the Table 1. The black squares correspond to pullulan standards with matching molar mass (MM).

Under milder temperatures (e.g. pH 1, 60 min at 70 °C), higher MM and broader MM distributions (PDI 8.5) suggested the presence of highly branched pectin components, which may be forming agglomerates of different polysaccharide or protein components (Table S2). The presence of other small polydisperse components contributing to agglomeration, such as hemicelluloses, is also feasible (Houben et al., 2011; Koubala et al., 2014).

For pectins extracted at 95 °C, their MM distribution presented a wider dispersity, except at pH 1. At this pH, a different peak close to 112 kDa was observed, this lower MM being similar to CP (Figure 2). This was possibly due to their less branched (or linear) homogalacturonan-based composition (Table 4, Table S2). MM for the harshest and for

optimum point conditions (section 3.7) also showed similar values (106.1 ± 2.7, 87.5 ± 0.8 kDa, respectively) (Table S4).

MM as a response factor for the mathematical model was taken from the average value of the main peak from each extract (Table S3). A very good fit was observed (Table 3), with a significant effect of all factors (time (*p=0.0031*), temperature (*p=0*) and pH (*p=0*)) over MM (Figure S1(d)). The results again evidenced the possibility to target different structures depending on the treatment applied, with either bigger, entangled, or branched structures (higher values of MM and distribution) at mild conditions, or a linear homogeneous pectin with harsher conditions, targeting different pectin functionalities.

4.7 Optimization and Validation

In order to validate the model with an optimized product, the optimum conditions boosting extraction yield were generated (Table 5), resulting in a maximum yield of 13.4%, which corresponded to an extraction temperature of 95 °C, during 90 min and at pH 1.36. Three more extraction conditions and their experimental and theoretical values are presented in supplementary material Table S4 for further comparison. Then, these extraction parameters were experimentally applied and the pectin obtained at these optimum conditions (OP) was characterized for the different responses and compared with the predicted values (Table 5). In most cases, a good correlation between experimental and predicted values was obtained, thus supporting the reliability of the generated models. The amount of pectin extracted at optimum yield point was similar to previously reported results using conventional acid extraction (Lee & Choo, 2020; Petkowicz et al., 2017). OP showed overall values comparable to traditional pectin sources (CP and AP; Table 1). The MM profile in OP was also comparable to CP or AP. On the other hand, the neutral sugar composition of OP showed higher Gal contents (Table 4) and a higher RG-I contribution and branching degree compared to commercial pectins (RG-I values of 9.7, 2.8 and 2.4 for OP, AP and CP, respectively; Table S2).

Table 5. Comparison of experimental and predicted values of different responses parameters of WRP using optimum conditions pectin.

Responses	Experimental value	Model value
Y (%)	13.4(0.05)	13.09
DE (%)	61.55(1.36)	61.19
MeO (%)	6.55(0.81)	6.88
AUA (%)	57.88(2.75)	64.27
MM (kDa)	106.1(2.69)	*-
GalA (µg/mg)	540.34(37.02)	558.19
Ara (µg/mg)	2.26(0.06)	5.37
Fuc (µg/mg)	3.47(0.23)	2.23
Gal (µg/mg)	204.95(5)	165.78
Xyl (µg/mg)	1.71(0.22)	1.77
Rha (µg/mg)	21.19(0.85)	23.5

*MM was not calculated due to peak heterogeneity of the sample measured.
Y: yield; DE: degree of esterification; MeO: methoxyl content; AUA: anhydrouronic acid content; MM: molar mass.

5 Conclusions

WR waste showed relatively high pectin contents (~30%), not recalcitrant to common acid treatments (~13% yield) and increased arabinogalactan side chain contribution compared to common commercial sources like apple (AP) and citrus pectin (CP). A Box-Behnken design was used to accurately model the effect of extraction time, pH and temperature on WRP yield and composition. The broad range of extraction conditions led to pectin with a broad range of esterification degree, molar mass and compositional or structural characteristics, all of which were accurately fitted to the polynomial models. Harshest conditions generated purer homogalacturonan fractions at the expense of yield, while mild extraction conditions (pH ≥ 2) produced highly branched entangled pectin structures. Optimum yield conditions led to more linear pectins with similar molecular mass as commercial AP or CP, but with

significantly higher RG-I, higher branching degree and small protein contents present, pointing towards a significant pectin-protein interaction. These unique structural features suggest that these specific pectins could have a better performance than commercial pectins as emulsifying agents and also having a double functionality as texturisers and stabilizing agents. The study underlines novel compositional features in WRP and how they relate to extraction parameters, offering the possibility of producing novel customized pectin ingredients with a wider potential application scope depending on the targeted structure. Further studies to relate the structural characteristics with the functionality of the different pectins will be conducted to unravel the potential of this new pectin source for the production of food additives.

6 Acknowledgements

This research was funded by the grant RTI-2018-094268-B-C22 (MCI/AEI/FEDER, EU). Mendez D. A. is supported by the Ministry of Science, Technology and Innovation (Minciencias) of the Colombian Government (783-2017). M. J. Fabra and A. Martinez-Abad are recipients of Ramon y Cajal (RYC-2014-158) and Juan de la Cierva (IJDC-2017-31255), respectively, from the Spanish Ministry of Economy, Industry and Competitiveness.

7 References

Al-Sayed, H. M. A., & Ahmed, A. R. (2013). Utilization of watermelon rinds and sharlyn melon peels as a natural source of dietary fiber and antioxidants in cake. *Annals of Agricultural Sciences*, *58*(1), 83–95. https://doi.org/10.1016/j.aoas.2013.01.012

AOAC. (1996). *Official Methods of Analysis* (16th ed.). Maryland: AOAC International.

Babbar, N., Dejonghe, W., Gatti, M., Sforza, S., & Elst, K. (2016). Pectic oligosaccharides from agricultural by-products: production, characterization and health benefits. *Critical Reviews in Biotechnology*, *36*(4), 594–606. https://doi.org/10.3109/07388551.2014.996732

Campbell, M. (2006). *Extraction of Pectin From Watermelon Rind*. Oklahoma State University.

Chen, H., Qiu, S., Gan, J., Liu, Y., Zhu, Q., & Yin, L. (2016). New insights into the functionality of protein to the emulsifying properties of sugar beet pectin. *Food Hydrocolloids*, *57*, 262–270. https://doi.org/10.1016/j.foodhyd.2016.02.005

Denman, L. J., & Morris, G. A. (2015). An experimental design approach to the chemical characterisation of pectin polysaccharides extracted from Cucumis melo Inodorus. *Carbohydrate Polymers*, *117*, 364–369. https://doi.org/10.1016/j.carbpol.2014.09.081

Dranca, F., & Oroian, M. (2018). Extraction, purification and characterization of pectin from alternative sources with potential technological applications. *Food Research International*, *113*(February), 327–350. https://doi.org/10.1016/j.foodres.2018.06.065

FAO. (2019). *The State of Food and Agriculture 2019, Moving forward on food loss and waste reduction*. Food and Agriculture Organization of the United Nations.

FAOSTAT. (2021). *CROPS*. http://www.fao.org/faostat/en/#data/QC/visualize

Fujihara, S., Kasuga, A., & Aoyagi, Y. (2001). Nitrogen-to-Protein Conversion Factors for Common Vegetables in Japan. *Journal of Food Science*, *66*(3), 412–415. https://doi.org/10.1111/j.1365-2621.2001.tb16119.x

Funami, T., Zhang, G., Hiroe, M., Noda, S., Nakauma, M., Asai, I., Cowman, M. K., Al-Assaf, S., & Phillips, G. O. (2007). Effects of the proteinaceous moiety on the emulsifying properties of sugar beet pectin. *Food Hydrocolloids*, *21*(8), 1319–1329. https://doi.org/10.1016/j.foodhyd.2006.10.009

Gómez-Mascaraque, L. G., Martínez-Sanz, M., Hogan, S. A., López-Rubio, A., & Brodkorb, A. (2019). Nano- and microstructural evolution of alginate beads in simulated gastrointestinal fluids. Impact of M/G ratio, molecular weight and pH. *Carbohydrate Polymers*, *223*, 115121. https://doi.org/10.1016/j.carbpol.2019.115121

Gómez, B., Gullón, B., Remoroza, C., Schols, H. A., Parajó, J. C., & Alonso, J. L. (2014). Purification, Characterization, and Prebiotic Properties of Pectic Oligosaccharides from Orange Peel Wastes. *Journal of Agricultural and Food Chemistry*, *62*(40), 9769–9782. https://doi.org/10.1021/jf503475b

Grassino, A. N., Brnčić, M., Vikić-Topić, D., Roca, S., Dent, M., & Brnčić, S. R. (2016). Ultrasound assisted extraction and characterization of pectin from tomato waste. *Food Chemistry*, *198*, 93–100. https://doi.org/10.1016/j.foodchem.2015.11.095

Grassino, A. N., Halambek, J., Djaković, S., Rimac Brnčić, S., Dent, M., & Grabarić, Z. (2016). Utilization of tomato peel waste from canning factory as a potential source for pectin production and application as tin corrosion inhibitor. *Food Hydrocolloids*, *52*, 265–274. https://doi.org/10.1016/j.foodhyd.2015.06.020

Hartati, I., & Subekti, E. (2015). Microwave assisted extraction of watermelon rind pectin. *International Journal of ChemTech Research*, *8*(11), 163–170.

Houben, K., Jolie, R. P., Fraeye, I., Van Loey, A. M., & Hendrickx, M. E. (2011). Comparative study of the cell wall composition of broccoli, carrot, and tomato: Structural characterization of the extractable pectins and hemicelluloses. *Carbohydrate Research*, *346*(9), 1105–1111. https://doi.org/10.1016/j.carres.2011.04.014

Ismail, N. S. M., Ramli, N., Hani, N. M., & Meon, Z. (2012). Extraction and characterization of pectin from dragon fruit (Hylocereus polyrhizus) using various extraction conditions. *Sains Malaysiana*, *41*(1), 41–45.

Jafari, F., Khodaiyan, F., Kiani, H., & Hosseini, S. S. (2017). Pectin from carrot pomace: Optimization of extraction and physicochemical properties. *Carbohydrate Polymers*, *157*, 1315–1322. https://doi.org/10.1016/j.carbpol.2016.11.013

Kacuráková, M., Capek, P., Sasinková, V., Wellner, N., & Ebringerová, A. (2000). FT-IR study of plant cell wall model compounds: Pectic polysaccharides and hemicelluloses.

Carbohydrate Polymers, *43*(2), 195–203. https://doi.org/10.1016/S0144-8617(00)00151-X

Karnik, D., Jung, J., Hawking, S., & Wicker, L. (2016). Sugar beet pectin fractionated using isopropanol differs in galacturonic acid, protein, ferulic acid and surface hydrophobicity. *Food Hydrocolloids*, *60*, 179–185. https://doi.org/10.1016/j.foodhyd.2016.03.037

Khamsucharit, P., Laohaphatanalert, K., Gavinlertvatana, P., Sriroth, K., & Sangseethong, K. (2018). Characterization of pectin extracted from banana peels of different varieties. *Food Science and Biotechnology*, *27*(3), 623–629. https://doi.org/10.1007/s10068-017-0302-0

Koh, J., Xu, Z., & Wicker, L. (2018). Blueberry Pectin Extraction Methods Influence Physico-Chemical Properties. *Journal of Food Science*, *83*(12), 2954–2962. https://doi.org/10.1111/1750-3841.14380

Korish, M. (2015). Potential utilization of Citrullus lanatus var. Colocynthoides waste as a novel source of pectin. *Journal of Food Science and Technology*, *52*(4), 2401–2407. https://doi.org/10.1007/s13197-014-1277-y

Koubala, B. B., Christiaens, S., Kansci, G., Van Loey, A. M., & Hendrickx, M. E. (2014). Isolation and structural characterisation of papaya peel pectin. *Food Research International*, *55*, 215–221. https://doi.org/10.1016/j.foodres.2013.11.009

Kumar, A., & Chauhan, G. S. (2010). Extraction and characterization of pectin from apple pomace and its evaluation as lipase (steapsin) inhibitor. *Carbohydrate Polymers*, *82*(2), 454–459. https://doi.org/10.1016/j.carbpol.2010.05.001

Kyomugasho, C., Christiaens, S., Shpigelman, A., Van Loey, A. M., & Hendrickx, M. E. (2015). FT-IR spectroscopy, a reliable method for routine analysis of the degree of methylesterification of pectin in different fruit- and vegetable-based matrices. *Food Chemistry*, *176*, 82–90. https://doi.org/10.1016/j.foodchem.2014.12.033

Lee, K. Y., & Choo, W. S. (2020). Extraction Optimization and Physicochemical Properties of Pectin from Watermelon (Citrullus lanatus) Rind: Comparison of Hydrochloric and Citric acid Extraction. *Journal of Nutraceuticals and Food Science*, *5*(1), 1. https://doi.org/10.36648/nutraceuticals.5.1.1

Lefsih, K., Giacomazza, D., Dahmoune, F., Mangione, M. R., Bulone, D., San Biagio, P. L., Passantino, R., Costa, M. A., Guarrasi, V., & Madani, K. (2017). Pectin from Opuntia ficus indica: Optimization of microwave-assisted extraction and preliminary characterization. *Food Chemistry*, *221*, 91–99. https://doi.org/10.1016/j.foodchem.2016.10.073

Levigne, S., Ralet, M. C., & Thibault, J. F. (2002). Characterisation of pectins extracted from fresh sugar beet under different conditions using an experimental design. *Carbohydrate Polymers*, *49*(2), 145–153. https://doi.org/10.1016/S0144-8617(01)00314-9

Mao, G., Wu, D., Wei, C., Tao, W., Ye, X., Linhardt, R. J., Orfila, C., & Chen, S. (2019). Reconsidering conventional and innovative methods for pectin extraction from fruit and vegetable waste: Targeting rhamnogalacturonan I. In *Trends in Food Science and Technology* (Vol. 94, pp. 65–78). Elsevier Ltd. https://doi.org/10.1016/j.tifs.2019.11.001

Marić, M., Grassino, A. N., Zhu, Z., Barba, F. J., Brnčić, M., & Rimac Brnčić, S. (2018). An overview of the traditional and innovative approaches for pectin extraction from plant food wastes and by-products: Ultrasound-, microwaves-, and enzyme-assisted extraction. *Trends in Food Science and Technology*, *76*(March), 28–37. https://doi.org/10.1016/j.tifs.2018.03.022

Martínez-Abad, A., Giummarella, N., Lawoko, M., & Vilaplana, F. (2018). Differences in extractability under subcritical water reveal interconnected hemicellulose and lignin recalcitrance in birch hardwoods. *Green Chemistry*, *20*(11), 2534–2546. https://doi.org/10.1039/c8gc00385h

Methacanon, P., Krongsin, J., & Gamonpilas, C. (2014). Pomelo (Citrus maxima) pectin: Effects of extraction parameters and its properties. *Food Hydrocolloids*, *35*, 383–391. https://doi.org/10.1016/j.foodhyd.2013.06.018

Mikshina, P. V., Makshakova, O. N., Petrova, A. A., Gaifullina, I. Z., Idiyatullin, B. Z., Gorshkova, T. A., & Zuev, Y. F. (2017). Gelation of rhamnogalacturonan I is based on galactan side chain interaction and does not involve chemical modifications. *Carbohydrate Polymers*, *171*, 143–151. https://doi.org/10.1016/j.carbpol.2017.05.013

Moorthy, I. G., Maran, J. P., Surya, S. M., Naganyashree, S., & Shivamathi, C. S. (2015). Response surface optimization of ultrasound assisted extraction of pectin from pomegranate peel. *International Journal of Biological Macromolecules*, *72*, 1323–1328. https://doi.org/10.1016/j.ijbiomac.2014.10.037

Müller-Maatsch, J., Bencivenni, M., Caligiani, A., Tedeschi, T., Bruggeman, G., Bosch, M., Petrusan, J., Van Droogenbroeck, B., Elst, K., & Sforza, S. (2016). Pectin content and composition from different food waste streams. *Food Chemistry*, *201*, 37–45. https://doi.org/10.1016/j.foodchem.2016.01.012

Muñoz-Almagro, N., Rico-Rodriguez, F., Villamiel, M., & Montilla, A. (2018). Pectin characterisation using size exclusion chromatography: A comparison of ELS and RI detection. *Food Chemistry*, *252*, 271–276. https://doi.org/10.1016/j.foodchem.2018.01.087

Ngouémazong, D. E., Kabuye, G., Fraeye, I., Cardinaels, R., van Loey, A., Moldenaers, P., & Hendrickx, M. (2012). Effect of debranching on the rheological properties of Ca2+-pectin gels. *Food Hydrocolloids*, *26*(1), 44–53. https://doi.org/10.1016/j.foodhyd.2011.04.009

Ngouémazong, D. E., Tengweh, F. F., Fraeye, I., Duvetter, T., Cardinaels, R., Van Loey, A., Moldenaers, P., & Hendrickx, M. (2012). Effect of de-methylesterification on network development and nature of Ca2+-pectin gels: Towards understanding

structure-function relations of pectin. *Food Hydrocolloids*, *26*(1), 89–98. https://doi.org/10.1016/j.foodhyd.2011.04.002

Ognyanov, M., Georgiev, Y., Petkova, N., Ivanov, I., Vasileva, I., & Kratchanova, M. (2018). Isolation and characterization of pectic polysaccharide fraction from in vitro suspension culture of Fumaria officinalis L. *International Journal of Polymer Science*, *2018*, 1–13. https://doi.org/10.1155/2018/5705036

Pasandide, B., Khodaiyan, F., Mousavi, Z. E., & Hosseini, S. S. (2017). Optimization of aqueous pectin extraction from Citrus medica peel. *Carbohydrate Polymers*, *178*, 27–33. https://doi.org/10.1016/j.carbpol.2017.08.098

Pasandide, B., Khodaiyan, F., Mousavi, Z., & Hosseini, S. S. (2018). Pectin extraction from citron peel: optimization by Box–Behnken response surface design. *Food Science and Biotechnology*, *27*(4), 997–1005. https://doi.org/10.1007/s10068-018-0365-6

Petkowicz, C. L. O., Vriesmann, L. C., & Williams, P. A. (2017). Pectins from food waste: Extraction, characterization and properties of watermelon rind pectin. *Food Hydrocolloids*, *65*, 57–67. https://doi.org/10.1016/j.foodhyd.2016.10.040

Prakash Maran, J., Sivakumar, V., Thirugnanasambandham, K., & Sridhar, R. (2014). Microwave assisted extraction of pectin from waste Citrullus lanatus fruit rinds. *Carbohydrate Polymers*, *101*(1), 786–791. https://doi.org/10.1016/j.carbpol.2013.09.062

Rasheed, A. M. (2008). Effect of Different Acids, Heating Time and Particle Size on Pectin Extraction from Watermelon Rinds. *Journal of Kerbala University*, *6*(4), 234–243.

Rodsamran, P., & Sothornvit, R. (2019). Microwave heating extraction of pectin from lime peel: Characterization and properties compared with the conventional heating method. *Food Chemistry*, *278*(November 2018), 364–372. https://doi.org/10.1016/j.foodchem.2018.11.067

Sanwiriya, P., & Suleiman, N. (2019). The effects of drying method and temperature on the nutritional quality of watermelon rinds. *International Food Research Journal*, *26*(3), 953–958.

Schols, H. A., Visser, R. G. F., & Voragen, A. G. J. (2009). Pectins and Pectinases. In H. A. Schols, R. G. F. Visser, & A. G. J. Voragen (Eds.), *Pectins and Pectinases*. Wageningen Academic Publishers. https://doi.org/10.3920/978-90-8686-677-9

Somashekar, D., Venkateshwaran, G., Srividya, C., Krishnanand, Sambaiah, K., & Lokesh, B. R. (2001). Efficacy of extraction methods for lipid and fatty acid composition from fungal cultures. *World Journal of Microbiology and Biotechnology*, *17*(3), 317–320. https://doi.org/10.1023/A:1016792311744

Wai, W. W., Alkarkhi, A. F. M., & Easa, A. M. (2009). Optimization of pectin extraction from durian rind (durio zibethinus) using response surface methodology. *Journal of Food Science*, *74*(8). https://doi.org/10.1111/j.1750-3841.2009.01331.x

Wusigale, Liang, L., & Luo, Y. (2020). Casein and pectin: Structures, interactions, and applications. In *Trends in Food Science and Technology* (Vol. 97, pp. 391–403). Elsevier Ltd. https://doi.org/10.1016/j.tifs.2020.01.027

Yapo, B. M. (2011). Rhamnogalacturonan-I: A structurally puzzling and functionally versatile polysaccharide from plant cell walls and mucilages. In *Polymer Reviews* (Vol. 51, Issue 4, pp. 391–413). https://doi.org/10.1080/15583724.2011.615962

8 Supplementary material

Table S1. Polynomial equations obtained for the prediction of responses properties for pectin extracted.

$$Y(\%)=8.81 - 0.24816X_1 - 0.11X_2 + 9.51X_3 + 0.002X_1^2 + 0.0005X_1X_2 - 0.013X_1X_3 + 0.0009X_2^2 - 0.011X_2X_3 - 2.68X_3^2 \quad \text{(Eq. 1)}$$

$$DE(\%)=-29.90 + 2.56X_1 - 0.083X_2 - 3.16X_3 - 0.021X_1^2 + 0.0006X_1X_2 + 0.404X_1X_3 - 0.00060X_2^2 + 0.048X_2X_3 - 4.95X_3^2 \quad \text{(Eq. 2)}$$

$$MeO(\%)=-19.99 + 0.68X_1 + 0.016X_2 - 1.32X_3 - 0.0047X_1^2 - 0.00008X_1X_2 + 0.068X_1X - 0.00020X_2^2 + 0.0075X_2X_3 - 1.23X_3^2 \quad \text{(Eq. 3)}$$

$$AUA(\%)=-92.90 + 3.86X_1 + 0.07X_2 - 11.51X_3 - 0.02X_1^2 - 0.0010X_1X_2 + 0.13X_1X_3 - 0.0004X_2^2 + 0.043X_2X_3 - 3.26X_3^2 \quad \text{(Eq. 4)}$$

$$MM\ (kDa)=-23579.3 + 582.54X_1 + 106.43X_2 + 2300.88X_3 - 3.86X_1^2 - 0.86 X_1X_2 + 16.65X_1X_3 - 0.35X_2^2 - 0.54X_2X_3 - 921.90X_3^2 \quad \text{(Eq. 5)}$$

$$GalA\ (\mu g/mg)=-362 + 17.3X_1 - 3.53X_2 - 27 X_3 - 0.047 X_1^2 + 0.0155 X_2^2 + 6.2 X_3^2 + 0.0073 X_1X_2 - 1.78 X_1X_3 + 0.707 X_2X_3 \quad \text{(Eq. 6)}$$

$$Ara\ (\mu g/mg)= -162.3+2.76 X_1 +0.352X_2 +80.62X_3 -0.0158 X_1^2 +0.0004X_1X_2 -0.40 X_1X_3 -0.0035 X_2^2 -0.025X_2X_3 -6.32X_3^2 \quad \text{(Eq. 7)}$$

$$Xyl\ (\mu g/mg)=-28.6+ 0.671X_1 - 0.1049X_2 +5.91X_3 -0.003X_1^2 +0.0015X_1X_2 -0.09X_1X_3+0.000013 X_2^2 -0.015X_2X_3 +1.10X_3^2 \quad \text{(Eq. 8)}$$

$$Rha\ (\mu g/mg)= -53.0 + 1.49X_1 - 0.004X_2 + 6.64X_3 - 0.0063X_1^2 -0.0010X_1X_2 -0.083X_1X_3 + 0.00067X_2^2 + 0.0172X_2X_3 -1.91X_3^2 \quad \text{(Eq. 9)}$$

$$Gal\ (\mu g/mg) = -303 +15.5X_1 +2.64X_2 -203X_3 -0.10X_1^2 + 0.0024 X_2^2 -5.3X_3^2 - 0.040X_1X_2 +1.88 X_1X_3 +0.31X_2X_3 \quad \text{(Eq. 10)}$$

Table S2. Composition ratios and pectin region % based on the mg/mg sample quantifiable neutral sugars and galacturonic acid (Denman & Morris, 2015).

Run	RB [a]	RL [b]	RS [c]	HG %[d]	RG-I %[e]	HG:RG-I
1	16.39	1.30	39.34	34.20	25.79	1.32
2	12.29	1.91	19.69	42.47	21.37	1.98
3	11.62	1.60	10.76	32.23	19.42	1.66
4	21.52	1.47	5.37	24.66	16.04	1.53
5	5.64	3.71	-	59.11	13.95	4.23
6	32.01	1.04	3.33	19.40	18.17	1.06
7	10.85	1.84	91.45	49.86	25.84	1.92
8	13.11	2.46	12.13	35.84	13.70	2.61
9	11.56	1.86	24.19	43.21	22.27	1.94
10	9.30	2.17	304.89	49.43	21.39	2.31
11	9.52	2.41	9.05	32.75	12.63	2.59
12	17.09	2.08	8.61	32.50	14.88	2.18
13	12.25	1.65	13.19	40.95	23.40	1.75
14	12.72	1.63	11.38	35.32	20.48	1.72
15	12.70	1.72	10.80	34.73	19.03	1.82
OP*	9.78	2.37	238.86	51.91	20.76	2.50
AP	2.80	4.39	26.09	45.77	6.84	6.69
CP	2.45	6.98	29.08	54.36	5.50	9.86

*Pectin extracted at optimum yield conditions
[a] A larger value is indicative of larger average size of the branching side chains. (Gal+Ara/Rha).
[b] A larger value suggests of more linear/less branched pectins. (GalA/(Xyl+Rha+Ara+Gal)).
[c] A larger value is indicative of more severe extraction conditions and loss of arabinofuranosyl (Araf) residues. (GalA/Ara).
[d] (GalA-Rha).
[e] (2Rha+Ara+Gal).

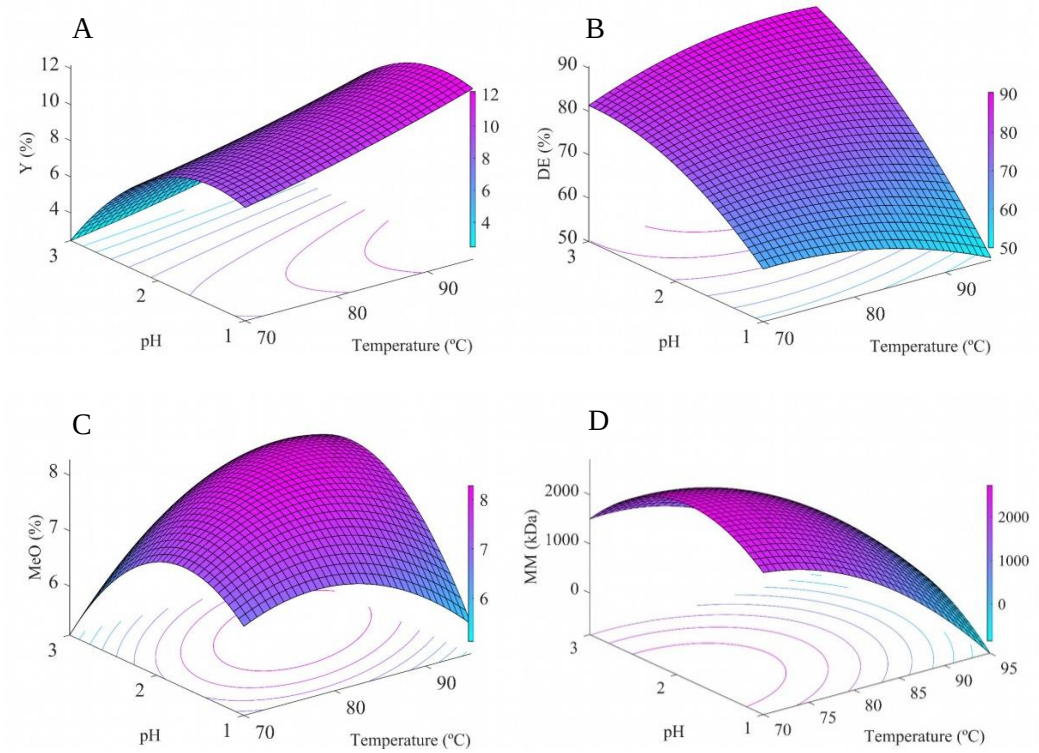

Figure S1. Response surface plot for the effects of temperature and pH with fixed time at 90 min on (A) yield (Y), (B) degree of esterification (DE), (C) methoxy content (MeO) and (D) molar mass (MM) (kDa), of pectin extracted.

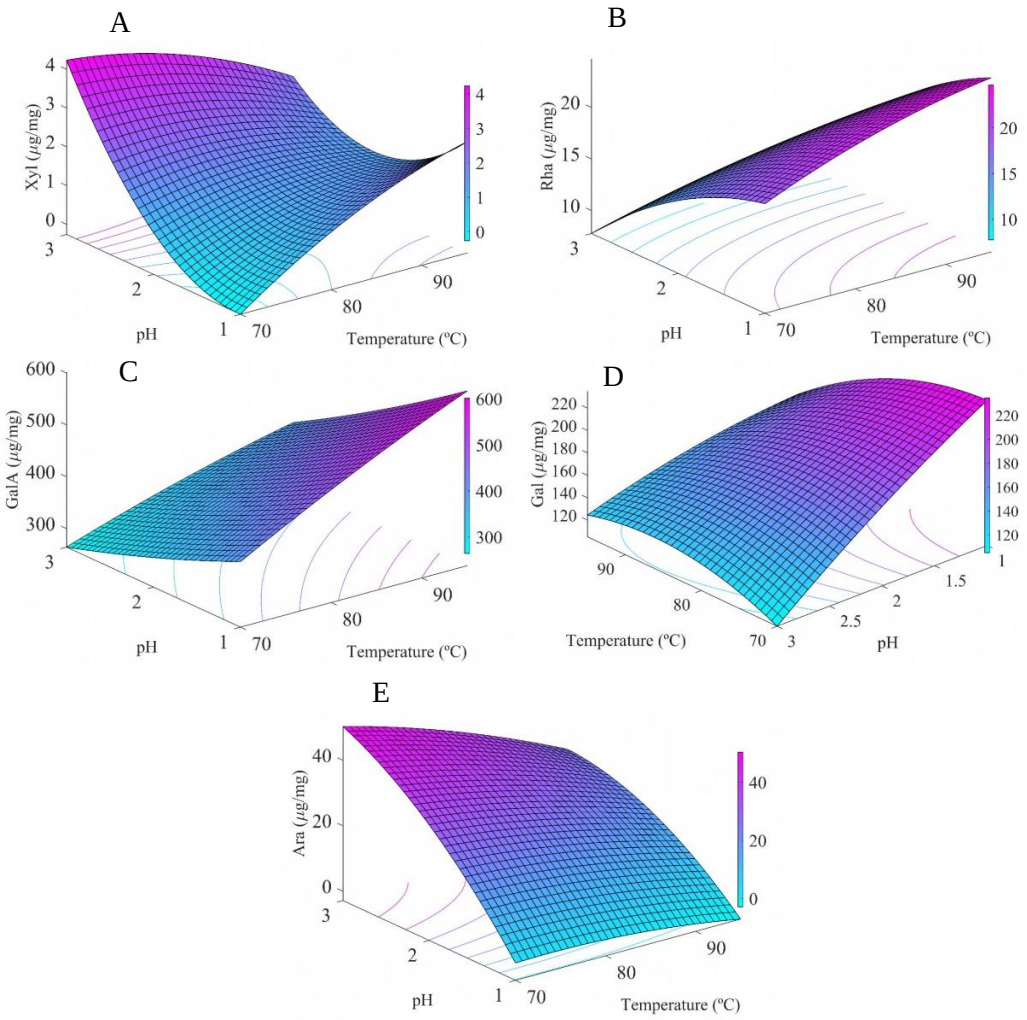

Figure S2. Response surface plot for the effects of temperature and pH with fixed time at 90 min on (A) xylose (Xyl), (B) rhamnose (Rha), (C) galacturonic acid (GalA), (D) galactose (Gal) and (e) arabinose (Ara) (μg/mg) content of pectin extracted.

Table S3. Molar mass (MM) at distinctive highest point, peak area and polydispersity index estimated with mathematical deconvolution calculated from the HPSEC runs evaluated.

	Peak 1			Peak 2			Peak 3		
Run	**MM (kDa)**	**Area %**	PDI	**MM (kDa)**	**Area %**	PDI	**MM (kDa)**	**Area %**	PDI
1	2348.4(65.24)	64(2.8)	8.5	19.94(0.42)	36(2.8)	1.6	0(0)	0(0)	0.0
2	1376.78(76.47)	77(4.1)	2.9	43.80(1.95)	19(4.1)	1.1	5.94(0.17)	3.7(0.2)	1.6
3	2687.38(77.45)	75(0.3)	1.8	59.90(1.51)	21(0.1)	2.6	5.54(0.22)	4.2(0.3)	1.0
4	1665.9(100.85)	50(1.6)	2.7	58.51(0.88)	28(0.7)	1.4	4.15(0.03)	22.2(2)	1.1
5	87.47(0.85)	87(0.8)	4.0	12.02(0.04)	13(0.8)	1.0	12.02(0.04)	12.7(0.8)	0.0
6	1708.41(44.34)	29(1.8)	2.9	58.83(0.15)	37(2.7)	1.5	5.48(0.02)	33.7(1)	1.0
7	1591.16(47.53)	83(14.5)	1.3	16.21(0.34)	25(0)	5.3	0(0)	0(0)	1.1
8	280(61.25)	55(4.2)	2.6	74.76(1.35)	33(2.9)	1.8	5.21(0.18)	11.4(1.8)	1.0
9	223.6(16.53)	76(2.2)	5.1	45.12(12.40)	20(2.3)	1.2	5.63(0.1)	3.2(0.1)	1.5
10	1148.72(114.91)	7(11.4)	1.8	198.79(4.47)	73(11.3)	4.0	14.22(0.11)	20.5(0.3)	1.1
11	2549(71.05)	68(0.3)	1.9	66.42(2.42)	15(0.1)	6.3	5.75(0.04)	16.2(0.2)	1.0
12	1157.93(65.51)	58(0.8)	2.9	63.31(1.28)	27(0.6)	1.7	4.94(0.07)	15(0.8)	1.0
13	2457.1(53.58)	76(0.6)	2.2	52.36(3.12)	20(0.6)	1.9	5.68(0.11)	4.6(0.1)	1.0
14	2678.84(66.55)	78(0.3)	1.9	55.52(2.15)	22(0.3)	9.5	0(0)	0(0)	1.0
15	2758.71(82.56)	77(0.1)	2.3	59.56(3.80)	18(0.3)	1.3	5.22(0.05)	5(0.1)	1.3
OP*	106.11(2.70)	79(0.3)	6.1	13.11(0.11)	21(0.3)	1.0	0(0)	0(0)	0.0
AP	339.4(11.4)	100(0)	8.9	0(0)	0(0)	0.0	0(0)	0(0)	0.0
CP	77.84(3.80)	100(0)	2.0	0(0)	0(0)	0.0	0(0)	0(0)	0.0

*Pectin extracted at optimum yield parameters (temp. 95 °C, pH 1.35 and time 90 min).

3.1.2

UNDERSTANDING THE DIFFERENT EMULSIFICATION MECHANISMS OF PECTIN: COMPARISON BETWEEN WATERMELON RIND AND TWO COMMERCIAL PECTIN SOURCES.

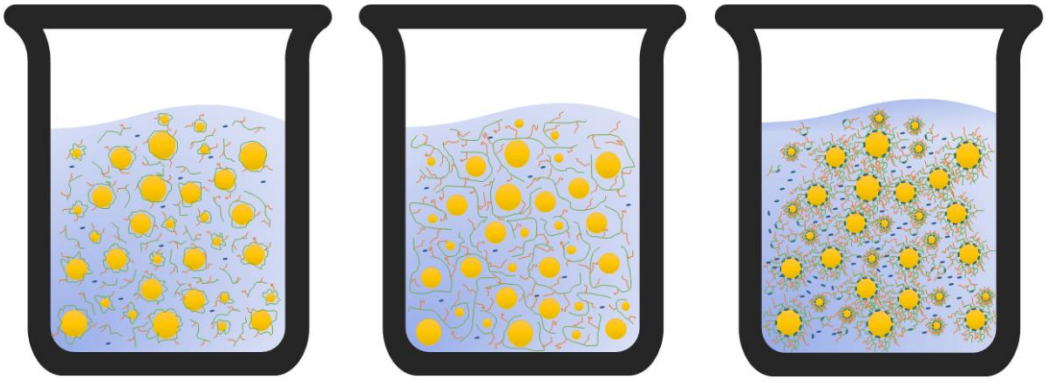

This section is an adapted version of the following published research article:

Méndez, D. A., Fabra, M. J., Martínez-Abad, A., Martínez-Sanz, Gorria, M., & López-Rubio, A. (2021). Understanding the different emulsification mechanisms of pectin: Comparison between watermelon rind and two commercial pectin sources. Food Hydrocolloids, 120, 106957.

---

1 Abstract

In this work, an advanced approach combining small angle X-ray scattering (SAXS) experiments, rheology and confocal laser scanning microscopy was used to explain the different emulsification mechanisms of three pectin sources (pectin extracted from watermelon rind -WRP- and commercial citrus -CP- and apple pectin -AP-). Very interestingly, three different emulsification mechanisms were identified, related to the structure and composition of the pectin extracts. WRP had significantly greater emulsifying capacity than commercial CP and AP. This enhanced emulsification ability was mainly ascribed to a combination of its relatively high protein content (mainly acting as the surface-active material), combined with the presence of longer sugar side chains in pectin, further contributing to stabilizing the oil droplets in the emulsions. All these structural features resulted in a reduction in the mean droplet size as the concentration increased, thus, hindering flocculation and coalescence during the short-term storage conditions at 4 °C. In contrast, AP had the lowest emulsification capacity, which was only related to its viscosifying effect (provided by its greater Mw), while CP, having the greatest homogalacturonan content, greatest linearity and a more balanced hydrophilic/ hydrophobic character (reflected in the degree of esterification), was able to form a better adsorbed layer at the o/w interphase, although it could not avoid flocculation and creaming at low pectin concentration during refrigerated storage.

2 Introduction

Pectin is a natural complex heteropolysaccharide extracted from plant cell walls, which can be currently found in multiple food, cosmetic, pharmaceutical and nutraceutical products, contributing to relevant technological and functional attributes, like fibre enrichment or rheology control (Ciriminna et al., 2015). It is a complex mixture of blocks of homogalacturonan (HG), the so-called “smooth region” and rhamnogalacturonan I (RG-I) and II (RG-II), constituting the “hairy regions” and having a greater degree of chemical complexity. The backbone of pectin is mainly composed of D-galacturonic acid (GalA) units connected by α-1,4-glucoside bonds which can be naturally methylesterified at the C-

6 carboxyl group (Prasanna et al., 2007; Schols et al., 2009; Schols & Voragen, 2003; Voragen et al., 2009). While commercial pectin are classified according to their methoxyl content and gel-forming rate (Ciriminna et al., 2017), the structural complexity of these polysaccharides, which depend on a number of factors like source or extraction conditions, define their properties, thus making it a very versatile natural polymer (Denman & Morris, 2015; Dranca & Oroian, 2018; Méndez et al., 2021).

Although most commercial pectin are extracted with mineral acids from citrus peels or apple pomace (waste materials from juice industries), other fruit waste materials have been investigated for pectin extraction, like banana peels (Oliveira et al., 2016), grape pomace (Minjares-Fuentes et al., 2014) or watermelon rinds (Campbell, 2006). Specifically, this last waste material can be envisaged as a highly promising pectin source, not only because of the economic importance of the crop, being the second world's largest fruit in terms of volume with around 100 million tons produced in 2019 (FAOSTAT, 2021) and constituting the rind about one third of the fruit, but also because of the good pectin yields obtained (Jiang et al., 2012; Lee & Choo, 2020; Petkowicz et al., 2017) and interesting structural features of the extracted pectin and related functional properties (Petkowicz et al., 2017).

The role of pectin as emulsifying agent has gained more attention in recent years, as apart from the obvious technological implications for many products, it can also have advantages from a nutritional viewpoint, having the European Food Standards Agency (EFSA) substantiated that at least 6 g of pectin daily consumed contribute towards the maintenance of normal blood cholesterol (Agostoni et al., 2010). In fact, it has been demonstrated that pectin is able to reduce lipid digestion rate and extent (Zhai et al., 2021), being lipolysis a potential factor contributing to blood lipid levels.

The emulsifying properties of pectin are mainly ascribed to the hydrophobic moieties in the pectin structure such as the methoxyl and acetyl groups, which abundance highly depend on the biomass source and extraction conditions (Wai et al., 2010).

The heterogeneity of neutral sugar branch chains, the presence of proteinaceous materials covalently linked to the side chains, ferulic acid, methoxyl or acetyl esterification and the

molecular weight also have a significant incidence on the balance of hydrophobic and hydrophilic regions and, thus, on the emulsifying properties of pectin (Fan et al., 2020; Nakauma et al., 2008). Currently, the most widely studied pectin regarding its emulsion capacity has been sugar beet pectin. Its remarkable proteinaceous content has been linked to a reduction in oil droplet size and improved emulsion stability. Proteins tend to act as anchor molecules for pectin in the oil phase, by adsorbing at the oil-water interface, decreasing the interfacial tension between water and oil (Funami et al., 2007, 2011; Nakauma et al., 2008; Schmidt et al., 2015).

In a recent work, pectin extraction from watermelon rinds was modelled and optimized in terms of yield, and its structural characterization pointed out to longer sugar side chains when compared with commercial citrus or apple pectin (Méndez et al., 2021). The presence of long branched chains in pectin has been correlated with improved emulsifying properties (Ngouémazong et al., 2015) and, in fact, acid-extracted watermelon rind pectin (WRP) has shown emulsion capacity similar to Arabic gum, a polysaccharide well-known for its emulsifying properties (Petkowicz et al., 2017). However, the mechanism for emulsion stabilization remains unknown and the emulsification potential of this novel pectin source for high oil concentration in comparison with commercial pectin also deserves to be studied to gain further insight for potential industrial applications.

Therefore, the aims of the present work were to (i) compare the emulsifying properties of WRP in comparison with apple pectin (AP) and citrus pectin (CP) as main market drivers during a short-term storage (ii) characterize the micro- and nanostructure and the rheological properties of the developed emulsions; and (iii) understand the main mechanisms for emulsion stabilization of the WRP pectin in relation with its structural features.

3 Materials and methods

3.1 Sample preparation

Fresh watermelon (*Citrullus lanatus*) fruits were kindly supplied by Anecoop S. Coop. during the summer season of 2019 from Almeria, Spain. The fruits were processed removing the red flesh and keeping the white rinds, which were later used for pectin extraction. The rinds were initially chopped in pieces of 0.5 – 2.5 cm and immersed in distilled water for 10 min with gentle agitation and, after draining the water, they were freeze-dried to keep them stable before pectin extraction. Citrus and apple pectin (CP and AP, respectively obtained from Sigma-Aldrich) were used for comparative purposes. Sunflower oil (SO) was obtained from a local supermarket.

3.2 Pectin extraction

Pectin extraction from WR was carried out following the optimal extraction conditions previously established (Méndez et al., 2021). Briefly, the ground WR was immersed in water acidified at pH 1.35 with a 1M HCl solution, with a solid-liquid ratio of 1:20 (w/v), and it was heated on a hotplate with magnetic stirring for 90 min at 95 °C. Subsequently, the extracted solution was filtered with a muslin cloth, followed by vacuum filtration using Whatman filter paper No. 4 at 60 °C and mixed with 96% (v/v) ethanol at a 1:2 (v/v) ratio and left overnight in the freezer. The coagulated pectin (WRP) was centrifuged at 23450 g for 20 min and consecutively washed with 96% (v/v) ethanol and acetone several times to remove water and low molecular weight or polar compounds. Finally, the material was dried at 60 °C in a hot air oven until constant weight, then grounded and stored in a desiccator until further analysis.

3.3 Pectin characterization

Methoxyl content (MeO%) and degree of esterification (DE) of extracted pectin were measured according to the method described by Grassino et al., (2016). Protein determination was carried out by the Dumas combustion method according to ISO/TS, 16634-2 (2016) and a nitrogen conversion factor of 6.25. The molecular weight of the pectin

was estimated by HPSEC as described in (Méndez et al., 2021). The sugar composition of the extracts was determined by high-performance anion exchange chromatography with pulsed amperometric detection (HPAEC-PAD) after acidic methanolysis as previously described (Martínez-Abad et al., 2018). Due the high lability of fructose (Fru) during methanolysis, the free Fru and Glc were measured using a sucrose, D-fructose and D-glucose (K-SUFRG) Assay Kit (Megazyme, Bray, Ireland), according to the manufacturers instructions. All measurements were carried out in triplicate.

3.4 Preparation of pectin solutions and emulsions

Pectin solutions (1.5 and 3.5% (w/v)) were prepared by dissolving weighed amounts of powdered samples of the extracted watermelon rind pectin (WRP) and the two commercial citrus and apple pectin (CP and AP, respectively) were solubilized into deionized water for 16 h at 25 °C with pH maintained in a range between (2.6–3.4).

Oil-in-water emulsions were obtained by dispersing 1 mL of SO each 30 seconds, using a high-speed homogenization equipment (Ultra-Turrax, MICCRA D-9 Homogenizer, IKA, Müllheim, Germany), until reaching a final oil concentration of 35% (v/v) or 60% (v/v). Samples' nomenclature was “xP- ySO’ where ‘x’ refers to the pectin solution concentration, “P” indicates pectin type (AP, CP or WRP) and “y” refers to the SO concentration.

3.5 Emulsion Microstructural Characterization

The microstructure of the O/W emulsions was studied using both optical microscopy and confocal laser scanning microscopy following the method reported by (Tang & Ghosh, 2020). Fluorescence images of the emulsions were characterized using a FV 1000-IX81 confocal laser scanning microscope (CLSM, Olympus, Japan) with a combination of 559 nm and 635 nm excitation wavelengths and with emission wavelength of 572 nm and 647 nm for Nile red and fast green, respectively, for the fluorescence field. SO was dyed before emulsion formation by adding 0.01% (w/v) Nile red, whereas 0.01% (w/v) fast green was added to the final emulsion samples prepared with 1.5% (w/v) pectin to stain the proteins present in the emulsion system. Images were analysed and processed by using FV10-ASW Version 4.02.03.06 (Olympus Corporation, Tokio, Japon).

3.6 Emulsion particle size analysis

The droplet size distribution and the volume-weighted mean diameter ($D_{4,3}$) were determined, in triplicate, with a laser scattering instrument (Mastersizer 2000, Malvern Instruments Ltd., Worcestershire, UK). Oil droplet size measurements were done in freshly prepared samples and after 6 days of storage under refrigerated conditions (4 °C). The droplet size distribution was determined based on the best fit between the experimental measurement and Mie theory (McClements, 2015).

3.7 Creaming index

The creaming index (CI) of the emulsions was measured following the methodology proposed by Verkempinck et al., (2018)). Capped, glass tubes were filled with 5 mL of each emulsion and the total height was measured using a calliper (BESTOOL-KANON, Japan.). The height of the upper cream layer was measured at different storage time (0 and 6) in order to calculate the creaming index. The creaming index (%) was expressed as the ratio of the height of the upper, cream layer (mm) to the height of the total emulsion (mm). Tubes were stored at refrigeration conditions (4 °C).

3.8 Rheological characterization

The rheological behaviour of the emulsions was analysed in triplicate at 25 °C using a rotational rheometer (HAAKE Rheostress 1, Thermo Electric Corporation, Karlsruhe, Germany) with a plate/plate measuring system (PP60Ti) using a gap of 1 mm. Samples were left to rest for 3 min before the measurements were taken. The shear stress (s) was obtained as a function of shear rate (g) between 0 and 100 s^{-1} and maintained during 1 min, taking 10 min for each (up and down) cycle. The power law model Eq. (1) was applied to determine consistency index (k) and flow behaviour index (n). Apparent viscosities were determined at 100 s^{-1}.

$$\sigma = K \gamma^n \qquad \text{(Eq. 1)}$$

3.9 Spreadability

Spreadability was measured using a TA.XT-Plus Texture Analyses (Stable Micro Systems Ltd., Godalming, UK), with a TTC Spreadability Rig (HDP/SR) attachment using 5 kg load cell and Heavy-Duty Platform (HDP/90). Samples were filled into a female cone (90° angle) with special attention to avoid bubbles formation. Any excess of sample was scraped off with a ruler. Then, the filled cone sample holder was put in the base holder and a 45-degree cone probe was used to penetrate the samples. Pre-test speed of 1 mm/s was set with trigger force of 1 g. Then, a test speed of 3 mm/s was applied until the sample reached 80% strain. Force, expressed in Newtons, was measured for the duration of the test. Firmness, spreadability and stickiness were determined. All measurements were made, at least, in triplicate.

3.10 Protein content

The protein content of the three pectin types was analysed for total nitrogen content using an Elemental Analyser Rapid N Exceed (Paralab S.L., Spain). About 100 mg of each of the powdered samples were pressed to form a pellet which was then analysed using the Dumas method, which is based on the combustion of the sample and subsequent detection of the released N_2 (Wiles et al., 1998). The total protein content was calculated from the nitrogen content multiplied by a factor of 6.25.

3.11 Small angle X-ray scattering (SAXS)

SAXS experiments were carried out in the Non Crystalline Diffraction beamline, BL-11, at ALBA synchrotron light source (www.albasynchrotron.es). Pectin solutions (in water) and emulsions were analysed at room temperature (25 °C). The samples were placed in sealed 2 mm quartz capillaries (Hilgenberg GmbH, Germany). The energy of the incident photons was 12.4 KeV or equivalently a wavelength, λ, of 1 Å. The SAXS diffraction patterns were collected by means of a photon counting detector, Pilatus 1M, with an active area of 168.7 x 179.4 mm^2, an effective pixel size of 172 x 172 μm^2 and a dynamic range of 20 bits. The sample-to-detector distance was set to 7570 mm, resulting in a q range with a maximum value of q = 0.19 $Å^{-1}$. An exposure time of 10 s was selected based on preliminary trials.

The data reduction was treated by pyFAI python code (ESRF) (Kieffer & Ashiotis, 2014), modified by ALBA beamline staff, to do on-line azimuthal integrations from a previously calibrated file. The calibration files were created from a silver behenate (AgBh) standard. The intensity profiles were then represented as a function of q using the IRENA macro suite (Ilavsky & Jemian, 2009) within the Igor software package (Wavemetrics, Lake Oswego, Oregon).

The scattering patterns from the emulsions were properly described using a fitting function consisting of a three-level unified model. This model considers that, for each individual level, the scattering intensity is the sum of a Guinier term and a power-law function (Beaucage, 1995, 1996):

$$I(q) = \sum_{i=1}^{N} G_i \exp\left(-q^2 \cdot \frac{R_{g,i}^2}{3}\right) + \frac{B_i\left[\text{erf}\left(qR_{g,i}/\sqrt{6}\right)\right]^{3P_i}}{q^{P_i}} + bkg \quad \text{(Eq. 2)}$$

where $G_i = c_i V_i \Delta SLD_i{}^2$ is the exponential prefactor (where V_i is the volume of the particle and ΔSLD_i is the scattering length density (SLD) contrast existing between the ith structural feature and the surrounding solvent), $R_{g,i}$ is the radius of gyration describing the average size of the ith level structural feature, B_i is a q-independent prefactor specific to the type of power-law scattering with power-law exponent, P_i, and bkg is the background. In this particular case, the largest structural level was modelled only by a power-law ($R_{g1}$was fixed at a value >> q_{min}^{-1} of 5000 Å), whereas the power-law exponent for the lowest structural level was fixed to 1, corresponding to rigid rods to account for the rod-like structure of the pectin molecules (Xu et al., 2018).

The obtained values from the fitting coefficients are those that minimize the value of Chi-squared, which is defined as:

$$\chi^2 = \sum \left(\frac{y - y_i}{\sigma_i}\right)^2 \quad \text{(Eq. 3)}$$

where y is a fitted value for a given point, y_i is the measured data value for the point and σ_i is an estimate of the standard deviation for y_i. The curve fitting operation is carried out iteratively and for each iteration, the fitting coefficients are refined to minimize χ^2.

3.12 Statistical analysis

All statistical analysis was performed using the statistical software Statgraphics Centurion XVI® (Manugistics Inc.; Rockville, MD, USA). Statistically significant differences were determined by using one-way analyses of variance (ANOVA) and sample comparison with LSD at 95% confidence level (p-value < 0.05).

4 Results and Discussion

The three pectin samples used in the present study have been previously characterized and key molecular characteristics relevant to their emulsifying capacity are reproduced in Table 1 (Méndez et al., 2021). Very briefly, their esterification degree was greater than 50% and, thus, all of them can be classified as high methyl-esterified (HM) pectin. WRP obtained under similar acid treatment conditions used in the industry, had intermediate average molecular weight, greater protein content and the presence of long side RG-I chains, in comparison with the commercial citrus (CP) and apple pectin (AP).

In order to comparatively evaluate the emulsification capacity of WRP with commercial CP and AP, oil-in-water emulsions were prepared using two different pectin concentrations (1.5 and 3.5% (w/v)) and two different soybean oil (SO) concentrations (35 and 60% (v/v)). Interestingly, only WRP was able to stabilize the emulsion with the greatest oil content, whereas immediate phase separation was observed when CP or AP commercial pectin were used (cf. Figure S1 from the Supplementary Material), thus pointing out the enhanced emulsifying capacity of WRP. Amongst the factors that affect the emulsifying properties of pectin, intrinsic factors like the degree of esterification, protein content, molecular weight (Mw) or monosaccharide composition play an important role. As for the degree of esterification (DE), higher values imply a greater content of hydrophobic groups (methyl

ester and acetyl groups) in the pectin structure providing the polysaccharide with the ability to be placed at the oil-water interphase (Verkempinck et al., 2018).

Table 1. Composition of pectin obtained from watermelon rind (WRP), and commercial apple (AP) and citrus pectin (CP). Adapted from Mendez et al. (2021).

	AP	CP	WRP
Degree of esterification [%]	77.2	55.2	61.6
Methoxyl content [%]	9.0	6.8	6.8
Molecular weight [kDa]	339.4(11.4)	77.8(3.8)	106.11(2.7)
Protein content [%]	2.5(0.2)	1.9(0.1)	9.2(1.4)
Monosaccharide composition [µg/mg]			
Galacturonic acid (GalA)	482.0(17.9)	565.9(22.3)	540.3(37.0)
Fucose (µg/mg)	1.65(0)	0.6(0.2)	2.5(1.0)
Rhamnose (µg/mg)	24.2(1.0)	22.3(0.5)	21.2(0.9)
Arabinose (µg/mg)	18.5(0.6)	19.5(0.7)	2.3(0.1)
Galactose (µg/mg)	49.4(1.7)	35.2(1.6)	204.9(5.0)
Xylose (µg/mg)	14.2(0.8)	3.1 (0.1)	1.9(0.2)
RG-I[a]	6.8	5.5	20.8
HG[b]	45.8	54.4	51.9
RL[c]	4.4	6.9	2.4
RB[d] ((Gal+Ara)/Rha)	2.8	2.5	9.8

[a] (2Rha+Ara+Gal).
[b] (GalA-Rha).
[c] A larger value suggests of more linear/less branched pectins. (GalA/(Xyl+Rha+Ara+Gal)).
[d] A larger value is indicative of larger average size of the branching side chains. ((Gal+Ara)/Rha). Values in brackets correspond to standard deviation.

WRP had a DE of ~62% and a methoxyl content (MeO) of 6.8% (cf. Table 1), which are similar to the DE and MeO contents of the commercial CP and AP (with DE between 50 and 77% and MeO >6.7%). Previous studies indicate that there is an optimal Mw promoting emulsion stability, which depends on the pectin source (e.g. 70kDa for the reference citrus pectin) (Akhtar et al., 2002; Leroux et al., 2003). In this work, the decreased emulsion

stability with AP might partly be explained by its higher molecular weight (339.4 ±11.4 kDa), compared to WRP (106.11 ±2.7 kDa) or CP (77.84 ±3.8 kDa). Nevertheless, WRP emulsions were more stable than CP, regardless of having similar Mw, suggesting other mechanisms are probably playing a role. Previous studies support the emulsion stabilization mechanism of WRP as explained by the steric hindrance induced by protein content and the electrostatic contribution of charged, non-esterified GalA units (Petkowicz et al., 2017). While CP and AP had 1.9 ±0.1 and 2.5 ±0.2% protein, respectively, a significantly greater amount of proteins was present in the WRP (9.2 ±1.4%).

Furthermore, and as previously commented in the introduction section, the lower relative abundance of rhamnose (Rha) and higher amounts of the combination of galactose (Gal) and arabinose (Ara) in comparison with CP and AP, indicated the presence of longer sugar side chains, which could have an influence on the emulsifying properties.

Therefore, in order to better understand how the different structural features and protein content of the three pectin types considered affected emulsion structure and properties, an in-depth analysis was carried out for O/W emulsions prepared with 1.5 and 3.5% (w/v) of AP, CP or WRP and containing 35% (v/v) SO. Moreover, WRP emulsions with 60% (w/v) SO concentration were also prepared to explore how this increased oil content influenced emulsion structure and properties.

4.1 Oil droplet size and emulsion stability

The study of the oil droplet size, as well as their distribution in the emulsions, is of interest because of its impact on the long-term stability. Initially, the stability of the emulsions was evaluated during storage for 6 days at 4 °C. As shown in Figure 1, all the emulsions had a creamy appearance, showing a thicker consistency for the ones with greater pectin concentration, consistent with the viscosifying function of the hydrocolloid. After 6 days of refrigerated storage, the emulsions prepared with 1.5% (w/v) CP or AP displayed a slight phase separation (see arrows in Figure 1), indicating that these were the least stable emulsions, fact which was further corroborated by the significant increase ($p<0.05$) in the average oil droplet size (see Table 2). The phase separation observed in CP and AP

emulsions prepared with the lower pectin concentration can be ascribed to bridging flocculation, coalescence and lower stabilization capacity. A previous study showed that pectin extracted from citrus peels but enriched in RG-I, showed excellent emulsion stability at 1.5% (w/v) concentration, although a lower oil content (20% (v/v)) was used in that case (Hu et al., 2021). Increasing pectin concentration led to enhanced emulsion stability, as no phase separation was observed during refrigerated storage. Interestingly, the samples prepared with the greater WRP concentration (3.5% (w/v)) and greater oil content (60% (v/v)) (see Figure 1) had a gel-like texture, similar to that of emulsion gels (Luo et al., 2019).

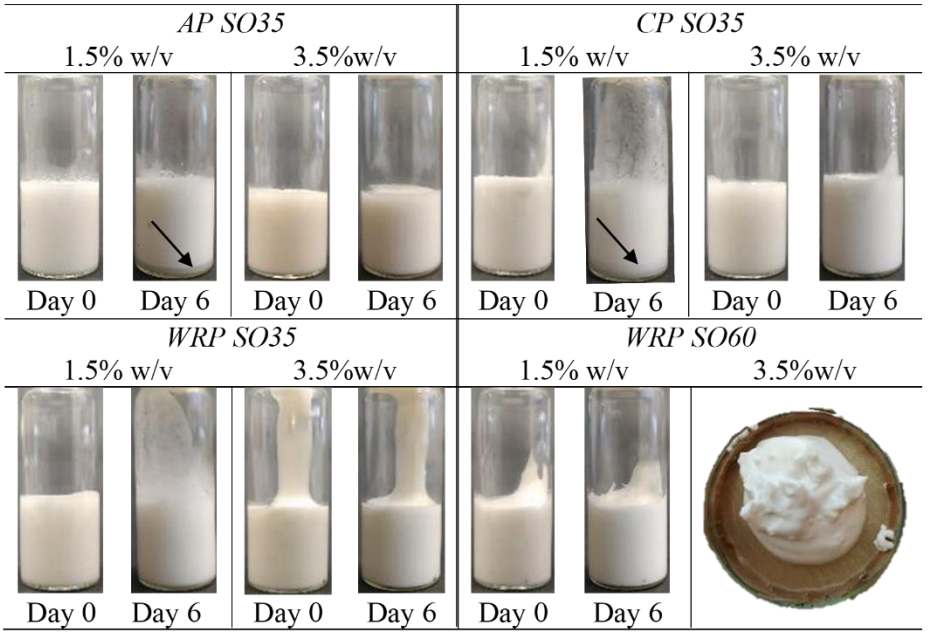

Figure 1. Macroscopic images of the different freshly prepared (day 0) emulsions and after 6 days of storage (day 6) at 4 °C. Black arrows point out to phase separation.

As already mentioned, the emulsifying properties of pectin can be partially ascribed to some structural features of the polysaccharide such as high acetyl content, presence of side chains or covalently bound proteins (Kpodo et al., 2018). As observed in Table 2, the mean particle size of the oil droplets in the AP emulsions prepared at low pectin concentration was smaller than that of their counterparts prepared with CP and WRP. However, while increasing pectin concentration led to a decrease in the average droplet size for the emulsions prepared with

CP and WRP, a slight increase was observed for the AP-stabilized emulsions with greater pectin content. This, together with the results related to emulsion stability and oil-holding capacity (as only WRP-stabilized emulsions were able to incorporate 60% (v/v) of oil), suggested different mechanisms of stabilization of the various pectin samples.

Table 2. Average oil (SO) droplet size of the emulsions stabilized with AP, CP and WRP, measured at two different times (freshly prepared samples and after 6 days of storage at 4 °C).

Sample	*Particle size $d_{4,3}$ (μm)*[a]		*CI (%)*
	day 0	*day 6*	*day 6*
1.5AP-SO35	15.29(0.32)^{d}	16.13(0.01)^{d}*	5.98
3.5AP-SO35	19.42(0.01)^{c}	19.73(0.01)^{c}*	-
1.5CP-SO35	24.58(0.02)^{a}	25(0.07)^{a}*	12.32
3.5CP-SO35	10.79(0)^{f}	10.6(0.01)^{g}*	-
1.5WRP-SO35	21.68(0.01)^{b}	21.49(0.05)^{b}*	-
3.5WRP-SO35	11.62(0.02)^{e}	12.24(0.08)^{e}*	-
1.5WRP-SO60	10.78(0)^{f}	10.84(0.01)^{f}*	-
3.5WRP-SO60	6.82(0.06)^{g}	7.44(0.23)^{h}*	

[a] The data are averages and standard deviations of triplicate measurements. Values in each column with different superscript letters (a-g) indicates significant differences ($p<0.05$) in the same column. (*) indicates significant differences ($p < 0.05$) in the same line (related to storage time). Values in brackets correspond to standard deviation.

4.2 Rheological characterization

Complete flow curves of both aqueous pectin solutions and their corresponding emulsions are shown in Figure 2. The rheological data of pectin solutions and emulsions were fitted to the Ostwald de Waale model (Eq.1). Table 3 gathers the flow (*n*) and consistency (k) indexes, together with the apparent viscosity (η_{ap}) values at a shear rate of 100 s^{-1} for the samples. As inferred from the rheology results, all samples (both solutions and emulsions) displayed shear thinning (behaving as pseudoplastic fluids), as previously reported for other pectin types (Cho et al., 2019; Hu et al., 2021; Rodsamran & Sothornvit, 2019). Solutions and emulsions prepared with AP were the most viscous ones, probably related to the greater Mw of this pectin sample (cf. Table 1). However, the rheological characteristics of pectin solutions are not only dependent on Mw, but also on the distribution of substituents along

the HG chains and the degree of branching (Cui et al., 2020). In fact, the presence of long sugar side chains in the WRP resulted in lower values of the flow index (n), thus indicating more pronounced shear thinning behaviour and the greatest consistency index (k) at 3.5% (w/v) WRP concentration, probably related to the entanglements between these long branch chains resulting in increased flow resistance at low shear rates (see Table 3). However, it seems that at high shear rates, these chain interactions are physically disrupted, causing chain rearrangements and a significant reduction in apparent viscosity (Sousa et al., 2015), more pronounced than that observed for the other two commercial pectin.

As observed from Figure 2 and Table 3, addition of SO promoted significant changes in the rheological behaviour, making the emulsions more viscous and more shear thinning than their counterpart solutions, mainly for those prepared with greater pectin concentration. An increased viscosity of the continuous phase of o/w emulsions contributes to emulsion stability, as oil droplet movement is slowed down, consequently limiting coalescence and flocculation (Ngouémazong et al., 2015). However, the viscosity of the continuous phase was not the determining factor for the stabilization ability of WRP, as having the lowest consistency index of the three emulsions prepared at 1.5% (w/v) concentration, it displayed the greatest emulsion stability. Regarding the shear thinning behaviour of emulsions, it has been previously explained by the disruption of the network of oil droplets by hydrodynamic forces, causing their rearrangement into a certain direction, resulting in less resistance to flow (Luo et al., 2019; Meng et al., 2018).

Increasing the oil concentration up to 60% (v/v) in the WRP-stabilized emulsions, further increased the consistency index and shear thinning behaviour, in agreement with the visual appearance (see Figure 1). In fact, the rheological behaviour of the emulsion with 3.5% (v/v) WRP and 60% (v/v) oil was so different (this sample having a solid-like behaviour) that it could not be adequately measured.

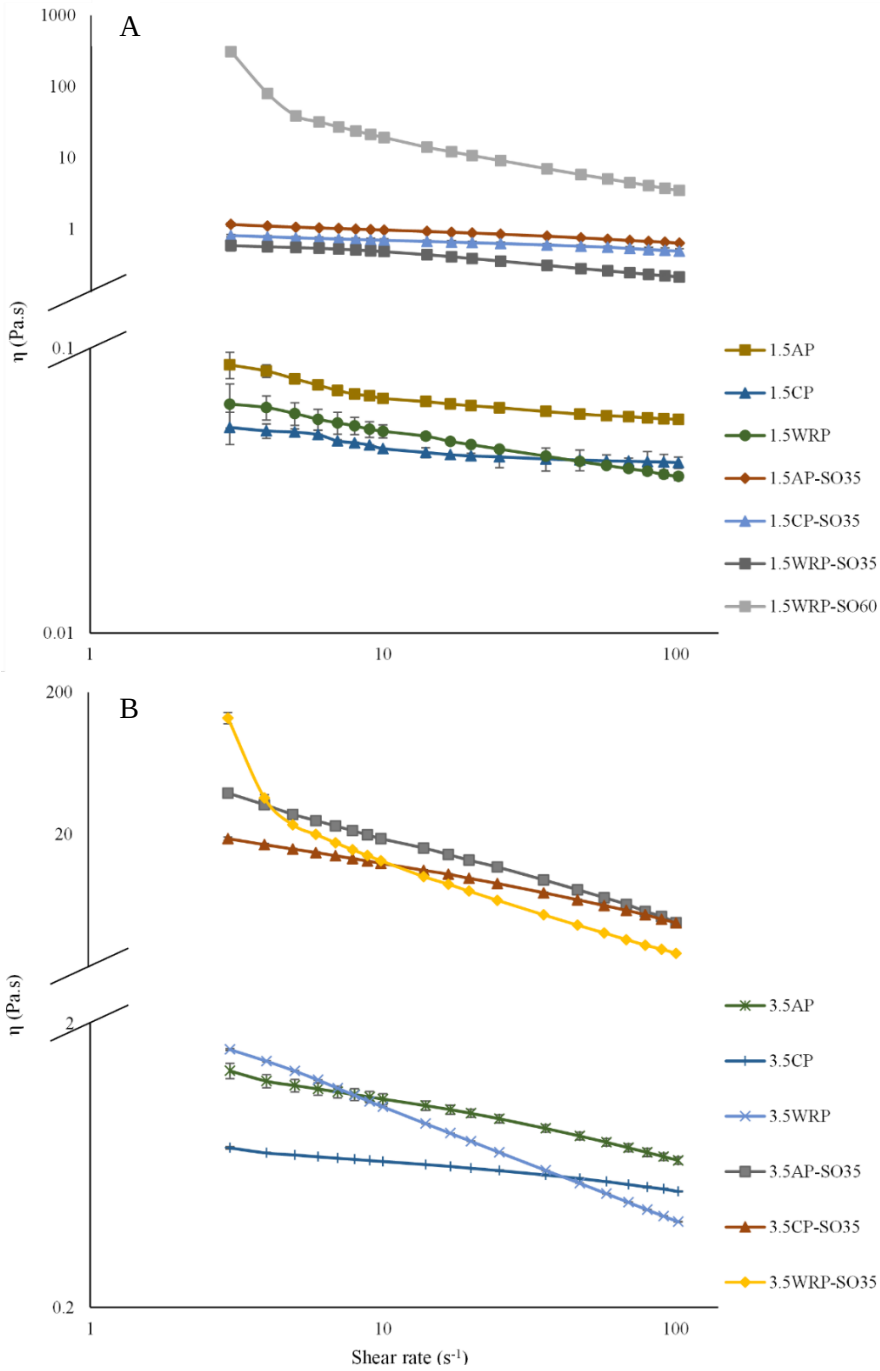

Figure 2. Apparent viscosity *vs*. shear rate curves for solutions and emulsions prepared with AP, CP and WRP at (a) 1.5% (w/v) and (b) 3.5% (w/v) pectin concentration.

Table 3. Flow behaviour index (n), consistency index (k) and apparent viscosity (η_{ap}) of the oil-in-water emulsions and their corresponding pectin solutions.

Sample	Ostwald de Wale model parameters			Apparent viscosity
	n	k	r^2	η_{ap} (Pa.s)
1.5AP-SO35	0.843	1.35	0.99	0.65
3.5AP-SO35	0.5106	51.09	0.95	5.36
1.5CP-SO35	0.8731	0.91	0.99	0.51
3.5CP-SO35	0.659	24.76	0.98	5.15
1.5WRP-SO35	0.69	0.88	0.99	0.21
3.5WRP-SO35	0.341	57.11	0.96	2.75
1.5WRP-SO60	0.266	97.3	0.90	3.31
3.5WRP-SO60	-	-		
1.5AP	0.90	0.08	0.99	0.05
3.5AP	0.82	1.60	0.99	0.69
1.5CP	0.92	0.05	0.99	0.04
3.5CP	0.91	0.78	0.99	0.53
1.5WPR	0.84	0.07	0.99	0.04
3.5WPR	0.62	2.30	0.99	0.41

4.3 Texture analysis.

The firmness of the emulsions was investigated by penetration and spreadability tests with a texture analyzer. Firmness reveals the hardness of the samples, spreadability indicates the capacity of a sample to be applied as a thin layer, while stickiness is related to the force needed to pull out the measuring probe (Öğütcü & Yilmaz, 2014). The obtained results, gathered in Figure 3, indicate that both firmness and spreadability were significantly affected ($p<0.05$) by the amount of pectin and SO, which is well correlated with the increase in the viscosity values reported in the previous section. Furthermore, for a given SO and pectin concentration, AP samples provided higher firmness and spreadability values, thus suggesting that the higher Mw of this pectin led to a greater viscosity of the aqueous phase, playing a major role on the textural parameters. It is worth mentioning that the spreadability values were not significantly different ($p>0.05$) for samples prepared with the lowest pectin and SO concentrations, probably ascribed to the fact that it is a more dynamic property than

firmness. Therefore, spreadability was influenced not only by the force required to obtain a given deformation but also by the progressive softening produced on the samples during the measurements (Bayarri et al., 2012).

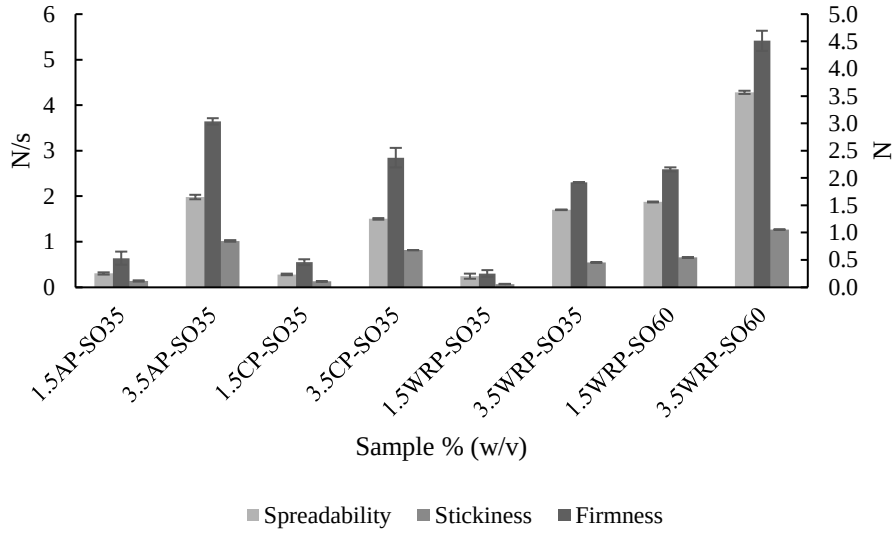

Figure 3. Firmness, spreadability and stickiness values of the pectin emulsions at two different pectin concentrations (1.5 and 3.5% (w/v)) with SO at 35% (w/v) and 60% (w/v).

Interestingly, the textural properties of the emulsion with 1.5% WRP and 60% SO were very similar to those of the 3.5% WRP emulsion containing 35% oil, further indicating the ability of this pectin for producing a well-structured oil droplet dispersion. In fact, the firmness and spreadability values of the emulsion with 3.5% WRP and 60% SO almost doubled the firmness and spreadability values of the 3.5% pectin-stabilized emulsions with 35% SO, thus pointing out at a compact microstructure.

4.4 Microstructural characterization of the emulsions

The microstructure of the freshly-prepared emulsions was further investigated by means of confocal microscopy by staining the SO with Nile red. Representative confocal images are shown in Figure 4, together with the size distribution of the oil droplets. It is interesting to note that at low pectin concentration, a more heterogeneous particle size distribution was observed for the emulsions stabilized with CP and WRP. In contrast, when increasing the

pectin concentration in the emulsions, apart from decreasing the average oil droplet size, more homogeneous particle size distribution was also attained when using CP or WRP as emulsifiers, while both the average particle size and size distribution remained almost unchanged in the AP-stabilized emulsion. This again suggests a different stabilization mechanism of the different pectin samples. In the case of AP, it is hypothesised that the mechanism of emulsion stabilization is based on the viscosity provided by the pectin to the continuous aqueous phase and not to a direct adsorption to the oil/water interphase, as increasing pectin concentration did not affect oil droplet size. Previous studies have also found that higher Mw pectin generates increased droplet sizes in emulsions as it is not able to properly adsorb at the oil/water interphase (Cui et al., 2020). In contrast, the decrease in oil droplet size when increasing CP or WRP concentration has been previously observed in other pectin samples and it is indicative of enhanced steric repulsion between droplets (Zhang et al., 2021).

Increasing the oil content of the WRP-stabilized emulsions, led to a further decrease in oil droplet size and to a very compacted microstructure formed by a great number of highly packed oil droplets (see Figure 4G and 4H). In fact, these two emulsions displayed the lowest average oil droplet sizes, an excellent storage stability and the rheological and textural properties were related to this characteristic microstructure, suggesting that a higher volume of smaller oil droplets in the emulsion lead to greater viscosity values as it has been previously observed (Schuch et al., 2015). In general, emulsions with smaller particle size have been seen to provide higher firmness, spreadability and stickiness, thus supporting the theory that a decreased droplet size results in a firmer and more adhesive emulsion (Lequeux, 1998), being thus this pectin type of great interest for the development of emulsion gels. As previously mentioned, the presence of branches in the pectin structure can also have an impact on emulsion stabilization. In fact, the molar ratio of (Ara+Gal)/Rha which is indicative of the length of the pectin side chains (greater values of the ratio indicating longer branches), has also been correlated with the emulsification capacity of pectin (Kpodo et al., 2018) and greater RG-I contents, apart from providing a range of bioactivities to this carbohydrate molecule (Zhang et al., 2021) also contribute to preventing oil droplet coalescence by steric stabilization (Ngouémazong et al., 2015).

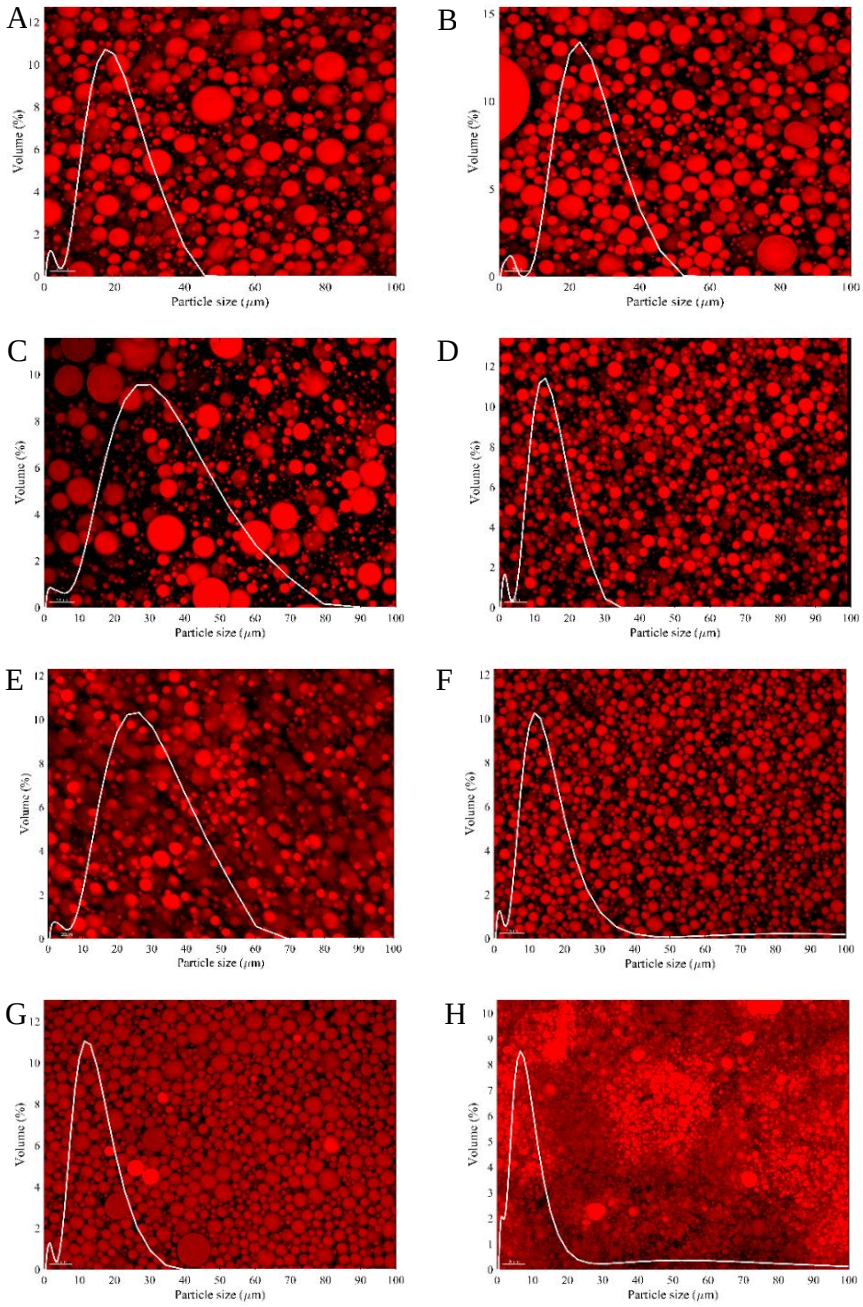

Figure 4. Confocal microscopy images of pectin-based emulsions and particle size distribution at day 0. The oil phase was labelled with Nile Red. All pictures were taken with

the same light intensity and magnification (scale bar corresponds to 20 μm). (A) 1.5AP-SO35, (B) 3.5AP-SO35, (C) 1.5CP-SO35, (D) 3.5CP-SO35, (E) 1.5WRP-SO35 (F) 3.5WRP-SO35, (G) 1.5WRP-SO60 and (H) 3.5WRP-SO60.

Another factor which influences the ability of a certain pectin molecule to stabilize an emulsion is related to its linearity and, thus, its flexibility, to be able to adsorb at the o/w interphase. Looking at Table 1, WRP had considerable longer side chains than CP or AP, while CP displayed the greatest linearity and HG content, thus suggesting that this latter pectin sample could have better interfacial properties than the other two. However, as previously explained, the emulsification capacity of WRP was significantly superior and, thus, proteins in this specific sample, seemed to play a key role in the stabilizing mechanism.

To better understand the role of the protein content in the microstructure of the emulsions, samples were stained with fast green dye, widely used for protein staining. As depicted in Figure 5, and in agreement with the measured protein content of the WRP sample (cf. Table 1), a much higher protein content was present in the aqueous phase of the WRP-stabilized emulsion. In fact, the magnified image of this specific emulsion evidenced the key role that proteins play in emulsion stabilization, as a protein layer could be identified in the o/w interphase. It has been previously described that the protein content of pectin plays a major role in its emulsifying capacity by increasing the surface activity of the overall structure, (Akhtar et al., 2002; Funami et al., 2007; Leroux et al., 2003). The combination of proteins and pectin (specially highly branched pectin), have been seen to synergistically stabilise emulsions, favouring the production of thick adsorbed hydrated layers which prevent the coalescence of droplets (Funami et al., 2011; Neckebroeck et al., 2021). This behaviour has, for instance, been reported for sugar beet pectin that is recognized for its high protein content and excellent emulsifying properties (Schmidt et al., 2015), and can be explained by a combination of electrostatic and steric effects provided by both hydrocolloid types (Damodaran, 2006; Petkowicz et al., 2017). This would explain the increased emulsifying capacity and emulsion stability provided by WRP as compared to the less branched CP and AP.

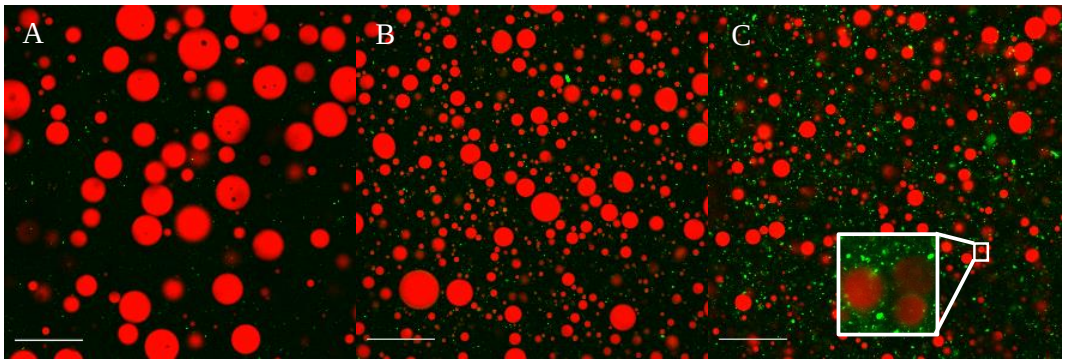

Figure 5. Confocal microscopy images of pectin-based emulsions. Oil droplets are stained with Nile red and Fast Green was used to label the proteins present in the emulsions. Scale bars correspond to 60 μm. (A) 1.5AP-SO35, (B) 1.5CP-SO35 and (C) 1.5WRP-SO35.

4.5 SAXS characterization of the emulsions

To further confirm the different emulsification mechanisms of the various pectin samples, the nanostructure of the developed emulsions was investigated by means of SAXS experiments. Figure 6 shows the SAXS patterns of the pectin emulsions and their corresponding solutions in water. As observed, the scattering patterns from all the samples were characterized by the appearance of a broad shoulder-like feature within the low-q region ($q < \sim 0.03$ Å^{-1}) and a more marked shoulder within the high-q region. Figure S2 from the Supplementary Material shows, as an example, the Kratky plots for the two solutions and emulsions prepared with 3.5 AP and CP, in which these structural features are better distinguished. This behaviour has already been reported for pectin samples (Alba et al., 2018) and suggests that at the tested concentrations, pectin chains do not have a random coil conformation typical from ideal solutions, but some degree of clustering takes place as a result of molecular interactions.

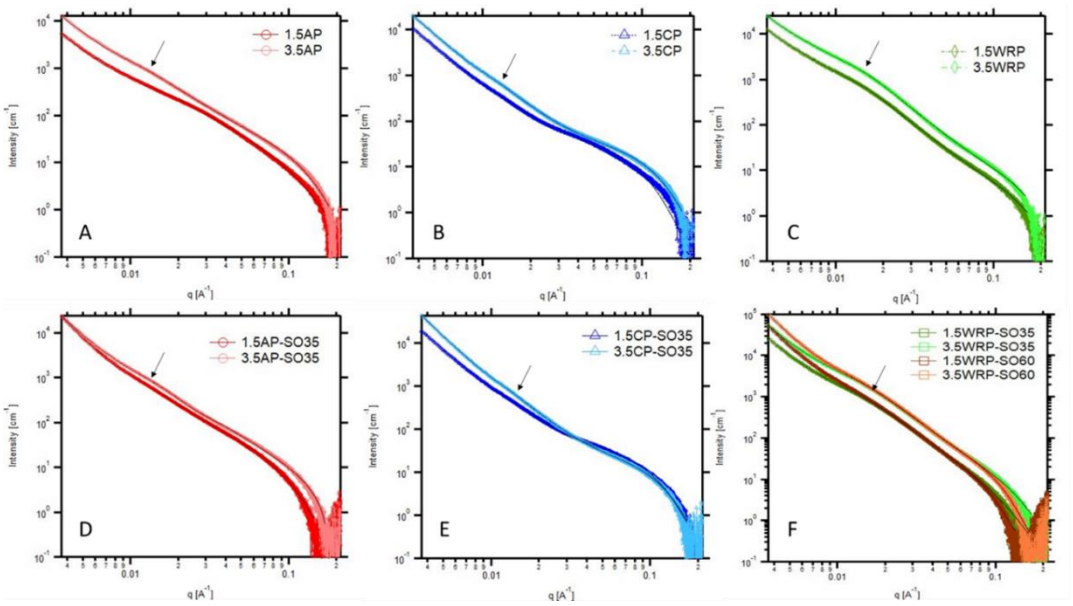

Figure 6. SAXS patterns from the pectin solutions (A-C) and corresponding emulsions (D-F). Markers represent the experimental data and solid lines show the fits obtained using the unified model. Arrows point towards the appearance of a shoulder-like feature in the low q region.

Whereas the low-q region is originated from intermolecular interactions and chain clusters, the high-q region arises from the scattering of rod-like pectin chains. As expected, the scattering intensity increased when increasing pectin concentration in all the samples. On the other hand, while the low-q shoulder was very faint in the case of the AP and CP samples, it was much more noticeable in the case of the WRP samples. This could be a consequence of the distinct composition of this pectin, which contains more protein than the two commercial grades. The presence of protein in the sample would decrease the overall scattering length density of the material, thus reducing the interfacial scattering length density contrast between the biopolymer and the surrounding bulk solvent; as a result, any scattering feature present in the low q region would be more visible. To extract more information from the results, the experimental data were fitted using an empirical three-level Beaucage model and the main structural parameters from the obtained fits are gathered in Table 4.

Table 4. Parameters obtained from the fits of the SAXS data from the pectin solutions and emulsions.

Samples	P_1	Rg_2 (nm)	P_2	Rg_3 (nm)
1.5AP	3.3	20.2	1.8	1.4
3.5AP	3.4	35.0	2.2	1.8
1.5AP-SO35	3.7	37.4	2.4	2.6
3.5AP-SO35	3.5	33.9	2.5	2.2
1.5CP	3.2	41.1	2.7	2.3
3.5CP	3.2	37.6	2.8	1.9
1.5CP-SO35	3.2	37.6	2.8	2.1
3.5CP-SO35	3.3	36.3	3.0	2.0
1.5WRP	3.4	27.3	2.7	1.5
3.5WRP	3.5	26.1	2.8	1.5
1.5WRP-SO35	3.6	28.0	2.6	2.1
3.5 WRP-SO35	3.7	27.4	2.7	1.7
1.5WRP-SO60	3.7	30.9	2.6	2.4
3.5 WRP-SO60	3.7	28.3	2.8	2.0

P_1: power-law coefficient for the largest structural level; Rg_2: radius of gyration associated to the largest structural level; P_2: power-law coefficient for the smallest structural level; Rg_3: radius of gyration associated to the smallest structural level.

Looking at the parameters from the lowest structural level (P_2 and Rg_3), it is evident that both the pectin type and the addition of oil has an impact on the structural arrangement of the pectin chains. The Rg_3 value for all the pectin solutions, characteristic of the cross-section of rod-like pectin chains, ranged from 1.4 to 2.3 nm. CP samples presented slightly larger Rg_3 values than AP and WRP, which may be related to the lower DE of the former. Previous work reported on the same behaviour for pectin with different DEs and attributed it to greater local chain bending originated by electrostatic interactions in low DE pectin (Alba et al., 2018). The power-law exponents corresponding to the smallest structural level, ranging from 1.8 to 2.8, also support the existence of flexible folded chains rather than ideal rigid rods. The incorporation of oil into the emulsions seemed to have a small impact on the conformation of pectin chains, slightly increasing their degree of folding. At the next structural level, Rg_2 values are characteristic of the size of the molecular clusters originated as a result of chain bending. The corresponding power-law exponents (P_1) were 3.2-3.5, characteristic of surface fractals, arise from the surface scattering of the rough particles

formed by pectin chain clusters. The Rg_2 values determined for pectin solutions (20-38 nm) fall within the range previously determined by SAXS (6.3-42 nm) and light scattering (~36 nm) for pectin with different DEs (Alba et al., 2018). Interestingly, CP samples showed greater radii of gyration, which again may be related to the lower DE and greater HG content of this pectin type. The greater chain bending in the CP samples confirm the greater flexibility of this pectin related to its greater linearity, and it may lead to the formation of less densely packed molecular clusters, i.e. more interwined structures. In general, the incorporation of oil into the systems led to greater P_1 and Rg_2 values, being this effect more obvious in the AP samples and the WRP samples with the greatest oil content. This suggests that the presence of oil difficulted to a certain extent the packing of the pectin chains, especially in the case of the pectin with the greatest DE.

4.6 Proposed mechanisms for emulsion stabilization of the three pectin samples

In view of all the previous results, a different mechanism of emulsion stabilization is proposed for each of the three pectin samples and is schematically represented in Figure 7. In the case of the emulsions prepared with AP, having this pectin the greatest DE and Mw and not very high linearity, a stabilising effect ascribed to its viscosifying capacity, was observed. That is, this pectin does not affect oil droplet size, but slows down oil droplet movement by providing viscosity to the continuous aqueous phase and, thus, it can be considered that AP works as a stabilizer rather than as an emulsifier. In fact, other studies have shown that AP has a low potential to decrease interfacial tension (Neckebroeck et al., 2021) and, thus, the stabilizing effect, which is a kinetic effect, leads to emulsion de-stabilization with storage time. CP, on the other hand, has the lowest DE (and thus, a more balanced amphiphilic character) and the greatest linearity and flexibility as inferred from the SAXS data, fact which could favour pectin adsorption at the o/w interphase.

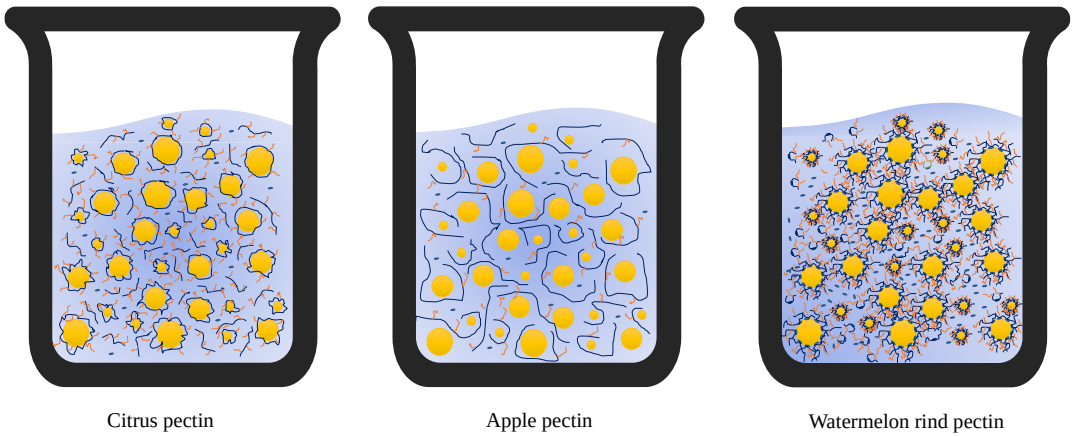

Figure 7. Schematic representation for emulsion stabilization proposed for each of the three pectin samples, pectin back bone ( ), branching sides ( ), protein moieties ( ) (AP, CP and WRP)

However, having short length branches, a limited steric repulsion is created, thus also leading to oil droplet coalescence and creaming with storage. WRP, having a greater protein content and very long RG-I branch chains despite being obtained under similar acid conditions as CP or AP, is the one displaying the better emulsifying properties and superior emulsion stability. The emulsification capacity of WRP is based on the combination of proteins, acting as surface active materials, surrounded by the pectin polysaccharides with long branch side chains, which are able to provide stable steric repulsions between oil droplets, guarantying long-term stability of the emulsions. Leroux et al., (2003) reported a similar behaviour, suggesting that the presence of a certain amount of protein covalently bound to a highly branched polysaccharide structure reduces the interfacial tension, thus facilitating the emulsifying capacity of beet pectin and citrus pectin. Despite some works having attributed good emulsifying properties to the presence of protein, neither high protein concentration nor the presence of proteins guarantee excellent emulsifying properties since both the protein accessibility and its chemical interaction with the branched neutral sugars have been seen to determine their emulsifying capacity (Alba & Kontogiorgos, 2017; Ngouémazong et al., 2015). Therefore, the structural features and composition of the WRP could explain its higher ability to trap a larger oil amount, producing stable emulsions at SO concentration up to 60% (v/v).

5 Conclusions

WR waste showed relatively high pectin contents (~30%), not recalcitrant to common acid treatments (~13% yield) and increased arabinogalactan side chain contribution compared to common commercial sources like apple (AP) and citrus pectin (CP). A Box-Behnken design was used to accurately model the effect of extraction time, pH and temperature on WRP yield and composition. The broad range of extraction conditions led to pectin with a broad range of esterification degree, molar mass and compositional or structural characteristics, all of which were accurately fitted to the polynomial models. Harshest conditions generated purer homogalacturonan fractions at the expense of yield, while mild extraction conditions ($pH \geq 2$) produced highly branched entangled pectin structures. Optimum yield conditions led to more linear pectins with similar molecular mass as commercial AP or CP, but with significantly higher RG-I, higher branching degree and small protein contents present, pointing towards a significant pectin-protein interaction. These unique structural features suggest that these specific pectins could have a better performance than commercial pectins as emulsifying agents and also having a double functionality as texturizers and stabilizing agents. The study underlines novel compositional features in WRP and how they relate to extraction parameters, offering the possibility of producing novel customized pectin ingredients with a wider potential application scope depending on the targeted structure. Further studies to relate the structural characteristics with the functionality of the different pectins will be conducted to unravel the potential of this new pectin source for the production of food additives.

6 Acknowledgements

This work was funded by the grant RTI-2018-094268-B-C22 (MCI/AEI/FEDER, EU). Mendez D. A. is supported by the Administrative Department of Science, Technology and Innovation (Colciencias) of the Colombian Government (783-2017). M. J. Fabra and A. Martinez-Abad are recipients of Ramon y Cajal (RYC-2014-158) and Juan de la Cierva (IJDC-2017-31255), respectively, from the Spanish Ministry of Economy, Industry and Competitiveness.

7 References

Agostoni, C., Bresson, J.-L., Fairweather-Tait, S., Flynn, A., Golly, I., Korhonen, H., Lagiou, P., Løvik, M., Marchelli, R., Martin, A., Moseley, B., Neuhäuser-Berthold, M., Przyrembel, H., Salminen, S., Sanz, Y., Strain, S., Strobel, S., Tetens, I., Tomé, D., … Verhagen, H. (2010). Scientific Opinion on the substantiation of health claims related to pectins and reduction of post-prandial glycaemic responses (ID 786), maintenance of normal blood cholesterol concentrations (ID 818) and increase in satiety leading to a reduction in ene. *EFSA Journal*, *8*(10), 1747. https://doi.org/10.2903/j.efsa.2010.1747

Akhtar, M., Dickinson, E., Mazoyer, J., & Langendorff, V. (2002). Emulsion stabilizing properties of depolymerized pectin. *Food Hydrocolloids*, *16*(3), 249–256. https://doi.org/10.1016/S0268-005X(01)00095-9

Alba, K., Bingham, R. J., Gunning, P. A., Wilde, P. J., & Kontogiorgos, V. (2018). Pectin Conformation in Solution [Research-article]. *Journal of Physical Chemistry B*, *122*(29), 7286–7294. https://doi.org/10.1021/acs.jpcb.8b04790

Alba, K., & Kontogiorgos, V. (2017). Pectin at the oil-water interface: Relationship of molecular composition and structure to functionality. *Food Hydrocolloids*, *68*, 211–218. https://doi.org/10.1016/j.foodhyd.2016.07.026

Bayarri, S., Carbonell, I., & Costell, E. (2012). Viscoelasticity and texture of spreadable cheeses with different fat contents at refrigeration and room temperatures. *Journal of Dairy Science*, *95*(12), 6926–6936. https://doi.org/10.3168/jds.2012-5711

Beaucage, G. (1995). Approximations Leading to a Unified Exponential/Power-Law Approach to Small-Angle Scattering. *Journal of Applied Crystallography*, *28*(6), 717–728. https://doi.org/10.1107/s0021889895005292

Beaucage, G. (1996). Small-angle scattering from polymeric mass fractals of arbitrary mass-fractal dimension. *Journal of Applied Crystallography*, *29*(2), 134–146. https://doi.org/10.1107/S0021889895011605

Campbell, M. (2006). *Extraction of Pectin From Watermelon Rind*. Oklahoma State University.

Cho, E. H., Jung, H. T., Lee, B. H., Kim, H. S., Rhee, J. K., & Yoo, S. H. (2019). Green process development for apple-peel pectin production by organic acid extraction. *Carbohydrate Polymers*, *204*, 97–103. https://doi.org/10.1016/j.carbpol.2018.09.086

Ciriminna, R., Chavarría-Hernández, N., Inés Rodríguez Hernández, A., & Pagliaro, M. (2015). Pectin: A new perspective from the biorefinery standpoint. *Biofuels, Bioproducts and Biorefining*, *9*(4), 368–377. https://doi.org/10.1002/bbb.1551

Ciriminna, R., Fidalgo, A., Delisi, R., Tamburino, A., Carnaroglio, D., Cravotto, G., Ilharco, L. M., & Pagliaro, M. (2017). Controlling the Degree of Esterification of Citrus Pectin for Demanding Applications by Selection of the Source. *ACS Omega*, *2*(11), 7991–7995. https://doi.org/10.1021/acsomega.7b01109

Cui, J., Ren, W., Zhao, C., Gao, W., Tian, G., Bao, Y., Lian, Y., & Zheng, J. (2020). The structure–property relationships of acid- and alkali-extracted grapefruit peel pectins. *Carbohydrate Polymers*, *229*, 115524. https://doi.org/10.1016/j.carbpol.2019.115524

Damodaran, S. (2006). Protein Stabilization of Emulsions and Foams. *Journal of Food Science*, *70*(3), R54–R66. https://doi.org/10.1111/j.1365-2621.2005.tb07150.x

Denman, L. J., & Morris, G. A. (2015). An experimental design approach to the chemical characterisation of pectin polysaccharides extracted from Cucumis melo Inodorus. *Carbohydrate Polymers*, *117*, 364–369. https://doi.org/10.1016/j.carbpol.2014.09.081

Dranca, F., & Oroian, M. (2018). Extraction, purification and characterization of pectin from alternative sources with potential technological applications. *Food Research International*, *113*(February), 327–350. https://doi.org/10.1016/j.foodres.2018.06.065

Fan, C., Chen, X., & He, J. (2020). Effect of calcium chloride on emulsion stability of methyl-esterified citrus pectin. *Food Chemistry*, *332*, 127366. https://doi.org/10.1016/j.foodchem.2020.127366

FAOSTAT. (2021). *CROPS*. http://www.fao.org/faostat/en/#data/QC/visualize

Funami, T., Nakauma, M., Ishihara, S., Tanaka, R., Inoue, T., & Phillips, G. O. (2011). Structural modifications of sugar beet pectin and the relationship of structure to functionality. *Food Hydrocolloids*, *25*(2), 221–229. https://doi.org/10.1016/j.foodhyd.2009.11.017

Funami, T., Zhang, G., Hiroe, M., Noda, S., Nakauma, M., Asai, I., Cowman, M. K., Al-Assaf, S., & Phillips, G. O. (2007). Effects of the proteinaceous moiety on the

emulsifying properties of sugar beet pectin. *Food Hydrocolloids*, *21*(8), 1319–1329. https://doi.org/10.1016/j.foodhyd.2006.10.009

Grassino, A. N., Halambek, J., Djaković, S., Rimac Brnčić, S., Dent, M., & Grabarić, Z. (2016). Utilization of tomato peel waste from canning factory as a potential source for pectin production and application as tin corrosion inhibitor. *Food Hydrocolloids*, *52*, 265–274. https://doi.org/10.1016/j.foodhyd.2015.06.020

Hu, W., Chen, S., Wu, D., Zhu, K., & Ye, X. (2021). Physicochemical and macromolecule properties of RG-I enriched pectin from citrus wastes by manosonication extraction. *International Journal of Biological Macromolecules*, *176*, 332–341. https://doi.org/10.1016/j.ijbiomac.2021.01.216

Ilavsky, J., & Jemian, P. R. (2009). Irena: Tool suite for modeling and analysis of small-angle scattering. *Journal of Applied Crystallography*, *42*(2), 347–353. https://doi.org/10.1107/S0021889809002222

Jiang, L. N., Shang, J. J., He, L. B., & Dan, J. M. (2012). Comparisons of Microwave-Assisted and Conventional Heating Extraction of Pectin from Seed Watermelon Peel. *Advanced Materials Research*, *550–553*, 1801–1806. https://doi.org/10.4028/www.scientific.net/amr.550-553.1801

Kieffer, J., & Ashiotis, G. (2014). PyFAI: a Python library for high performance azimuthal integration on GPU. *Powder Diffraction*, *28*(SUPPL.2), 3.

Kpodo, F. M., Agbenorhevi, J. K., Alba, K., Oduro, I. N., Morris, G. A., & Kontogiorgos, V. (2018). Structure-Function Relationships in Pectin Emulsification. *Food Biophysics*, *13*(1), 71–79. https://doi.org/10.1007/s11483-017-9513-4

Lee, K. Y., & Choo, W. S. (2020). Extraction Optimization and Physicochemical Properties of Pectin from Watermelon (Citrullus lanatus) Rind: Comparison of Hydrochloric and Citric acid Extraction. *Journal of Nutraceuticals and Food Science*, *5*(1), 1. https://doi.org/10.36648/nutraceuticals.5.1.1

Lequeux, F. (1998). Emulsion rheology. *Current Opinion in Colloid and Interface Science*, *3*(4), 408–411. https://doi.org/10.1016/S1359-0294(98)80057-5

Leroux, J., Langendorff, V., Schick, G., Vaishnav, V., & Mazoyer, J. (2003). Emulsion stabilizing properties of pectin. *Food Hydrocolloids*, *17*(4), 455–462. https://doi.org/10.1016/S0268-005X(03)00027-4

Luo, S. Z., Hu, X. F., Jia, Y. J., Pan, L. H., Zheng, Z., Zhao, Y. Y., Mu, D. D., Zhong, X. Y., & Jiang, S. T. (2019). Camellia oil-based oleogels structuring with tea polyphenol-palmitate particles and citrus pectin by emulsion-templated method: Preparation, characterization and potential application. *Food Hydrocolloids*, *95*, 76–87. https://doi.org/10.1016/j.foodhyd.2019.04.016

Martínez-Abad, A., Giummarella, N., Lawoko, M., & Vilaplana, F. (2018). Differences in extractability under subcritical water reveal interconnected hemicellulose and lignin recalcitrance in birch hardwoods. *Green Chemistry*, *20*(11), 2534–2546. https://doi.org/10.1039/c8gc00385h

McClements, D. J. (2015). *Food Emulsions*. CRC Press. https://doi.org/10.1201/b18868

Méndez, D. A., Fabra, M. J., Gómez-Mascaraque, L., López-Rubio, A., & Martinez-Abad, A. (2021). Modelling the Extraction of Pectin towards the Valorisation of Watermelon Rind Waste. *Foods*, *10*(4), 738. https://doi.org/10.3390/foods10040738

Meng, Z., Qi, K., Guo, Y., Wang, Y., & Liu, Y. (2018). Macro-micro structure characterization and molecular properties of emulsion-templated polysaccharide oleogels. *Food Hydrocolloids*, *77*, 17–29. https://doi.org/10.1016/j.foodhyd.2017.09.006

Minjares-Fuentes, R., Femenia, A., Garau, M. C., Meza-Velázquez, J. A., Simal, S., & Rosselló, C. (2014). Ultrasound-assisted extraction of pectins from grape pomace using citric acid: A response surface methodology approach. *Carbohydrate Polymers*, *106*(1), 179–189. https://doi.org/10.1016/j.carbpol.2014.02.013

Nakauma, M., Funami, T., Noda, S., Ishihara, S., Al-Assaf, S., Nishinari, K., & Phillips, G. O. (2008). Comparison of sugar beet pectin, soybean soluble polysaccharide, and gum arabic as food emulsifiers. 1. Effect of concentration, pH, and salts on the emulsifying properties. *Food Hydrocolloids*, *22*(7), 1254–1267. https://doi.org/10.1016/j.foodhyd.2007.09.004

Neckebroeck, B., Verkempinck, S. H. E., Van Audenhove, J., Bernaerts, T., de Wilde d'Estmael, H., Hendrickx, M. E., & Van Loey, A. M. (2021). Structural and emulsion stabilizing properties of pectin rich extracts obtained from different botanical sources. *Food Research International*, *141*, 110087. https://doi.org/10.1016/j.foodres.2020.110087

Ngouémazong, D. E., Christiaens, S., Shpigelman, A., van Loey, A., & Hendrickx, M. (2015). The Emulsifying and Emulsion-Stabilizing Properties of Pectin: A Review. *Comprehensive Reviews in Food Science and Food Safety*, *14*(6), 705–718. https://doi.org/10.1111/1541-4337.12160

Öğütcü, M., & Yilmaz, E. (2014). Oleogels of virgin olive oil with carnauba wax and monoglyceride as spreadable products. *Grasas y Aceites*, *65*(3). https://doi.org/10.3989/gya.0349141

Oliveira, T. Í. S., Rosa, M. F., Cavalcante, F. L., Pereira, P. H. F., Moates, G. K., Wellner, N., Mazzetto, S. E., Waldron, K. W., & Azeredo, H. M. C. (2016). Optimization of pectin extraction from banana peels with citric acid by using response surface methodology. *Food Chemistry*, *198*, 113–118. https://doi.org/10.1016/j.foodchem.2015.08.080

Petkowicz, C. L. O., Vriesmann, L. C., & Williams, P. A. (2017). Pectins from food waste: Extraction, characterization and properties of watermelon rind pectin. *Food Hydrocolloids*, *65*, 57–67. https://doi.org/10.1016/j.foodhyd.2016.10.040

Prasanna, V., Prabha, T. N., & Tharanathan, R. N. (2007). Fruit ripening phenomena-an overview. *Critical Reviews in Food Science and Nutrition*, *47*(1), 1–19. https://doi.org/10.1080/10408390600976841

Rodsamran, P., & Sothornvit, R. (2019). Microwave heating extraction of pectin from lime peel: Characterization and properties compared with the conventional heating method. *Food Chemistry*, *278*(November 2018), 364–372. https://doi.org/10.1016/j.foodchem.2018.11.067

Schmidt, U. S., Schmidt, K., Kurz, T., Endreß, H. U., & Schuchmann, H. P. (2015). Pectins of different origin and their performance in forming andstabilizing oil-in-water-emulsions. *Food Hydrocolloids*, *46*, 59–66. https://doi.org/10.1016/j.foodhyd.2014.12.012

Schols, H. A., Visser, R. G. F., & Voragen, A. G. J. (2009). Pectins and Pectinases. In H. A. Schols, R. G. F. Visser, & A. G. J. Voragen (Eds.), *Pectins and Pectinases*. Wageningen Academic Publishers. https://doi.org/10.3920/978-90-8686-677-9

Schols, H. A., & Voragen, A. G. J. (2003). Pectic Polysaccharides. In J. R. Whitaker, A. G. J. Voragen, & D. W. S. Wong (Eds.), *Handbook of food enzymology* (Vol. 353, Issue 2, pp. 829–843). Dekker. https://doi.org/10.1201/9780203910450-68

Schuch, A., Schuchmann, H., & Gaukel, V. (2015). Rheology of Emulsions. In *Encyclopedia of Membranes* (pp. 1–2). Springer Berlin Heidelberg. https://doi.org/10.1007/978-3-642-40872-4_1884-1

Sousa, A. G., Nielsen, H. L., Armagan, I., Larsen, J., & Sørensen, S. O. (2015). The impact of rhamnogalacturonan-I side chain monosaccharides on the rheological properties of citrus pectin. *Food Hydrocolloids*, *47*, 130–139. https://doi.org/10.1016/j.foodhyd.2015.01.013

Tang, Y. R., & Ghosh, S. (2020). Stability and rheology of canola protein isolate-stabilized concentrated oil-in-water emulsions. *Food Hydrocolloids*, 106399. https://doi.org/10.1016/j.foodhyd.2020.106399

Verkempinck, S. H. E., Kyomugasho, C., Salvia-Trujillo, L., Denis, S., Bourgeois, M., van Loey, A. M., Hendrickx, M. E., & Grauwet, T. (2018). Emulsion stabilizing properties of citrus pectin and its interactions with conventional emulsifiers in oil-in-water emulsions. *Food Hydrocolloids*, *85*, 144–157. https://doi.org/10.1016/j.foodhyd.2018.07.014

Voragen, A. G. J. J., Coenen, G.-J. J., Verhoef, R. P., & Schols, H. A. (2009). Pectin, a versatile polysaccharide present in plant cell walls. *Structural Chemistry*, *20*(2), 263–275. https://doi.org/10.1007/s11224-009-9442-z

Wai, W. W., Alkarkhi, A. F. M., & Easa, A. M. (2010). Effect of extraction conditions on yield and degree of esterification of durian rind pectin: An experimental design. *Food and Bioproducts Processing*, *88*(2–3), 209–214. https://doi.org/10.1016/J.FBP.2010.01.010

Wiles, P. G., Gray, I. K., Kissling, R. C., Delahanty, C., Evers, J., Greenwood, K., Grimshaw, K., Hibbert, M., Kelly, K., Luckin, H., McGregor, K., Morris, A., Petersen, M., Ross, F., & Valli, M. (1998). Routine Analysis of Proteins by Kjeldahl and Dumas Methods: Review and Interlaboratory Study Using Dairy Products. *Journal of AOAC INTERNATIONAL*, *81*(3), 620–632. https://doi.org/10.1093/jaoac/81.3.620

Xu, A. Y., Melton, L. D., Ryan, T. M., Mata, J. P., Rekas, A., Williams, M. A. K., & McGillivray, D. J. (2018). Effects of polysaccharide charge pattern on the microstructures of β-lactoglobulin-pectin complex coacervates, studied by SAXS and SANS. *Food Hydrocolloids*, *77*, 952–963. https://doi.org/10.1016/J.FOODHYD.2017.11.045

Zhai, H., Gunness, P., & Gidley, M. J. (2021). Depletion and bridging flocculation of oil droplets in the presence of β-glucan, arabinoxylan and pectin polymers: Effects on lipolysis. *Carbohydrate Polymers*, *255*, 117491. https://doi.org/10.1016/j.carbpol.2020.117491

Zhang, S., He, Z., Cheng, Y., Xu, F., Cheng, X., & Wu, P. (2021). Physicochemical characterization and emulsifying properties evaluation of RG-I enriched pectic polysaccharides from Cerasus humilis. *Carbohydrate Polymers*, *260*, 117824. https://doi.org/10.1016/j.carbpol.2021.117824

8 Supplementary material

1.5AP-60SO	3.5AP-60SO	1.5CP-60SO	3.5CP-60SO
			

Figure S1. Macroscopic images evidencing phase separation of freshly prepared emulsions prepared with AP or CP and 60% (w/v) SO.

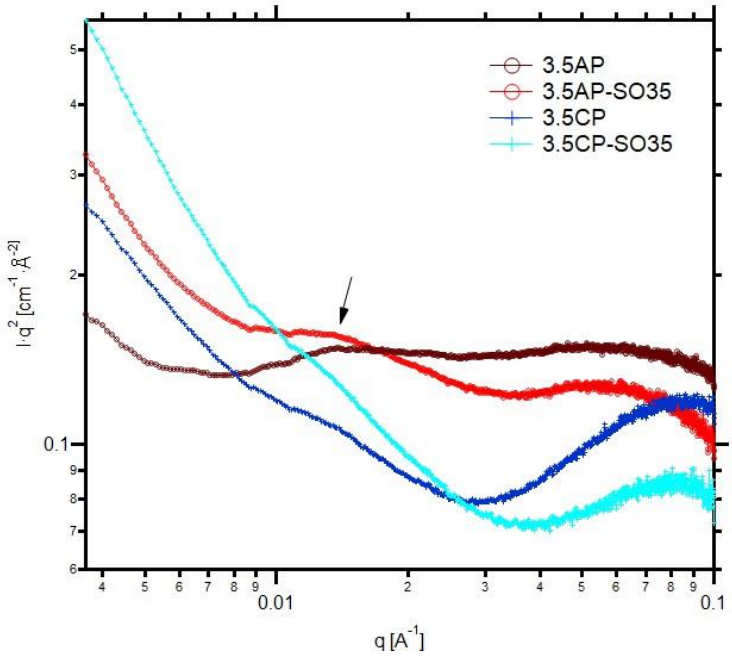

Figure S2. Kratky plot of the SAXS data from the pectin solutions (3.5AP and 3.5 CP) and corresponding emulsions (3.5 AP-SO35 and 3.5CP-SO35). Arrow points out to the structural feature observed at low q.

3.1.3

TAILORING STRUCTURAL, RHEOLOGICAL AND GELLING PROPERTIES OF WATERMELON RIND PECTIN BY ENZYMATIC TREATMENTS.

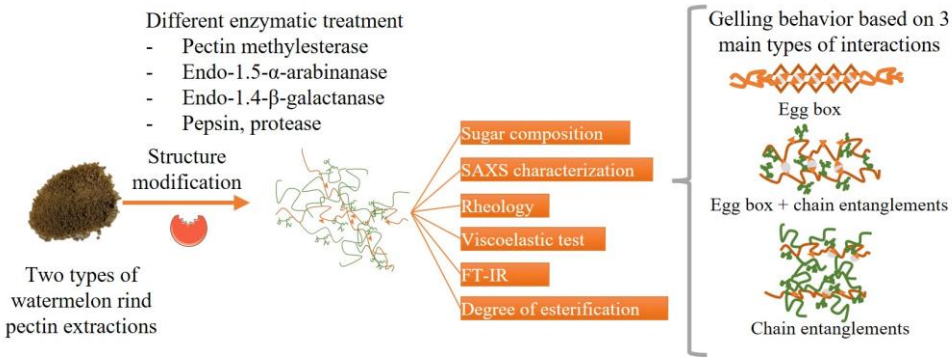

This section is an adapted version of the following published research article:

Méndez, D. A., Martínez-Abad, A., Martínez-Sanz, M., López-Rubio, A., & Fabra, M. J. (2022). Tailoring structural, rheological and gelling properties of watermelon rind pectin by enzymatic treatments. Food Hydrocolloids, 135, 108119.

---

1 Abstract

In this work, pectin extracts from watermelon rind (WRP) were enzymatically treated to evaluate their potential for preparing hydrogels with the addition of $CaCl_2$. Based on a previous work, two different conditions were selected to obtain WRP extracts according to the 1) highest yield (OP) or 2) highest yield without negatively affecting the branching and native structure of pectin (OPA). Firstly, both WRP extracts were enzymatically modified using different treatments (de-esterification and/or de-branching of galacturonic and arabinose side chains, and deproteinization), and their impact on the esterification degree, monosaccharide composition and changes on their structural properties (linearity and branching degree) were analysed. Then, the effect of the structural properties of the resulting pectin on the rheological behaviour and nanostructure of the hydrogels was investigated. The presence of long branched side chains and high methyl-esterified galacturonic acid chains promoted the formation of weaker hydrogels whereas de-esterification of the original pectin enabled intermolecular association giving rise to stronger hydrogels with the formation of ordered and densely packed structures (as deduced from SAXS results). However, the presence of small arabinogalactans side chains in the de-branched and de-esterified pectin extracts acted as reinforcement agents, inducing the formation of more densely packed networks and stronger hydrogels than their less-branched counterpart. These results demonstrated the impact of the pectin structure on the hydrogel-forming capacity.

2 Introduction

Pectin is a family of complex heteropolysaccharides consisting of homogalacturonan (HG), rhamnogalacturonan I (RG-I) and rhamnogalacturonan II (RG-II). HG is a linear chain of 1,4-linked α-D-galacturonic acid (GalA) residues, which can be methoxylated at C-6 and/or acetylated on the O-2 and/or O-3 position. The degree and distribution of methoxylation are important parameters for their gelling properties (Ngouémazong et al., 2012; Voragen et al., 2009). HG is often referred to as the pectin smooth region, whereas RG-I is called the hairy region since its backbone can be abundantly substituted by neutral sugars like arabinose and galactose forming arabinan, galactan and arabinogalactans on the side chains,

predominantly attached to the O-4 position of rhamnose (Lara-Espinoza et al., 2018). In contrast, RG-II is composed of a HG backbone, which is branched with chains at C-2 and C-3. These side chains include arabinose, fucose, galactose, rhamnose, glucuronic acid, galacturonic acid, xylose, apiose and fucose units.

The worldwide application of pectin in the food industry as gelling, thickening, and stabiliser agents (Schols & Voragen, 2003a) together with the global aim towards sustainability, has prompted the interest in valorising by-products or residues from the food chain to find new pectin sources following circular economy principles. Specifically, watermelon (*Citrillus lanatus*), has been considered a promising pectin source, ascribed to the high amounts of biomass waste generated by the global production that accounts 100 million tonnes in 2019 (FAOSTAT, 2021), of which one third (rind) is discarded (Petkowicz et al., 2017). Although different approaches for the extraction and characterization of watermelon rind pectin (WRP) have been proposed and discussed in the literature (Campbell, 2006; Hartati & Subekti, 2015; Lee & Choo, 2020; Méndez, Fabra, Gómez-Mascaraque, et al., 2021; Petkowicz et al., 2017; Prakash Maran et al., 2014), the understanding of the relationship between watermelon pectin structure and functionality could provide an opportunity to customize their functional and technological properties depending on the final application.

In a previous work, a Box–Behnken response surface experimental design was carried out to optimize the pectin extraction process from watermelon rind (Méndez, Fabra, Gómez-Mascaraque, et al., 2021) and, the conditions in which the yield was the highest (OP) were used to evaluate the emulsifying properties of this pectin extract. The compositional features showed relevant structural differences compared to other conventional pectin, related to the higher content of neutral sugars. At optimum yield conditions, WRP yield (13.4%), purity (464.6 µg/g galacturonic acid) and molar mass (106.1 kDa) were comparable to traditional pectin sources but showed branching degree with longer galactan side chains and higher protein interaction (Méndez, Fabra, Gómez-Mascaraque, et al., 2021; Méndez, Fabra, Martínez-Abad, et al., 2021). Its greater emulsifying capacity as compared to commercial citrus or apple pectin was ascribed to the presence of longer side chains in the WRP

combined with its relatively high protein content (mainly acting as the surface-active material) (Méndez, Fabra, Martínez-Abad, et al., 2021).

Pectin-modifying enzymes are of great interest to make controlled changes on the molecular structure of this polysaccharide and several works have reported about the effects of side chain- and backbone-modifying enzymes on i) the composition and structure of pectin, ii) the rheological behaviour of the resulting pectin dispersions and iii) the gelling capacity of the corresponding gels (Funami et al., 2007, 2011; Nakauma et al., 2008). In this study, the gelling capacity of WRP before and after enzymatic treatments was explored. In contrast to previous studies, the aim of the present work was not only to investigate the effect of controlled enzymatic debranching, de-esterification and protein removal on watermelon rind pectin composition and molecular structure but also to deeply characterize the structure of the pectin hydrogels using small angle X-ray scattering (SAXS) and rheology, in order to understand the role of the RG-I side chains and protein moieties on the molecular structure of the gel of the resulting pectin.

3 Materials and methods

3.1 Sample preparation

Fresh watermelon (*Citrullus lanatus*) fruits were kindly supplied by Anecoop S. Coop. during the summer season of 2019 from Almeria, Spain. The fruits were processed removing the red flesh and keeping the rind, which were later used for pectin extraction. The rinds were initially chopped in pieces of 0.5 – 2.5 cm and immersed in distilled water for 10 min with gentle agitation and, after draining the water, they were freeze-dried to keep them stable before pectin extraction. Sodium hydroxide (pharma grade) and hydrochloric acid was supplied by Sigma-Aldrich (Stenheim, Germany). Acetone (99%) and ethanol (96% v/v, USP grade) were purchased from WVR chemicals and Panreac Applichem (Darmstadt, Germany), respectively. The enzymes pectin methyl-esterase (PME) from orange peel (≥150 units/mg protein), alcohol oxidase solution from *Pichia pastoris* (EC 1.1.3.13), pepsin (EC 3.4.23.1), protease from *Aspergillus oryzae* (EC 232.752.2), 2,4-pentanedione (≥99%) and the analytical standards: D-(+)-galactose, D-(+)-galacturonic acid

monohydrate, L-rhamnose monohydrate, D-glucuronic Acid D-(+)-mannose, D-(+)-glucose, D-(-)-fructose, L-(-)-fucose, D-(+)-xylose, L-(+)-arabinose were all purchased from Sigma-Aldrich. Polygalacturonic acid from citrus pectin low methoxy (5%) (LMCP), endo-1,5-α-arabinanase (EAR) (*Aspergillus niger*, EC 3.2.1.99) and endo-1,4-β-galactanase (EGA) (*Aspergillus niger*, EC 3.2.1.89), were supplied by Megazyme Ltd., (Wicklow, Ireland).

3.2 Pectin extraction

Following the Box-Behnken response surface experimental design carried out to optimize the pectin extraction process from watermelon rind (Méndez, Fabra, Gómez-Mascaraque, et al., 2021), two different conditions were selected for this work: i) where the yield was the highest (OP) (95 °C pH 1.36 and 90 min) and, ii) where the yield was the highest without negatively affecting the branching and native structure of pectin (OPA) (81.7 °C pH 2.15 and 90 min). Briefly, the ground WR was immersed in water and acidified using a 1 M HCl solution, with a solid-liquid ratio of 1:20 (w/v). Subsequently, after acid extraction the extracted solution was filtered with a muslin cloth, followed by vacuum filtration using Whatman filter paper No. 4 at 60 °C, mixed with 96% (v/v) ethanol at a 1:3 (v/v) ratio and left overnight in the freezer. The coagulated pectin (WRP) was centrifuged at 12000 rpm for 20 min and consecutively washed with 96% (v/v) ethanol and acetone twice to remove water and low molecular weight or polar compounds. Finally, the material was dried at 60 °C in a hot air oven until constant weight, then grounded and stored in a desiccator until further analysis.

3.3 Preparation of enzymatically modified pectin samples

Both pectin extracts (OP and OPA) were enzymatically modified using six different treatments. Briefly, stock solutions of each pectin extract were prepared by dispersing 1% (w/v) in 100 mM PBS (pH 7.2) or in 100 mM citrate buffer (pH 4.0), overnight, under gentle magnetic stirring. These two stock solutions were prepared according to the optimum pH conditions provided by the supplier: PME optimum pH was around the neutral whereas EGA, EAR, pepsin and proteases were active at pH 4.0. The enzymes were added and

incubated at 40 °C for 24 h under gentle stirring, as described below and with the following aims:

i) De-esterification: PME (10 units per 1.0 g WRP) was incorporated in the pectin solutions prepared with PBS. Potential side activities of PME due to lack of purity were ruled out as no increase in reducing sugars was noted, following the 3,5- dinitrosalicilic colorimetric assay.

ii) De-branching of galacturonic side chains: EGA (10 units per 1.0 g WRP) was added to the pectin solutions prepared with citrate buffer.

iii) De-branching of arabinose side chains: EAR (10 units per 1.0 g WRP) was dissolved in the pectin/citrate buffer-stock solutions.

iv) De-esterification and de-branching of galacturonic side chains: EGA and PME were used at the concentrations reported for i) and ii) and gently stirred in the pectin/PBS-stock solutions.

v) De-esterification and de-branching of arabinose side chains: EAR and PME were dissolved in pectin/PBS-stock solutions and used at the concentrations stated at i) and iii).

vi) Deproteinization: pectin/citrate buffer stock solutions were used and, both pepsin (700 unit per 1.0 g WRP) and protease (70 unit per 1.0 g WRP) (PP) were added and incubated at 40 °C for 24 h with gentle stirring.

All enzyme-treated pectin solutions were heated at 90 °C for 5 min to stop the enzymatic reaction. The resulting solutions were then rapidly cooled in an ice bath and dialyzed against deionized water at 20 °C through a dialysis membrane with a 3.5 kDa molecular weight cut-off, followed by freeze-drying. The freeze-dried samples were stored in a desiccator at 20 °C until analysis. Sample's nomenclature was "*x*-*y*' where '*x*' refers to the type of pectin extract, and "*y*" specifies the enzymes used for each treatment.

3.4 Compositional characterization

3.4.1 Monosaccharide composition

The sugar composition of the samples was determined after acidic methanolysis as previously described by Méndez, Fabra, Gómez-Mascaraque, et al., (2021). The monosaccharides were analysed using high performance anion exchange chromatography with pulsed amperometric detection (HPAEC-PAD) with an ICS-6000 system (Dionex) equipped with a CarboPac PA1 column (4 × 250 mm, Dionex). Control samples of known concentrations of mixtures of glucose (Glc), fucose (Fuc), rhamnose (Rha), galactose (Gal), arabinose (Ara), xylose (Xyl), mannose (Man), galacturonic acid (GalA) and glucuronic acid (GlcA) were used for calibration.

3.4.2 Determination of the degree of esterification (DE)

The DE of all pectin samples was calculated as the ratio of the molar number of methyl-groups (as methanol) to the molar amount of GalA estimated per gram of sample and expressed in percentage. The methyl esters of all pectin samples were hydrolysed and the methanol produced during pectin saponification was determined based on a colorimetric method (Klavons & Bennett, 1986). The GalA content of the pectin was taken from monosaccharide composition. All concentrations were determined on dry basis.

3.4.3 Protein content

The protein content of the two pectin types was analysed for total nitrogen content using an Elemental Analyser Rapid N Exceed (Paralab S.L., Spain). About 100 mg of each of the powdered samples were pressed to form a pellet which was then analysed using the Dumas method, which is based on the combustion of the sample and subsequent detection of the released N_2 (Wiles et al., 1998). The total protein content was calculated from the nitrogen content multiplied by a factor of 6.25.

3.5 Rheological characterization

3.5.1 Flow-curves of pectin solutions

The viscosity of the pectin solutions was analysed using a rheometer HR20, (TA Instruments, Montreal, QC, Canada) with a 40 mm parallel plate geometry. Briefly, pectin solutions at 2% (w/v) were dissolved in Milli-Q water (18.2 MΩ.cm resistance, Millipore, USA). Samples were loaded on the bottom of a Peltier plate. The viscosity was measured by applying a rotational shear between the two parallel plates at 20 °C with a gap of 500 µm as a function of increasing shear rate from 0.1 s^{-1} to 200 s^{-1}. The rheological behaviour of the samples was recorded with the TRIOS software version 5.1.1.46572 (TA Instruments, Montreal, QC, Canada. The power law model Eq. (1) was applied to determine the consistency index (k) and the flow behaviour index (n). The apparent viscosities were determined at 100 s^{-1}.

$$\sigma = K \gamma^n \qquad \text{(Eq. 1)}$$

3.5.2 Preparation of Ca^{2+} pectin hydrogels

Each pectin sample was initially dissolved in Milli-Q water (18.2 MΩcm resistance, Millipore, USA) in order to obtain 1% (w/v) pectin solutions. The pH of the solution was adjusted to 5.0 using NaOH solutions of concentrations varying from 0.1 to 1 M, and under continuous vigorous stirring. The resulting solutions were immediately used for gel preparation.

Then, a 3 M $CaCl_2$ stock solution was prepared using Milli-Q water. Prior to its use, this stock solution was diluted so as to produce gels with defined Ca^{2+} concentration expressed as the stoichiometric ratio ($R = 2[Ca^{2+}]/[COO^-]$) (Capel et al., 2006). The R-value of each prepared gel was 2.0.

Ca^{2+} pectin gels were prepared on the lower plate of a stress controlled HR20, rheometer (TA Instruments, Montreal, QC, Canada). A few microliters of pectin and $CaCl_2$ solutions were preheated to 50 °C. Meanwhile, the Peltier controlled lower plate of the rheometer was

preheated to 50 °C. Specifically, 670 µL of the pre-heated pectin solution were placed at the centre of the lower plate. Subsequently, 35 µL of the preheated $CaCl_2$ was added dropwise over the entire pectin surface. The upper geometry (40 mm B parallel plate) was then lowered to the set measuring gap (0.5 mm). The edge of the sample was covered with a layer of paraffin oil to prevent evaporation during gel formation and measurements. To limit temperature fluctuations within the sample, the upper plate was preheated and lowered over the loaded sample.

3.5.3 Small-amplitude oscillatory shear tests

The loaded (time zero of the experiment) sample with Ca^{2+} cations mixed was allowed to equilibrate for 5 min (to ensure complete calcium diffusion through the 670 µL pectin solution), and was subsequently cooled to 20 °C at a rate of 6 °C/min. After that, the sample was maintained for 1 h at 20 °C to ensure a complete gel formation. Before measurements, linear viscoelastic sweeps were performed from 0.01 to 100% strain at a frequency of 1 rad/s, in order to define the linear viscoelastic region of the gels at 20 °C. A dynamic viscoelastic test was conducted in the frequency range from 0.01 to 100 rad/s, and the viscoelastic properties (storage moduli -G'- and loss moduli -G''-) of the hydrogels were recorded as a function of the frequency. Although the aforementioned gel preparation method and rheological measurements have been reported to be reproducible (Doungla & Vandebril, 2009), all experiments were performed in duplicate, on freshly prepared gels.

3.6 Fourier transform infrared (FTIR)

The IR spectra of samples were measured in the wavenumber range of 600–4000 cm^{-1} by a Jasco FT-IR-4100 spectrometer (Tokyo, Japan) coupled with a TGS detector. The spectral resolution was 4 cm^{-1}. Each spectrum was the average of 32 scans. During the whole experiment, the temperature was kept at about 25 °C and the humidity was kept at a stable level in the laboratory.

3.7 SAXS analysis of pectin hydrogels

SAXS experiments were carried out in the Non-Crystalline Diffraction beamline, BL-11, at ALBA synchrotron light source (www.albasynchrotron.es). Briefly, the samples were prepared at 1% (w/v), following the same procedure in section 2.5.2. Initially, the $CaCl_2$ solution was added to the capillaries keeping the same stoichiometric ratio as commented before for the rheology measurements. Then, the pectin solution was slowly added to obtain the hydrogel inside the capillary. The samples were placed in sealed 2 mm quartz capillaries (Hilgenberg GmbH, Germany). The energy of the incident photons was 12.4 KeV or equivalently a wavelength, λ, of 1 Å. The SAXS diffraction patterns were collected by means of a photon counting detector, Pilatus 1M, with an active area of 168.7 x 179.4 mm^2, an effective pixel size of 172 x 172 μm^2 and a dynamic range of 20 bits. The sample-to-detector distance was set to 7570 mm, resulting in a q range with a maximum value of q = 0.19 $Å^{-1}$. An exposure time of 10 s was selected based on preliminary trials. The data reduction was treated by pyFAI python code (ESRF) (Kieffer & Ashiotis, 2014), modified by ALBA beamline staff, to do on-line azimuthal integrations from a previously calibrated file. The calibration files were created from a silver behenate (AgBh) standard. The intensity profiles were then represented as a function of q using the IRENA macro suite (Ilavsky & Jemian, 2009) within the Igor software package (Wavemetrics, Lake Oswego, Oregon).

The scattering patterns were properly described using different fitting functions depending on the sample: (i) correlation length, (ii) two-level unified model or (iii) three-level unified model.

The correlation length model is described by the following equation:

$$I(q) = \frac{A}{q^n} + \frac{C}{1+(q\xi_L)^m} + bkg \qquad \text{(Eq. 2)}$$

The first term in equation (2) is described by a power-law function and accounts for the scattering from large clusters in the low q region, while the second term, consisting of a Lorentzian function, describes scattering from polymer chains in the high q region. n is the power-law exponent, A is the power-law coefficient, m is the Lorentzian exponent, C is the

Lorentzian coefficient and ξ_L is the correlation length for the polymer chains (which gives an indication of the gel's mesh size). The third term accounts for the incoherent background.

The unified model considers that, for each individual level, the scattering intensity is the sum of a Guinier term and a power-law function (Beaucage, 1995, 1996):

$$I(q) = \sum_{i=1}^{N} G_i \, exp\left(-q^2 \cdot \frac{R_{g,i}^2}{3}\right) + \frac{B_i\left[erf\,(qR_{g,i}/\sqrt{6})\right]^{3P_i}}{q^{P_i}} + bkg \qquad \text{(Eq. 3)}$$

where $G_i = c_i V_i \Delta SLD_i{}^2$ is the exponential prefactor (where V_i is the volume of the particle and ΔSLD_i is the scattering length density (SLD) contrast existing between the ith structural feature and the surrounding solvent), $R_{g,i}$ is the radius of gyration describing the average size of the ith level structural feature, B_i is a q-independent prefactor specific to the type of power-law scattering with power-law exponent, P_i, and bkg is the background. In this particular case, the two (i=2) or three (i=3) levels were considered, depending on the sample. In all cases, the largest structural level was modelled only by a power-law ($R_{g1}$was fixed at a value >> q_{min}^{-1} of 5000 Å).

The obtained values from the fitting coefficients are those that minimize the value of Chi-squared, which is defined as:

$$\chi^2 = \sum \left(\frac{y - y_i}{\sigma_i}\right)^2 \qquad \text{(Eq. 4)}$$

where y is a fitted value for a given point, y_i is the measured data value for the point and σ_i is an estimate of the standard deviation for y_i. The curve fitting operation is carried out iteratively and for each iteration, the fitting coefficients are refined to minimize χ^2.

3.8 Statistical analysis

All statistical analysis was performed using the statistical software Statgraphics Centurion XVI® (Manugistics Inc.; Rockville, MD, USA). Statistically significant differences were determined by using one-way analyses of variance (ANOVA) and sample comparison with LSD at 95% confidence level (*p-value* < 0.05).

4 Results and Discussion

4.1 Sugar constituents, composition and structure of the enzymatically-treated WRP extracts

Compositional and structural analyses were firstly carried out on WRP extracts (OP and OPA) and on the resulting enzymatically-treated pectin samples. Sugar ratios were also calculated based on previous literature (Denman & Morris, 2015; Houben et al., 2011; Méndez, Fabra, Gómez-Mascaraque, et al., 2021; Ognyanov et al., 2018) to estimate the linearity (RL) and branching (RB) degree of the various pectin and, thus, to get a better understanding on their structural differences. Table 1 summarizes the results from the compositional analysis. When comparing OPA and OP, it was clearly seen that the branching degree and relative content of Ara was significantly higher in OPA, and suggests the presence of high and long distribution of arabinan and/or arabinogalactan side chains. This is explained by the harsher acid conditions in the extraction process, which are known to more specifically cleave the neutral sugar side chains, especially arabinosyl residues (Méndez, Fabra, Gómez-Mascaraque, et al., 2021; Ngouémazong et al., 2012; Schols & Voragen, 2003b; Verhoef et al., 2009). As reported in our previous works, WRP generally displayed a lower rhamnose content compared to typical industrial pectin from citrus or apple. In this sense, the relative content of Rha was even lower in OPA than in OP, suggesting the presence of longer sugar side chains in the rhamnogalacturonan (RG-I) region. Furthermore, the protein content was significantly higher in OPA, ascribed to the milder extraction conditions used in this case and attributed to the protein interaction with arabinogalactan side chains in the highly branched structures, as previously reported (Méndez, Fabra, Gómez-Mascaraque, et al., 2021).

Table 1. Chemical composition and sugar content of the different enzymatic treatments (pectin methyl esterase (PME), endo-1,5-α-arabinanase (EAR), endo-1,4-β-galactanase (EGA), pepsin, protease (PP)) with OP and OPA.

Sample	Protein (%)	DE (%)	Fuc (µg/mg)	Rha (µg/mg)	Ara (µg/mg)	Gal (µg/mg)	GalA (µg/mg)	RB [a]	RL[b]	RG-I %[c]
OPA	18.0(1.5)^{bc}	57.1(4.6)^{c}	5.1(0.4)^{c}	9.4(0.8)^{f}	30.9 (2.7)^{a}	170.9(14.8)^{ab}	345.7(28.9)^{g}	21.38	1.63	20.20
OPA-PME	21.1(2.6)^{a}	3.7(0.1)^{hi}	3.8(1.2)^{hi}	15.2(0.4)^{bc}	25.3(1.8)^{b}	103.5(16.4)^{d}	529.4(0.3)^{a}	8.45	3.67	12.91
OPA-EAR	20.6(3.3)^{ab}	35.9(0.1)^{f}	5.1(0.6)^{f}	11.2(1.0)^{cd}	15.4(0.4)^{d}	163.7(1.8)^{a}	393.9(12.3)^{defg}	16.01	2.07	17.93
OPA-EGA	17.3(0.1)^{c}	33.4(0.4)^{e}	4.9(0.6)^{e}	10.6(0.2)^{ef}	22.9(0.3)^{bc}	149.3(4.2)^{bc}	364.1(1.3)^{fg}	16.27	1.97	17.25
OPA-PME/EAR	19.0(0.2)^{abc}	13.1(0.2)^{i}	1.3(0.1)^{i}	17.5(0.9)^{b}	20(1.0)^{c}	29.1(1.4)^{f}	505.5(24.5)^{ab}	2.80	7.59	4.95
OPA-PME/EGA	19.6(1.7)^{abc}	13.7(0.3)^{h}	1.5(0.1)^{h}	15.6(0.9)^{bc}	24.5(1.3)^{b}	34.1(1.8)^{f}	402.5(20.9)^{defg}	3.76	5.44	5.90
OPA-PP	11.9(1.4)^{d}	42.6(2.6)^{c}	2.5(0.1)^{c}	17.4(1.9)^{b}	29.6(2.8)^{a}	71.0(2.6)^{e}	451.8(53.9)^{abcd}	5.77	3.81	10.09
OP	8.2(0.4)^{e}	50.1(2.1)^{b}	4.8(0.5)^{b}	16.4(4.6)^{a}	0.5(0.9)^{e}	158.8(11.1)^{ab}	464.6(42.2)^{abc}	9.73	2.62	15.97
OP-PME	9.6(0.1)^{de}	4.9(0.1)^{i}	1.0(0.1)^{i}	20.8(0.9)^{a}	1.4(0.1)^{e}	22.9(1.1)^{f}	517.7(23.5)^{a}	1.17	11.52	2.47
OP-EAR	8.2(2.0)^{e}	22.4(0.3)^{d}	2.9(0.2)^{d}	12.1(1.7)^{de}	1.5(0.1)^{e}	90.7(0.2)^{de}	415.8(63.1)^{cdef}	7.59	3.99	9.25
OP-EGA	7.3(0.1)^{e}	31.0(0.6)^{de}	3.9(0.0)^{de}	15.2(1.3)^{bc}	1.3(0.1)^{e}	135.8(2.4)^{c}	367.7(23.2)^{efg}	9.02	2.42	13.74
OP-PME/EAR	9.2(0.4)^{de}	4.8(0.07)^{g}	0.9(0.1)^{g}	11.0(0.6)^{ef}	2.8(0.1)^{e}	28.5(1.5)^{f}	383.5(20.0)^{defg}	2.84	9.08	3.15
OP-PME/EGA	8.1(0.01)^{e}	7.7(0.3)^{g}	0.3(0.4)^{g}	17.2(1.3)^{b}	1.4(0.1)^{e}	14.3(1.6)^{f}	479.6(21.7)^{abc}	0.91	14.44	1.60
OP-PP	8.9(0.8)^{e}	42.6(2.6)^{a}	0.9(0.1)^{a}	20.4(0.1)^{a}	1.3(0.1)^{e}	22.8(0.1)^{f}	393.4(17.01)^{defg}	1.18	8.86	2.45
LMCP*	1	5	0	9.07	0.2	9.07	852	1.02	45.45	27.41

[a] A larger value is indicative of larger average size of the branching side chains. (Gal+Ara/Rha).
[b] A larger value suggests of more linear/less branched pectins. (GalA/(Rha+Ara+Gal)).
[c] (2Rha+Ara+Gal).
* LMCP: commercial low methoxy citrus pectin. Datac provided by the company.
Means of each characteristic followed by different letters in the same column (a–j) are significantly different ($p \leq 0.05$), traces or cero values were found for Xyl, Glc, Fru, Man and GlcA. Values in brackets correspond to standard deviation.

As seen in Table 1, the treatment with PME had a significant impact on pectin structure, greatly reducing the esterification degree (DE) of the carbohydrates and significantly modifying the composition, linearity and branching ratios. In fact, enzymes with activity on the neutral side chains (EAR and EGA) produced a smaller reduction in Gal and Ara than that of PME. This shows that a pectin structure with long branched chains and a relatively high content of methylated carboxyl groups (>50%) somehow limited the accessibility of the EAR and EGA to the Ara and Gal active sites, as previously stated for carrot, apple and citrus pectin (Funami et al., 2011; Ngouémazong et al., 2012). This effect was more clearly observed for Gal rather than Ara content, probably because Ara units may be more accessible as loose arabinan structures or external arobinosyl residues in the branched side chains. PME catalyses the de-methyl esterification of galacturonic acid units of pectin, generating free carboxyl groups. This may have had an impact on lower molecular weight non-covalently bound neutral sugar chains, resulting in their removal through dialysis. This effect was more patent in the case of the OP extract, probably ascribed to shorter galactan side chains. On the other hand, the combination of PME with enzymes acting on the neutral sugar side chains (PME-EAR and PME-EGA) produced a substantial reduction in both Gal and Ara content. The reduction of Ara in OP samples was not significant due to the negligible quantities in the starting OP sample. This confirms that the PME facilitated the action of EAR and EGA enzymes, more significantly in less branched pectin. Despite the low contents in RG-II (Méndez, Fabra, Gómez-Mascaraque, et al., 2021) in WRP, de-branching of pectin with enzymatic treatments was also associated to a decrease in the Fuc content.

Arabinogalactan-proteins (AGP) are widely distributed in plant cell walls, consisting of a protein backbone that is rich in hydroxyproline and to which arabinogalactan polysaccharides are covalently attached, although there are many structural subclasses (Hromadová et al., 2021). This interaction between arabinogalactan and protein moieties has been reported in different studies for sugar beet pectin (Bindereif et al., 2021; Oosterveld et al., 2002). The depolymerisation of larger arabinogalactan-protein structures by proteases might result in the removal of smaller protein-carbohydrate fragments through dialysis. As observed in Table 1, the impact of proteolytic enzymes (pepsin and protease; PP) on pectin

was clearly demonstrated by a significant decrease in the Gal content for PP-treated pectin. The removal of arabinogalactan- or galactan-protein complexes results in a significant increase in the linearity (RL) in both OP-PP and OPA-PP samples. In OPA-PP samples, a significant reduction in protein content was observed, probably owed to the initial higher protein content. In OP-PP samples, protein content was not significantly reduced, suggesting both protein and carbohydrates (AGP fragments) were removed in equal amounts. This further explains a higher impact in the branching degree of OP-PP compared to OPA-PP samples.

FT-IR analyses were also carried out to assess the compositional differences between the different pectin samples. The obtained spectra in the wavelength region where pectin characteristic bands are typically detected (1700-600 cm^{-1}) are shown in Figure 1. The bands located at 1022 and 1106 cm^{-1}, which are attributed to glycosidic linkages (C-C, C-O stretching bond, respectively) were observed in all the samples. Their appearance indicated that the pectin had high HG content (Baum et al., 2017; Méndez, Fabra, Gómez-Mascaraque, et al., 2021). In addition, the band at 1046 cm^{-1}, indicative of the presence of neutral sugars, such as arabinose, xylose, and galactose (Baum et al., 2017) was also visible in OPA and OP extracts as a broad shoulder, although the relative intensity was not the same for all the enzymatically-treated samples, being significantly less intense for those in which the enzymatic hydrolysis included PME. This is related to the debranching and, thus, to the lower amount of neutral sugar side chains (as shown in Table 1) which were removed during the dialysis carried out after the enzymatic treatment. It should be noted that the relative intensity of this band also decreased after the PP treatment. All these results are in good agreement with the compositional analysis (cf. Table 1) and evidenced the presence of small amounts of AGP (Chen et al., 2016; Funami et al., 2011) which were lost after the proteolytic treatment.

In agreement with DE analysis (cf. Table 1), the relative intensity of the bands related to the free carboxyl groups COO^-, located at *ca*. 1625 cm^{-1} , and the weaker symmetric vibrating band centred at 1410 cm^{-1} (Baum et al., 2017; Karnik et al., 2016), were clearly increased in the pectin samples hydrolysed with PME (alone or in combination with EAR or EGA),

whereas the band centred at *ca.* 1740 cm^{-1}, ascribed to the vibration of the esterified carbonyl group C=O, decreased in PME-treated samples.

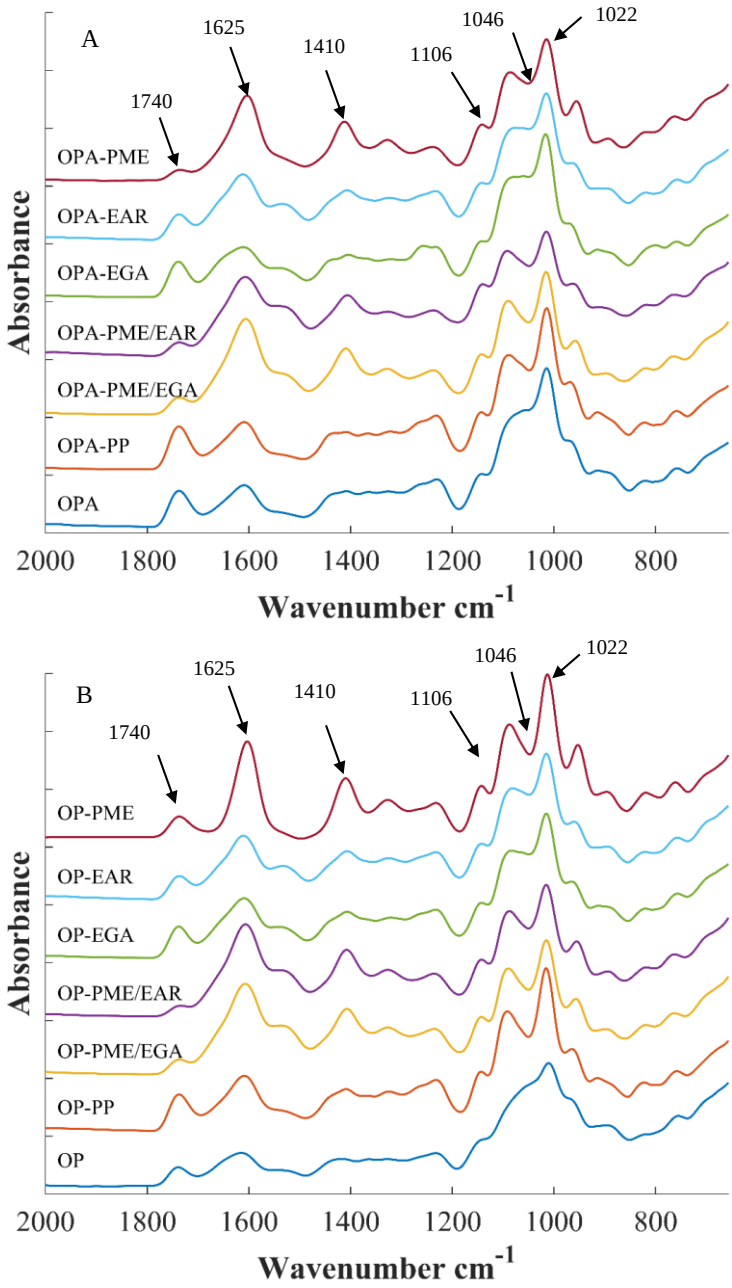

Figure 1. FT-IR spectra of OPA (A) and OP (B) pectin after the different enzymatic treatments.

4.2 Rheological properties of pectin-based solutions and gels

4.2.1 Effect of de-branching on steady shear flow behavior

The rheological behavior of the native and enzymatically-treated pectin extracts was also evaluated and they were compared with a commercial low-methoxyl citrus pectin (LMCP) with a DE 5% in order to understand the role of pectin composition and structure on the viscosity and gelling properties of the corresponding pectin. LMCP was chosen as a reference since it is well-known that low DE pectin have excellent gelling properties.

Complete flow curves presented in Figure 2 show a shear-thinning behavior (pseudoplastic), which was accentuated in the more branched structures (OPA). The presence of highly branched pectin components contributed to the formation of chain entanglements, probably a higher hydrodynamic radius and, consequently, a higher pseudoplastic character of the pectin solution (Celus et al., 2018; Chan et al., 2017). The rheological data of the resulting solutions were accurately fitted to the Ostwald-de Waale model ($r^2 \sim 0.99$) and, the flow (n) and consistency (k) indexes together with the apparent viscosity (η_{ap}) values at a shear rate of 200 s^{-1} are summarized in Table 2. The flow index (n) indicates the degree of Non-Newtonian ($n<1$) characteristics of the fluid whereas the consistency index gives an idea of the viscosity of the fluid. As a general observation, the enzymatic treatments promoted a decrease in the apparent viscosity and consistency index whereas the flow index increased. This result indicated that enzymatic digestion made the pectin solutions less viscous and less shear thinning, which again was related to the de-branching of OP and OPA. However, when OPA or OP were enzymatically treated only with PME, they were more viscous and more shear thinning that their untreated counterparts. This is probably ascribed to the presence of a higher amount of non-esterified groups which are able to form strong interactions (most likely hydrogen bonds) with the neutral sugar side chains. Uncharged carboxyl groups may form hydrogen bonds inside the polymer molecule and between two neighboring chains (Gawkowska et al., 2018; Walkinshaw & Arnott, 1981). Additionally, the removal of the lower molecular weight fraction of these neutral sugar side chains might further increase the viscosity and shear-thinning behavior. This is in line with the DE values and compositional analysis. These results further confirmed that the molecular structure of

pectin significantly affect the steady-shear flow behavior of the resulting solutions, i.e. longer sugar side chains provided more viscous solutions by means of chain entanglements (Chan et al., 2017; Méndez, Fabra, Martínez-Abad, et al., 2021).

As observed in Figure 2, the viscosity of the pectin modified with EAR was significantly lower from other enzymatic modifications. This is explained by the loss of arabinan structures or external arabinosyl residues (see Table 1), which confer pectin with a higher hydrophilic character and higher water holding capacity (Ramasamy et al., 2015).

Finally, a LMCP solution was also prepared as a reference and compared with WRP solutions. As seen in Table 2, it behaved near to a Newtonian fluid, supporting the key role of sugar side chains on the rheological behavior.

Table 2. Parameters of flow curves obtained by fitting the Ostwald–de Waele model for the different pectin at 2% (w/v).

Samples	n**	K	r^2	η_{ap} (Pa.s) at 200 s^{-1}
OPA	0.436	9.210	0.997	0.464
OPA-PME	0.314	20.566	0.991	0.543
OPA-EAR	0.899	0.022	0.990	0.013
OPA-EGA	0.764	0.150	0.998	0.043
OPA-PME/EAR	0.671	0.012	0.994	0.002
OPA-PME/EGA	0.306	4.510	0.980	0.114
OPA-PP	0.928	0.131	0.999	0.089
OP	0.780	0.057	0.995	0.018
OP-PME	0.889	0.103	0.999	0.057
OP-EAR	0.977	0.001	0.992	0.0009
OP-EGA	0.9205	0.013	0.9983	0.009
OP-PME/EAR	0.6709	0.0117	0.990	0.002
OP-PME/EGA	0.841	0.0196	0.990	0.009
OP-PP	0.866	0.006	0.999	0.003
LMCP*	0.9898	0.032	0.999	0.030

* Citrus pectin with 5% DE.

** Depending on the value of the flow index (n), the fluid can be classified as being pseudoplastic ($n < 1$), Newtonian ($n = 1$), or dilatant ($n > 1$).

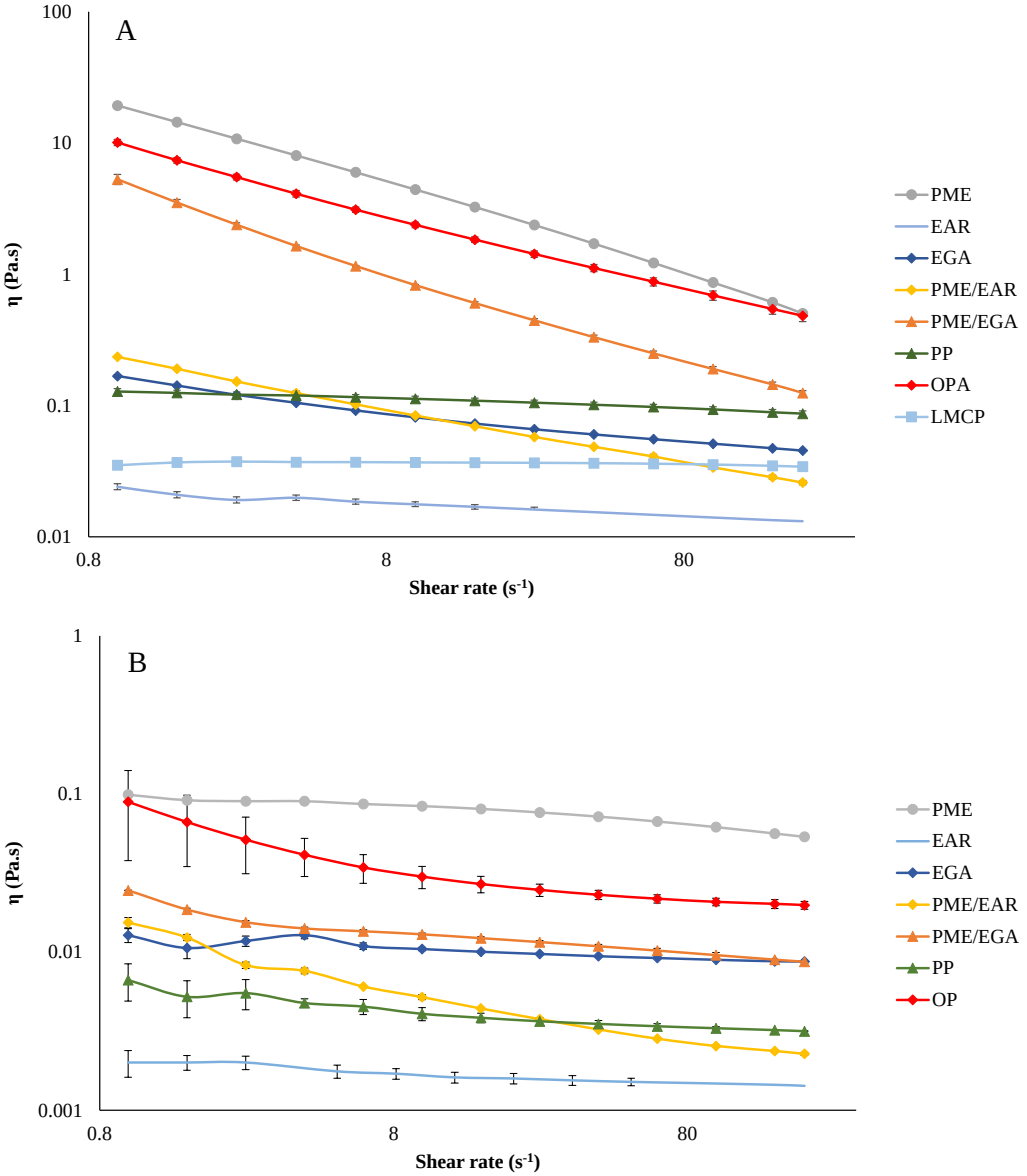

Figure 2. Apparent viscosity of enzymatically treated, (A) OPA, and (B) OP watermelon rind pectin samples at a concentration of 2% (w/v). Commercial LMCP is also shown for comparison.

4.2.2 Dynamic-viscoelastic behavior of enzymatically-treated pectin

The effect of the enzymatic treatment in the gel properties of the different pectin fractions with Ca^{2+} divalent ions was investigated by performing dynamic oscillatory tests. G' and G'' were measured as a function of frequency (rad·s^{-1}), at a fixed strain depending on previous amplitude sweep tests. As a general observation, the presence of long branched side chains decreased the gelation capacity of pectin, indicating that the presence of less branched non-methyl esterified galacturonic acid chains facilitated their association with the divalent ions to originate the network structures responsible for hydrogel formation. In fact, very weak hydrogels were formed with the pure pectin extracts (OPA and OP). However, this gelling network was lost in ERA and EGA treated samples in which the results revealed that the G' was higher than G'' only at low angular frequency range (< 1 rad s^{-1}). This corresponds to the loss of solid-related and elastic gel-like properties in these samples, as it was further confirmed by SAXS, and suggests that both the presence of longer sugar side chains in RG, as evidenced by the higher RB ratio (which refers to the side chain length) together with the high content of methyl esterified galacturonic acid chains negatively affected the interactions between the negative charge of non-esterified groups and Ca^{2+}.

As observed from Figure 3, all hydrogels formed with PME-treated samples exhibited a storage modulus (G') higher than the loss modulus (G''), denoting that the elastic character was always dominant when a load was applied and evidencing the formation of a packaged gelling network by means of the electrostatic interactions through cooperative binding of the Ca^{2+} to the non-methyl esterified galacturonic acid (NMGalA) blocks, as later supported by SAXS (see section 3.3) and in agreement with the gel strength values of the hydrogels formed (see Supplementary Material S1). There were not great differences between G' values of the hydrogels formed with only PME-treated OP or OPA samples, suggesting that, even though more linear backbone with low DE values facilitated the generation of Ca^{2+} gel networks, the presence of some sugar side chains (higher RB values for OPA-PME samples) could play an important role as reinforcement in hydrogels formed by means of intermolecular associations. Similar behavior was also found in a previous work, where regardless of Ca^{2+} concentration, a reduction in polymer chain entanglements in de-

branched pectin, provoked a drastic reduction of the gel strength in carrot pectin (Ngouémazong et al., 2012).

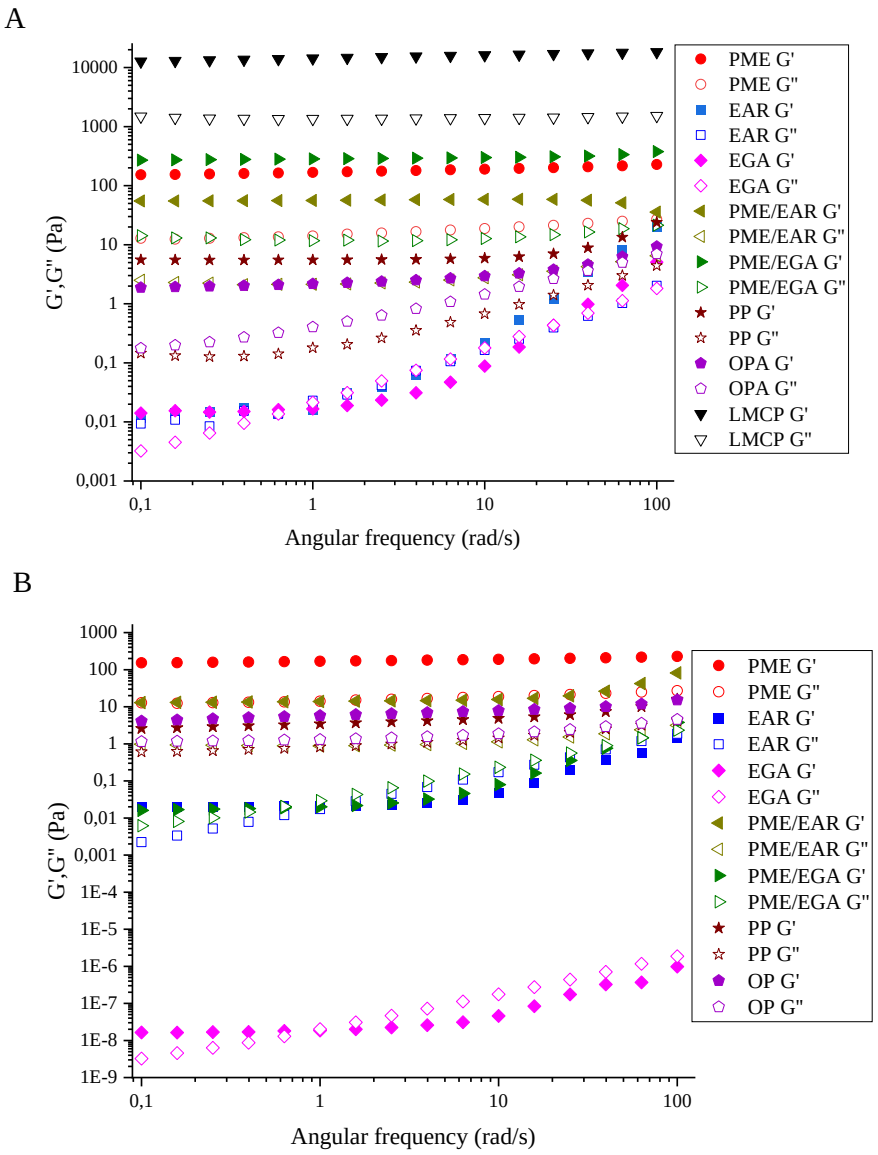

Figure 3. Dynamical oscillatory frequency sweep test curves of Ca^{2+} gels enzymatically modified from OPA (A) and OP (B) pectin. plot of storage modulus (G'), loss modulus (G'') vs. angular frequency. Filled and open symbols correspond to G' and G'' respectively. LMCP corresponds to low methoxy citrus pectin used for comparison.

With regards to the samples treated with both enzymes, stronger hydrogels were formed for OPA, being higher in those treated with PME/EGA. This is consistent with the hypothesis of small sugar side chains, being able to promote the intermolecular association of polymer chains through hydrogen bonding.

Based on these experimental results, it seems that in the presence of Ca^{2+}, a rapid cooperative binding of Ca^{2+} to the NMGalA blocks is stimulated throughout the polymer, thereby generating a number of energetically stable and strong junction zones. However, it is postulated that in the de-branched and de-methyl-esterified pectin, although a similar size and distribution of NMGalA blocks through the polymer could occur in PME/EGA and PME/EAR treated samples, there is a certain critical DE value in which the presence of short branched chains favour the formation of side chain entanglements, thereby increasing the overall entanglement of the polymer and thus, resulting in stronger gels. This effect is schematically represented in Figure 4.

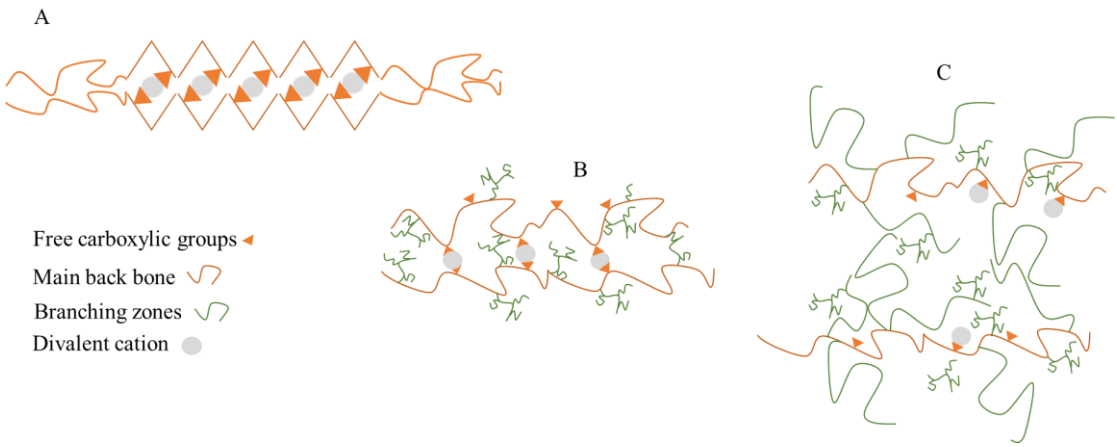

Figure 4. Schematic representation for pectin hydrogels proposed for (A) LMCP, (B) low DE and RB pectin (i.e. PA-PME/EGA) and (C) high DE and RB pectin (i.e. OPA/EGA).

When pectin extracts were treated with proteolytic enzymes, stronger hydrogels were observed in OP-PP treated samples which can be ascribed to the removal of smaller protein-arabinogalactan complexes in equal amounts, thus favoring the accessibility of Ca^{2+} ions to

the non-esterified acid groups (see Table 1). In contrast, OPA-PP gels behaved similar to its OPA counterpart.

4.3 Nanostructural characterization of pectin gels

To investigate the effect of the different enzymatic treatments on the nanostructure of the pectin, gelling formulations were characterized by means of SAXS and the obtained patterns are shown in Figure 5. When comparing the patterns from the untreated pectin (OP and OPA) with the commercial citrus pectin, it was evident that while the citrus pectin showed a marked broad shoulder feature, indicative of the formation of a gelling network, the untreated pectin showed very weak scattering features, which can be more clearly visualized in the corresponding Kratky plots (cf. Figure S2). The patterns from OP and OPA pectin are similar to those previously reported for pectin solutions at concentrations at which intermolecular interactions take place (Méndez, Fabra, Martínez-Abad, et al., 2021). In particular, one broad shoulder-like feature appears within the low-q region ($q < \sim 0.03$ Å^{-1}), which is associated to intermolecular interactions and chain clusters, and a more marked shoulder is observed within the high-q region, which originates from the scattering of rod-like pectin chains. Interestingly, the unmodified OPA and OP pectin showed almost identical patterns, indicating their similarity at the nanoscale level. The scattering data were fitted using different empirical models and the obtained fitting parameters are gathered in Table 3. As observed, the OPA and OP pectin showed very similar structural parameters, with power-law exponents around 3 within the whole q range studied, denoting the existence of mass fractals, in particular, clustered networks. This means that, at the size range covered by the SAXS experiments, none of the samples showed a linear rod-like structure, but instead they presented branched networks. In fact, the Rg_3 values, characteristic of the cross-section of rod-like pectin chains, were around 6 nm, much larger than the typical cross-sections reported for pectin rod-like structures (Méndez, Fabra, Gómez-Mascaraque, et al., 2021). On the other hand, the Rg_2 values, characteristic of the size of the molecular clusters, were around 18-23 nm, which is in agreement with previous studies (Alba et al., 2018; Méndez, Fabra, Martínez-Abad, et al., 2021).

As evidenced by the results shown in Figures 5B and 5C, the enzymatic treatments seemed to have a stronger effect on the nanostructure of the OP pectin samples. In particular, the OP-EAR and OP-EGA samples showed a significant decrease in the scattering intensity, suggesting that the physical density of the samples may have been decreased as a result of weaker intermolecular networks being formed. On the contrary, the PME treatment led to a slight increase in the scattering intensity and the low-q shoulder was not observed. The fact that this scattering feature was not detected may be a consequence of a larger interfacial scattering length density contrast (i.e. greater contrast between the pectin network and the surrounding solvent) or simply because the scattering feature appeared at lower q values out of the covered range. In any case, this may be indicative of the formation of a more densely packed gelling network, more similar to that observed for the citrus pectin. The enzymatic treatments with PME/EGA, PME/EAR and PP did not produce strong modification on the nanostructure, although there was a slight reduction in the mesh size of the gel network and in the radius of gyration associated to the rod-like pectin chains.

In the case of the OPA pectin samples, although the enzymatic treatments did not produce strong changes in the scattering intensity of the samples, some of the applied treatments induced the formation of different types of nanostructures to those observed in the unmodified OPA sample. In particular, the EGA treatment had the strongest effect, hindering the formation of intermolecular networks, similarly to what was observed for the OP-EAR and OP-EGA samples. On the other hand, all the PME treated samples showed a distinct behaviour, with slightly higher scattering intensity than the unmodified OPA pectin and the low-q scattering feature being absent. This might be indicative of the formation of stronger gelling networks in these samples, in agreement with the rheological characterization.

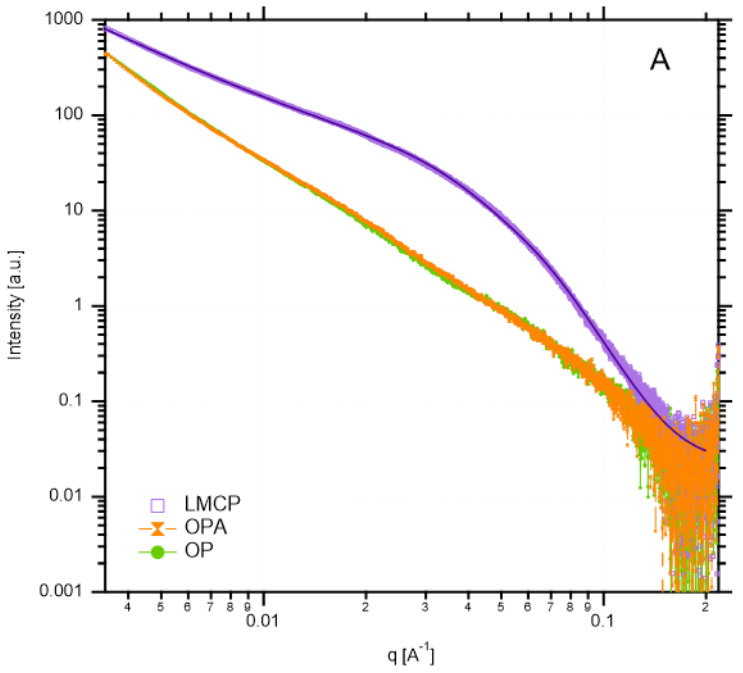
A
Intensity [a.u.]
q [A^{-1}]
LMCP
OPA
OP

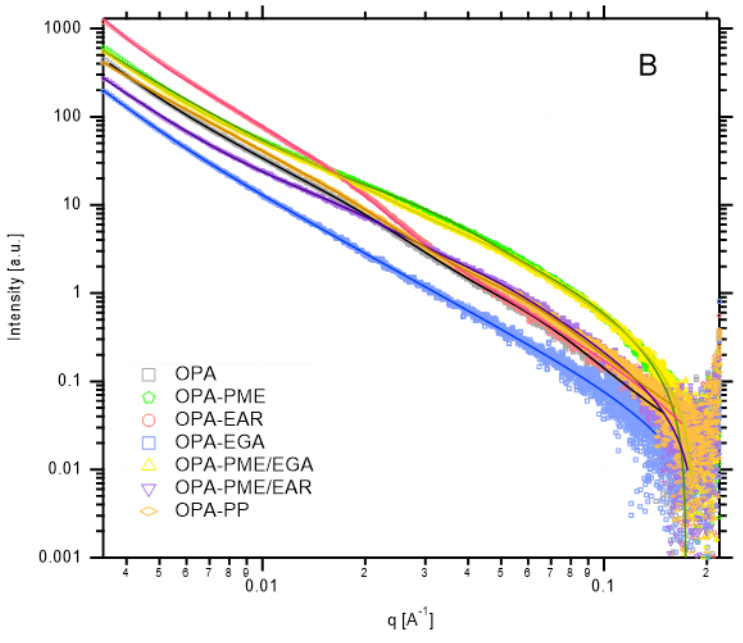
B
Intensity [a.u.]
q [A^{-1}]
OPA
OPA-PME
OPA-EAR
OPA-EGA
OPA-PME/EGA
OPA-PME/EAR
OPA-PP

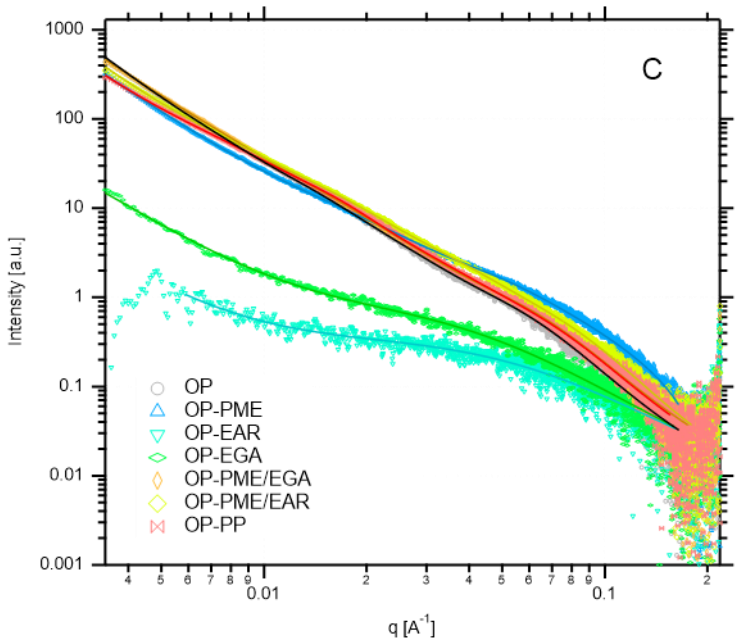

Figure 5. SAXS patterns from the pectin samples. (A) OPA and OP pectin compared to the low methoxy citrus pectin. (B) OPA enzymatically modified pectin. (C) OP enzymatically modified pectin. Markers represent the experimental data and solid lines show the fits obtained using the corresponding fitting models.

Table 3. Parameters obtained from the fits of the SAXS data for the different pectin samples.

	Unified model					Correlation length		
Samples	P_1	Rg_2 (nm)	P_2	Rg_3 (nm)	P_3	*n*	*m*	ξ_L *(nm)*
OPA	2.9	18.3	3.2	6.2	3.3	---	---	---
OPA-PME	---	---	2.4	5.1	2.5	---	---	---
OPA-EAR	3.6	24.0	3.5	3.2	3.8	---	---	---
OPA-EGA	---	---	---	---	---	2.7	2.0	6.2
OPA-PME/EGA	---	---	2.6	9.5	2.1	---	---	---
OPA-PME/EAR	---	---	2.7	8.9	2.3	---	---	---
OPA-PP	2.6	22.0	3.1	6.6	3.1	---	---	---
OP	3.0	23.4	3.4	6.3	3.4	---	---	---
OP-PME	---	---	2.6	8.6	1.9	---	---	---
OP-EAR	---	---	---	---	---	2.4	2.2	1.8
OP-EGA	---	---	---	---	---	2.3	2.4	2.4
OP-PME/EGA	2.6	20.6	3.5	5.9	3.3	---	---	---
OP-PME/EAR	3.0	19.4	3.7	4.5	3.7	---	---	---
OP-PP	2.9	19.6	4.0	5.4	3.4	---	---	---
LMCP	---	---	2.4	9.3	4.0	---	---	---

Unified model: P_i: power-law coefficient for the structural level i; Rg_2: radius of gyration associated to the structural level i (i=1,2,3).
Correlation length model: *n*: power-law exponent; *m*: Lorentzian exponent; ξ_L: correlation length.

5 Conclusions

In this work, two watermelon rind pectin extracts (OP and OPA) were enzymatically modified using six different treatments, including de-esterification, de-branching of arabinose and galactose side chains, their combinations and de-proteinization. The compositional analyses indicated that the de-esterification and its combination with de-branching enzymes had the most significant impact on the pectin structure, greatly reducing the esterification degree (DE) of both pectin extracts and significantly modifying the linearity and branching ratios. Furthermore, the proteolytic enzymes hydrolysed the protein moieties linked to the arabinogalactan part of pectin, which results in a significant increase in the linearity in both OP-PP and OPA-PP samples. This effect was more accentuated in

OP-PP samples in which the arabinogalactan-protein (AGP) fragments were removed in equal amounts.

The presence of highly branched pectin components contributed to the formation of chain entanglements and, consequently, to a higher pseudoplastic character of the pectin solution. In general, enzymatic treatments made the pectin solutions less viscous and less shear thinning. Pectin solutions in which carbohydrates were enzymatically treated only with PME, were more viscous and more shear thinning than their untreated counterparts. The presence of long branched side chains and high methyl esterified galacturonic acid chains promoted the formation of weaker hydrogels whereas de-esterification of the original pectin enabled intermolecular association giving rise to more viscous solutions and stronger hydrogels with the formation of ordered and densely packed structures. However, after de-esterifying and de-branching the galacturonic side chains, the presence of small arabinogalactans side chains in the pectin extracts could act as reinforcement agents, inducing the formation of more densely packed networks and stronger hydrogels.

Thus, enzymes acting on neutral sugar side chains (EAR and EGA) alone were not capable of debranching the pectin structure, resulting in weaker gels. In contrast, PME-treated samples might break electrostatic interaction between smaller sugar side chains and these were removed during dialysis, especially in OP, which resulted more viscous solutions and stronger gels. When both enzymes were combined, debranching produced the strongest gels similar to the benchmark LMCP. However, composition and SAXS analysis revealed that the gelling mechanisms involved densely packed structures where the small side chains remaining in the OPA acted as reinforcement. PP treatment had a greater impact on OP samples by removing small AGP fractions.

Understanding the gelation mechanism of WRP hydrogels depending on its composition and structure and their implication on the nanostructure will open the possibility of designing hydrogels with specific properties for targeted applications, such as encapsulation systems for the controlled release of bioactive compounds. Therefore, the composition and structure of WRP can be tailored depending on the final intended used such as thickeners, gelling or stabilizing additives in food. These results evidence that enzymatic treatments

greatly modified the composition and structure of watermelon pectin extracts and provide the basis for a rational design of pectin hydrogels depending of the targeted applications within the food industry.

6 Acknowledgements

Grant RTI-2018-094268-B-C22 funded by MCIN/AEI/10.13039/501100011033 and by "ERDF A way of making Europe". This work was also funded by the grant INNVAL10-19-009 - CA8250 from Agència Valenciana d´Innovació (AVI). D.A. Méndez. is supported by the Administrative Department of Science, Technology and Innovation (Colciencias) of the Colombian Government (783-2017). This research is part of the CSIC program for the Spanish Recovery, Transformation and Resilience Plan funded by the Recovery and Resilience Facility of the European Union, established by the Regulation (EU) 2020/2094. Interdisciplinary Platform for Sustainable Plastics towards a Circular Economy+. (PTI-SusPlast+) is also acknowledged for financial support.

7 References

Alba, K., Bingham, R. J., Gunning, P. A., Wilde, P. J., & Kontogiorgos, V. (2018). Pectin Conformation in Solution [Research-article]. *Journal of Physical Chemistry B*, *122*(29), 7286–7294. https://doi.org/10.1021/acs.jpcb.8b04790

Baum, A., Dominiak, M., Vidal-Melgosa, S., Willats, W. G. T. T., Søndergaard, K. M., Hansen, P. W., Meyer, A. S., & Mikkelsen, J. D. (2017). Prediction of Pectin Yield and Quality by FTIR and Carbohydrate Microarray Analysis. *Food and Bioprocess Technology*, *10*(1), 143–154. https://doi.org/10.1007/s11947-016-1802-2

Beaucage, G. (1995). Approximations Leading to a Unified Exponential/Power-Law Approach to Small-Angle Scattering. *Journal of Applied Crystallography*, *28*(6), 717–728. https://doi.org/10.1107/s0021889895005292

Beaucage, G. (1996). Small-angle scattering from polymeric mass fractals of arbitrary mass-fractal dimension. *Journal of Applied Crystallography*, *29*(2), 134–146. https://doi.org/10.1107/S0021889895011605

Bindereif, B., Eichhöfer, H., Bunzel, M., Karbstein, H. P., Wefers, D., & van der Schaaf, U. S. (2021). Arabinan side-chains strongly affect the emulsifying properties of acid-extracted sugar beet pectins. *Food Hydrocolloids*, *121*. https://doi.org/10.1016/J.FOODHYD.2021.106968

Campbell, M. (2006). *Extraction of Pectin From Watermelon Rind*. Oklahoma State University.

Capel, F., Nicolai, T., Durand, D., Boulenguer, P., & Langendorff, V. (2006). Calcium and acid induced gelation of (amidated) low methoxyl pectin. *Food Hydrocolloids*, *20*(6), 901–907. https://doi.org/10.1016/j.foodhyd.2005.09.004

Celus, M., Kyomugasho, C., Van Loey, A. M., Grauwet, T., & Hendrickx, M. E. (2018). Influence of Pectin Structural Properties on Interactions with Divalent Cations and Its Associated Functionalities. In *Comprehensive Reviews in Food Science and Food Safety* (Vol. 17, Issue 6, pp. 1576–1594). Blackwell Publishing Inc. https://doi.org/10.1111/1541-4337.12394

Chan, S. Y., Choo, W. S., Young, D. J., & Loh, X. J. (2017). Pectin as a rheology modifier: Origin, structure, commercial production and rheology. In *Carbohydrate Polymers* (Vol. 161, pp. 118–139). Elsevier Ltd. https://doi.org/10.1016/j.carbpol.2016.12.033

Chen, H., Qiu, S., Gan, J., Liu, Y., Zhu, Q., & Yin, L. (2016). New insights into the functionality of protein to the emulsifying properties of sugar beet pectin. *Food Hydrocolloids*, *57*, 262–270. https://doi.org/10.1016/j.foodhyd.2016.02.005

Denman, L. J., & Morris, G. A. (2015). An experimental design approach to the chemical characterisation of pectin polysaccharides extracted from Cucumis melo Inodorus. *Carbohydrate Polymers*, *117*, 364–369. https://doi.org/10.1016/j.carbpol.2014.09.081

Doungla, E., & Vandebril, S. (2009). Quick and reliable method of preparation of strong homogeneous calcium-pectin gels. *… Symposium on Food …*, 2–3.

FAOSTAT. (2021). *CROPS*. http://www.fao.org/faostat/en/#data/QC/visualize

Funami, T., Nakauma, M., Ishihara, S., Tanaka, R., Inoue, T., & Phillips, G. O. (2011). Structural modifications of sugar beet pectin and the relationship of structure to functionality. *Food Hydrocolloids*, *25*(2), 221–229. https://doi.org/10.1016/j.foodhyd.2009.11.017

Funami, T., Zhang, G., Hiroe, M., Noda, S., Nakauma, M., Asai, I., Cowman, M. K., Al-Assaf, S., & Phillips, G. O. (2007). Effects of the proteinaceous moiety on the emulsifying properties of sugar beet pectin. *Food Hydrocolloids*, *21*(8), 1319–1329. https://doi.org/10.1016/j.foodhyd.2006.10.009

Gawkowska, D., Cybulska, J., & Zdunek, A. (2018). Structure-related gelling of pectins and linking with other natural compounds: A review. *Polymers*, *10*(7), 762. https://doi.org/10.3390/polym10070762

Hartati, I., & Subekti, E. (2015). Microwave assisted extraction of watermelon rind pectin. *International Journal of ChemTech Research*, *8*(11), 163–170.

Houben, K., Jolie, R. P., Fraeye, I., Van Loey, A. M., & Hendrickx, M. E. (2011). Comparative study of the cell wall composition of broccoli, carrot, and tomato: Structural characterization of the extractable pectins and hemicelluloses. *Carbohydrate Research*, *346*(9), 1105–1111. https://doi.org/10.1016/j.carres.2011.04.014

Hromadová, D., Soukup, A., & Tylová, E. (2021). Arabinogalactan Proteins in Plant Roots - An Update on Possible Functions. *Frontiers in Plant Science*, *12*. https://doi.org/10.3389/FPLS.2021.674010

Ilavsky, J., & Jemian, P. R. (2009). Irena: Tool suite for modeling and analysis of small-angle scattering. *Journal of Applied Crystallography*, *42*(2), 347–353. https://doi.org/10.1107/S0021889809002222

Karnik, D., Jung, J., Hawking, S., & Wicker, L. (2016). Sugar beet pectin fractionated using isopropanol differs in galacturonic acid, protein, ferulic acid and surface hydrophobicity. *Food Hydrocolloids*, *60*, 179–185. https://doi.org/10.1016/j.foodhyd.2016.03.037

Kieffer, J., & Ashiotis, G. (2014). PyFAI: a Python library for high performance azimuthal integration on GPU. *Powder Diffraction*, *28*(SUPPL.2), 3.

Klavons, J. A., & Bennett, R. D. (1986). Determination of Methanol Using Alcohol Oxidase and Its Application to Methyl Ester Content of Pectins. *Journal of Agricultural and Food Chemistry*, *34*(4), 597–599. https://doi.org/10.1021/jf00070a004

Lara-Espinoza, C., Carvajal-Millán, E., Balandrán-Quintana, R., López-Franco, Y., & Rascón-Chu, A. (2018). Pectin and pectin-based composite materials: Beyond food

texture. In *Molecules* (Vol. 23, Issue 4, p. 942). MDPI AG. https://doi.org/10.3390/molecules23040942

Lee, K. Y., & Choo, W. S. (2020). Extraction Optimization and Physicochemical Properties of Pectin from Watermelon (Citrullus lanatus) Rind: Comparison of Hydrochloric and Citric acid Extraction. *Journal of Nutraceuticals and Food Science*, *5*(1), 1. https://doi.org/10.36648/nutraceuticals.5.1.1

Méndez, D. A., Fabra, M. J., Gómez-Mascaraque, L., López-Rubio, A., & Martinez-Abad, A. (2021). Modelling the Extraction of Pectin towards the Valorisation of Watermelon Rind Waste. *Foods*, *10*(4), 738. https://doi.org/10.3390/foods10040738

Méndez, D. A., Fabra, M. J., Martínez-Abad, A., Martínez-Sanz, Gorria, M., & López-Rubio, A. (2021). Understanding the different emulsification mechanisms of pectin: Comparison between watermelon rind and two commercial pectin sources. *Food Hydrocolloids*, *120*, 106957. https://doi.org/10.1016/j.foodhyd.2021.106957

Nakauma, M., Funami, T., Noda, S., Ishihara, S., Al-Assaf, S., Nishinari, K., & Phillips, G. O. (2008). Comparison of sugar beet pectin, soybean soluble polysaccharide, and gum arabic as food emulsifiers. 1. Effect of concentration, pH, and salts on the emulsifying properties. *Food Hydrocolloids*, *22*(7), 1254–1267. https://doi.org/10.1016/j.foodhyd.2007.09.004

Ngouémazong, D. E., Kabuye, G., Fraeye, I., Cardinaels, R., van Loey, A., Moldenaers, P., & Hendrickx, M. (2012). Effect of debranching on the rheological properties of Ca2+-pectin gels. *Food Hydrocolloids*, *26*(1), 44–53. https://doi.org/10.1016/j.foodhyd.2011.04.009

Ognyanov, M., Georgiev, Y., Petkova, N., Ivanov, I., Vasileva, I., & Kratchanova, M. (2018). Isolation and characterization of pectic polysaccharide fraction from in vitro suspension culture of Fumaria officinalis L. *International Journal of Polymer Science*, *2018*, 1–13. https://doi.org/10.1155/2018/5705036

Oosterveld, A., Voragen, A. G. J., & Schols, H. A. (2002). Characterization of hop pectins shows the presence of an arabinogalactan-protein. *Carbohydrate Polymers*, *49*(4), 407–413. https://doi.org/10.1016/S0144-8617(01)00350-2

Petkowicz, C. L. O., Vriesmann, L. C., & Williams, P. A. (2017). Pectins from food waste: Extraction, characterization and properties of watermelon rind pectin. *Food Hydrocolloids*, *65*, 57–67. https://doi.org/10.1016/j.foodhyd.2016.10.040

Prakash Maran, J., Sivakumar, V., Thirugnanasambandham, K., & Sridhar, R. (2014). Microwave assisted extraction of pectin from waste Citrullus lanatus fruit rinds. *Carbohydrate Polymers*, *101*(1), 786–791. https://doi.org/10.1016/j.carbpol.2013.09.062

Ramasamy, U. R., Gruppen, H., & Kabel, M. A. (2015). Water-holding capacity of soluble and insoluble polysaccharides in pressed potato fibre. *Industrial Crops and Products*, *64*, 242–250. https://doi.org/10.1016/J.INDCROP.2014.09.036

Schols, H. A., & Voragen, A. G. J. (2003a). Pectic Polysaccharides. In J. R. Whitaker, A. G. J. Voragen, & D. W. S. Wong (Eds.), *Handbook of food enzymology* (Vol. 353, Issue 2, pp. 829–843). Dekker. https://doi.org/10.1201/9780203910450-68

Schols, H. A., & Voragen, A. G. J. (2003b). Pectins and their Manipulation. In G. B. Seymour & J. P. Knox (Eds.), *Pectins and their manilpulation* (p. 29). Blackwell.

Verhoef, R., Lu, Y., Knox, J. P., Voragen, A. G. J., & Schols, H. A. (2009). Fingerprinting complex pectins by chromatographic separation combined with ELISA detection. *Carbohydrate Research*, *344*(14), 1808–1817. https://doi.org/10.1016/j.carres.2008.09.030

Voragen, A. G. J. J., Coenen, G.-J. J., Verhoef, R. P., & Schols, H. A. (2009). Pectin, a versatile polysaccharide present in plant cell walls. *Structural Chemistry*, *20*(2), 263–275. https://doi.org/10.1007/s11224-009-9442-z

Walkinshaw, M. D., & Arnott, S. (1981). Conformations and interactions of pectins: I. X-ray diffraction analyses of sodium pectate in neutral and acidified forms. *Journal of Molecular Biology*, *153*(4), 1055–1073. https://doi.org/10.1016/0022-2836(81)90467-8

Wiles, P. G., Gray, I. K., Kissling, R. C., Delahanty, C., Evers, J., Greenwood, K., Grimshaw, K., Hibbert, M., Kelly, K., Luckin, H., McGregor, K., Morris, A., Petersen, M., Ross, F., & Valli, M. (1998). Routine Analysis of Proteins by Kjeldahl and Dumas Methods: Review and Interlaboratory Study Using Dairy Products. *Journal of AOAC INTERNATIONAL*, *81*(3), 620–632. https://doi.org/10.1093/jaoac/81.3.620

8 Supplementary material

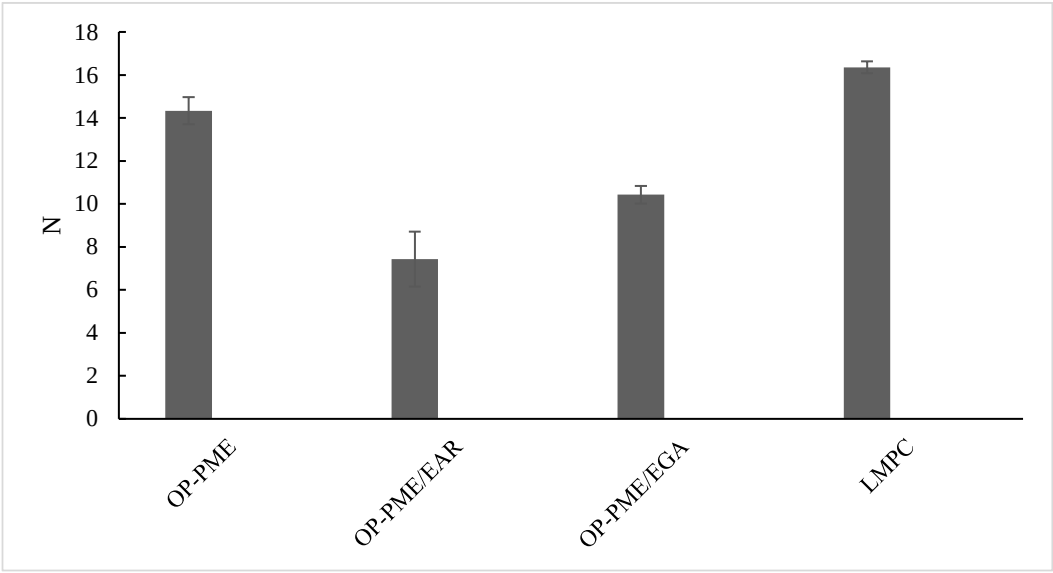

Figure S1. Firmness by compression (pre-test speed 5 mm/s, test speed 1 mm/s, strain 80%). of pectin hydrogel beads via dripping method in gelation bath at 1.5% (w/v) of calcium chloride. The measurements correspond to the compression of ten beads per run, made in triplicates.

Table S1. Parameters obtained from the fits of the SAXS data for the different pectin samples.

	Unified model					Correlation length		
Samples	P_1	Rg_2 (nm)	P_2	Rg_3 (nm)	P_3	*n*	*m*	ξ_L *(nm)*
OPA	2.9	18.3	3.2	6.2	3.3	---	---	---
OPA-PME	---	---	2.4	5.1	2.5	---	---	---
OPA-EAR	3.6	24.0	3.5	3.2	3.8	---	---	---
OPA-EGA	---	---	---	---	---	2.7	2.0	6.2
OPA-PME/EGA	---	---	2.6	9.5	2.1	---	---	---
OPA-PME/EAR	---	---	2.7	8.9	2.3	---	---	---
OPA-PP	2.6	22.0	3.1	6.6	3.1	---	---	---
OP	3.0	23.4	3.4	6.3	3.4	---	---	---
OP-PME	---	---	2.6	8.6	1.9	---	---	---
OP-EAR	---	---	---	---	---	2.4	2.2	1.8
OP-EGA	---	---	---	---	---	2.3	2.4	2.4
OP-PME/EGA	2.6	20.6	3.5	5.9	3.3	---	---	---
OP-PME/EAR	3.0	19.4	3.7	4.5	3.7	---	---	---
OP-PP	2.9	19.6	4.0	5.4	3.4	---	---	---
LMCP	---	---	2.4	9.3	4.0	---	---	---

Unified model: P_i: power-law coefficient for the structural level i; Rg_2: radius of gyration associated to the structural level i (i=1,2,3).
Correlation length model: *n*: power-law exponent; *m*: Lorentzian exponent; ξ_L: correlation length.

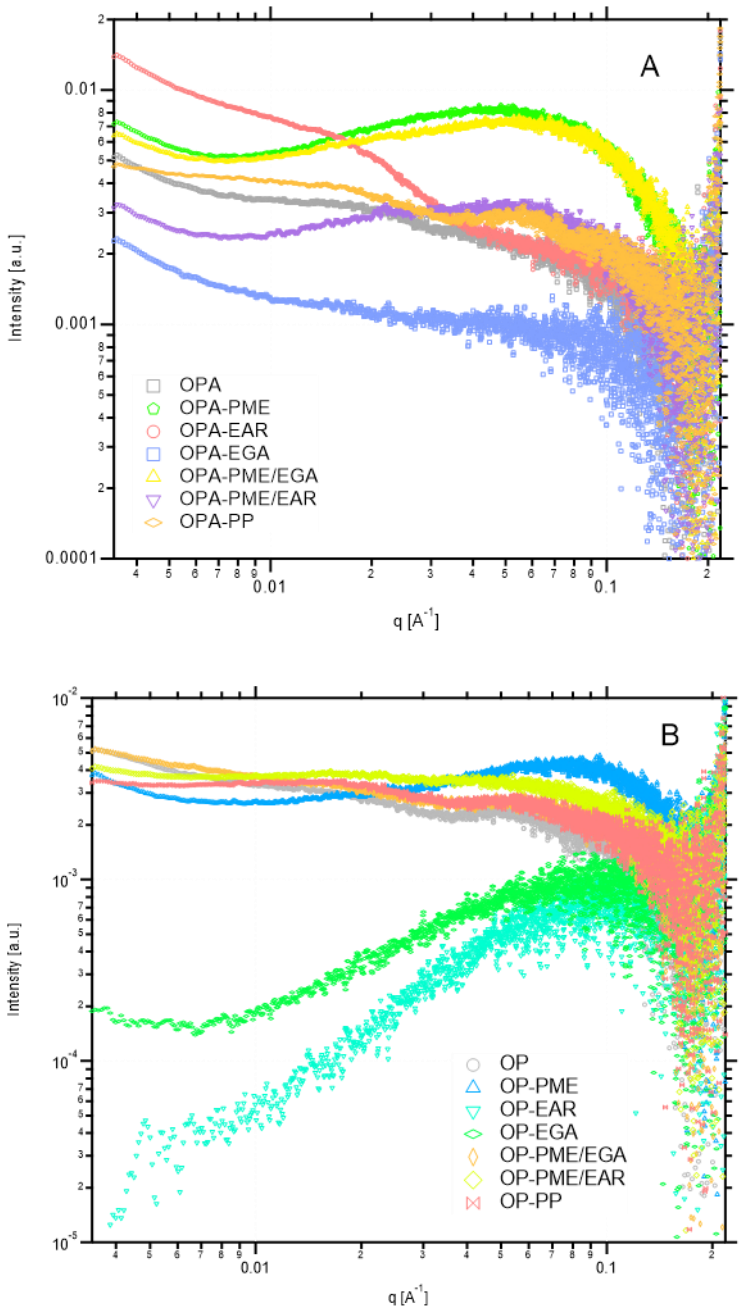

Figure S2. SAXS Kratky plots from the (A) OPA and (B) OP pectin samples.

3.1.4

PECTIN-BASED AEROGEL PARTICLES FOR DRUG DELIVERY: EFFECT OF PECTIN COMPOSITION ON AEROGEL STRUCTURE AND RELEASE PROPERTIES

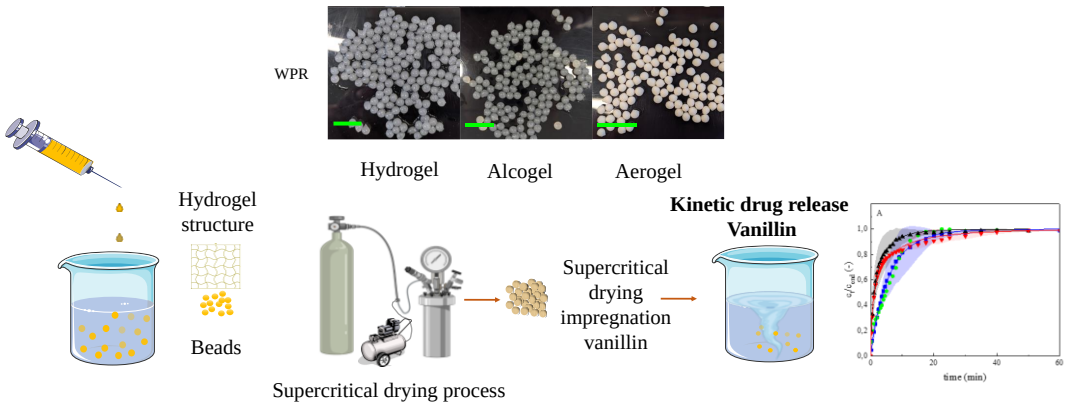

This section is an adapted version of the following submitted research article:

D. A. Mendez, B. Schroeter, A. Martínez-Abad, M. J. Fabra, P. Gurikov and A. López-Rubio. Pectin-based aerogel particles for drug delivery: effect of pectin composition on aerogel structure and release properties. Carbohydrate Polymers (submitted)

---

1 Abstract

In this work, nanostructured pectin aerogels were prepared via a sol-gel process and subsequent drying under supercritical conditions. To this end, three commercially available citrus pectins and an in-house produced and enzymatically modified watermelon rind pectin (WRP) were compared. Then, the effect of pectin's structure and composition on the aerogel properties were analysed and its potential application as a delivery system was explored by impregnating them with vanillin. Results showed that the molecular weight, degree of esterification and branching degree of the pectin samples played a main role in the production of hydrogels and subsequent aerogels. The developed aerogel particles showed high specific surface areas (468-584 m^2/g) and low bulk density (0.025-0.10 g/cm^3). The shrinkage effect during aerogel formation was significantly affected by the pectin concentration and structure, while vanillin loading in aerogels and its release profile was also seen to be influenced by the affinity between pectin and vanillin. Furthermore, the results highlight the interest of WRP as a carrier of active compounds which might have potential application in food and biomedical areas, amongst others.

2 Introduction

The development of delivery systems is an area of immense importance for human health and well-being, having applications in the food, pharma and cosmetic industries. In this sense, aerogels from biopolymers are especially attractive due to their stability, availability, renewability and low toxicity (Mehling et al., 2009). The remarkable aerogels properties (homogeneous structure, tuneable mesh size, interconnected pores, and increased surface area) are advantageous features for exploring the capabilities of aerogels as carrier systems (García-González et al., 2021). Moreover, the so-called second generation of aerogels (which have shifted from inorganic to organic-based ones) has facilitated the penetration of these materials in the food market since they consist on biopolymer-based aerogels, including food-grade polysaccharides and proteins (Manzocco et al., 2021). However, the evaluation and feasibility of different biopolymers for aerogel uses are still in early research phases, because a number of factors including biopolymer source, extraction process,

seasonality, and gelation process among others, drastically affect the properties and functionality of the obtained aerogel materials. Amongst the potential biopolymer sources, fruit and vegetable wastes have a huge potential being among the categories of residues with the largest production (Esparza et al., 2020) and rich in many functional biopolymers of interest. As an example, pectin obtained from novel sources open up the possibility to new applications and improvements (Chen et al., 2016), also satisfying the increasing demand for pectin polymer already existing in the food sector.

Different authors have characterized and evaluated the potential of pectin as an aerogel material and drug carrier mainly from commercial citrus pectins (García-González et al., 2012, 2015; Groult et al., 2021a, 2021b; Groult & Budtova, 2018; Ne et al., 2018; Preibisch et al., 2018; Veronovski, Tkalec, Knez, & Novak, 2014; White et al., 2010). However, to the best of our knowledge, these studies emphasized in the structural and mechanical properties of the developed aerogel and in the gelation mechanism, not considering the intrinsic factors related to the compositional and chemical characteristics of the pectin itself which, as can be noticed in other pectin applications, played a key role in the thickening, emulsifier and gelation process. It should be highlighted that pectin has been considered a prebiotic fibre as it is resistant to protease and amylase enzymes, both of which are active within the upper gastrointestinal tract, thus being used by gut bacteria in the lower gastrointestinal tract. Therefore, it could be a promising drug vehicle from the mouth to the colon (Veronovski, Tkalec, Knez, & Novak, 2014). However, factors such as the pectin structure, composition, and physicochemical properties, may affect the aerogel formation and the interaction with the drug of interest.

Watermelon rind, with a very high global production, is a promising source of pectin. Several works have optimized the extraction conditions from watermelon rind pectin (WRP) and, its structure and properties have demonstrated the potential of this novel pectin source for a number of applications (Campbell et al., 2015; Hartati & Subekti, 2015; Méndez, Fabra, Gómez-Mascaraque, et al., 2021; Méndez, Fabra, Martínez-Abad, et al., 2021; Petkowicz et al., 2017; Zubairu et al., 2018). However, the ability of different pectin samples to form gels depend on their sources and extraction process as they are greatly affected by important parameters such as molecular weight distribution, degree of esterification,

structure distribution and compositional sugars (Méndez, Fabra, Gómez-Mascaraque, et al., 2021; Veronovski, Tkalec, Knez, & Novak, 2014). Based on previous studies, it was evidenced that the degree of esterification of the WRP extracted is usually greater than 50% (Méndez, Fabra, Gómez-Mascaraque, et al., 2021), which is not favorable for gel formation through crosslinking with divalent cations and further aerogel production. Different enzyme treatments were evaluated for tailoring the rheological properties of WRP (Méndez et al., 2022), and it was observed that the application of pectin methyl esterase (PME) combined with Endo-1,5-α-arabinanase resulted in the best treatment to produce improved gel strength with divalent cation addition.

In light of the above, it was hypothesized that depending on the structural, physicochemical properties and concentration of pectin, the aerogel structure and its suitability as drug delivery systems can be significantly affected. Therefore, the aim of this work was to evaluate an enzymatically modified WRP for aerogel bead production and to compare it with three commercially available citrus pectin samples with different composition. The evaluation of these pectin-based aerogels as delivery systems was also carried out using vanillin as a model compound. Vanillin (4-hydroxy-3-methoxybenzaldehyde) is a phytochemical generally regarded as a safe (GRAS) flavouring compound widely used in ice creams, beverages, biscuits, chocolate, confectionery, desserts, etc. (Rupasinghe et al., 2006). Moreover, its bioactive properties, including antimicrobial, antioxidant, anticarcinogenic activities (Sinha et al., 2009), medium polarity and the simplicity to track its release via UV-Vis spectroscopy, make it a perfect candidate as a model active compound to test the release kinetics from porous polymer-carriers. Both aerogel formation and vanillin impregnation were done through supercritical CO_2 treatments and a detailed study on the effects of initial pectin composition on the final structural and release properties of the materials was carried out.

3 Materials and methods

3.1 Material

Three commercially available citrus pectins and an in-house produced and enzymatically modified watermelon rind pectin (WRP) were used in this study: a low methoxy (5%) citrus pectin (denoted as C1 from now on that was supplied by Megazyme Ltd., (Wicklow, Ireland) and two other citrus pectin of low (C2) and high molecular weight (C3) kindly provided by Herbstreith and Fox KG, (Neuenbürg/Württ, Germany). Watermelon rind pectin was produced at laboratory conditions and enzymatically modified with an endo-1,5-α-arabinanase and a methyl-esterase as previously reported (Méndez et al., 2022). Anhydrous ethanol was provided by Carl Roth GmbH & Co. KG (Karlsruhe, Germany).

3.2 Pectin characterization

3.2.1 Carbohydrate composition

The sugar composition of the extracts was determined after acidic methanolysis as previously described (Méndez et al., 2022). Freeze-dried samples (1 mg) were incubated with 1 mL of 2 M HCl in dry methanol for 5 h at 100 °C. Samples were then neutralized with pyridine, dried under a stream of air, and further hydrolysed with 2 M TFA at 100 °C for 1 h. The samples were again dried under a stream of air and re-suspended in milliQ, filtered and injected. The monosaccharides were analysed using high performance anion exchange chromatography with pulsed amperometric detection (HPAEC-PAD) with a ICS-6000 system (Thermofisher) equipped with a CarboPac PA1 column (4 × 250 mm, Dionex). Control samples of known concentrations of mixtures of glucose (Glc), fucose (Fuc), rhamnose (Rha), galactose (Gal), arabinose (Ara), xylose (Xyl), mannose (Man), galacturonic acid (GalA) and glucuronic acid (GlcA) were used for calibration (Merck, Germany).

3.2.2 Ash content

The ash content was determined according to the standard method TAPPI T211 om-07. All measurements were carried out in triplicate.

3.2.3 Protein content

The protein content was carried out by the Dumas combustion method (nitrogen conversion factor 6.25) according to ISO/TS, 16634–2 (2016).

3.3 Molecular weight distribution

The molecular weight of the pectin was estimated by HPSEC using Waters ACQ Arc Sys Core 1-30 cm CH (Waters, USA). The HPLC system was equipped with a Waters 2998 PAD module, a Waters 2414 refractive index detector (Waters, USA), and 2475 FLR module (Waters, USA). 0.1 M NaCl was used as the mobile phase. The samples (3 mg/mL) were dissolved in the mobile phase under magnetic stirring at 40 °C, filtered through 0.22 μm pore syringe filters. Then, the samples were injected into columns in series (PolySep-GFC-P 4000 and 2000 (300 mm x 7.8 mm) Phenomenex Inc., CA, USA) equilibrated at 40 °C. The injection volume was 20 μL and the flow rate was 0.5 mL/min. Calibration was performed using a pullulan standards kit (PSS polymer standards service GmbH, Mainz, Germany).

3.4 Rheological characterization

The viscosity of the pectin solutions was determined using a rheometer HR20, (TA Instruments, Montreal, QC, Canada) with a 40 mm parallel plate geometry. Briefly, pectin solutions at 2% (w/w) and 4% (w/w) were dissolved in deionized water and adjusted to pH 4.0. Samples were loaded on the bottom Peltier plate. The viscosity was measured by rotational shear between the two parallel plates at 20 ºC with a gap of 500 μm as a function of increasing shear rate from 0.1 s^{-1} to 200 s^{-1}. The samples were recorded with the TRIOS software version 5.1.1.46572 (TA Instruments, Montreal, QC, Canada. The power law

model Eq. (1) was applied to determine the consistency index (k) and the flow index behaviour (n). The apparent viscosities were determined at 100 s^{-1}.

$$\sigma = K\gamma^n \quad \text{(Eq. 1)}$$

3.5 Preparation of hydrogel beads and particles

3.5.1 Dripping method

Pectin solutions at 2 and 4% (w/w) in de-mineralized water were prepared and pH adjusted to 4.0 to avoid acidic induced gelation during the process (Groult & Budtova, 2018). The solutions were extruded at 4 mL/min through a stainless-steel needle (0.4 mm inner diameter) into an aqueous gelation bath containing $CaCl_2$ at 0.5% (w/w) which was slowly agitated with a magnetic stirrer. The distance between the syringe tip and the coagulation bath was 3 cm. After bead formation, the beads were kept in the coagulation bath for 24 h to stabilize the gel network.

3.5.2 Jet cutting method

Hydrogel particles were produced with the JetCutter Type S from geniaLab GmbH, Braunschweig, Germany. A gelation bath was previously prepared at 0.5% (w/w) of $CaCl_2$ as a crosslinker. Four process parameters were fixed: the cutting frequency (f_{cut} 2000 rpm), the nozzle diameter (d_{nozzle}=0.3 mm), the jet flow (F_{jet}=0.25 g/s), the falling distance (1.5 m) and the pectin solution concentrations of 2 and 4% (w/w).

3.6 Aerogel production

A sequential solvent exchange was carried out by immersion of the resulting hydrogels in 20, 40, 60 and 80 wt% ethanol for 24 hours each. Then, the samples were immersed in 99.9 wt% ethanol until a minimum final concentration of 98 wt% ethanol inside the hydrogels was reached (controlled by density measurements, Anton Paar, DMA 4500 M). A hydrogel solvent ratio of 1:10 was kept during the solvent exchange.

After the solvent exchange, the alcogel particles and beads were sealed into a filter paper bag and placed into a high-pressure autoclave with an overall volume of 3.9 L for supercritical drying with CO_2. The supercritical drying was performed at a temperature of 60 °C and pressure of 120 bars. A continuous flow of CO_2 (flow rate = 80 – 110 g/min) was set through the autoclave until complete extraction of the ethanol was achieved after 4 h. The aerogel materials were collected after slow de-pressurization (1 bar/min) of the autoclave and stored in sealed tubes (25 mL, Sarstedt) in a desiccator prior to analysis.

3.7 Supercritical impregnation with vanillin

Vanillin was selected due its proven good solubility under supercritical conditions (temperature 34.8-44.8 ºC, pressure 85-500 bars) (Liu et al., 2006; Rojas-Ávila et al., 2016), and proven impregnation efficiency on aerogels, as previously reported by Schroeter, Yonkova, Goslinska, et al., (2021). For the impregnation process, vanillin was placed at the bottom of the high-pressure autoclave keeping a vanillin:aerogel weight ratio of 1:2. The aerogel materials were sealed into a filter paper bag. The supercritical impregnation was performed in a closed system at a temperature of 60 °C and pressure of 120 bars of supercritical CO_2 for 16 hours. The impregnated material was collected after slow depressurization (1 bar/min) of the autoclave and stored in sealed tubes (25 mL, Sarstedt) in a desiccator prior to analysis.

3.8 Aerogel characterization

The bulk density of aerogel particles and beads were measured using a graduated cylinder. Dry and impregnated aerogel particles (0.3 g) were filled in the cylinder up to a certain volume without tapping. The bulk density was calculated as a ratio of the weight and the occupied volume.

Furthermore, low temperature N_2 adsorption–desorption analysis was performed to investigate the microstructural properties of the aerogels (Nova 3000e Surface Area Analyzer, Quantachrome Instruments, Boynton Beach, USA). A single determination was carried out for aerogel produced. An overall sample mass of 20–30 mg was used for each analysis. The specific surface area was determined using the BET (Brunauer–Emmett–

Teller) method (Brunauer et al., 1938). The pore volume (Vpore) and average pore diameter (Dpore) were estimated by the BJH (Barrett–Joyner–Halendia) method (Barrett et al., 1951). All samples were degassed under vacuum at 60 °C for 6 h prior to analysis.

3.9 Scanning electron microscope

The surface properties and the inner structure of the aerogels were characterized via scanning electron microscopy (SEM, Zeiss Supra VP55, Jena, Germany). The intact and cut beads were sputtered with a thin layer of gold (approx. 6 nm thickness, Sputter Coater SCD 050, BAL-TEC) before analysis. The measurements were carried out under high vacuum at an accelerating voltage of 3 kV and a working distance of 4.2–5.6 mm.

3.10 Image analysis

The size and shape of beads via dripping method was determined based on image analysis of pictures. 50 beads per experiment were evaluated to determine the mean particle diameter (Dparticle), perimeter and projection surface area (ImageJ software). In case of irregular shaped beads, the average of the maximum and minimum diameter was used to calculate the Dparticle.

Size and shape of dry aerogel particles from jet cutting process were determined with a Camsizer XT system (Retsch Technology) in free fall mode. All characterizations were carried out according to DIN 66,141. $d_{particle}$ was calculated from the longest feret-diameter and the shortest chord-diameter of each particle projection as follows:

$$d_{particle} = \sqrt{x_{Femax}^2 - x_{cmin}^2} \qquad \text{(Eq. 2)}$$

Where x_{Femax} is the longest feret-diameter and x_{cmin} being the shortest chord-diameter of each particle projection.

3.11 FTIR

FTIR measurements were recorded in transmission mode in a controlled chamber at 21 °C and dry air in order to avoid humidity and CO_2 using a Cary 630 FTIR spectrometer (Agilent, USA). The spectra were taken at 4 cm^{-1} resolution in a wavelength range of 400–4000 cm^{-1} and average a minimum of 32 scans. Spectra acquired were processed using Origin pro 2019 software (OriginLab Corporation, Northampton, MA, USA).

3.12 Vanillin release kinetics

A kinetic study on vanillin release from the impregnated aerogel beads prepared at two different pectin concentrations (2 and 4% w/w) in water was monitored using a spectrophotometer (Evolution™ 300, Thermo Fisher Scientific, USA) at 280 nm. Around 180 mg of impregnated bead samples where immersed in 500 mL of distilled water at 30, 40 and 50 °C with magnetic stirring (180 rpm). The range of temperature was selected to evaluate any influence of this factor on vanillin release, also keeping in mind the body temperature which falls within the selected range. At pre-determined time periods, an aliquot (1 mL) from the solution was taken out and analysed, and then returned back into the release medium. The vanillin concentration was calculated through a calibration curve constructed beforehand using vanillin solutions with known concentrations. The kinetic experimental data collected was analysed and adjusted according to previous work (Schroeter, Yonkova, Goslinska, et al., 2021) with the Weibull model approach (Eq. 2) using origin 9.6 (OriginLab Corporation, Northampton, MA, USA).

$$c_t = c_{max} - e^{-\left(\frac{t}{\alpha}\right)^{\beta}} \quad \text{(Eq. 3)}$$

with c_t being the concentration at time t, c_{max} being the vanillin concentration in the water phase at the end of the measurement. α is the scale constant and β is the shape constant.

3.13 Statistical analysis

All statistical analysis was performed using the statistical software Statgraphics Centurion XVI® (Manugistics Inc.; Rockville, MD, USA). Statistically significant differences were

determined by using one-way analyses of variance (ANOVA) and sample comparison with LSD at 95% confidence level (p-value < 0.05).

4 Results and discussion

4.1 Initial pectin characterization

A compositional characterization of the different pectin samples used for aerogel production was conducted in order to assess and correlate composition with their gelling capacity, aerogel structure, subsequent vanillin impregnation and release profiles. The three commercial pectin samples (C1, C2 and C3) showed a high purity, with a total carbohydrate content near to 100% and very high Gal A content, typical for industrial pectin (Table 1). Only small differences between these citrus pectin samples were found, with a higher content in protein in the low molecular weight citrus pectin (C2) and a slightly higher branching degree in the medium molecular weight pectin (C3). In contrast, the enzymatically-modified watermelon rind pectin (WRP) obtained in the laboratory showed remarkable differences compared to the citrus pectin samples. Specifically, it was a relatively less pure pectin extract due to the presence of a certain amount of protein and ashes and, more interestingly, this WRP had a much larger branching degree pointing out at the predominance of long galactan side chains (Méndez, Fabra, Gómez-Mascaraque, et al., 2021).

Table 1. Composition of pectin samples. Degree of esterification (DE %), protein and ash content (%) and structural ratio of pectin powder C1, C2, C3 and WRP.

Sample	DE**** (%)	Ashes (% d.w.)	Protein content (%)	Rha (µg/mg)	Ara (µg/mg)	Gal (µg/mg)	GalA (µg/mg)	RB*	RL**	HG*** (%)
C1	5	0.47(0.01)[a]	5.78(0.07)[c]	45.1(6.41)[a]	7.02 (0.98)[a]	91.28 (15.54)[a]	856.42 (132.05)[a]	2.2	5.8	81.1
C2	6.5	3.08(0.08)[b]	7.44(0.004)[b]	43.32(0.66)[a]	17.05 (0.34)[b]	91.36 (6.66)[a]	885.94 (43.87)[a]	2.5	5.6	84.2
C3	5.6	1.91(0.00)[c]	5.82(0.08)[c]	41.05(4.81)[a]	23.72 (3.01)[c]	98.9 (10.87)[a]	831.97 (89.53)[a]	2.9	4.9	79.1
WRP	4.8	1.47(0.02)[d]	7.95)0.021)[a]	19.4(3.52)[b]	1.72 (0.13)[d]	120.14 (3.58)[b]	633.35 (46.05)[b]	6.2	4.4	61.4

* RB A larger value is indicative of larger average size of the branching side chains. (Gal+Ara/Rha).
**RL A larger value suggest of more linear/less branched pectins. (GalA/(Xyl+Rha+Ara+Gal).
*** (GalA-Rha).
**** DE values were given by the suppliers, DE of WRP was estimated according to the method described in Méndez et al., (2022).
Numbers in brackets corresponds to standard deviation
The rest of sugars were detected in minor amounts (See supplementary material Fig.S1)
The data are averages and standard deviations (brackets) of triplicate measurements. Values in each column with different superscript letters (a-d) indicates significant differences ($p<0.05$) among samples.

The presence of longer branches in the WRP pectin have been seen to affect the rheological properties of the gels formed with Ca^{2+} (Méndez et al., 2022). However, there are other factors which could affect the structure and physical properties of the gels and of the subsequent aerogels, such as degree of blockiness or esterification degree (DE), among others (Ngouémazong, Kabuye, et al., 2012). As observed from Table 1, WRP had the lowest DE and the greatest protein content and branching degree (RB), with a considerable lower homogalacturonan percentage, thus suggesting less gel strength as observed in previous works with WRP compared with C1 (Méndez et al., 2022; Ngouémazong, Jolie, et al., 2012) that could be highly co-related to the methyl-esterification pattern and available junction zones (Ngouémazong, Jolie, et al., 2012).

The FTIR of the various pectin powders showed the typical fingerprint for pectin (Figure 1A), identified by the two strong absorption bands at 1012 and 1084 cm^{-1} which are attributed to glycosidic linkages (C-O and C-C stretching bonds) and is typical for backbone vibrations of pectin (Bichara et al., 2016; Kacuráková et al., 2000; Mikshina et al., 2017; Pasandide et al., 2017). The band at 1077 cm^{-1} has been previously attributed to neutral Ara-based glycans or RG regions (Kacuráková et al., 2000). Other characteristic pectin FTIR vibrational bands are the one at 1730 cm^{-1}, ascribed to esterified carbonyl groups (C=O), the band at 1598 cm^{-1}, corresponding to free carboxylic groups COO^-, and another symmetric vibrational band at 1406 cm^{-1} which is also related to the free carboxyl groups (Kozioł et al., 2022; Pasandide et al., 2017). Due to the low degree of esterification in all selected pectins (low methoxy degree), a high intensity is observed for the bands representative for free carboxylic (1598 cm^{-1}) groups (Gnanasambandam & Proctor, 2000; Méndez, Fabra, Gómez-Mascaraque, et al., 2021) which is desirable for divalent cation interaction and hydrogel-forming.

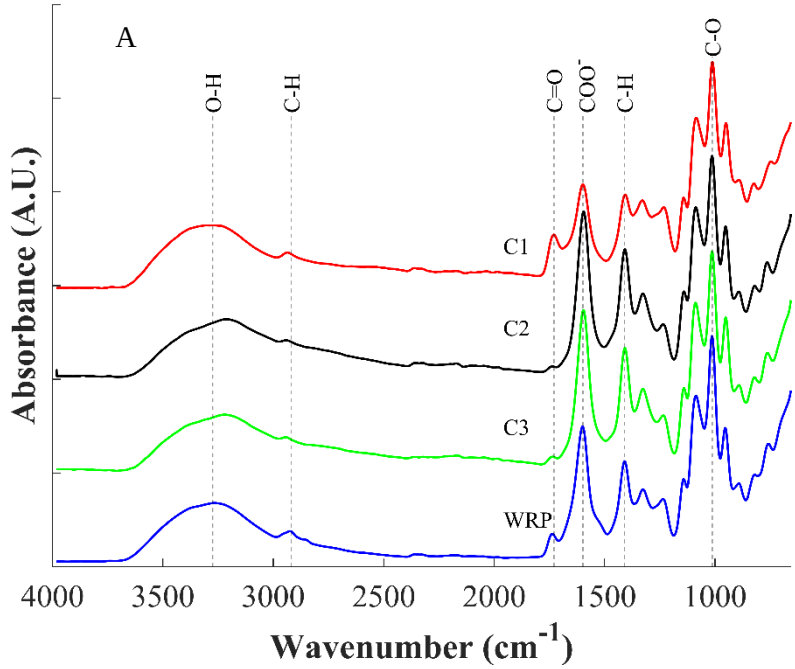
A
O-H
C-H
C=O
COO-
C-H
C-O
C1
C2
C3
WRP
Absorbance (A.U.)
4000
3500
3000
2500
2000
1500
1000
Wavenumber (cm-1)

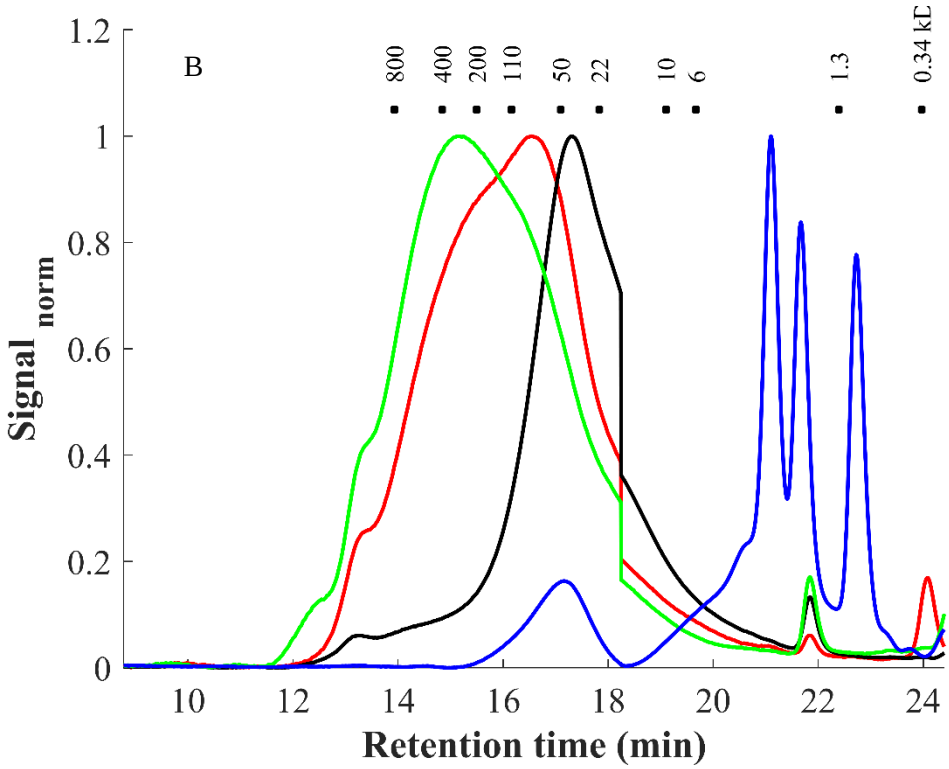
B
800
400
200
110
50
22
10
6
1.3
0.34 kD
Signal norm
1.2
1
0.8
0.6
0.4
0.2
0
10
12
14
16
18
20
22
24
Retention time (min)

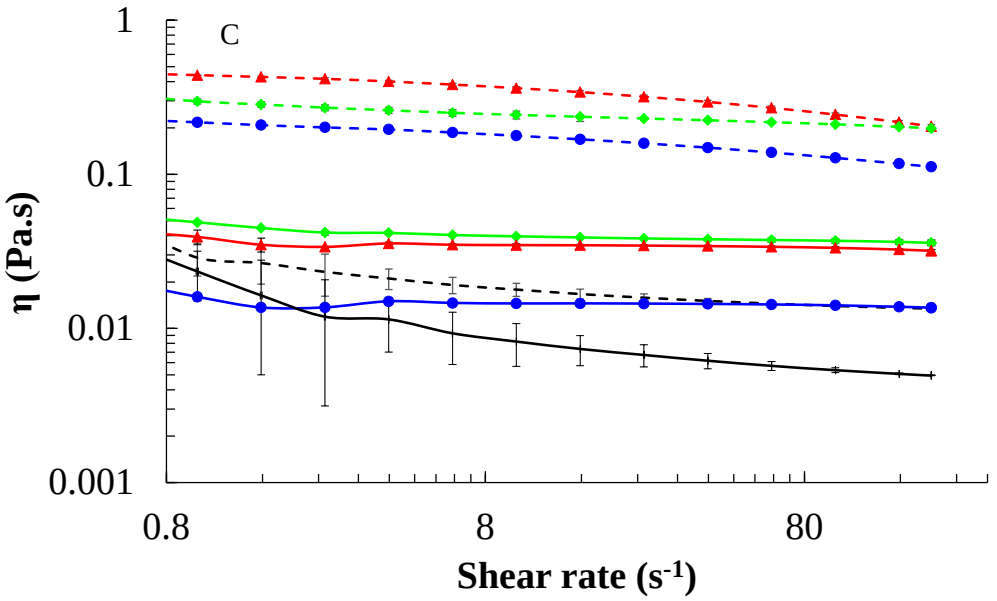

Figure 1. (A) FT-IR spectra for initial pectin powder C1, C2, C3 and WRP. (B) Molar mass (MM) distribution of the pectin samples, the black squares correspond to pullulan standards with the matching MM. (C) Apparent viscosity vs. shear rate curves for solutions prepared with, at 2% (w/w) (continuous line) and 4% (w/w) (dotted line) pectin concentration, WRP (▬), C1 (▬), C2 (▬), and C3 (▬).

Another factor which is closely related to the rheological behaviour of pectin is the molar mass distribution (MM) (Figure 1B), as apart from affecting the viscosity of pectin solutions, also plays a key role in the gelation process itself and in the shape of the gels and final aerogel structure (Schroeter, Yonkova, Niemeyer, et al., 2021). A broad polydisperse peak was observed for the three industrial pectin samples (C1, C2 and C3). In contrast, a much narrower MM was observed for the WRP pectin, which could be a result of the specificity of the enzymatic process and subsequent dialysis steps. WRP had a very similar average MM as the C2 sample (the lower molecular weight pectin) and C3 sample showed the broadest distribution. Smaller peaks (lower than 1.5 kDa) were observed for samples C1, C2 and C3, that were higher with the increase arabinose content of each sample, which

is in accordance with previous reports (Brigand et al., 1990). Interestingly, the WRP also showed three less intense peaks under 2.3 kDa that probably corresponds to the degradation products of pectin or the associated lignin (Sun & Hughes, 1998). These differences may be due to the different extraction conditions, pectin source and the harvest conditions (el Fihry et al., 2022).

The rheological behaviour of pectin solutions was also evaluated as it has been considered a key factor in the production of quality hydrogel beads. Higher viscosities usually induce more spherical beads resistant to impact forces when hitting the coagulation bath surface (Schroeter, Yonkova, Niemeyer, et al., 2021). As expected, higher pectin concentrations (e.g. 4% (w/w)) resulted in increased viscosity and a more shear thickening behaviour ($n<1$) (see Table 2). At the lower pectin concentration (2% (w/w)), the apparent viscosity of the solutions was related with their MM, being the C3 pectin the one giving raise to the more viscous solutions, followed by C1. In the case of C2 and WRP, as shown in Figure 1C, at 2% (w/w) concentration, C2 showed a higher apparent viscosity than WRP only at lower shear rates. At higher shear rates, the hydrophobic interaction caused by the higher DE which is related to more viscous pectins, was surpassed and their resistance to shear stress was lowered as expected for the reduced MM (Chan et al., 2017). Furthermore, it was observed a high standard deviation during the first shear rate steps, due to the low viscosity and high variability during the polymer reorganization of this sample At higher pectin concentration, the closer polymer-polymer interactions affected the rheological behaviour and, although the MM distribution was displaced towards lower molecular weights for the C1 pectin, a greater resistance to shear stress was observed probably ascribed to better electrostatic interactions amongst the pectin chains (Chan et al., 2017; Petkowicz et al., 2017). On the other hand, although samples WRP and C2 share similar MM, WRP had a superior viscosity. This suggests that the branching degree (RB) had a significant impact in the viscosity and rheological properties, caused by the entanglements interactions as previously reported for branched pectin gels (Ngouémazong, Kabuye, et al., 2012; Petkowicz et al., 2017).

Table 2. Flow behaviour index (n), consistency index (k) and apparent viscosity (η_{ap}) of the pectin solutions prepared at (A) 2 and (B) 4% (w/w).

Sample	n	K	R^2	η_{ap} (Pa.s) at 100 s^{-1}
C1 (A)	0.97	0.03	0.999	0.033
C1 (B)	0.85	0.4	0.998	0.244
C2 (A)	0.77	0.015	0.997	0.005
C2 (B)	0.85	0.026	0.998	0.014
C3 (A)	0.96	0.04	0.999	0.037
C3 (B)	0.93	0.28	0.999	0.210
WRP (A)	0.98	0.014	0.999	0.014
WRP (B)	0.87	0.22	0.999	0.129

4.2 Development and characterization of aerogels beads

The substantial differences found amongst the pectin samples studied were expected to affect the microstructure and release properties of aerogel beads produced thereof. Initially, the effect of pectin concentration on aerogel structure was evaluated. To this end, pectin hydrogels were initially obtained by dripping pectin solutions (at 2% and 4% w/w) onto a gelling bath containing 0.5% (w/w) $CaCl_2$ and subsequently, aerogels from the four different pectin samples were obtained through supercritical drying. The average diameter for hydrogel beads was 2.89 ±0.2, 3.43 ±0.3, 2.8 ±0.1 and 2.48 ±0.2 mm for C3, C2, C1 and WRP samples respectively (Table S1. supplementary material), at 2% (w/w). At higher pectin concentration, the size of the beads increased around 20% for samples C2, C3 and WRP. Interestingly, the size of the aerogel particles prepared with C1 increased ~66% at 4% (w/w), which was presumably ascribed to the higher viscosity, increasing the size of the drop during the dripping process.

Figure 2 shows representative images of the visual appearance of the various pectin gels before (hydrogels and alcogels) and after (aerogels) supercritical drying. As observed from this Figure, the morphology of the hydrogel, alcogel and aerogel structures depended on the pectin source. Round shape hydrogel and alcogel capsules obtained from WRP presented a

whitish hue which could be ascribed to the presence of some impurities (like proteins) with different refractive indices which provoked light dispersion. In contrast, those prepared with commercial citrus pectin were more transparent, indicative of a greater homogeneity. Besides, it is worth mentioning that C1 and C3 pectin gave rise to round shaped and translucent beads whereas capsules prepared with C2 had a noticeable irregular shape after the gelling process, even in those prepared at the higher pectin concentration. This suggests that not only the esterification degree but also the molecular weight, linearity and purity played a role on the gel´s formation. The significantly lower viscosity of C2 together with the greater DE and protein content could explain the morphology obtained in this case, in agreement with previous research studies (Fitri et al., 2021; Schroeter, Yonkova, Niemeyer, et al., 2021; Shi et al., 2011).

A

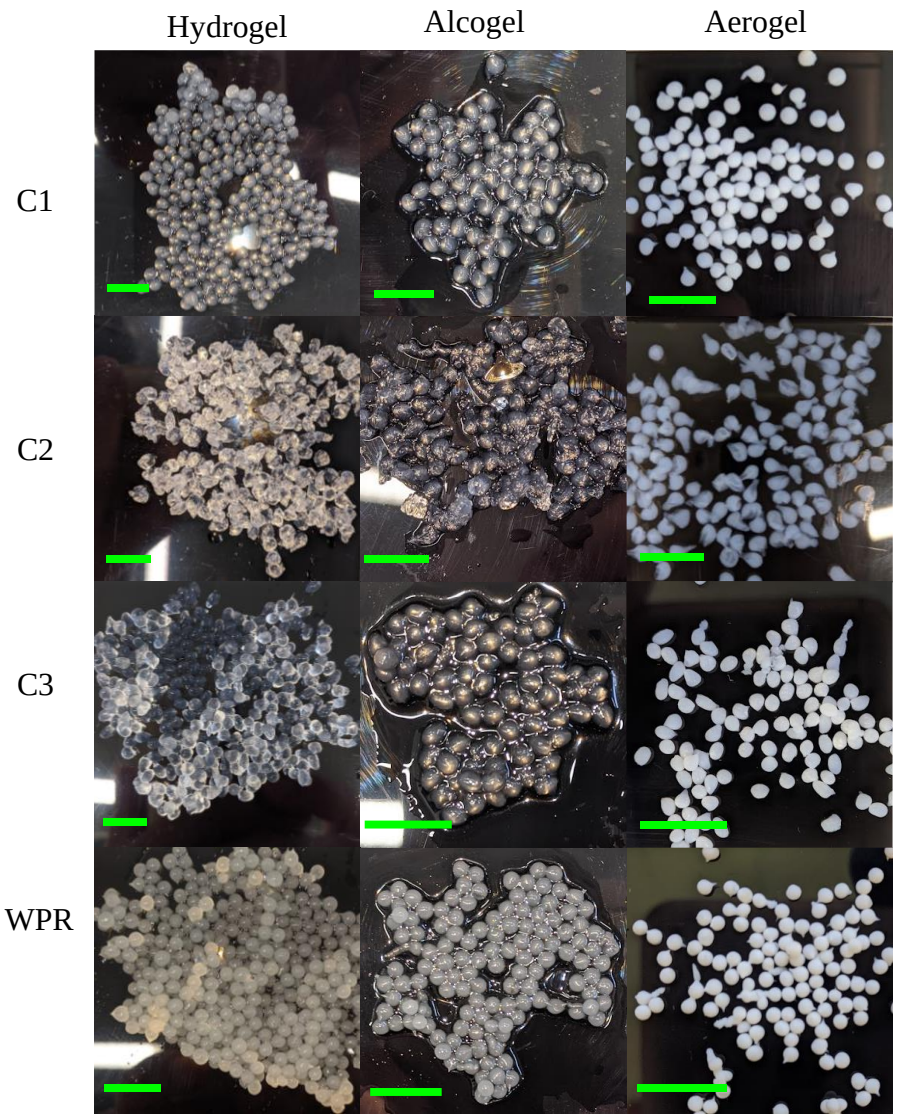

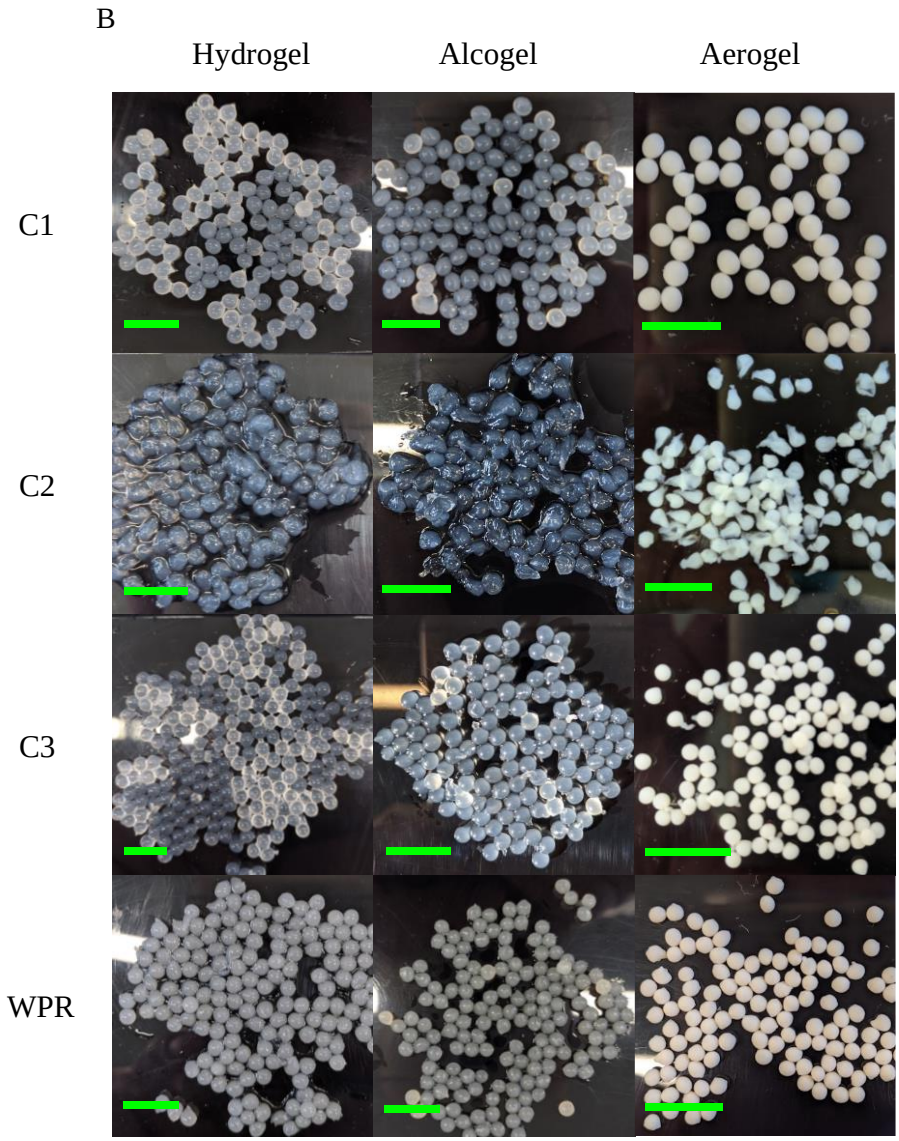

Figure 2. Beads produced by dripping method with gelation bath at 0.5% (w/w) $CaCl_2$ at two pectin concentration solution a) 2% (w/w) and b) 4% (w/w). (green scale bar corresponds to 1 cm).

In order to quantitatively evaluate the morphological changes related to the type of pectin used, the sample volumetric shrinkage was monitored from hydrogel to aerogel for samples prepared at 2 and 4% (w/v) pectin and the results are displayed in Figure 3. The shrinkage phenomenon has been frequently reported for other pectin and bio-based aerogels, and it is

an important parameter for evaluating the quality of aerogels in terms of preservation of the fragile microporous structure, dimensional stability and quality of the aerogel pore system (Chartier et al., 2022; Dirauf et al., 2021; El-naggar et al., 2020; Groult et al., 2021a; Liebner et al., 2009; Schroeter, Yonkova, Niemeyer, et al., 2021). A multistep solvent exchange was used as it has been reported to greatly limit the shrinkage phenomenon. However, at lower pectin concentrations, a significant size reduction was observed already during solvent exchange process. This phenomenon has been previously reported, as hydrogels with low solid contents are prone to significant shrinkage, losing about half of their volume during solvent exchange (Gurikov et al., 2019). In contrast, shrinkage decreased with the increase of pectin concentration, as previously reported for other aerogels, as more concentrated solutions are generally more robust, undergoing less changes during solvent exchange and subsequent drying (Groult & Budtova, 2018; Gurikov et al., 2019). From Figure 3, one could see the relevance of the homogalacturonan (HG) content and DE in the shrinking phenomenon and, thus, the commercial C3 pectin, with a 79% HG content and DE 5.6 exhibited the greatest shrinkage, even when prepared at the higher concentration (4% (w/w)). While the WRP had a substantially lower HG content of 61%, the lower DE (4.8%) partially prevented shrinkage during aerogel formation, probably due to a stronger hydrogel network formed through the interactions between free carboxyl groups and the positively charged divalent ions present in the gelation bath. The C1 pectin, having the lowest DE (5) and a high HG content (81%), probably leading to the strongest hydrogels, was the one suffering from less shrinkage, especially at the higher pectin concentration. Other factors which affect gel strength are also expected to influence the shrinkage degree. Interestingly, a substantial shrinkage was observed in C3 pectin at the greater concentration (cf. Figure 3b), which seems to point out the greater degree of branching, responsible of its greater molecular weight and probably leading to a lower gel strength. In fact, similar effects were previously reported for polyethylene aerogels (Khedaioui et al., 2019; Leven et al., 2021; Liebner et al., 2009). Rodríguez-Dorado et al., (2019) also reported that high molecular weight alginate induced a higher shrinkage degree and less porous materials.

Therefore, it could be concluded that the shrinkage phenomenon was not only affected by the biopolymer concentration, as it has been previously reported, but also by compositional,

structural, molecular interactions and the collapse due to surface tension effects at the vapor–liquid interfaces (Benali & Boumghar, 2014; Groult & Budtova, 2018; Schroeter, Yonkova, Niemeyer, et al., 2021).

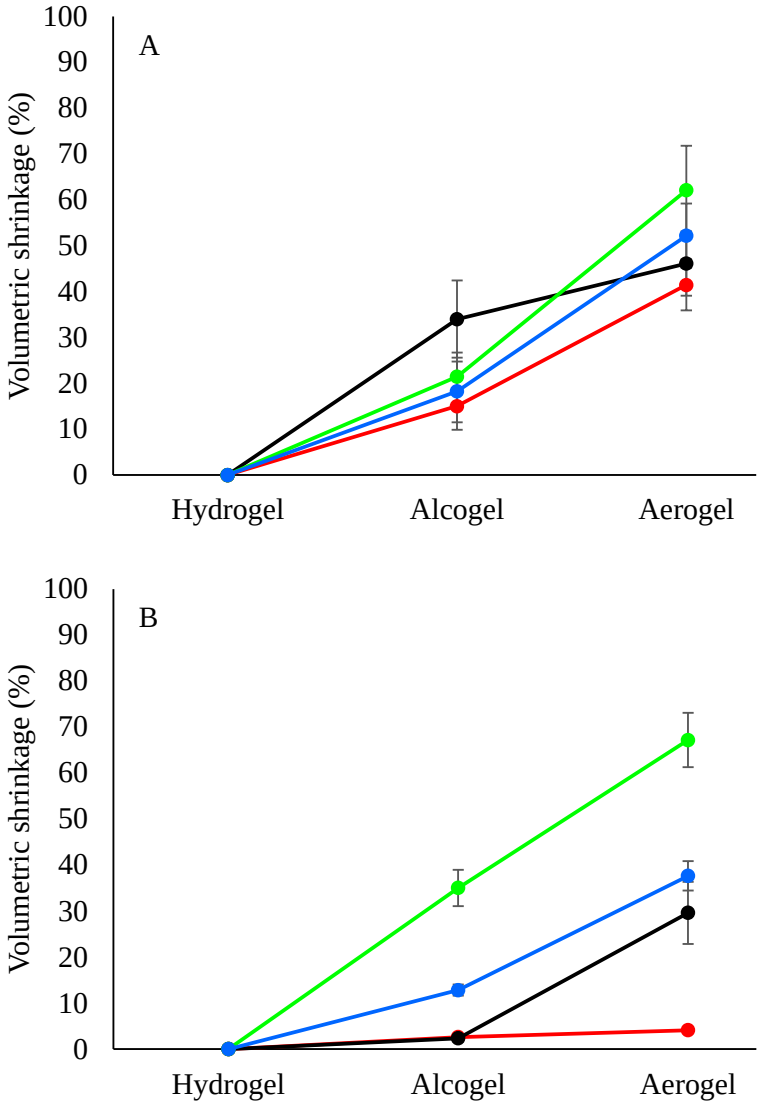

Figure 3. Volumetric shrinkage during the aerogel preparation (C1 (▬), C2 (▬), C3 (▬) and WRP (▬)) as a function of pectin concentration: A) 2% (w/w) and B) 4% (w/w). The hydrogels were formed by dripping the pectin solutions in a 0.5% (w/w) $CaCl_2$ coagulating bath. Lines are drawn to guide the eye.

The microstructure and porosity of the aerogels formed were also examined by scanning electron microscopy (SEM). Figure 4 shows representative micrographs of the inner structure of the aerogel capsules formed using WRP and the commercial pectin samples (C1, C2 and C3) prepared at both concentrations. Although a porous three-dimensional network was observed in the different samples, from the SEM images it was difficult to draw conclusions about the microstructure and, thus, the surface area, bulk density and average pore size were measured through the BET method and the results are displayed in Table 3.

Table 3 displays the surface area, bulk density, and average pore diameter of the various pectin aerogels. In general, the specific surface area of the aerogels ranged between 469 and 585 m^2/g, in agreement with previous works (Preibisch et al., 2018; Veronovski, Tkalec, Knez, & Novak, 2014). Interestingly, while surface area could not be directly related with shrinkage, the bulk density clearly reflected the changes taking place during aerogel formation. In fact, while the surface area of the developed aerogels did not significantly increase as the pectin concentration increased, as it was the case in previous studies (Buchtová & Budtova, 2016; Chartier et al., 2022; Groult & Budtova, 2018), concentration and shrinkage affected the bulk density of the samples, being the C1 and C2 the less dense aerogels, in accordance with their lower shrinkage observed. These lower densities were also correlated with greater average pore diameters (cf. Table 3). pore volume varying from 2.37-8.65 cm^3/g, with noticeable changes among samples (supplementary material Table S4). The fact that increasing the pectin concentration did not lead to a significant increase in the surface area, could be related to the $CaCl_2$ concentration used as a crosslinker, which was fixed at 0.5% (w/w) and, therefore, the amount of calcium ions able to interact with ionized groups of non-methylated galacturonic acid on the pectin backbone was limited (Dronnet et al., 1996; Groult & Budtova, 2018; Thibault & Rinaudo, 1986). Bulk density values were in agreement with the results recently reported by (Groult et al., 2021b), C3 and WRP aerogels presented greater densities, explained by their greater shrinkage degree.

Table 3. Surface Area (m^2/g), bulk density (g/cm^3), and Dpore (**Å**), of aerogel samples (C1, C2, C3 and WRP) produced by the dripping method at (A) 2% (w/w) and (B) 4% (w/w) of pectin solutions and impregnation % (w/w) and bulk density (g/cm^3), of loaded aerogel pectin.

Sample	Surface area (m^2/g)	Bulk density (g/cm^3) Non impregnated	Average Dpore (Å)	Impregnation (% (w/w))	Bulk density (g/cm^3) impregnated
C1(A)	469 (76)[a]	0.025 (0.003)[g]	202	60.5	0.093 (0.001)[e]
C2(A)	527 (31)[a]	0.026 (0.002)[g]	208	57.1	0.091 (0.002)[e]
C3(A)	525 (86)[a]	0.059 (0.004)[c]	137	57.6	0.285 (0.002)[b]
WRP(A)	524 (69)[a]	0.052 (0.002)[d]	137	59.3	0.304(0.02)[a]
C1(B)	523 (53)[a]	0.035 (0.003)[f]	206	9.3	0.049 (0.004)[g]
C2(B)	537 (63)[a]	0.041 (0.003)[e]	207	19.4	0.070 (0.002)[f]
C3(B)	523 (57)[a]	0.104 (0.002)[a]	137	18.3	0.151 (0.005)[c]
WRP(B)	585 (62)[a]	0.070 (0.003)[b]	139	15.2	0.122 (0.003)[d]

The data are averages and standard deviations (brackets) of triplicate measurements. Values in each column with different superscript letters (a-d) indicates significant differences ($p<0.05$) among samples.

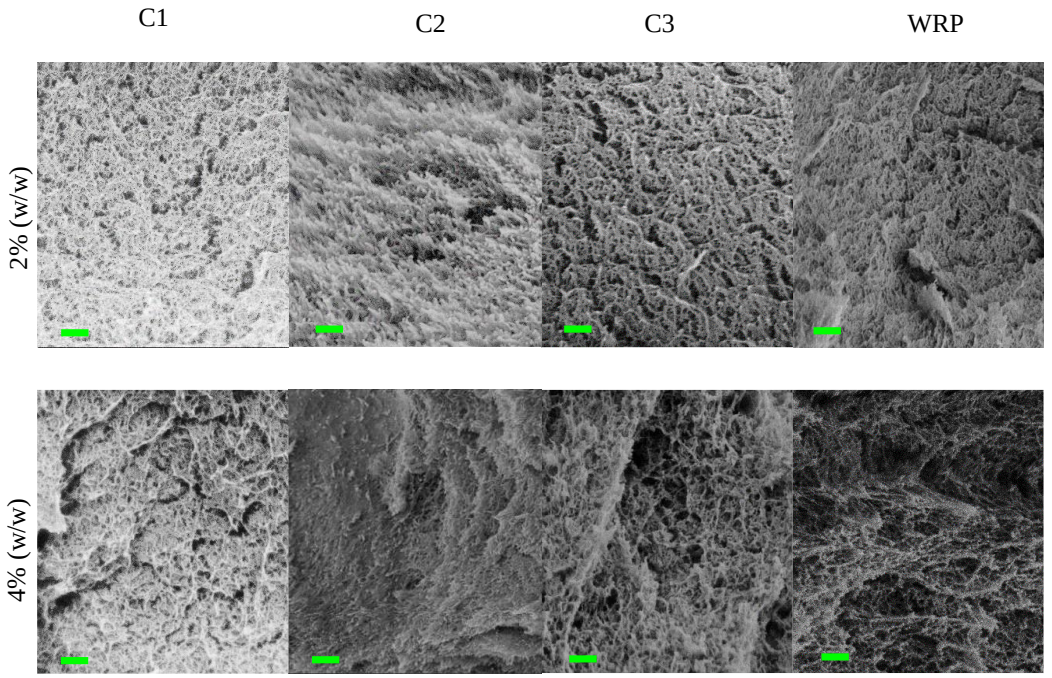

Figure 4. SEM micrographs of pectin aerogels produced via dripping method at two different concentrations: 2% (w/w) and 4% (w/w). Scale markers corresponds to 400 nm.

The various aerogels formed were up-scaled through a jet cutting methodology to check on the validity of the conditions used and the results are shown in the supplementary material (Table S3) which confirmed the reproducibility of the methodology used.

4.3 Pectin aerogels as drug delivery systems

In the last part of this work, highly porous pectin aerogels obtained by means of the dripping methodology were subsequently impregnated with vanillin and the drug loading efficiency and kinetics release were analysed. The impregnation process provided a brief insight of possible chemical interaction and affinity between pectin and vanillin. During the impregnation process, the aerogel beads suffer a size reduction of 8.4, 9.0, 3.1 and 15% for C1, C2, C3 and WRP respectively, as the structure collapses due to the high pressures in the supercritical impregnation process (Fig S2. Table S1 Supplementary material). As

observed in Table 3, the impregnation efficiency varied between 9% and 60%, in agreement with previous works using other biopolymers (García-González et al., 2015; Groult et al., 2021b; Mehling et al., 2009; Tkalec et al., 2016; Veronovski, Tkalec, Knez, Novak, et al., 2014). It is worth mentioning that the loading capacity was significantly higher and very similar in all the pectin aerogels prepared at 2% (w/w) concentration. In contrast, lower vanillin loading was observed when increasing pectin concentration. The results seem to point out to the low chemical affinity between vanillin and low methoxy pectin. Vanillin is a phenolic aldehyde with three functional groups (aldehyde, ether and hydroxyl groups), with a tendency to form aggregates stemming from the hydrophobicity of aromatic compounds (Frenkel & Havna-Frenkel, 2006). The results seem to indicate that at low pectin concentrations, most of the carboxyl groups from pectin are interacting with the calcium cations to form the so-called egg-box junctions, leaving a relatively hydrophobic inner aerogel structure, where vanillin molecules can penetrate and stack together and, thus, similar loadings were observed irrespective of the pectin used. In contrast, at high pectin concentrations, only some of the carboxyl groups were interacting with the calcium ions, thus leaving a more hydrophilic environment within the aerogels. In this case, the composition of the various pectin samples affected aroma loading. C1 pectin, having the lower DE, a high homogalacturonan content, the lower protein content and a low shrinkage, was the one having less vanillin affinity and thus, displaying the lower impregnation. C2 and C3 pectin aerogels displayed the greatest vanillin loading when prepared at 4% (w/w) pectin concentration, probably ascribed to their higher DE, thus presenting a more hydrophobic inner aerogel environment. Interestingly, WRP, even though having the lowest DE, was able to incorporate much more vanillin than the C1 aerogels, explained by the lower HG content (61%) and greater protein content, as aromatic compounds such as vanillin are prone to interact with proteins (Tromelin et al., 2006).

4.4 Release kinetics

The release kinetics are influenced by the drug and carrier material. For instance, when a hydrophilic drug is loaded into a hydrophilic aerogel, hydration and drug dissolution are often fast, facilitating drug desorption. Likewise, different phases could occur depending on the interaction with the media, such as erosion, swelling, and in some cases, dissolution of the carrier matrix. During the first phase, hydration and swelling of the carbohydrate-based aerogels normally takes place, finally resulting in the collapse of the pores and the formation of a hydrogel-like matrix. It has been reported that the velocity of the pore collapse and hydrogel formation affects drug release kinetics (García-González et al., 2021), which will be affected by the pectin type, pectin-vanillin interactions and release media.

In order to characterize the vanillin release profiles from the various pectin aerogels, a Weibull model-based approach was used for description of release kinetics. While the approach is purely empiric, it has demonstrated suitability for highly correlated non-linear kinetic description of chemical reactions in previous works (Kokkinidou et al., 2014; Schroeter et al., 2019; Schroeter, Yonkova, Goslinska, et al., 2021). In this work, the influence of temperature was also evaluated (30, 40 and 50 ºC) but according to the kinetic data, vanillin release was temperature-independent, supporting the hypothesis of low pectin-vanillin interactions. Therefore, the rate constants were calculated from the average profiles of the three kinetic release temperatures. Vanillin release profiles of all samples were fitted with a high correlation (R^2 0.985-0.999) up to complete release by the Weibull model, except the C3 aerogel at 2% (w/w), which showed a differentiated release behaviour starting with a linear release (0 order) followed by a swelling step up to ~ 80% and a final slower release (Figure 5). The data from Table 4 indicate that release kinetics, at least during the first minutes, were mainly influenced by aerogel shrinkage, bulk density and average pore size and, thus, the greatest shrinkage experienced by the C3 aerogel obtained with a pectin concentration of 4% w/w, probably hindered water diffusion within the aerogel, thus limiting the initial vanillin release. WRP also showed slower initial vanillin release, also explained by the lower average pore size limiting solvent diffusion. However, in the case of WRP, once the water penetrated within the structure, a burst vanillin release occurred, again confirming the low chemical affinity between both materials.

The obtained data showed a faster release kinetics compared with previous works from cellulose aerogels loaded with vanillin (Schroeter, Yonkova, Goslinska, et al., 2021) and pectin aerogels loaded with theophylline (Groult et al., 2021a). The use of aerogels for fast release is also desirable in some cases, e.g. in drug release for dermal treatments (Siepmann & Siepmann, 2012).

Table 4. Fitting of kinetic parameters and times of vanillin released to the media at 50% (t50%) and 90% (t90%) of the different impregnated pectin aerogels at (A) 2% (w/w) and (B) 4% (w/w)

Sample	R^2	$\alpha^{-1}(min^{-1})$	β (-)	t50% (min)	t90% (min)
C1(A)	0.985	2.53(0.11)	0.49(0.02)	1.20	13.69
C2(A)	0.996	1.95(0.04)	0.63(0.01)	1.10	7.20
C3(A)	-	-	-	6.7*	12.4*
WRP(A)	0.999	5.81(0.04)	0.89(0.01)	3.96	14.77
C1(B)	0.991	3.35(0.10)	0.58(0.02)	1.80	13.96
C2(B)	0.994	3.9(0.10)	0.56(0.015)	2.05	17.26
C3(B)	0.997	17.9(0.24)	1.36(0.03)	13.69	32.91
WRP(B)	0.996	4.47(0.07)	1.04(0.02)	3.18	9.96

Mean value (standard deviation)
* Average point

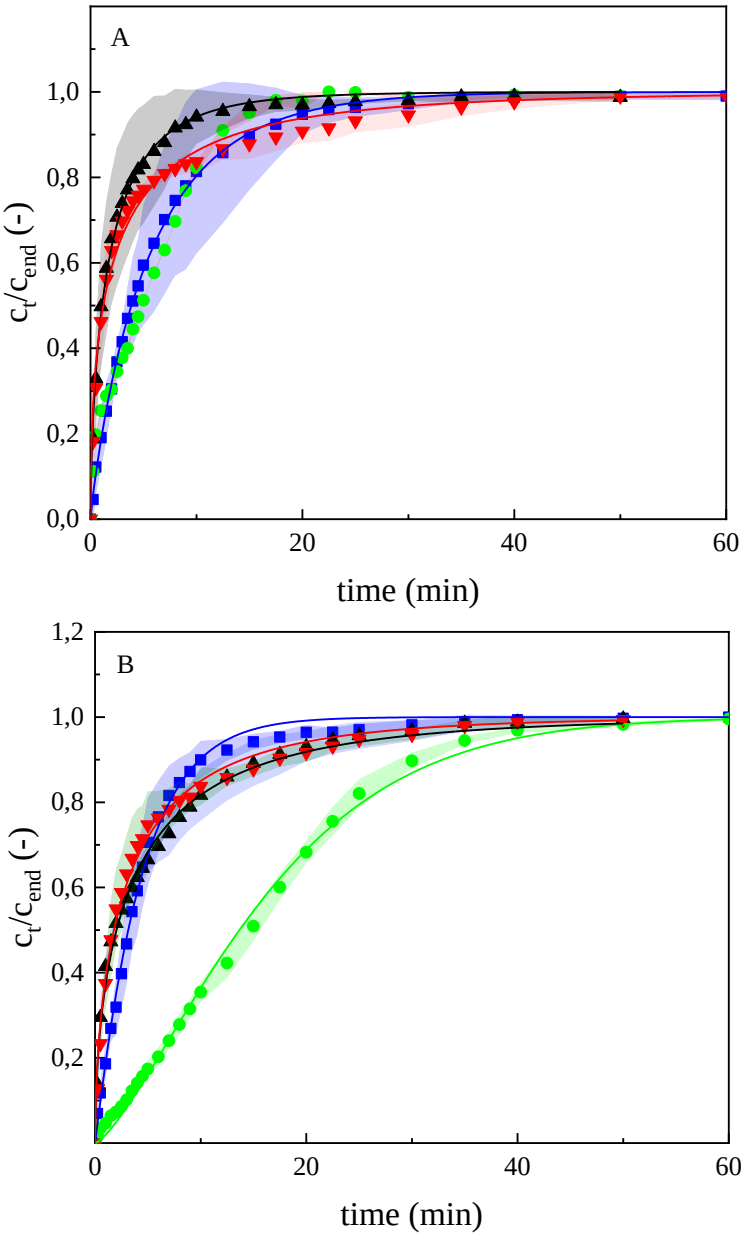

Figure 5. Release patterns of vanillin from impregnated pectin beads (C1 (▬), C2 (▬), C3 (▬) and WRP (▬)) at (A) 2 and (B) 4% (w/w). All data is averaged from 30, 40 and 50 ºC release data and normalized to 100% release. The solid lines correspond to Weibull model fitting. The shaded part of each line corresponds to standard deviation of the average of the three temperature values (30, 40 and 50 ºC).

5 Conclusions

Three commercial citrus pectin samples (C1, C2 and C3) and an enzymatically-modified watermelon rind pectin (WRP) with different physicochemical characteristics were investigated for the production of aerogel beads at two pectin concentrations (2 and 4% (w/w)) and they were evaluated as potential drug carriers. Results showed that pectin concentration, the degree of esterification, composition and molecular weight, affected hydrogel and subsequent aerogel particle formation. The aerogel particles obtained presented high surface areas and low-density values, thus making them attractive vehicles for delivery applications. Shrinkage during aerogel formation was highly dependent on the pectin concentration and structure and, thus, C1 pectin at 4% concentration, having the lowest DE and a high HG content, was the one with the lowest shrinkage, while C3 and WRP with lower HG contents suffered from substantial shrinkage, thus having higher bulk density values and lower average pore diameters. Vanillin, as a model compound, was loaded by impregnation, in the different aerogel structures. The low chemical affinity between pectin and vanillin explained greater aroma loading in the aerogels prepared at 2% (w/w) pectin concentration, while the vanillin content of the aerogels prepared with 4% pectin was seen to depend on the inherent pectin characteristics and, thus, those having more hydrophobic groups were the ones incorporating more vanillin. The low chemical affinity between pectin and vanillin also affected the release kinetics (not influenced by temperature) and, in this case, slower release, especially in the initial phase was observed for the samples with smaller average pore sizes (C3 and WRP), probably due to the limited solvent diffusion towards the inner part of the aerogels. Therefore, the WRP aerogel can be considered as a promising carrier of active compounds of interest in the food and pharma areas. Further experiments are needed to explore their potential as a carrier of hydrophobic compounds and to mimic human conditions.

6 Acknowledgements

D.A. Mendez is recipient of a predoctoral grant from the Ministry of Science Technology and Innovation of the Colombian Government (783-2017). D.A. Mendez also

acknowledges financial support from the also AERoGELS COST action CA18125 of the EU Horizon 2020 Framework Programme. The project RTI2018-094268-B-C22 was funded by MCIN/AEI/10.13039/501100011033 and by "ERDF A way of making Europe". Project INNEST/2021/27 was granted by Agencia Valenciana de Innovación (AVI) and co-financed by the European Union through the Operative Programme of FEDER from Comunitat Valenciana 2014-2020.

7 References

Barrett, E. P., Joyner, L. G., & Halenda, P. P. (1951). The Determination of Pore Volume and Area Distributions in Porous Substances. I. Computations from Nitrogen Isotherms. *Journal of the American Chemical Society*, *73*(1), 373–380. https://doi.org/10.1021/JA01145A126/ASSET/JA01145A126.FP.PNG_V03

Benali, M., & Boumghar, Y. (2014). Supercritical Fluid-Assisted Drying. In A. S. Mujumdar (Ed.), *Handbook of Industrial Drying* (pp. 1291–1300). CRC Press. https://doi.org/10.1201/b17208

Bichara, L. C., Alvarez, P. E., Fiori Bimbi, M. v., Vaca, H., Gervasi, C., & Brandán, S. A. (2016). *Structural and spectroscopic study of a pectin isolated from citrus peel by using FTIR and FT-Raman spectra and DFT calculations*. *76*, 315–327. https://www.sciencedirect.com/science/article/pii/S1350449516300688?via%3Dihub

Brigand, G., Denis, A., Grall, M., & Lecacheux, D. (1990). Insight into the structure of pectin by high performance chromatographic methods. *Carbohydrate Polymers*, *12*(1), 61–77. https://doi.org/10.1016/0144-8617(90)90104-Z

Brunauer, S., Emmett, P. H., & Teller, E. (1938). Adsorption of Gases in Multimolecular Layers. *Journal of the American Chemical Society*, *60*(2), 309–319. https://doi.org/10.1021/JA01269A023/ASSET/JA01269A023.FP.PNG_V03

Buchtová, N., & Budtova, T. (2016). Cellulose aero-, cryo- and xerogels: towards understanding of morphology control. *Cellulose*, *23*(4), 2585–2595. https://doi.org/10.1007/s10570-016-0960-8

Campbell, M., Lee, K. Y., Choo, W. S., Sandarani, M., Kute, A., Mohapatra, D., Babu, B., Sawant, B. P., Hartati, I., & Subekti, E. (2015). Extraction of pectin from watermelon rind. *Journal of Pharmacognosy & Natural Products*, *03*(1), 1–8.

Chan, S. Y., Choo, W. S., Young, D. J., & Loh, X. J. (2017). Pectin as a rheology modifier: Origin, structure, commercial production and rheology. *Carbohydrate Polymers*, *161*, 118–139. https://doi.org/10.1016/j.carbpol.2016.12.033

Chartier, C., Buwalda, S., Van Den Berghe, H., Nottelet, B., & Budtova, T. (2022). Tuning the properties of porous chitosan: Aerogels and cryogels. *International Journal of Biological Macromolecules*, *202*, 215–223. https://doi.org/10.1016/j.ijbiomac.2022.01.042

Chen, H., Qiu, S., Gan, J., Liu, Y., Zhu, Q., & Yin, L. (2016). New insights into the functionality of protein to the emulsifying properties of sugar beet pectin. *Food Hydrocolloids*, *57*, 262–270. https://doi.org/10.1016/j.foodhyd.2016.02.005

Dirauf, M. P., Hajnal, A., Gurikov, P., & Braeuer, A. S. (2021). Protein gel shrinkage during solvent exchange: Quantification of gel compaction, mass transfer and compressive strength. *Food Hydrocolloids*, *120*, 106916. https://doi.org/10.1016/J.FOODHYD.2021.106916

Dronnet, V. M., Renard, C. M. G. C., Axelos, M. A. V., & Thibault, J. F. (1996). Characterisation and selectivity of divalent metal ions binding by citrus and sugar-beet pectins. *Carbohydrate Polymers*, *30*(4), 253–263. https://doi.org/10.1016/S0144-8617(96)00107-5

el Fihry, N., el Mabrouk, K., Eeckhout, M., Schols, H. A., Filali-Zegzouti, Y., & Hajjaj, H. (2022). Physicochemical and functional characterization of pectin extracted from

Moroccan citrus peels. *LWT*, *162*, 113508. https://doi.org/10.1016/J.LWT.2022.113508

El-naggar, M. E., Othman, S. I., Allam, A. A., & Morsy, O. M. (2020). Synthesis, drying process and medical application of polysaccharide-based aerogels. *International Journal of Biological Macromolecules*, *145*, 1115–1128. https://doi.org/10.1016/j.ijbiomac.2019.10.037

Esparza, I., Jiménez-Moreno, N., Bimbela, F., Ancín-Azpilicueta, C., & Gandía, L. M. (2020). Fruit and vegetable waste management: Conventional and emerging approaches. *Journal of Environmental Management*, *265*, 110510. https://doi.org/10.1016/j.jenvman.2020.110510

Fitri, A., Salahuddin, H., Izzuddin, M., Shafiq, I., Huda, Y., Radziah, R., & Hakimah, A. (2021). Optimisation of alginate-pectin bead formulation using central composite design guided electrospray technique. *International Food Research Journal*, *28*(4), 860–870.

Frenkel, C., & Havna-Frenkel, D. (2006). Vanilla Material properties: The Physics and Chemistry of Vanillin - Research sheds light on practical ways to prevent losses of vanillin during production. *Perfumer and Flavorist*, *31*(3).

García-González, C. A., Carenza, E., Zeng, M., Smirnova, I., & Roig, A. (2012). Design of biocompatible magnetic pectin aerogel monoliths and microspheres. *RSC Advances*, *2*(26), 9816–9823. https://doi.org/10.1039/c2ra21500d

García-González, C. A., Jin, M., Gerth, J., Alvarez-lorenzo, C., & Smirnova, I. (2015). Polysaccharide-based aerogel microspheres for oral drug delivery. *Carbohydrate Polymers*, *117*, 797–806. https://doi.org/10.1016/j.carbpol.2014.10.045

García-González, C. A., Sosnik, A., Kalmár, J., de Marco, I., Erkey, C., Concheiro, A., & Alvarez-Lorenzo, C. (2021). Aerogels in drug delivery: From design to application.

Journal of Controlled Release, *332*, 40–63. https://doi.org/10.1016/J.JCONREL.2021.02.012

Gnanasambandam, R., & Proctor, A. (2000). Determination of pectin degree of esterification by diffuse reflectance Fourier transform infrared spectroscopy. *Food Chemistry*, *68*(3), 327–332. https://doi.org/10.1016/S0308-8146(99)00191-0

Groult, S., & Budtova, T. (2018). Tuning structure and properties of pectin aerogels. *European Polymer Journal*, *108*(July), 250–261. https://doi.org/10.1016/j.eurpolymj.2018.08.048

Groult, S., Buwalda, S., & Budtova, T. (2021a). Pectin hydrogels, aerogels, cryogels and xerogels: Influence of drying on structural and release properties. *European Polymer Journal*, *149*, 110386. https://doi.org/10.1016/J.EURPOLYMJ.2021.110386

Groult, S., Buwalda, S., & Budtova, T. (2021b). Tuning bio-aerogel properties for controlling theophylline delivery. Part 1: Pectin aerogels. *Materials Science and Engineering: C*, *126*, 112148. https://doi.org/10.1016/J.MSEC.2021.112148

Gurikov, P., S. P., R., Griffin, J. S., Steiner, S. A., & Smirnova, I. (2019). 110th Anniversary: Solvent Exchange in the Processing of Biopolymer Aerogels: Current Status and Open Questions. *Industrial & Engineering Chemistry Research*, *58*(40), 18590–18600. https://doi.org/10.1021/acs.iecr.9b02967

Hartati, I., & Subekti, E. (2015). Microwave assisted extraction of watermelon rind pectin. *International Journal of ChemTech Research*, *8*(11), 163–170.

Kacuráková, M., Capek, P., Sasinková, V., Wellner, N., & Ebringerová, A. (2000). FT-IR study of plant cell wall model compounds: Pectic polysaccharides and hemicelluloses. *Carbohydrate Polymers*, *43*(2), 195–203. https://doi.org/10.1016/S0144-8617(00)00151-X

Khedaioui, D., Boisson, C., D'Agosto, F., & Montarnal, D. (2019). Polyethylene Aerogels with Combined Physical and Chemical Crosslinking: Improved Mechanical

Resilience and Shape-Memory Properties. *Angewandte Chemie International Edition*, *58*(44), 15883–15889. https://doi.org/10.1002/ANIE.201908257

Kokkinidou, S., Floros, J. D., & Laborde, L. F. (2014). Kinetics of the Thermal Degradation of Patulin in the Presence of Ascorbic Acid. *Journal of Food Science*, *79*(1), T108–T114. https://doi.org/10.1111/1750-3841.12316

Kozioł, A., Środa-Pomianek, K., Górniak, A., Wikiera, A., Cyprych, K., & Malik, M. (2022). Structural Determination of Pectins by Spectroscopy Methods. *Coatings*, *12*(4). https://doi.org/10.3390/coatings12040546

Leven, F., Ulbricht, M., Limberg, J., & Ostermann, R. (2021). Novel finely structured polymer aerogels using organogelators as a structure-directing component. *Journal of Materials Chemistry A*, *9*(36), 20695–20702. https://doi.org/10.1039/D1TA06161E

Liebner, F., Haimer, E., Potthast, A., Loidl, D., Tschegg, S., Neouze, M.-A., Wendland, M., & Rosenau, T. (2009). Cellulosic aerogels as ultra-lightweight materials. Part 2: Synthesis and properties 2nd ICC 2007, Tokyo, Japan, October 25–29, 2007. *Holzforschung*, *63*(1), 3–11. https://doi.org/10.1515/HF.2009.002

Manzocco, L., Mikkonen, K. S., & García-González, C. A. (2021). Aerogels as porous structures for food applications: Smart ingredients and novel packaging materials. *Food Structure*, *28*, 100188. https://doi.org/10.1016/j.foostr.2021.100188

Mehling, T., Smirnova, I., Guenther, U., & Neubert, R. H. H. (2009). Polysaccharide-based aerogels as drug carriers. *Journal of Non-Crystalline Solids*, *355*(50–51), 2472–2479. https://doi.org/10.1016/j.jnoncrysol.2009.08.038

Méndez, D. A., Fabra, M. J., Gómez-Mascaraque, L., López-Rubio, A., & Martinez-Abad, A. (2021). Modelling the Extraction of Pectin towards the Valorisation of Watermelon Rind Waste. *Foods*, *10*(4), 738. https://doi.org/10.3390/foods10040738

Méndez, D. A., Fabra, M. J., Martínez-Abad, A., Martínez-Sanz, Gorria, M., & López-Rubio, A. (2021). Understanding the different emulsification mechanisms of pectin:

Comparison between watermelon rind and two commercial pectin sources. *Food Hydrocolloids*, *120*, 106957. https://doi.org/10.1016/j.foodhyd.2021.106957

Méndez, D. A., Martínez-Abad, A., Martínez-Sanz, M., López-Rubio, A., & Fabra, M. J. (2022). Tailoring structural, rheological and gelling properties of watermelon rind pectin by enzymatic treatments. *Food Hydrocolloids*, 108119. https://doi.org/10.1016/j.foodhyd.2022.108119

Mikshina, P. v., Makshakova, O. N., Petrova, A. A., Gaifullina, I. Z., Idiyatullin, B. Z., Gorshkova, T. A., & Zuev, Y. F. (2017). Gelation of rhamnogalacturonan I is based on galactan side chain interaction and does not involve chemical modifications. *Carbohydrate Polymers*, *171*, 143–151. https://doi.org/10.1016/j.carbpol.2017.05.013

Ne, A., Gordi, M., Davidovi, S., Radovanovi, Ž., Nedeljkovi, J., Smirnova, I., Gurikov, P., Nešić, A., Gordić, M., Davidović, S., Radovanović, Ž., Nedeljković, J., Smirnova, I., & Gurikov, P. (2018). Pectin-based nanocomposite aerogels for potential insulated food packaging application. *Carbohydrate Polymers*, *195*(March), 128–135. https://doi.org/10.1016/j.carbpol.2018.04.076

Ngouémazong, D. E., Jolie, R. P., Cardinaels, R., Fraeye, I., van Loey, A., Moldenaers, P., & Hendrickx, M. (2012). Stiffness of Ca 2+-pectin gels: Combined effects of degree and pattern of methylesterification for various Ca 2+ concentrations. *Carbohydrate Research*, *348*, 69–76. https://doi.org/10.1016/j.carres.2011.11.011

Ngouémazong, D. E., Kabuye, G., Fraeye, I., Cardinaels, R., van Loey, A., Moldenaers, P., & Hendrickx, M. (2012). Effect of debranching on the rheological properties of Ca2+-pectin gels. *Food Hydrocolloids*, *26*(1), 44–53. https://doi.org/10.1016/j.foodhyd.2011.04.009

Pasandide, B., Khodaiyan, F., Mousavi, Z. E., & Hosseini, S. S. (2017). Optimization of aqueous pectin extraction from Citrus medica peel. *Carbohydrate Polymers*, *178*, 27–33. https://doi.org/10.1016/j.carbpol.2017.08.098

Petkowicz, C. L. O., Vriesmann, L. C., & Williams, P. A. (2017). Pectins from food waste: Extraction, characterization and properties of watermelon rind pectin. *Food Hydrocolloids*, *65*, 57–67. https://doi.org/10.1016/j.foodhyd.2016.10.040

Preibisch, I., Niemeyer, P., Yusufoglu, Y., Gurikov, P., Milow, B., & Smirnova, I. (2018). Polysaccharide-based aerogel bead production via jet cutting method. *Materials*, *11*(8). https://doi.org/10.3390/ma11081287

Rodríguez-Dorado, R., López-Iglesias, C., García-González, C. A., Auriemma, G., Aquino, R. P., & Del Gaudio, P. (2019). Design of aerogels, cryogels and xerogels of alginate: Effect of molecular weight, gelation conditions and drying method on particles' micromeritics. *Molecules*, *24*(6). https://doi.org/10.3390/molecules24061049

Rupasinghe, H. P. V., Boulter-Bitzer, J., Ahn, T., & Odumeru, J. A. (2006). Vanillin inhibits pathogenic and spoilage microorganisms in vitro and aerobic microbial growth in fresh-cut apples. *Food Research International*, *39*(5), 575–580. https://doi.org/10.1016/J.FOODRES.2005.11.005

Schroeter, B., Bettermann, S., Semken, H., Melchin, T., Weitzel, H. P., & Pauer, W. (2019). Kinetic Description of Ascorbic Acid Decomposition in Redox Initiator Systems for Polymerization Processes. *Industrial and Engineering Chemistry Research*, *58*(29), 12939–12952. https://doi.org/10.1021/ACS.IECR.9B00710/ASSET/IMAGES/MEDIUM/IE-2019-007109_M013.GIF

Schroeter, B., Yonkova, V. P., Goslinska, M., Orth, M., Pietsch, S., Gurikov, P., Smirnova, I., & Heinrich, S. (2021). Spray coating of cellulose aerogel particles in a miniaturized spouted bed. *Cellulose*, *28*(12), 7795–7812. https://doi.org/10.1007/s10570-021-04032-0

Schroeter, B., Yonkova, V. P., Niemeyer, N. A. M. M., Jung, I., Preibisch, I., Gurikov, P., & Smirnova, I. (2021). Cellulose aerogel particles: control of particle and textural

properties in jet cutting process. *Cellulose*, *28*(1), 223–239. https://doi.org/10.1007/s10570-020-03555-2

Shi, P., He, P., Teh, T. K. H., Morsi, Y. S., & Goh, J. C. H. (2011). Parametric analysis of shape changes of alginate beads. *Powder Technology*, *210*(1), 60–66. https://doi.org/10.1016/J.POWTEC.2011.02.023

Siepmann, J., & Siepmann, F. (2012). Modeling of diffusion controlled drug delivery. *Journal of Controlled Release*, *161*(2), 351–362. https://doi.org/10.1016/J.JCONREL.2011.10.006

Sinha, A. K., Sharma, U. K., & Sharma, N. (2009). A comprehensive review on vanilla flavor: Extraction, isolation and quantification of vanillin and others constituents. *Http://Dx.Doi.Org/10.1080/09687630701539350*, *59*(4), 299–326. https://doi.org/10.1080/09687630701539350

Sun, R., & Hughes, S. (1998). Extraction and Physico-Chemical Characterization of Pectins from Sugar Beet Pulp. *Polymer Journal 1998 30:8*, *30*(8), 671–677. https://doi.org/10.1295/polymj.30.671

Thibault, J. F., & Rinaudo, M. (1986). Chain association of pectic molecules during calcium-induced gelation. *Biopolymers*, *25*(3), 455–468. https://doi.org/10.1002/BIP.360250306

Tkalec, G., Knez, Ž., & Novak, Z. (2016). PH sensitive mesoporous materials for immediate or controlled release of NSAID. *Microporous and Mesoporous Materials*, *224*, 190–200. https://doi.org/10.1016/J.MICROMESO.2015.11.048

Tromelin, A., Andriot, I., & Guichard, E. (2006). Protein–flavour interactions. In *Flavour in Food* (pp. 172–207). Elsevier. https://doi.org/10.1533/9781845691400.2.172

Veronovski, A., Tkalec, G., Knez, Ž., & Novak, Z. (2014). Characterisation of biodegradable pectin aerogels and their potential use as drug carriers. *Carbohydrate Polymers*, *113*, 272–278. https://doi.org/10.1016/j.carbpol.2014.06.054

Veronovski, A., Tkalec, G., Knez, Z., Novak, Z., Veronovski, A., Tkalec, G., Knez, Z., & Novak, Z. (2014). Characterisation of biodegradable pectin aerogels and their potential use as drug carriers. *Carbohydrate Polymers*, *113*, 272–278. https://doi.org/10.1016/j.carbpol.2014.06.054

White, R. J., Budarin, V. L., & Clark, J. H. (2010). Pectin-derived porous materials. *Chemistry - A European Journal*, *16*(4), 1326–1335. https://doi.org/10.1002/CHEM.200901879

Zubairu, A., Gimba, A. S. B., Mamza, W. J., & Highina, B. K. (2018). Proximate Analysis of Dry Watermelon (Citrullus lanatus) Rind and Seed Powder. *Available Online Www.Jsaer.Com Journal of Scientific and Engineering Research 473 Journal of Scientific and Engineering Research*, *5*(3), 473–478.

8 Supplementary Material

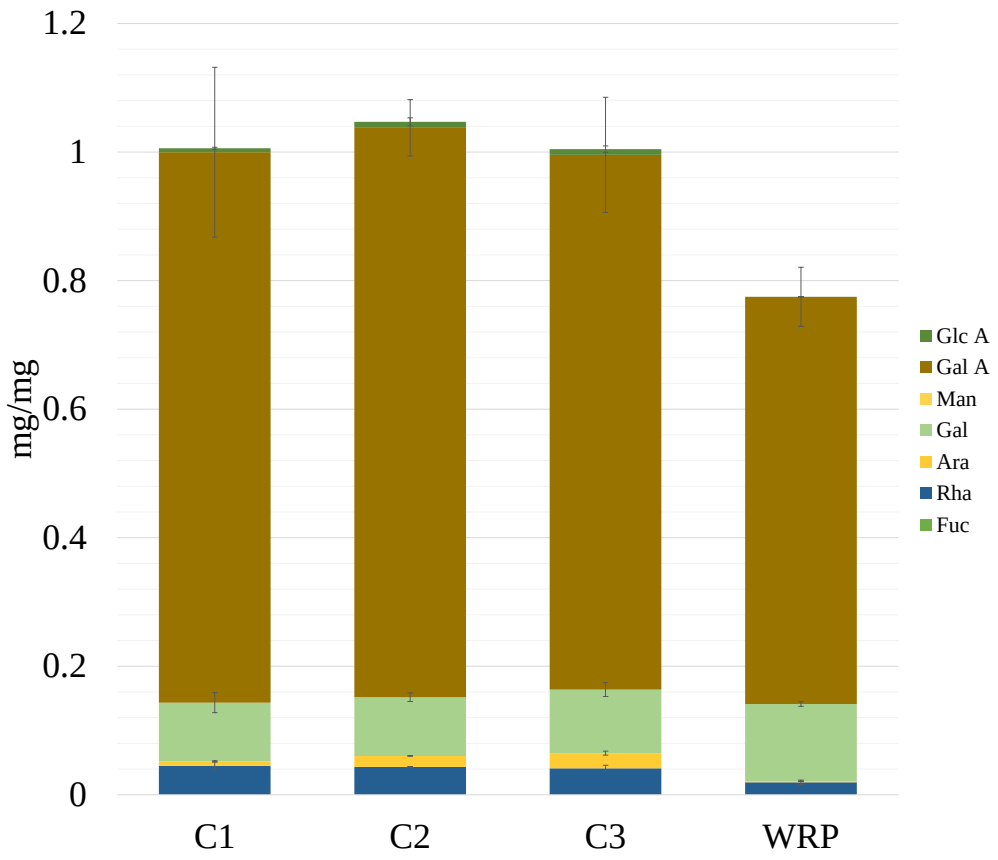

Figure S1. Sugar constituents of the three different pectins, citrus pectin with different characteristics (C1, C2 and C3) and WRP enzymatically modified.

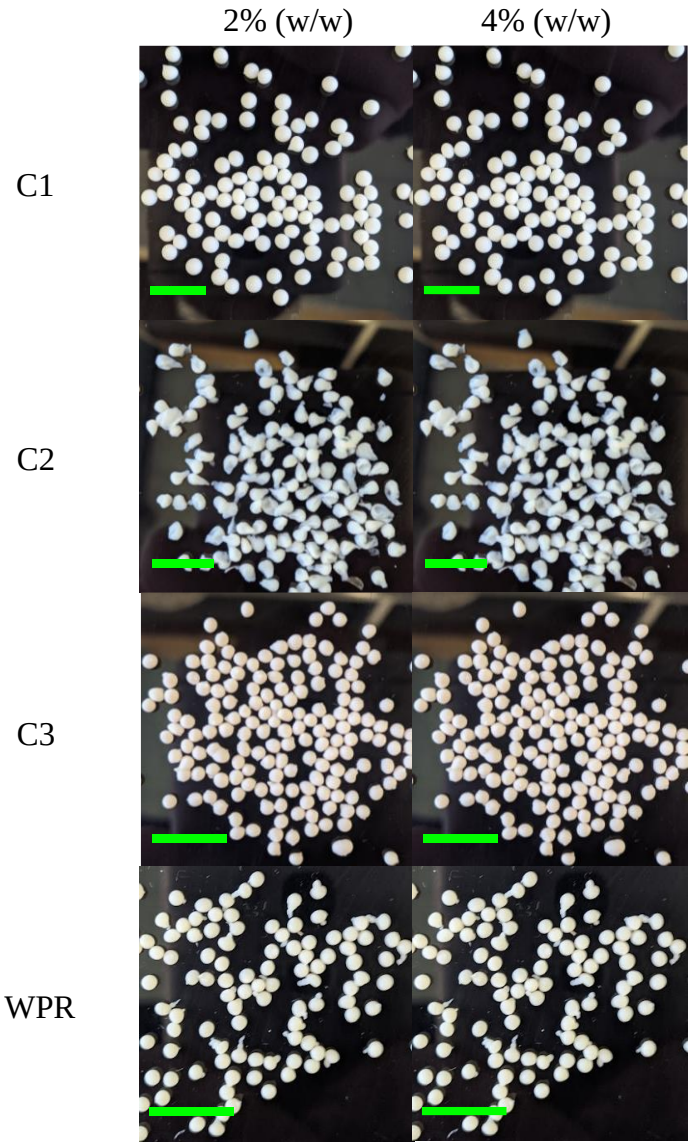

Figure S2. Beads impregnated with vanillin by dripping method with gelation bath at 0.5%(w/w) $CaCl_2$ at two pectin concentration solution a) 2% (w/w) and b) 4% (w/w). (green scale bar corresponds to 1 cm).

Table S1. Morphological characteristics of aerogel beads analyzed by ImageJ software.

Samples	Process	Area mm^2	Perimeter (mm)	SPH	Radius (mm)	Diameter (mm)
			2% (w/w)			
C1	Hydrogel	6.7(1.1)	11.3(1.5)	0.6(0.1)	1.4(0.1)	2.9(0.2)
	Alcogel	5.8(1.4)	11.6(2.5)	0.5(0.1)	1.3(0.2)	2.6(0.3)
	Aerogel	3.9(0.5)	7.6(0.7)	0.8(0.06)	1.1(0.09)	2.2(0.2)
	Impregnated	2.7(0.4)	6.5(0.6)	0.8(0.07)	0.9(0.07)	1.8(0.1)
C2	Hydrogel	9.3(1.8)	12.1(1.2)	0.7(0.07)	1.7(0.1)	3.4(0.3)
	Alcogel	6.1(1.5)	9.7(1.3)	0.8(0.07)	1.3(0.1)	2.7(0.3)
	Aerogel	5.0(0.76)	9.3(1.0)	0.7(0.08)	1.2(0.09)	2.5(0.2)
	Impregnated	2.7(0.36)	6.7(0.5)	0.7(0.09)	0.9(0.06)	1.8(0.1)
C3	Hydrogel	6.6(0.8)	9.6(0.7)	0.8(0.05)	1.4(0.09)	2.8(0.1)
	Alcogel	5.1(0.7)	8.4(0.6)	0.9(0.028)	1.2(0.1)	2.5(0.2)
	Aerogel	2.5(0.3)	5.9(0.6)	0.8(0.058)	0.8(0.07)	1.7(0.1)
	Impregnated	1.1(0.2)	4.1(0.4)	0.8(0.05)	0.6(0.061)	1.2(0.1)
WRP	Hydrogel	4.9(0.9)	9.4(1.4)	0.7(0.1)	1.2(0.1)	2.4(0.2)
	Alcogel	4.1(0.5)	8.1(0.9)	0.7(0.1)	1.1(0.07)	2.2(0.1)
	Aerogel	2.3(0.2)	5.7(0.4)	0.8(0.06)	0.8(0.04)	1.7(0.08)
	Impregnated	1.0(0.1)	3.8(0.3)	0.8(0.06)	0.5(0.03)	1.1(0.06)
			4% (w/w)			
C1	Hydrogel	7.8(1.1)	11.5(1.0)	0.7(0.1)	1.5(0.1)	4.8(0.2)
	Alcogel	7.5(0.8)	11.0(0.856)	0.7(0.1)	1.5(0.08)	4.2(0.7)
	Aerogel	7.4(0.5)	10.2(0.409)	0.9(0.01)	1.5(0.06)	4.8(0.1)
	Impregnated	6.2(0.5)	9.2(0.371)	0.9(0.02)	1.412(0.059)	4.4(0.1)
C2	Hydrogel	7.2(1.3)	10.7(1.261)	0.7(0.09)	1.5(0.1)	3.02(0.2)
	Alcogel	7.1(2.1)	12.7(2.837)	0.5(0.1)	1.4(0.2)	2.9(0.5)
	Aerogel	5.1(1.1)	9.3(1.457)	0.7(0.106)	1.2(0.1)	2.5(0.2)
	Impregnated	4.2(0.9)	8.1(1.1)	0.7(0.07)	1.1(0.1)	2.3(0.2)
C3	Hydrogel	8.3(1.3)	11.3(0.9)	0.8(0.07)	1.6(0.1)	3.2(0.2)
	Alcogel	5.4(0.6)	9.6(0.9)	0.7(0.104)	1.3(0.07)	2.6(0.1)
	Aerogel	2.7(0.2)	6.2(0.4)	0.8(0.065)	0.9(0.04)	1.8(0.08)
	Impregnated	2.9(0.4)	6.4(0.6)	0.8(0.071)	0.9(0.07)	1.9(0.1)
WRP	Hydrogel	6.1(1.2)	10.3(1.5)	0.7(0.135)	1.3(0.1)	2.7(0.3)
	Alcogel	5.3(0.5)	9.1(0.7)	0.8(0.09)	1.3(0.06)	2.6(0.1)
	Aerogel	3.8(0.3)	7.2(0.4)	0.9(0.04)	1.1(0.04)	2.2(0.09)
	Impregnated	2.7(0.2)	6.2(0.6)	0.8(0.08)	0.9(0.04)	1.8(0.09)

Table S2. Surface area (m^2/g), bulk density (g/cm^3) and impregnation rate (%) of the pectin aerogels produced by jet-cutting method at 2% (w/w) and 4% (w/w) pectin solutions.

	Surface area (m^2/g)		Impregnation (% (w/w)		Bulk density (g/cm^3) Non impregnated		Bulk density (g/cm^3) impregnated	
Sample	2% (w/w)	4% (w/w)	2% (w/w)	4% (w/w)	2% (w/w)	4% (w/w)	2% (w/w)	4% (w/w)
C1	437.2	533.4	39.0	14.3	0.02(0.001)	0.04(0.01)	0.23(0.003)	0.07(0.001)
C2	581.3	630.6	33.4	15.3	0.03(0.004)	0.06(0.02)	0.14(0.001)	0.06(0.002)
C3	520.2	541.8	39.2	13.8	0.05(0.001)	0.10(0.02)	0.48(0.003)	0.17(0.001)
WRP	451.6	627.1	40.8	14.1	0.06(0.001)	0.09(0.02)	0.53(0.004)	0.12(0.002)

Table S3. Particle diameter (Dparticle mm), sphericity (SPTH) and span (g/cm^3), and impregnation rate (%) of aerogel pectin samples produced by jet-cutting method at 2% (w/w) and 4% (w/w) pectin solutions.

Sample	Dparticle mm		Mean value SPHT3		Span	
	2%	4%	2%	4%	2%	4%
C1	0.26(0.19)	0.36(0.023)	0.83(0.078)	0.87(0.005)	0.372(0.484)	0.875(0.011)
C2	0.53(0.033)	0.34(0.02)	0.65(0.024)	0.77(0.001)	0.89(0.028)	0.988(0.036)
C3	0.56(0.06)	0.59(0.012)	0.69(0.022)	0.7(0.026)	0.965(0.058)	0.976(0.074)
WRP	0.42(0.021)	0.36(0.051)	0.73(0.006)	0.81(0.024)	1.233(0.033)	1.023(0)

Table S4. Pore volume (Vpore-BJH) of beads produced by dripping method at 2%(w/w) and 4%(w/w).

Sample	**Average Vpore (cm^3/g)**	
	2% (w/w)	4% (w/w)
C1	2.37	3.63
C2	3.95	6.23
C3	7.32	5.40
WRP	8.65	7.37

CHAPTER 2

VALORISATION OF PERSIMMON FRUITS.

3.2.1 Influence of the extraction conditions on the carbohydrate and phenolic composition of functional pectin from persimmon waste streams.

3.2.2 Bioactive extracts from persimmon waste: Influence of extraction conditions and ripeness.

3.2.3 Sustainable bioactive pectin-based films to improve fruit safety via a circular economy approach.

INTRODUCTION TO CHAPTER 2

The seasonality, artificial over-ripening and high perishability during post-harvest of persimmon fruit produce a huge amount of rejected fruit, not suitable for consumption or commercialization. One possible strategy to alleviate this problem would be to valorise this by-product. In this regard, the demonstrated high polyphenol (tannin) content of this fruit generates the opportunity to obtain biofunctional compounds with potential applications, as an antioxidant, antimicrobial, and antiviral among other properties, in food or other applications. Likewise, a characterization of the main components in the rejected fruits to determine which fruit maturity state contains higher amounts of valuable compounds (e.g. pectin) is crucial to optimize the extraction and consequent valorisation of persimmon biomass waste.

First, the extraction of a phenolic-rich fraction from two different maturity stages of persimmon fruit was evaluated using a central composite design, and evaluated in terms of antioxidant activity and polyphenol content. The optimum extract with the conditions set by the experimental design was industrially up-scaled and its composition, cytotoxicity and advanced functional properties, such as antiviral, anti-ageing effect and fat reduction, were evaluated.

Having found an interesting relationship between pectin and polyphenol extraction, persimmon fruit was characterized to select the best maturity stage, triggering both the highest pectin and polyphenol content. Then, extraction parameters of these compounds from the selected fruits were evaluated through a 3-level full factorial design. Response factors included sugar constituents, polyphenol content, and antioxidant activity with insight on pectin structure and the polyphenol profile.

Finally, the application of this functional pectin in edible coatings was tested. According to the positive results regarding antiviral activity from the previous works, films were prepared with two different types of persimmon pectin obtained from the second part of this chapter. These pectins were mixed with commercial citrus pectin separately. The physicochemical

properties were evaluated and the functionality of the antiviral edible coatings was investigated with application on blueberry fruits.

3.2.2

BIOACTIVE EXTRACTS FROM PERSIMMON WASTES: INFLUENCE OF EXTRACTION CONDITIONS AND RIPENESS.

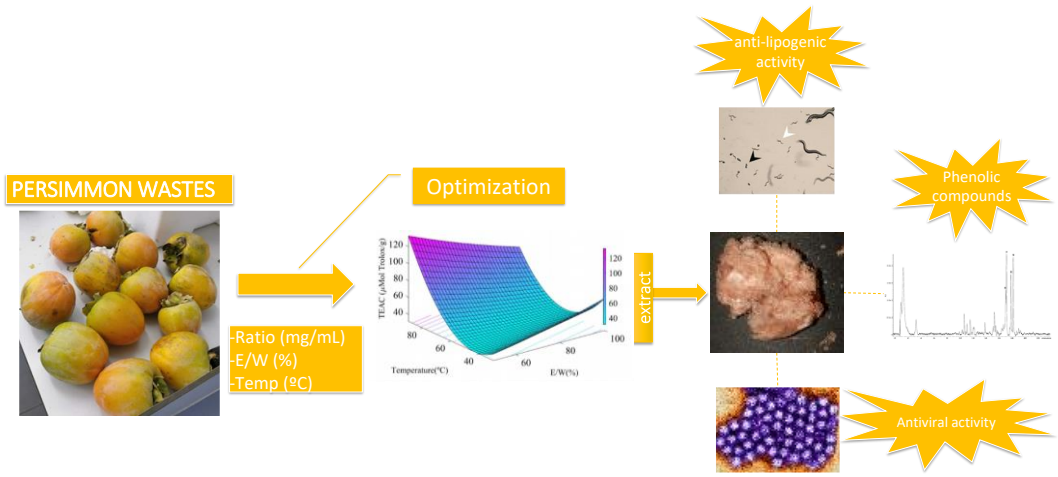

This section is an adapted version of the following published research article:

Méndez, D. A., Fabra, M. J., Falcó, I., Sánchez, G., Aranaz, P., Vettorazzi, A., … López-Rubio, A. (2021). Bioactive extracts from persimmon waste: influence of extraction conditions and ripeness. *Food & Function, 12*(16), 7428–7439. https://doi.org/10.1039/D1FO00457C

1 Abstract

In this work, a bioactive persimmon extract was produced from discarded fruits. A central composite design was used to evaluate the effect of different extraction parameters and ripeness stage of persimmon fruits on the total phenolic content and antioxidant activity of the resulting extracts. Significantly greater phenolic contents were obtained from immature persimmon (IP) fruits. The optimum IP extract with the conditions set by the experimental design was industrially up-scaled and its composition and functional properties were evaluated and compared with that obtained at lab-scale conditions. Both extracts contained significant protein (>20%) and phenolic contents (11-27 mg GA/g dry extract) and displayed significant antiviral activity against murine norovirus hepatitis A virus. Moreover, the extract showed no toxicity and significantly reduced the fat content and the cellular ageing of *Caenorhabditis. elegans* (*C. elegans*) without affecting the worm development. These effects were mediated by down-regulation of fat-7, suggesting an anti-lipogenic activity of this extract.

2 Introduction

According to the Food and Agriculture Organization (FAO), around 14 percent of the food produced worldwide every year is lost from the post-harvest stage to the retail stage and, of this, fruit and vegetables have the second highest wastage rate of the different commodity groups after roots and tubers (FAO, 2019). being the reduction of food loss and waste an important target of the Sustainable Development Goals (SDGs), relating to food security, nutrition and environmental sustainability.

To date, most agro-industrial wastes have been extensively used as a source of fuel, animal feed or as organic fertilizer (Venkata Mohan et al., 2016). However, there is a growing interest in the valorisation of agro-industrial by-products and wastes as abundant, cheap and renewable sources of high added value molecules with specific functional properties (Méndez et al., 2021; Müller-Maatsch et al., 2016).

Persimmon (*Diospyros kaki Thunb*.) fruits are rich in various nutrients and phytochemicals, including carbohydrates, vitamins, proanthocyanidins, flavonoid oligomers, tannins, phenolic acids, dietary fibre and carotenoids, which significantly contribute to their taste, colour, nutritional and medicinal value (Yoo et al., 2019). Although China is by far the larger producer, a significant amount of persimmon is also produced in Spain, being the main exporter of the fruit, particularly in Europe (Domínguez Díaz et al., 2020). Currently, the seasonality and overproduction, together with problems associated with storage, ripening processes, fruit disease and stringent standard demands in terms of fruit appearance, give raise to huge amounts of discarded fruit at different stages of ripeness, which is estimated to be around 5-20% of the fruit harvested (Munera et al., 2019). In this sense, and given the existing evidence related to beneficial functional attributes derived from phytochemicals (and more specifically polyphenols) present in the persimmon fruits (Domínguez Díaz et al., 2020; Kamimoto et al., 2014), a plausible strategy for its valorisation can be obtaining polyphenol-rich extracts from the discarded fruits. It is also well-known that composition changes with fruit ripeness and, thus, exploring these functional attributes in different stages of development can also be helpful to determine the best ripening stage if aiming to this type of valorisation.

Although a few research works have focused on obtaining purified tannins from persimmon pulp (Gu et al., 2008; Liu et al., 2018), from an application view point, obtaining polyphenol-rich extracts with simple, green and scalable processes may be desirable. Therefore, the main goals of this work were first to optimize the extraction protocol to obtain polyphenol-rich extracts from persimmon fruit at two different ripeness stages, selecting the optimal one in terms of polyphenol content and antioxidant capacity. Subsequently, the selected extract was industrially up-scaled to check on the validity of the extraction process and various functional properties of interest for its practical application as food ingredient were evaluated, including antioxidant, antiviral, anti-obesity and anti-ageing capacity both using *in-vitro* and *in- vivo* (*Caenorhabditis elegans*) methods. A complete characterization of the selected extract was carried out, including protein content, monosaccharide analysis, polyphenolic profile and a preliminary genotoxicity screening assay through an SOS/*umu*-

test. Overall, the results presented in this work will provide the basis for the production of a potential antioxidant extract produced by a valorisation of persimmon fruit.

3 Materials and methods

3.1 Materials

Persimmon (*Diospyros kaki* Thunb) "Rojo brillante-Ribera del Xuquer" discarded fruits in two ripeness stages: immature (I) and mature (M) (see photos in Figure S1 from the Supplementary Material), astringent variety, were kindly supplied by Anecoop S. Coop. during the autumn season of 2019 (Spain). The unpeeled whole fruits, after removal of the calix and peduncle, were cut into pieces of around 0.5 – 2.5 cm and they were kept in sealed bags at - 20 °C and subsequently freeze-dried before further processing. Folin-Ciocalteu's reagent, Trolox (97% purity) and gallic acid (≥98.0% purity), were supplied by Sigma-Aldrich (Stenheim, Germany). Ethanol (96% (v/v), USP grade) was purchased from Panreac Applichem (Darmstadt, Germany).

3.2 Experimental design for obtaining the persimmon extracts (PE)

A response surface methodology with central composite design (CCD) was carried out in lab scale to investigate the effect of solid:liquid ratio (mg/mL) (X_1), ethanol:water ratio (E/W %) (X_2) and temperature (°C) (X_3) on the extraction of polyphenolic compounds and antioxidant capacity of the extracts from persimmon fruit, at two different ripeness stages (I and M). The whole design consisted of 20 experimental points carried out in random order, which included 8 factorial points, 6 centre points and 6 axial points (Table 1). Experimental data were fitted to a second-order polynomial equation. For the extractions, 5 g of freeze-dried samples were used in the various ethanol:water solutions, adjusting the volume and ratio of the solvent. Then, they were heated on a hotplate with magnetic stirring during 1 hour. After that, the different persimmon extracts obtained (IPE and MPE for the extracts obtained from the immature and mature fruits, respectively) were filtered with a muslin cloth, freeze-dried and stored in a desiccator with silica gel until subsequent

characterization. After freeze-drying, the various extracts obtained were weighed to evaluate the yield.

Tables of the analysis of variance (ANOVA) were generated, and the effect and regression coefficients of individual linear, quadratic, and interactive terms were determined. Quality of fit (coefficient of determination (R^2)), adjusted coefficient of determination (adj-R^2) and lack of fit, were attained using software Minitab version 15 (Minitab Inc., Philadelphia, U.S.A.). Differences were considered significant at $p \leq 0.05$.

A principal component analysis (PCA) using Minitab 15 Software was also performed for a better evaluation of the results. Then, the better extraction conditions in terms of TPC and antioxidant activity was used for up-scaling.

3.3 Total phenolic content (TPC)

TPC of the extracts was determined using a spectrophotometric method (Singleton et al., 1999). Previously, the freeze-dried IPE and MPE was dissolved in PBS at 5 mg/mL. The reaction mixture was prepared by mixing 0.2 mL of the extract solutions for each treatment, 1 mL of 10% Folin-Ciocalteu's reagent dissolved in distilled water and 0.8 mL 7.5% $NaHCO_3$. The samples were thereafter incubated in a thermostat at 50 °C for 10 min and the mean absorbance of a triplicate analysis determined at λ_{max} = 750 nm. The same procedure was repeated for the standard solution of gallic acid and the content of phenolic compounds in the various extracts was expressed in terms of gallic acid equivalents (mg GAE/g extract).

3.4 Antioxidant activity

The Trolox Equivalent Antioxidant Capacity (TEAC) of the persimmon extracts was determined using a modification of the original TEAC method (Re et al., 1999). Trolox (6-hydroxy-2,5,7,8-tetramethylchroman-2-carboxylic acid), was used as a standard of antioxidant capacity. Samples were solubilized in distilled water for 12 hours and analyzed for $ABTS^{+\cdot}$ (2,2-azinobis (3-4ethylbenzothiazoline)-6-sulfonic acid) radical scavenging activity. First, the ABTS+·solution with an initial absorbance at 734 nm of 0.70 ± 0.08 was

prepared, then 20 µL of the various IPE and MPE were added to 230 µL of the ABTS+·solution and the absorbance was registered at 6 min. For calibration, Trolox standards of different concentrations were prepared, and the same procedure was followed. The TEAC of the persimmon extracts was determined by comparing the corresponding percentage of absorbance reduction at 6 min with the Trolox concentration-response curve. All the determinations were carried out, at least, six times using a spectrophotometer (CLARIOstar, BMG LABTECH, Germany) and water as blank.

3.5 Up-scaled extraction of the selected persimmon extract

The extraction process using the optimized conditions in terms of total polyphenolic content and antioxidant activity was industrially scaled up by the Kimitec Group (Vícar, Spain). In order to make the process industrially viable, ethanol was replaced by isopropanol and, instead of freeze drying, the extract was concentrated with a semi-industrial concentrator at mild temperatures. Briefly, 200 kg of fresh immature persimmon samples were washed and ground with an industrial mixer. The extraction was carried out by recirculation in a helical mill at 60 °C for 1 h using a solid:liquid ratio of 83.3 g L^{-1} and a mixture of 75:25 isopropanol : water solution. The extract was subsequently filtered with a vibrating sieve and concentrated using a semi-industrial concentrator with a capacity of 350 L h^{-1} and a rotary evaporator. An aliquot of the scaled-up extract was freeze-dried to quantify its solid content, determine the yield (50 g concentrated extract /100 g dried sample) and use it for subsequent functional analysis.

3.6 Compositional characterization of the selected persimmon extract

3.6.1 Protein content.

Samples were analysed, in triplicate, for total nitrogen content using an Elemental Analyser Rapid N Exceed (Paralab S.L., Spain). Approximately 100 mg of dry extracts were pressed into pellets and then analyzed using the Dumas method, which is based on the combustion of the sample and subsequent detection of the released N_2 (Wiles et al., 1998). The protein content was calculated from the nitrogen content multiplied by a factor of 6.25.

3.6.2 Carbohydrate composition.

The carbohydrate composition in both the lab-scale and up-scale obtained samples was determined after acid methanolysis of the extracts. Briefly, the dried extracts were submitted to methanolysis, with acid methanol (HCl 2 M) during 5 h at 100 °C, followed by neutralization and drying with inert air. Subsequently, the methoxy group was hydrolyzed with trifluoroacetic acid (2 M, 1 h at 100 °C) and the volatile acid was eliminated with air flow. The samples were then re-suspended in bi-distilled water at the suitable dilution and analysed by anionic chromatography with pulsed amperometric detector (HPAEC-PAD) using a Dionex ICS-3000 equipped with a CarbopacPA1 column. Calibration was carried out with commercial standards of the different monosaccharides (fucose, arabinose, rhamnose, galactose, glucose, xylose, mannose, glucuronic acid and galacturonic acid). The experiments were carried out in triplicate.

3.6.3 Polyphenolic profile (UPLC-DAD-MS2 analysis).

The phenolic profile of the lab-scale and up-scale persimmon extracts was determined in an UPLC-DAD-MS system equipped with diode array (DAD) and triple quadrupole mass spectrometer (MS) detectors using electrospray ionization interface (Waters, Milford, MA, USA). The freeze dried lab-scale extract (50 mg) was first suspended in 1 mL 85% methanol, sonicated for 5 min and centrifuged at 12,000 rpm for 10 minutes. The clear supernatant was dissolved (1:8.5) in 0.1% (v/v) formic acid, filtered through PTFE (0.2 μm) and injected into the chromatographic system. The concentrated liquid pilot plant persimmon extract (50 mg) was directly dissolved in 0.5 mL 0.1% (v/v) formic acid, filtered and injected into the chromatographic system. Separation was performed in a reversed-phase Acquity UPLC BEH Shield 1.7 μm 1.0 × 150 mm column (Waters, Milford, MA, USA), using a mobile phase composed of A (0.1% v/v formic acid) and B (acetonitrile), under isocratic elution (1% B) from 0 to 5 min and linear gradient (1%-40% B) from 5 to 25 min.

Parent molecular ions (m/z) were obtained by MS scan mode experiments using cone voltage at 30 V. MS^2 fragmentation patterns were obtained using cone voltage at 30 V and

collision energy at 25 V. Phenolic compounds were quantified using DAD signal and external calibration curves with pure standards: gallic acid, vanillic acid, hesperetin, quercetin, kaempferol and naringenin (Sigma-Aldrich, Madrid, Spain).

3.7 Functional activity of the selected persimmon extract

3.7.1 Antiviral capacity. - Virus propagation and cell lines.

Murine norovirus (MNV-1), used as a human norovirus surrogate, was propagated and assayed in RAW 264.7 cells, both kindly provided by Prof. H. W. Virgin (Washington University School of Medicine, USA). Hepatitis A virus (HAV, strain HM-175/18f) was purchased from ATCC (VR-1402) and was propagated and assayed in confluent FRhK-4 cells (kindly provided by Prof. A. Bosch, University of Barcelona, Spain). Semi-purified MNV and HAV viruses were harvested at 2 days and 12 days after infection, respectively, by three freeze-thaw cycles of infected cells followed by centrifugation at 660 ´ g for 30 min to remove cell debris. Infectious viruses were enumerated by determining the 50% tissue culture infectious dose (TCID50) with eight wells per dilution and 20 µL of inoculum per well using the Spearman-Karber method (Pintó et al., 1994).

- Evaluation of antiviral activity of the persimmon extract. Both the lab-scale and pilot plant scale obtained persimmon extracts were dissolved in PBS (pH 7.2) and mixed with an equal volume of HAV and MNV suspensions (ca. 5 log $TCID_{50}$/mL) getting a final concentration of the extracts of 0.5 and 5 mg/mL and incubated overnight at 37 °C. The positive control was virus suspensions in PBS under the same experimental conditions. Each treatment was performed in triplicate. Confluent RAW 264.7 and FRhK-4 monolayers in 96-well plates were used to evaluate the effect of the extracts as described above. The antiviral activity of the persimmon extracts was estimated by comparing the number of infectious viruses on suspensions without the extracts and on the extract-treated virus suspensions. The decay of HAV and MNV titers was calculated as log10 (Nx/N0), where N0 is the infectious virus titer for untreated samples and Nx is the infectious virus titer for persimmon extract-treated samples.

3.7.2 Anti-obesity and anti-ageing capacity of the persimmon extract. - *C. elegans* culture and persimmon extract supplementation.

C. elegans was cultured as previously described (Navarro-Herrera et al., 2018). Wild type N2 Bristol strain was obtained from the *Caenorhabditis Genetics Center* (CGC, University of Minnesota, MN), and was grown at 20 °C on Nematode Growth Medium (NGM) with *Escherichia coli* OP50 as normal nematode diet. Experiments were performed in 6-well cell culture plates with 4 mL of NGM per well. Supplemented media was prepared as follows: Persimmon extract was dissolved in distilled water and mixed with the NGM at the doses of 10, 100, 200 and 1000 µg/mL. Each concentration was tested in four replicates, including the vehicle (distilled water) as control. Orlistat supplemented plates (6 µg/mL Orlistat; Sigma-Aldrich, St. Louis, MO) were used as fat reduction control (Navarro-Herrera et al., 2018). Once the treatments were added to NGM, plates were allowed to solidify and dry in a dark environment to protect them from light oxidation. Afterwards, 150 µL of an overnight culture of *E. coli* OP50 were seeded and plates were incubated in darkness at room temperature until dry. For all experiments, age-synchronized L4 worms were obtained by standard hypochlorite treatment of gravid animals and eggs were let hatch overnight in M9 medium. Then, about 1000-2000 L1 larvae were transferred onto plates and were grown during 46 h until they reached the L4 stage, in which worms were collected and experiments were performed.

- *Nile Red staining.* Nile Red (#N3013, Sigma-Aldrich, St. Louis, MO) staining, a dye for neutral lipids, was performed as previously described with minor modifications (Navarro-Herrera et al., 2018; Pino et al., 2013). Briefly, L4 worms were harvested in 1.5 mL tubes and washed twice with PBST (0.01% of Triton X-100 in Phosphate Buffered Saline). Then, worms were kept on ice for 15 min to stop pharyngeal activity and fixed in 40% isopropanol for 3 min. The staining was performed adding 150 µL of Nile Red solution (3 µg/mL) to fixed worms followed by incubation (30 min) at 20 °C in the dark with gentle rocking. Finally, worms were washed in PBST and mounted on a 2% agarose pad for microscopy visualization.

- *C. elegans ageing visualization*. Synchronized 500 L1 larvae were transferred onto plates containing DMSO (control) or persimmon extract (200 µg/mL), and were grown until the L4 stage of adulthood. Worms were collected, washed and mounted onto 2% agarose pads with a 1% of sodium azide. Lipofuscin pigment was determined by auto-fluorescence as marker of ageing (Gardner et al., 2004).

- *Image acquisition, quantification and statistical analyses.* For all conditions tested, approximately 300 animals were fixed and stained. Fluorescent images of Nile Red stained worms were captured at 100x magnification on a Nikon SMZ18 research stereomicroscope equipped with an epi-fluorescence system and a DS-FI1C refrigerated colour digital camera (Nikon Instruments Inc., Tokyo, Japan). Images were taken at the same conditions and integration time under a GFP filter (Ex 480-500; DM 505; BA 535-550). The dihydroethidium (DHE)-labelled ROS formation and the lipofuscin auto-fluorescence were detected by measuring the fluorescence intensity using a Nikon Eclipse 80i epi-fluorescent microscope, equipped with a TRITC filter (Ex 540-625; DM 565; BA 605-655) and the DAPI filter (with excitation at 340-380 nm and emission at 435-485 nm), respectively (Nikon Instruments Inc., Tokyo, Japan). In all cases, the image analysis of the Nile Red, DHE and lipofuscin assays were quantified by determining the average pixel intensity per worm (mean value) using ImageJ software as previously described (Navarro-Herrera et al., 2018). Approximately 25-40 worms were examined in three independent experiments for each condition. *C. elegans* body-fat reduction (Nile Red) between treated and untreated control condition (NGM group), together with oxidative stress (DHE), were evaluated by a hierarchical ANOVA test, where replicates were nested in treatments, followed by multiple comparison (Fisher's protected Least Significant Difference, LSD) tests. Lipofuscin determinations between treated (200 µg/mL) and untreated control worms were statistically compared using Student's t test. All statistical tests were performed using StataSE v12 software (StataCorp LLC, College Station, TX).

- *Egg lying and worm length*. Egg lying was observed in young adult nematodes (day 3 of growth) grown on NGM agar plates supplemented or not with the persimmon extract (200 µg/mL). The images were taken at 135 magnifications using a Nikon SMZ18 stereomicroscope equipped with a Nikon DS-Fi1C high-definition colour camera. Worm

length (µm) was calculated with the Nikon NIS-ELEMENTS Software (Nikon Instruments Inc., Tokyo, Japan), and determinations between treated (200 µg/mL) and untreated samples were statistically compared using Student's t test.

- *RNA extraction and quantitative PCR analysis.* Total RNA from *C. elegans* N2 strain were extracted using Trizol® RNA isolation reagent (Thermo Fisher Scientific, Paisley, UK) according to the manufacturer's instructions. Concentration and purity of RNA were determined at 260/280 nm using a NanoDrop ND-1000 spectrophotometer (Thermo Fisher Scientific, Wilmington, DE, USA). Then, 1000 ng of RNA were treated with DNAse (Ambion™ DNase I, RNase-free; Thermo Fisher Scientific Inc., Waltham, MA, USA) according the manufacturer's protocol. For the quantitative gene expression analyses, DNA-free RNA was reverse-transcribed into cDNA following the protocol previously described (Navarro-Herrera et al., 2018). Gene expression analyses were performed by quantitative-real time PCR (qPCR) using the TaqMan Universal PCR master mix and specific probes (Table S1 in Supplementary Material) from Applied Biosystems Technologies (Thermo Fisher Scientific Inc., Waltham, MA, USA) and Integrated DNA Technologies Inc., (Coralville, Iowa, USA). All reactions were performed using a CFX384 Touch™ Real-Time PCR Detection System (BioRad, Hercules, CA, USA). The expression level of each gene was normalized comparing to the expression of the *pmp3* gene from Life Technologies (TaqMan Gene Expression Assays), which was used as housekeeping gene control. Gene expression differences between treated and untreated worms were quantified using the relative quantification $2^{-\Delta\Delta Ct}$ method (Livak & Schmittgen, 2001). Real-time PCR data was statistically analysed using Wilcoxon test comparing ERE and control data.

3.7.3 Genotoxicity evaluation of the persimmon extract (SOS/*umu*-test).

The SOS/*umu*-test was used to determine the DNA-damaging effect and was carried out according to the method of Reifferscheid *et al.*(Reifferscheid et al., 1991), with some modifications. The test strain *S. typhimurium* TA1535/pSK1002 (German Collection for microorganisms and Cell cultures (DSMZ)) from stock (-80 °C; in TGA medium containing 10% DMSO as cryoprotective agent) was thawed and 0.5 mL of bacteria were suspended in 100 mL TGA medium supplemented with ampicillin (50 µg/mL). The tester strain

suspension was incubated overnight at 37 °C with slight orbital shaking (155 rpm) until an optical density was reached (OD 600 between 0.5 and 1.5). Thereafter, the overnight culture was diluted with fresh (not supplemented with ampicillin) TGA medium and incubated for 2 h at 37 °C, 155 rpm in order to get log-phase bacteria exponential growth culture (OD 600 between 0.15 and 0.4).

The test was performed in absence and presence of external metabolic activation system (10% of rat S9 mix, prepared from S9 SD rat liver Aroclor KCl frozen, Trinova, Germany) in order to also determine the possible genotoxic effects of any metabolite. In each test performed negative and positive controls were included, water was used as solvent control (negative control), and 4-nitroquinoline-N-oxide (4-NQO) (Sigma-Aldrich, China) and 2-aminoanthracene (2-AA) (Sigma-Aldrich, Germany) were used as positive controls in the absence and presence of S9 mix, respectively.

Test procedure was as follows: firstly, the extract was dissolved in water at 80 mg/mL (for a final concentration in the assay of 1 mg/mL) and 11 serial ½ dilutions were prepared in a 96-well plate (plate A; final volume in each well was 10 µL). The highest concentrations in DMSO used for the positive controls were 100 µg/mL for 4-NQO (final concentration: 2.5 µg/mL) and 0.5 mg/mL for 2-AA (final concentration: 0.0125 mg/mL). Then, 70 µL water was added to each well. At this point, each well was checked in order to detect any precipitation of the compounds. In other two 96-well plates (plates B; one for the test with S9 and the other without S9), 10 µL S9 mix or 10 µL PBS, respectively were added and afterwards, 25 µL of each concentration of compound previously prepared. Finally, 90 µL of exponentially growing bacteria were added to each well and both plates were incubated during 4 hours by shaking (500 rpm) at 37 °C. After the incubation period, absorbance at 600 nm was measured in order to evaluate toxicity on *S. typhimurium* TA1535/pSK1002.

Genotoxicity is related to survival percentage, which has been calculated as follows:

Survival percentage e= (A_{600} for each concentration tested/media A_{600} for negative control)*100

Afterwards, for the determination of β-galactosidase activity, in two new 96-well plates (plates C), 150 µL ONPG solution (2-nitrophenyl-β-D-galactopyranoside, Sigma-Aldrich, Switzerland) (0.9 mg/mL in B-buffer prepared according to Reifferscheid et al., (1991) was added to each well and 30 µL of the content of each well of the plates B was transferred to these plates C. Both plates C were incubated 30 minutes by shaking (500 rpm) at 28 °C avoiding direct light exposure. After the incubation period, 120 µL stop reagent (Na_2CO_3, 1M) was added to stop the reaction. Absorbance at 420 nm was then measured immediately, and β-galactosidase activity (relative units; RU) was calculated as follows:

β-galactosidase enzymatic units=A_{420} for each concentration tested/A_{600} for each concentration tested

And finally, the induction factor (IF) was calculated as follows:

IF=β-galactosidase RU for each concentration tested/average β-galactosidase RU for negative control

Where: average β-galactosidase RU for negative control=average A_{420} for negative control/average A_{600} for negative control

In the same way, β-galactosidase relative units were calculated for both positive controls and the test was only considered valid if the positive controls reached an IF ≥2 under the given test conditions.

An extract is considered genotoxic when in any of the conditions studied (with or without metabolic activation) the induction factor is ≥2 at non-toxic concentrations (bacteria survival percentage ≥80%).

Any well where compound precipitation was observed, was discarded from analysis

4 Results and discussion

A central composite design based on response surface methodology was used to determine the optimal parameters giving raise to persimmon (*Diospyros kaki* Thunb) extracts with the greatest polyphenol content and antioxidant capacity (cf. Table 1), aiming to provide relevant information for further industrial up-scaling and evaluation of the bioactive properties. The extracts were obtained from persimmon fruits in two different ripeness stages (IPE and MPE) and the effects of the solid:liquid ratio (g/mL), the ethanol/water solvent ratio E/W (%) and the extraction temperature (°C) on the total polyphenolic content (TPC) as well as on the antioxidant capacity of the extracts were evaluated. The overall extraction yields for the different extraction conditions and raw materials (both immature and mature persimmons) ranged between 50 g/100 g dry weight and 75 g/100 g dry weight, indicating that the range of parameters selected for extraction was suitable, as excellent yields were obtained in all cases. The high yield obtained in this case can be attributed to the extractions of other components, such as free sugars (glucose and fructose) which constitute around 66-83% dry weight of the whole fruit (data not show).

Table 1. Full central composite design with the experimental data.

Run	Ratio (mg/mL)	E/W (%)	Temp (°C)	IPE		MPE	
				TPC (mg GAE/g extract)	TEAC (µmol TE/g extract)	TPC (mg GAE/g extract)	TEAC (µmol TE/g extract)
1	12.50	75.0	60.0	26.68	119.36	3.44	40.18
2	12.50	75.0	60.0	26.00	122.26	3.61	35.53
3	12.50	100.0	60.0	2.41	44.49	1.92	35.99
4	5.00	75.0	60.0	15.33	129.37	1.78	35.27
5	8.04	60.1	77.8	5.69	49.29	9.34	81.71
6	20.00	75.0	60.0	20.54	167.57	3.87	40.04
7	12.50	75.0	90.0	20.79	160.64	15.19	114.72
8	8.04	89.8	42.1	8.59	97.67	2.91	39.59
9	16.96	60.1	42.1	23.55	119.87	4.53	35.80
10	12.50	50.0	60.0	15.66	160.50	8.59	46.44
11	12.50	75.0	60.0	26.47	130.82	2.93	37.27
12	8.04	89.8	77.8	17.36	134.68	3.69	49.48
13	12.50	75.0	60.0	27.14	137.96	2.98	39.41
14	16.96	60.1	77.8	19.72	141.72	4.19	67.44
15	12.50	75.0	60.0	28.94	162.43	4.42	37.83
16	12.50	75.0	30.0	20.19	142.19	4.39	45.83
17	16.96	89.8	42.1	4.73	51.31	3.04	48.59
18	16.96	89.8	77.8	11.41	116.88	3.14	62.20
19	8.04	60.1	42.1	16.08	132.26	3.74	34.00
20	12.50	75.0	60.0	27.10	122.38	3.17	37.57

4.1 Selection of extraction conditions

All the results were statistically analyzed through an analysis of variance (ANOVA) and the results are compiled in Table S2 from the Supplementary Material. The regression models were highly significant with satisfactory coefficients of determination for total phenolic content (TPC) (R^2 = 0.93–0.96). The values of the adjusted determination coefficients (adj R^2 = 0.87–0.92) also validated that the models were highly significant. Moreover, the lack-of-fit test, which measures the competence of the model, did not result in a significant P-value, highlighting that the models were sufficiently precise for predicting the phenolic

content of the extracts. ABTS response also exhibited a high model accuracy for the mature fruits, showing R^2 of 94.61% for MPE, although it was lower for IPE (R^2 68.92%), indicating a lower reliability of the developed model. The response surface plots were also generated (cf. Figure 1) to better understand the effect of extraction conditions on both TPC and antioxidant potential.

Both the total phenolic content (TPC) and antioxidant capacity (using the ABTS assay) of the samples were taken into account to select the optimum extraction conditions for subsequent up-scale. The first remarkable result was that the TPC and antioxidant capacity showed a clear dependence on fruit stage. As expected, the immature fruit samples showed significantly higher TPC (28.9 mg GAE/g) and antioxidant capacity values (167.6 µmol Trolox/g extract) than the mature ones (15.2 mg GAE/g and 114.7 µmol Trolox/g extract, respectively). This is explained by the ripeness stage, as less mature fruits have been reported to contain a greater amount of soluble tannins which are usually degraded or transformed into insoluble ones during ripening (Yoo et al., 2019), having a positive impact on the astringency (Mamet et al., 2018; Taira et al., 1997).

Interestingly, remarkable differences were observed in the factors affecting the responses depending on the starting material. While for IPE, the E/W ratio had the highest effect on both response parameters, for MPE, the TPC and antioxidant capacity were mainly influenced by the extraction temperature (greater temperatures fostering phenolic extraction) (cf. Table S2). This is clearly patent when looking at the response-surface plots for TPC values (Figure 1). For IPE, a combination of

intermediate E/W ratios and high temperature is necessary to maximize polyphenol and antioxidant performance (Figure 1a and 1b), while only high temperatures are most significantly affecting these for MPE (Figure 1c and 1d). This is probably related to the different nature of the polyphenolic compounds present in the persimmon fruits depending on the ripeness stage. Whereas intermediate E/W ratio favor the extraction of soluble tannins from the immature fruits, these temperatures were insufficient in the case of the mature persimmons, since higher temperatures are required in these cases to solubilize the complexes formed between insoluble tannins and other compounds, such as pectin, which

have been associated to the ripening process (Taira et al., 1997). The TPC values obtained in this work were similar to the values reported for dried persimmon peel extract (2.30 to 18.31 mg GAE/g) (Hwang et al., 2011), and higher than other fruit extracts (3.09 - 9.44 mg GAE/g elderberry, blueberry 5.58 mg GAE/g, and blackberry 2.72 mg GAE/g DW) (Domínguez et al., 2020; Huang et al., 2012), confirming the potential use of persimmon fruit as an important source of phenolic compounds for bioactive applications. A PCA was also carried out to evaluate the variance related to the extraction conditions and the results are included in the Supplementary Material (Figure S2).

In view of the results, immature fruits showed the highest antioxidant and TPC values and thus, this stage was selected as raw material for the up-scaled process. The extraction conditions were set at 60 °C and an E/W ratio of 75%. The extract was up-scaled by Kimitec Group, but in order to make the process more sustainable from an economical view point, ethanol was substituted by isopropanol. Both, the optimized IPE obtained at lab and industrial scale were characterized in terms of composition and functional properties.

4.2 Compositional Characterization of the "Immature Persimmon Extract" (IPE)

4.2.1 Protein content.

The protein content of the lab-scale and up-scaled IP was 4.48 ±0.13 g/100g dry weight and 1.35 ±0.11 g/100g dry weight, respectively. The contents are higher than those reported in the literature for mature persimmon **(***Diospyros kaki L*) (1.14 - 1.56 g/100 g dry weight) (Karaman et al., 2014), indicating that most of the proteins present in the fruits are enriched in the IPE under the applied extraction conditions. Ripeness, variety and nitrogen cultivation vastly affect the protein content of the fruits, as observed in a couple of studies in which higher protein contents were generally observed in earlier stages of maturation (S. T. Choi et al., 2012; S.-T. Choi et al., 2011; Yoon et al., 2014).

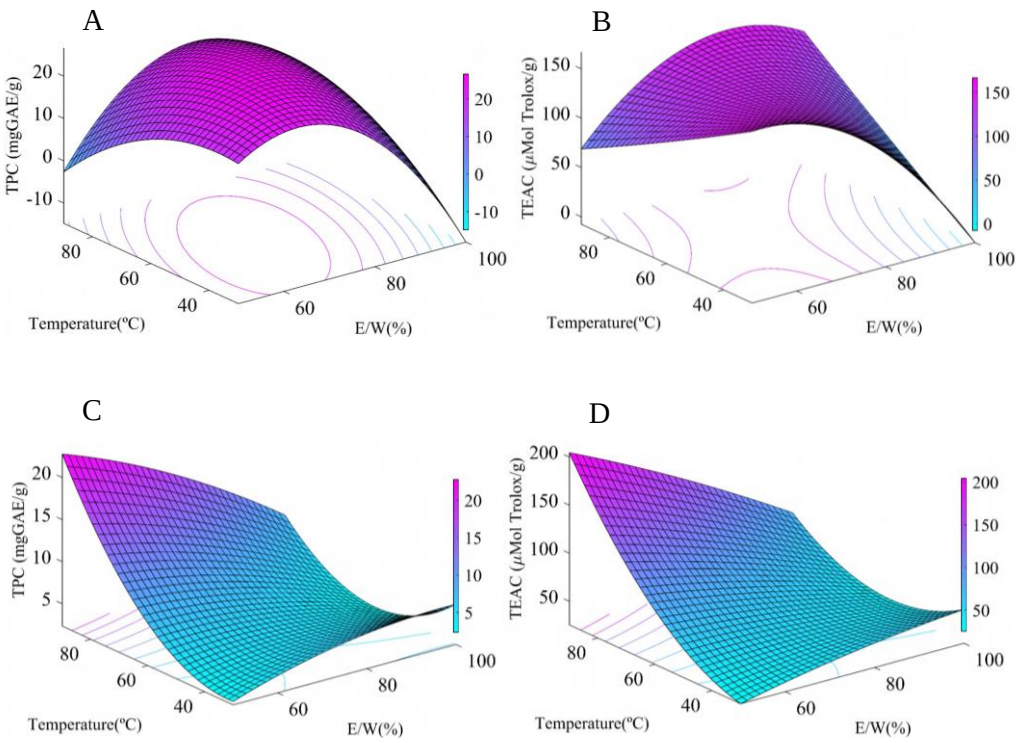

Figure 1. Response surfaces of the TPC and antioxidant activity of extracts from (A, B) IPE and (C, D) MPE as a function of temperature and E/W with a fixed solid:liquid ratio (12.5 mg/mL).

4.2.2 Carbohydrate composition.

The carbohydrate composition of the persimmon extracts mainly consisted on glucose, arising from free glucose mainly, as well as from xyloglucan hemicelluloses, pectin components, such as galacturonic acid, galactose, rhamnose and arabinose, and xylose from xyloglucan (Table S3 in Supplementary Material), in agreement with the major soluble carbohydrate components found in persimmon (Cutillas-Iturralde et al., 1998). Although similar total carbohydrate contents were found in both lab- and up-scaled extracts (45-50%), glucose was much enriched in the up-scaled extract (45%) in comparison with the lab-scale IPE (20%), where significant quantities of xyloglucan and pectin were to be found. These

differences may be ascribed to the different solvent used, as ethanol is more polar and thus able to extract low molecular weight pectin and xyloglucan components.

4.2.3 Polyphenolic Profile.

To gain further insights on the composition of the selected extract obtained both at lab and industrial scale, their polyphenolic profile was also characterized and the results are compiled in Table 2. Details about the quantification and the obtained chromatograms can be found in the Supplementary Material (Table S4 and Figures S3-S7). Several phenolic compounds were identified in the persimmon extracts on the basis of their DAD, MS and MS^2 information and comparison with pure standards and/or bibliographic data (Heras et al., 2016; Jiménez-Sánchez et al., 2015; Sentandreu et al., 2015). The main phenolic compound in both extracts was the hydrolysable tannin gallic acid, which was more abundant in the up-scaled IPE than in the one produced in laboratory conditions. Other phenolic compounds such as naringin, hesperidin or naringenin were only present in the industrially up-scaled extract (see Table S4 in the Supplementary Material). Again, the solvent combination used for extraction seems to play an important role in the solvation and extraction of specific phenolic molecules, fact which also has an impact on the antioxidant properties of the extract, as commented on later and also observed in previous studies (Venkatesan et al., 2019).

4.3 Functional activity of the “Immature Persimmon Extract” (IPE)

4.3.1 Antiviral capacity.

The antiviral activity of the lab-scale and up-scaled IPE was evaluated on HAV and MNV (a human surrogate), and the results are compiled in Table 3. Both extracts greatly decreased the titer of MNV detection limits) at the greatest concentration tested (5 mg/mL), although only the up-scaled extract produced a significant reduction at lower concentrations (0.5 mg/mL). The up-scaled extract also showed a marked antiviral effect on HAV, with a titer reduction of 2.83 log. The antiviral capacity of persimmon extracts has been previously reported and has been correlated to the persimmon tannins present (Kamimoto et al., 2014).

Table 2. Content of the different phenolic compounds tentatively identified (mg kg^{-1}) in the lab scale and up-scaled immature persimmon extracts (IPE) (mean (standard deviation), n = 3). Nd: not detected.

Peak	Tentative identification	Labscale IPE	Up-scaled IPE
1	Gallic acid	728.5(122.9)	998.1(37.2)
2	Galloyl hexoside	nd	64.8(1.3)
3	Vanillic acid hexoside	15.9(1.6)	28.2(1.2)
4	Naringin	Nd	73.2(3.0)
5	Hesperidin	nd	277.8(86.8)
6	Quercetin hexoside I	22.3(3.3)	13.4(0.5)
7	Quercetin hexoside II	46.1(8.9)	28.3(2.0)
8	Kaempferol hexoside I	19.0(0.4)	18.4(2.2)
9	Kaempferol hexoside II	29.4(0.6)	16.7(2.7)
10	Kaempferol hexoside gallate I	nd	1.5(0.3)
11	Kaempferol hexoside gallate II	nd	3.4(0.6)
12	Naringenin	nd	27.0(15.5)

The overall higher antiviral effectiveness of the up-scaled extract could thus be related with a higher polyphenol content. In fact, it was found that tannin concentrations greater than 0.11 mg/mL were needed to reduce the infectivity of a human norovirus surrogate by more than 2.5 log, (Kamimoto et al., 2014) which explains why only the greatest extract concentration tested was seen to be effective in the reduction of the viral load.

4.3.2 Anti-obesity and anti-ageing capacity.

As it has been previously described (see Table 2), As it has been previously described (see Table 2), the IPE extracts obtained contain a relevant content of polyphenols, including naringin, hesperidin and derivatives of quercetin and kaempferol, together with different phenolic acids, such as gallic and vanillic acids. All these phenolic compounds are considered bioactive compounds with reported antioxidant and anti-ageing activities

(Kawai, 2018; Peng et al., 2014). Therefore, the *in-vivo* antioxidant activity was carried out using the model *C. elegans*, and, its potential activity over other parameters associated with the nematode health, such as development, ageing or energy homeostasis regulation, was also evaluated.

C. elegans has been demonstrated to be a powerful *in-vivo* model for the screening of food ingredients and bioactive compounds with health-related benefits, such as antioxidant and anti-ageing activities (Saul et al., 2011; Shen et al., 2018). Besides, due to the highly conserved regulatory pathways of energy homeostasis between mammals and *C. elegans*, this nematode is considered a popular model for exploring the ability of different functional ingredients modulating fat storage, commonly determined by quantification of the triglyceride accumulation with lipid-specific stains such as Oil Red O or Nile Red (Pino et al., 2013). Thus, this model has been widely used to identify bioactive compounds with potential application in the prevention of obesity-related disorders (Navarro-Herrera et al., 2018; Shen et al., 2018).

To determine the in-vivo antioxidant capacity, synchronized L1 worms were grown in presence of different concentrations of the IRE extract (100 and 200 µg/mL) until L4 stage, when nematodes were collected and stained with dihydroethidium (DHE) staining, (Wei & Kenyon, 2016) after treatment with ERE extract (100 and 200 µg/mL) were initially calculated. Surprisingly, despite the high content in antioxidant compounds, no differences were observed in the ROS levels of the IRE extract-treated and untreated worms.

However, it was observed that all tested doses (10, 100, 200 and 1000 µg/mL) of the IRE extract were able to reduce the lipid accumulation of *C. elegans*, in comparison with untreated-control worms (Figure 2A), as it was determined by a reduction in the Nile Red staining (Figure 2B). As a result, the up-scaled IPE was able to modulate the *C. elegans* lipid homeostasis when treated from L1 to L4 stages.

Table 3. Effect of the persimmon extracts on the infectivity of murine norovirus (MNV) and hepatitis A virus (HAV) after overnight incubation at 37 °C.

Sample	Concentration (mg/mL)	MNV		HAV	
		Log $TCID_{50}$/mL	R	Log $TCID_{50}$/mL	R
Lab-scale IPE	0	5.41(0.29)[a]		5.78(0.19)[a]	
	0.5	4.16(0.19)[c]	1.25	5.37(0.1)[a]	0.42
	5	UDL*[b]	> 4.26	6.07(0.37)[a]	- 0.29
Up- scaled IPE	0	4.03(0.29)[d]		5.32(0.22)[b]	
	0.5	5.53(0.19)[d]	-0.50	5.16(0.19)[b]	0.17
	5	UDL*[e]	>2.88	2.49(0.07)[c]	2.83

R: Reduction; UDL*: Under the detection limits (1.15). Within each column for each concentration, different letters denote significant differences between treatments ($P < 0.05$).

In order to determine if the reduction in the lipid content was related to an effect over the worm development, a qualitative analysis was performed by microscopy on day 1 of adulthood (day 3 of treatment). In this experiment (Figure 2C), it was observed that both control and IPE-treated plates exhibited the presence of eggs (black arrows) and L1 larvae (white arrows), with no differences in the time of appearance of these eggs. The analysis of the worm size of the adults revealed no differences in length between control and treated-worms (Figure 2D), indicating that the lipid-reducing effect of the persimmon extract was not related to differences in the worm development. Moreover, it was observed that persimmon extract-treated worms (200 µg/mL) exhibited a significant reduction of the intestinal lipofuscin pigment, an auto-fluorescent molecule commonly used as marker of the rate of ageing (Liao, 2018) (Figure 2E-F), in comparison with the untreated-control worms. Therefore, this result evidenced that the treatment with IPE during L1 to adulthood reduced the *C. elegans* fat content without having an effect on the worm development, and this activity was accompanied by a reduction in the cellular ageing of the nematode.

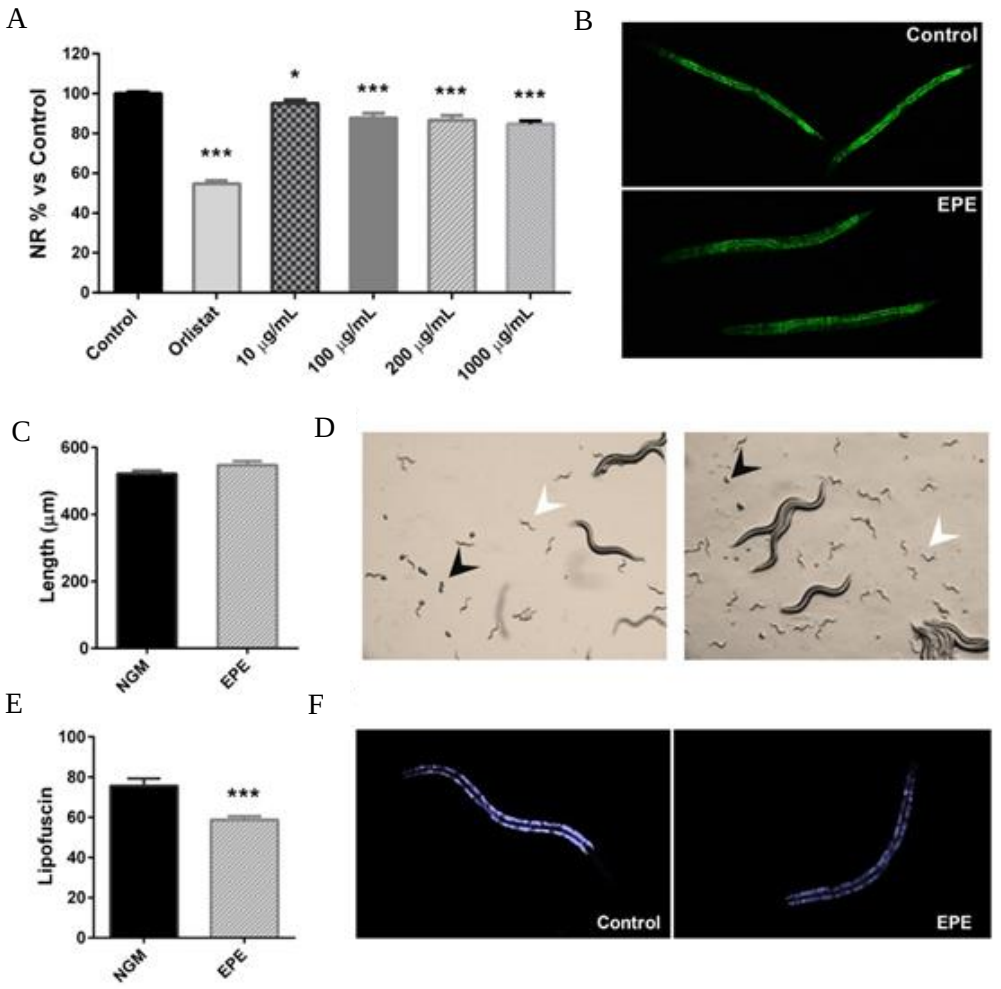

Figure 2. A) *C. elegans* lipid quantification data (relative to NGM) obtained after treatment with different doses (10-100-200-1000 µg/mL) of the persimmon enriched-polyphenolic extract (EPE) and measured by Nile Red staining. Orlistat (6 µg/mL)-supplemented wells were used as positive control of fat loss. All data correspond to the mean ± SEM. Significance refers to the effect of persimmon extract with respect to control worms (ANOVA followed by LSD test, * $p < 0.05$; *** $p < 0.001$). B) Nile Red staining of the control and EPE extract (200 µg/mL)-treated worms. C) Size (µM) of the treated- and un-treated worms on day 1 of adulthood (mean ± SEM). D) Microscope observation of the presence of eggs (black arrows) and L1 larvae (white arrows) in both control (left) and EPE-

supplemented (right) plates. E) Quantification of lipofuscin aging-pigment of EPE-treated worms compared to control (mean ± SEM). *** Show the level of statistical significance of the differences (T test, $p < 0.001$). F) Visualization of *C. elegans* lipofuscin pigment auto-fluorescence by microscopy of control and EPE-treated worms.

Finally, the plausible mechanisms underlying the lipid- and ageing-reducing activities of the persimmon extract were determined by evaluating the expression of genes involved in different processes related with lipid synthesis (fat-7 and fat-5), lipid oxidation (acox-1 and maoc-1), and oxidative stress (skn-1). As it can be observed in Figure 3, treatment with IPE induced a significant downregulation (Wilcoxon test $p=0.047$) of fat-7. This gene encodes a Δ9 desaturase that catalyses the insertion of the first double bond into a saturated fatty acid (stearic acid, C18:0) at the C9 position, constituting a key enzyme in the synthesis of fatty acids (Watts, 2009). Inhibition of this gene is associated with a reduced total triacylglyceride content, (Ashrafi, 2007) so the down-regulation by the persimmon extract might indicate a reduction in the fat synthesis rate. No changes were observed in the expression of fat-5, encoding for a palmitic acid-specific desaturase, (Ashrafi, 2007) nor in that of the maoc-1 and acox-1 genes, involved in the fatty acid β–oxidation. These results suggest that the fat-reducing activity of the persimmon enriched-polyphenolic extract might be attributed to a reduced lipogenesis rate through down-regulation of fat-7, not to an increased lipolysis and subsequent β-oxidation. Finally, no changes were observed in the expression of skn-1, ortholog of human Nrf/CNC proteins which are activated under oxidative stress conditions (An et al., 2005) which might contribute to explain the result obtained in the DHE staining. However, it should be mentioned that the experiments were performed without applying any type of chemical or thermal stress to the nematode, so further studies are needed to investigate the antioxidant activity of this persimmon extract in *C. elegans*.

4.3.3 Genotoxicity screening assay.

Finally, the genotoxicity of the up-scaled IPE was also determined in order to evaluate its applicability in food related products. All the controls used for the SOS/*umu*-test were correct (IF < 2 for negative and IF>2 for positive controls). The wells corresponding to the

higher concentrations tested (final concentrations: 2, 1 and 0.5 mg/mL) showed precipitation in the wells and were discarded from analysis. The well corresponding to the final concentration of 0.25 mg/mL showed some turbidity. The extract was considered non genotoxic as the induction factor was always lower than 2 at non-toxic concentrations with or without the persimmon extract (see Figure S8 in the Supplementary Material).

Even if a high degree of agreement between the SOS/*umu*-test and the standardized Ames test (OECD guideline 471) for mutagenicity testing has been found, (Reifferscheid & Heil, 1996) it should be noted that the SOS/*umu*-test is used for screening purposes. For regulatory purposes, the negative results obtained with the SOS/*umu*-test should be further evaluated with the standardized Ames test.

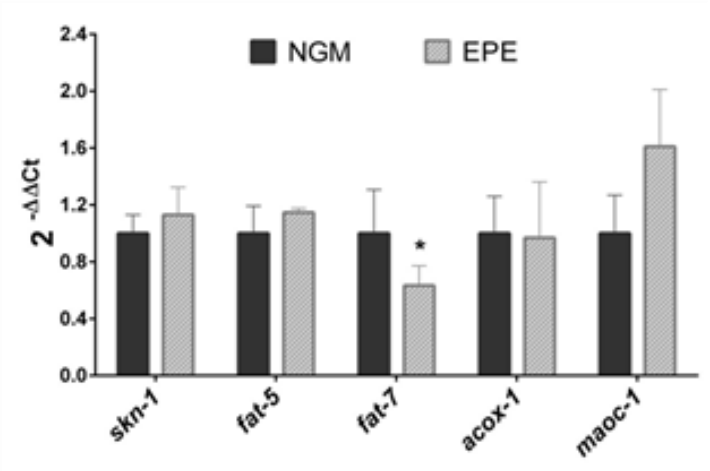

Figure 3. qPCR analysis performed in EPE-treated and untreated control worms. Results are expressed as the fold-difference expression levels of each gene in the EPE-treated group compared to the untreated-control group, calculated with the 2−ΔΔCt method. Significance refers to the effect of EPE with respect to control worms (Student t test, * $p < 0.05$).

5 Conclusions

In this work, an optimization for extraction of a polyphenol-rich extract from persimmon fruits was carried out using a central composite design. The ripeness degree of the fruits was seen to affect, not only the extract composition (greater in phenolic compounds in those

obtained from immature fruits), but also the determining factors for extraction. Specifically, in the mature fruits, increased phenolic content and antioxidant capacity was seen upon temperature increase, while in the case of the immature persimmons, the solvent composition was the main relevant factor in determining polyphenol extraction. The best extract in terms of phenolic content and antioxidant capacity (from immature persimmon fruits-IPE) was industrially up-scaled and compositionally characterized, being very rich in gallic acid and other phenolic compounds previously described to have diverse bioactive properties. Specifically, in this work, the IPE demonstrated a good antiviral capacity, with a significant reduction in the titers of hepatitis A virus and murine norovirus. Moreover, treatment of *C. elegans* with IPE during L1 to adulthood was able to reduce the fat content and the cellular ageing of the nematode without affecting the worm development. These effects were mediated by down-regulation of fat-7, suggesting an anti-lipogenic activity of this extract. Although further studies are needed to investigate the antioxidant activity of the extract in *C. elegans*, as well as to confirm the anti-obesity and anti-ageing activities of persimmon extract in superior mammalian models, these preliminary data would suggest the potential application of this persimmon extract in the prevention of obesity and ageing-related diseases.

6 Acknowledgements

This work was financially supported by the grant RTI-2018-094268-B-C22 (MCI/AEI/FEDER, EU). Mendez D. A. is supported by the Ministry of Science, Technology and Innovation (Minciencias) of the Colombian Government (783-2017). M. J. Fabra and A. Martinez-Abad are recipients of Ramon y Cajal (RYC-2014-158) and Juan de la Cierva (IJDC-2017-31255), respectively, from the Spanish Ministry of Economy, Industry and Competitiveness. We also appreciate the funding of the CERCA program (Centres de Recerca de Catalunya) of the Generalitat de Catalunya and from the CIEN project “BIOPRO” from CDTI. Nune Sahakyan is kindly acknowledged for experimental support.

7 References

An, J. H., Vranas, K., Lucke, M., Inoue, H., Hisamoto, N., Matsumoto, K., & Blackwell, T. K. (2005). Regulation of the Caenorhabditis elegans oxidative stress defense protein SKN-1 by glycogen synthase kinase-3. *Proceedings of the National Academy of Sciences of the United States of America*, *102*(45), 16275–16280. https://doi.org/10.1073/pnas.0508105102

Ashrafi, K. (2007). Obesity and the regulation of fat metabolism. *WormBook*, 1–20. https://doi.org/10.1895/wormbook.1.130.1

Choi, S. T., Park, D. S., Kang, S. M., & Kang, S. K. (2012). Influence of leaf-fruit ratio and nitrogen rate on fruit characteristics, nitrogenous compounds, and nonstructural carbohydrates in young persimmon trees. *HortScience*, *47*(3), 410–413. https://doi.org/10.21273/hortsci.47.3.410

Choi, S.-T., Park, D.-S., & Hong, K.-P. (2011). Status of nitrogenous and carbohydrate compounds as affected by nitrogen fertigation rates in young persimmon trees. *Scientia Horticulturae*, *130*(1), 354–356. https://doi.org/10.1016/j.scienta.2011.05.035

Cutillas-Iturralde, A., Peña, M. J., Zarra, I., & Lorences, E. P. (1998). A xyloglucan from persimmon fruit cell walls. *Phytochemistry*, *48*(4), 607–610. https://doi.org/10.1016/S0031-9422(98)00026-0

Domínguez Díaz, L., Dorta, E., Maher, S., Morales, P., Fernández-Ruiz, V., Cámara, M., Sánchez-Mata, M.-C. C., Díaz, L. D., Dorta, E., Maher, S., Morales, P., Fernández-Ruiz, V., Cámara, M., Sánchez-Mata, M.-C. C., Domínguez Díaz, L., Dorta, E., Maher, S., Morales, P., Fernández-Ruiz, V., … Sánchez-Mata, M.-C. C. (2020). Potential Nutrition and Health Claims in Deastringed Persimmon Fruits (Diospyros kaki L.), Variety 'Rojo Brillante', PDO 'Ribera del Xúquer'. *Nutrients*, *12*(5), 1397. https://doi.org/10.3390/nu12051397

Domínguez, R., Zhang, L., Rocchetti, G., Lucini, L., Pateiro, M., Munekata, P. E. S., & Lorenzo, J. M. (2020). Elderberry (Sambucus nigra L.) as potential source of antioxidants. Characterization, optimization of extraction parameters and bioactive properties. *Food Chemistry*, *330*, 127266. https://doi.org/10.1016/j.foodchem.2020.127266

FAO. (2019). *The State of Food and Agriculture 2019, Moving forward on food loss and waste reduction*. Food and Agriculture Organization of the United Nations.

Gardner, M. P., Gems, D., & Viney, M. E. (2004). Aging in a very short-lived nematode. *Experimental Gerontology*, *39*(9), 1267–1276. https://doi.org/10.1016/j.exger.2004.06.011

Gu, H.-F. F., Li, C.-M. M., Xu, Y. juan, Hu, W. feng, Chen, M. hong, & Wan, Q. hong. (2008). Structural features and antioxidant activity of tannin from persimmon pulp. *Food Research International*, *41*(2), 208–217. https://doi.org/10.1016/j.foodres.2007.11.011

Heras, R. M. Las, Quifer-Rada, P., Andrés, A., & Lamuela-Raventós, R. (2016). Polyphenolic profile of persimmon leaves by high resolution mass spectrometry (LC-ESI-LTQ-Orbitrap-MS). *Journal of Functional Foods*, *23*, 370–377. https://doi.org/10.1016/j.jff.2016.02.048

Huang, W., Zhang, H., Liu, W., & Li, C. (2012). Survey of antioxidant capacity and phenolic composition of blueberry, blackberry, and strawberry in Nanjing. *Journal of Zhejiang University SCIENCE B*, *13*(2), 94–102. https://doi.org/10.1631/jzus.B1100137

Hwang, I.-W. W., Jeong, M. C., & Chung, S. K. (2011). The Physicochemical Properties and the Antioxidant Activities of Persimmon Peel Powders with Different Particle Sizes. *Journal of the Korean Society for Applied Biological Chemistry*, *54*(3), 442–446. https://doi.org/10.3839/jksabc.2011.068

Jiménez-Sánchez, C., Lozano-Sánchez, J., Marti, N., Saura, D., Valero, M., Segura-Carretero, A., & Fernández-Gutiérrez, A. (2015). Characterization of polyphenols, sugars, and other polar compounds in persimmon juices produced under different technologies and their assessment in terms of compositional variations. *Food Chemistry*, *182*, 282–291. https://doi.org/10.1016/j.foodchem.2015.03.008

Kamimoto, M., Nakai, Y., Tsuji, T., Shimamoto, T., & Shimamoto, T. (2014). Antiviral Effects of Persimmon Extract on Human Norovirus and Its Surrogate, Bacteriophage MS2. *Journal of Food Science*, *79*(5), M941–M946. https://doi.org/10.1111/1750-3841.12462

Karaman, S., Toker, O. S., Çam, M., Hayta, M., Doğan, M., & Kayacier, A. (2014). Bioactive and Physicochemical Properties of Persimmon as Affected by Drying Methods. *Drying Technology*, *32*(3), 258–267. https://doi.org/10.1080/07373937.2013.821480

Kawai, Y. (2018). Understanding metabolic conversions and molecular actions of flavonoids in vivo: Toward new strategies for effective utilization of natural polyphenols in human health. In *Journal of Medical Investigation* (Vol. 65, Issues 3–4, pp. 162–165). University of Tokushima. https://doi.org/10.2152/jmi.65.162

Lattin, J. M., Carroll, J. Douglas., Green, P. E., & Green, P. E. (2003). *Analyzing multivariate data*. Thomson Brooks/Cole.

Liao, V. H. C. (2018). Use of Caenorhabditis elegans to Study the Potential Bioactivity of Natural Compounds. In *Journal of Agricultural and Food Chemistry* (Vol. 66, Issue 8, pp. 1737–1742). American Chemical Society. https://doi.org/10.1021/acs.jafc.7b05700

Liu, M., Wang, J., Yang, K., Qi, Y., Zhang, J., Fan, M., & Wei, X. (2018). Optimization of ultrasonic-assisted extraction of antioxidant tannin from young astringent persimmon (Diospyros kaki L.) using response surface methodology. *Journal of Food Processing and Preservation*, *42*(7), e13657. https://doi.org/10.1111/jfpp.13657

Livak, K. J., & Schmittgen, T. D. (2001). Analysis of relative gene expression data using real-time quantitative PCR and the 2-ΔΔCT method. *Methods*, *25*(4), 402–408. https://doi.org/10.1006/meth.2001.1262

Mamet, T., Ge, Z. zhen, Zhang, Y., & Li, C. mei. (2018). Interactions between highly galloylated persimmon tannins and pectins. *International Journal of Biological Macromolecules*, *106*(2018), 410–417. https://doi.org/10.1016/j.ijbiomac.2017.08.039

Méndez, D. A., Fabra, M. J., Gómez-Mascaraque, L., López-Rubio, A., & Martinez-Abad, A. (2021). Modelling the Extraction of Pectin towards the Valorisation of Watermelon Rind Waste. *Foods*, *10*(4), 738. https://doi.org/10.3390/foods10040738

Müller-Maatsch, J., Bencivenni, M., Caligiani, A., Tedeschi, T., Bruggeman, G., Bosch, M., Petrusan, J., Van Droogenbroeck, B., Elst, K., & Sforza, S. (2016). Pectin content and composition from different food waste streams. *Food Chemistry*, *201*, 37–45. https://doi.org/10.1016/j.foodchem.2016.01.012

Munera, S., Aleixos, N., Besada, C., Gómez-Sanchis, J., Salvador, A., Cubero, S., Talens, P., & Blasco, J. (2019). Discrimination of astringent and deastringed hard 'Rojo Brillante' persimmon fruit using a sensory threshold by means of hyperspectral imaging. *Journal of Food Engineering*, *263*, 173–180. https://doi.org/10.1016/j.jfoodeng.2019.06.008

Navarro-Herrera, D., Aranaz, P., Eder-Azanza, L., Zabala, M., Hurtado, C., Romo-Hualde, A., Martínez, J. A., González-Navarro, C. J., & Vizmanos, J. L. (2018). Dihomo-gamma-linolenic acid induces fat loss in: C. Elegans in an omega-3-independent manner by promoting peroxisomal fatty acid β-oxidation. *Food and Function*, *9*(3), 1621–1637. https://doi.org/10.1039/c7fo01625e

Peng, C., Wang, X., Chen, J., Jiao, R., Wang, L., Li, Y. M., Zuo, Y., Liu, Y., Lei, L., Ma, K. Y., Huang, Y., & Chen, Z. Y. (2014). Biology of ageing and role of dietary

antioxidants. In *BioMed Research International* (Vol. 2014). Hindawi Publishing Corporation. https://doi.org/10.1155/2014/831841

Pino, E. C., Webster, C. M., Carr, C. E., & Soukas, A. A. (2013). Biochemical and high throughput microscopic assessment of fat mass in Caenorhabditis elegans. *Journal of Visualized Experiments*, *73*. https://doi.org/10.3791/50180

Pintó, R. M., Diez, J. M., & Bosch, A. (1994). Use of the colonic carcinoma cell line CaCo-2 for in vivo amplification and detection of enteric viruses. *Journal of Medical Virology*, *44*(3), 310–315. https://doi.org/10.1002/jmv.1890440317

Re, R., Pellegrini, N., Proteggente, A., Pannala, A., Yang, M., & Rice-Evans, C. (1999). Antioxidant activity applying an improved ABTS radical cation decolorization assay. *Free Radical Biology and Medicine*, *26*(9–10), 1231–1237. https://doi.org/10.1016/S0891-5849(98)00315-3

Reifferscheid, G., & Heil, J. (1996). Validation of the SOS/umu test using test results of 486 chemicals and comparison with the Ames test and carcinogenicity data. *Mutation Research - Genetic Toxicology*, *369*(3–4), 129–145. https://doi.org/10.1016/S0165-1218(96)90021-X

Reifferscheid, G., Heil, J., Oda, Y., & Zahn, R. K. (1991). A microplate version of the SOS/umu-test for rapid detection of genotoxins and genotoxic potentials of environmental samples. *Mutation Research/Environmental Mutagenesis and Related Subjects*, *253*(3), 215–222. https://doi.org/10.1016/0165-1161(91)90134-T

Saul, N., Pietsch, K., Stürzenbaum, S. R., Menzel, R., & Steinberg, C. E. W. (2011). Diversity of Polyphenol Action in Caenorhabditis elegans : Between Toxicity and Longevity. *Journal of Natural Products*, *74*(8), 1713–1720. https://doi.org/10.1021/np200011a

Sentandreu, E., Cerdán-Calero, M., Halket, J. M., & Navarro, J. L. (2015). Rapid screening of low-molecular-weight phenols from persimmon (Diospyros kaki) pulp using liquid

chromatography/UV-visible/electrospray mass spectrometry analysis. *Journal of the Science of Food and Agriculture*, *95*(8), 1648–1654. https://doi.org/10.1002/jsfa.6867

Shen, P., Yue, Y., & Park, Y. (2018). A living model for obesity and aging research: Caenorhabditis elegans. In *Critical Reviews in Food Science and Nutrition* (Vol. 58, Issue 5, pp. 741–754). Taylor and Francis Inc. https://doi.org/10.1080/10408398.2016.1220914

Singleton, V. L., Orthofer, R., & Lamuela-Raventós, R. M. (1999). Analysis of total phenols and other oxidation substrates and antioxidants by means of folin-ciocalteu reagent. *Methods in Enzymology*, *299*, 152–178. https://doi.org/10.1016/S0076-6879(99)99017-1

Sun, C., Wu, Z., Wang, Z., & Zhang, H. (2015). Effect of ethanol/water solvents on phenolic profiles and antioxidant properties of Beijing propolis extracts. *Evidence-Based Complementary and Alternative Medicine*, *2015*. https://doi.org/10.1155/2015/595393

Taira, S., Ono, M., & Matsumoto, N. (1997). Reduction of persimmon astringency by complex formation between pectin and tannins. *Postharvest Biology and Technology*, *12*(3), 265–271. https://doi.org/10.1016/S0925-5214(97)00064-1

Venkata Mohan, S., Nikhil, G. N., Chiranjeevi, P., Nagendranatha Reddy, C., Rohit, M. V., Kumar, A. N., & Sarkar, O. (2016). Waste biorefinery models towards sustainable circular bioeconomy: Critical review and future perspectives. *Bioresource Technology*, *215*, 2–12. https://doi.org/10.1016/j.biortech.2016.03.130

Venkatesan, T., Choi, Y. W., & Kim, Y. K. (2019). Impact of Different Extraction Solvents on Phenolic Content and Antioxidant Potential of Pinus densiflora Bark Extract. *BioMed Research International*, *2019*, 1–14. https://doi.org/10.1155/2019/3520675

Watts, J. L. (2009). Fat synthesis and adiposity regulation in Caenorhabditis elegans. In *Trends in Endocrinology and Metabolism* (Vol. 20, Issue 2, pp. 58–65). https://doi.org/10.1016/j.tem.2008.11.002

Wei, Y., & Kenyon, C. (2016). Roles for ROS and hydrogen sulfide in the longevity response to germline loss in Caenorhabditis elegans. *Proceedings of the National Academy of Sciences*, *113*(20), E2832–E2841. https://doi.org/10.1073/pnas.1524727113

Wiles, P. G., Gray, I. K., Kissling, R. C., Delahanty, C., Evers, J., Greenwood, K., Grimshaw, K., Hibbert, M., Kelly, K., Luckin, H., McGregor, K., Morris, A., Petersen, M., Ross, F., & Valli, M. (1998). Routine Analysis of Proteins by Kjeldahl and Dumas Methods: Review and Interlaboratory Study Using Dairy Products. *Journal of AOAC INTERNATIONAL*, *81*(3), 620–632. https://doi.org/10.1093/jaoac/81.3.620

Yoo, S. K., Kim, J. M., Park, S. K., Kang, J. Y., Han, H. J., Park, H. W., Kim, C. W., Lee, U., & Heo, H. J. (2019). Chemical compositions of different cultivars of astringent persimmon (Diospyros kaki Thunb.) and the effects of maturity. *Korean Journal of Food Science and Technology*, *51*(3), 248–257. https://doi.org/10.9721/KJFST.2019.51.3.248

Yoon, Y. W., Choi, S. T., Park, D. S., Rho, C. W., Kim, D. H., & Kang, S. M. (2014). Changes in organic and inorganic nutrients in terminal shoots of ‘Fuyu’ persimmon during spring growth. *Korean Journal of Horticultural Science and Technology*, *32*(3), 279–288. https://doi.org/10.7235/hort.2014.13099

8 Supplementary material

Figure S1. Photos of the persimmon fruits at the two ripeness stages: A) Immature (I) and B) Mature (M).

Table S1. *C. elegans*-specific gene expression probes used for qPCR analyses*.

PrimeTime qPCR Probe Assays (Integrated DNA Technologies, Inc)			
C.elegans gene	Fw sequence (5' – 3')	Rv sequence (5' – 3')	Probe sequence (5' – 3')
fat-5	CGTGTAGAAGG CGATGAAGG	GATTTGTACGAG GATCCGGTG	/56FAM/ACGACTGGA/Zen/ATGAAG GTGGGCA/3IABkFQ/
fat-7	ACAAGTTAAGG AGCATGGAGG	TCTCCTTCCAGA AATAAACGGG	/56-FAM/CAGAGAAAG/Zen/CACTAT TTCCCACTGGTCA/3IABkFQ/
acox-1	AGCAAACTGGA AAGCGTAGG	AACAAGATACTC GGCAGTGAG	/56FAM/CGGGCGATG/Zen/AATGGG AAGAGACG/3IABkFQ/
maoc-1	CAGTAACCAATG TTTGTCCTGG	TCATGGATTGTG CAGTCTGG	/56FAM/CTGCTTGGG/Zen/CTGGAA ATGATTCTGAC/3IABkFQ/
TaqMan® Gene Expression Assays (Thermo Fisher Scientific)			
C.elegans gene	TaqMan reference probe	Assay	
daf-2	Ce02444349_m1	Made to order	
daf-16	Ce02422838_m1	Inventoried	
skn-1	Ce02407447_g1	Inventoried	
pmp-3 *	Ce02485188_m1	Inventoried.	

* The expression level of each gene was normalized comparing to the expression of the *pmp3* as housekeeping gene control.

Table S2. Analysis of variance for the predicted quadratic polynomial models for TPC and antioxidant capacity of extracts from persimmon fruit.

		IPE				MPE			
		TPC (mg GAE/g)		TEAC (μmol TE/g)		TPC (mg GAE/g)		TEAC (μmol TE/g)	
Source	d.f.	SS	p-value	SS	p-value	SS	p-value	SS	p-value
Model	9	1122.3	0	17267	0.088	260.552	0	22361	0
Linear	3	198.39	0.004	4991	0.159	174.132	0	16362	0
X_1 S/L	1	32.35	0.07	469	0.455	7.655	0.021	2101	0.002
$X_{2\ E/W}$	1	165.84	0.001	4137	0.044	30.633	0	2465	0.001
$X_{3\ T}$	1	0.21	0.875	384	0.498	135.844	0	11795	0
Square	3	679.67	0	4104	0.219	58.366	0	2156	0.016
X_1X_1	1	92.92	0.001	15	0.954	0.869	0.688	26	0.463
X_2X_2	1	505.1	0	4083	0.047	5.516	0.141	111	0.603
X_3X_3	1	81.65	0.009	5.	0.936	51.981	0	2018	0.003
2-Way interaction	3	244.21	0.002	8171	0.058	28.055	0.003	3842	0.002
X_1X_2	1	126.77	0.002	2599	0.098	0.808	0.396	1.4	0.92
X_1X_3	1	3.16	0.54	2223	0.122	5.141	0.049	2232	0.002
X_2X_3	1	114.28	0.003	3349	0.065	22.105	0.001	1609	0.005
Lack of fit	5	34.93	0.592	6479	0.052	7.649	0.134	735	0.37
Pure error	5	43.43		1308		2.64		538	
Total	19	1200.7		25055		270.841		23634	
R^2		0.9347		0.689		0.962		0.946	
R^2-adj		0.876		0.409		0.9278		0.897	

Principal Components Analysis (PCA)

A PCA was carried out to evaluate the variance related to the extraction conditions and the results are presented as scatterplots showing the relationship between the factors and variables (score plot A) and samples (loading plot B) in Figure S2. If variables are highly related, they can be incorporated into a component that accounts for the most variance in the observations. The second component explains the second highest amount of variance and will not be correlated to the first component (Lattin et al., 2003).

The multivariate treatment of the data obtained for the samples permitted the reduction of the variables to two principal components, which together explained 88.5% of the total variability. The first axis accounted for 58.8% and the second axis for 26.7%. According the factor loadings plot (Figure S2b), the bioactive extracts from the mature fruits-MPE (TPC and antioxidant activity), were positively correlated to the PC1 axis which was highly represented by temperature, whereas the IPE extracts were positively correlated to the PC2 axis highly correlated to E/W(%) ratios and thus, supporting the differences between factors evaluated over the effect of extraction process of polyphenol content which was also significantly affected by the maturity stage of the fruit. Phenolic compounds extracted at low temperatures, and high E/W (%) (8, 17, 3) were rated low in TPC, indicating a high amount of polyphenolic compounds easily extracted by polar solvents. However, the center points conditions, had the best values allowing higher extraction degree of phenolic compounds and indicating that the E/W of 75% with moderate temperatures, were the best conditions for IPE. Similarly, this E/W ratio was also reported as the best in polyphenolic extraction from propolis (Sun et al., 2015).

In summary, the discrimination of samples based on the scatter-plots highlighted a correlation with the response surface methodology results commented on in the manuscript.

A

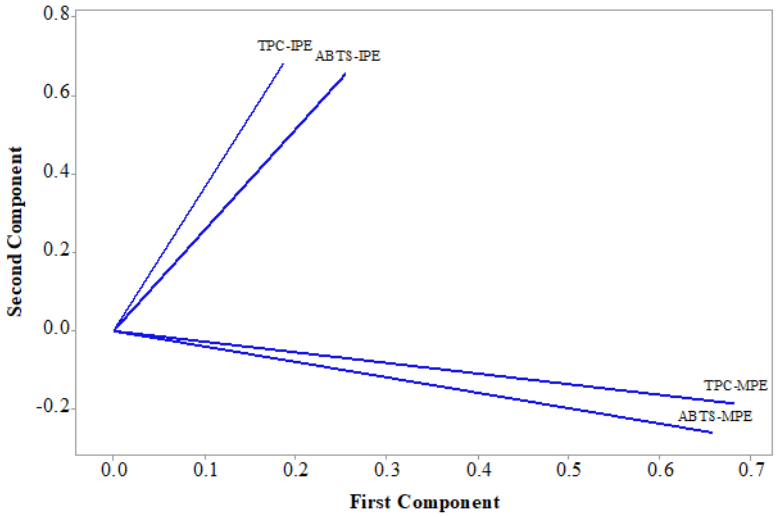

B

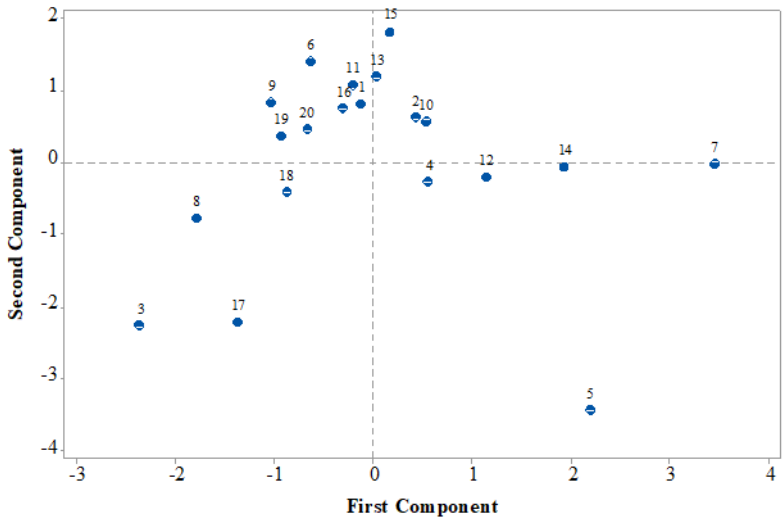

Figure S2. (A) Principal component analysis of the extracted samples for TPC and antioxidant activity (for the codes of the samples, see Table 1) (B) Factor loadings for principal component analysis.

Carbohydrate composition

Table S3. Monosaccharide composition of the persimmon extracts.

mg/g extract	Fuc	Rha	Ara	Gal	Glc	Xyl	GalA
lab-scale IPE	2 ±1	4 ±1	15 ±2	12 ±2	286 ±27	25 ±9	155 ±31
Up-scaled IPE	<2	<2	3 ±0	<2	459±15	<2	<2

Fuc: Fucose, Rha: rhamnose, Ara: arabinose, Gal: galacose, Glc: glucose, Xyl: xylose, GalA: Galacturonic acid. Mannose and Glucuronic acid were not detected or detected in trace amounts.

Characterization of the polyphenolic profile of the persimmon extracts

Table S4 compiles the different phenolic compounds identified in the lab scale and upscaled immature persimmon extract. Quantification of gallic acid and naringenin was performed with the response of the corresponding pure standards at 280 nm. Tentatively identified peaks (2-11) were quantified with the response of pure standards of their aglycones. Vanillic acid hexoside, naringin and hesperidin were quantified at 280 nm with the response of vanillic acid, naringenin and hesperetin, respectively (Figures S3-S4). Galloyl hexoside was quantified at 254 nm with the response of gallic acid (Figure S5). Quercetin glycosides (two hexosides) were quantified at 350 nm with the response of quercetin, while kaempferol glycosides (two hexosides and two hexoside-gallates) were quantified with the response of kaempferol (Figures S6 and S7).

Table S4. UPLC-DAD-MS information of phenolic compounds detected in the persimmon extracts (IPE) obtained at lab scale (A) and industrially upscaled (B).

Peak	Tentative identification	RT (min)	Extracts	UV-vis (nm)	[M-H]- *m/z*	MS^2
1	Gallic acid	3.7	A, B	270	169	125 (100%), 79 (20%)
2	Galloyl hexoside	7.6	B	254	331	169 (100%)
3	Vanillic acid hexoside	12.2	A, B	280	329	167 (100%), 191 (30%)
4	Naringin	16.5	B	283	579	271 (100%), 170 (30%), 296 (20%)
5	Hesperidin	16.9	B	284	609	301 (100%)
6	Quercetin hexoside I	17.0	A, B	254, 353	463	301 (100%)
7	Quercetin hexoside II	17.1	A, B	254, 353	463	301 (100%)
8	Kaempferol hexoside I	17.8	A, B	266, 352	447	285 (100%), 227 (20%)
9	Kaempferol hexoside II	18.2	A, B	266, 352	447	285 (100%)
10	Kaempferol hexoside gallate I	18.7	B	268, 352	599	285 (100%)
11	Kaempferol hexoside gallate II	19.0	B	268, 352	599	285 (100%)
12	Naringenin	22.9	B	280	271	151 (100%), 119 (30%)

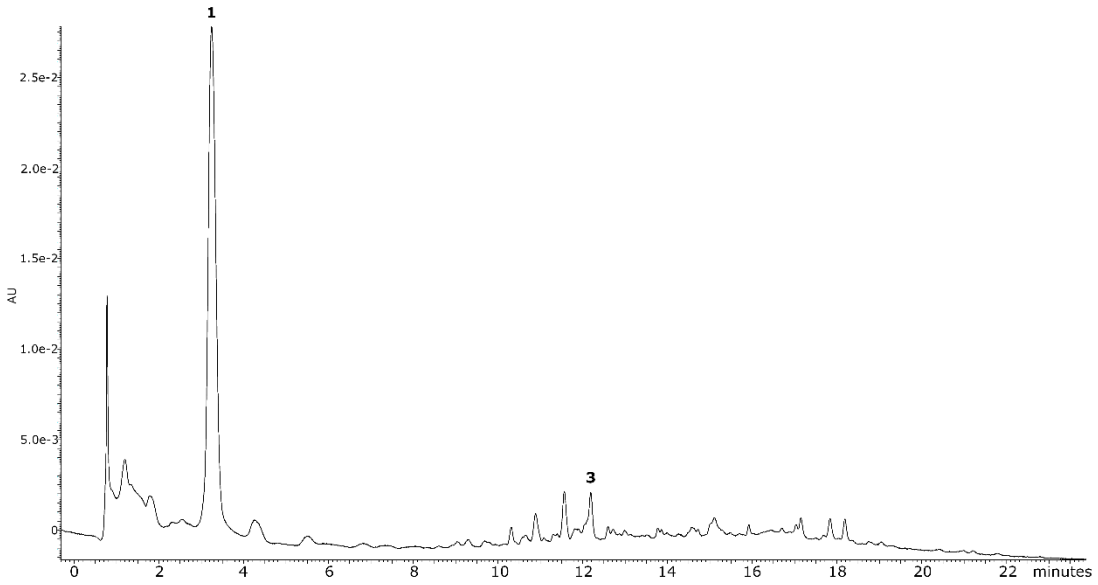

Figure S3. UPLC chromatogram of lab scale IPE (extract A) at 280 nm. For peaks identification see Table S4.

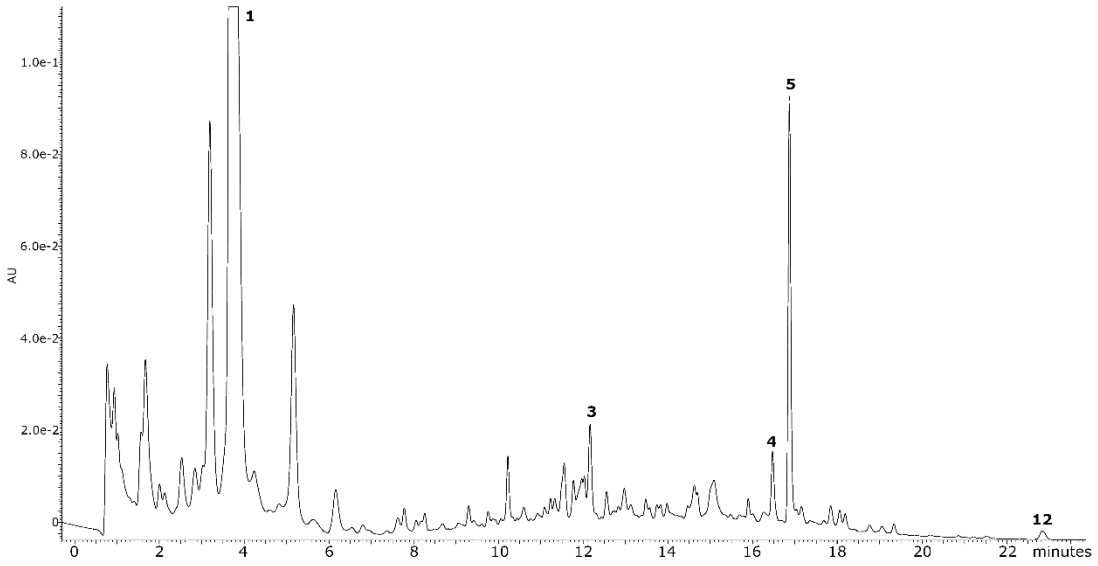

Figure S4. UPLC chromatogram of upscaled IPE (extract B) at 280 nm. For peaks identification see Table S4.

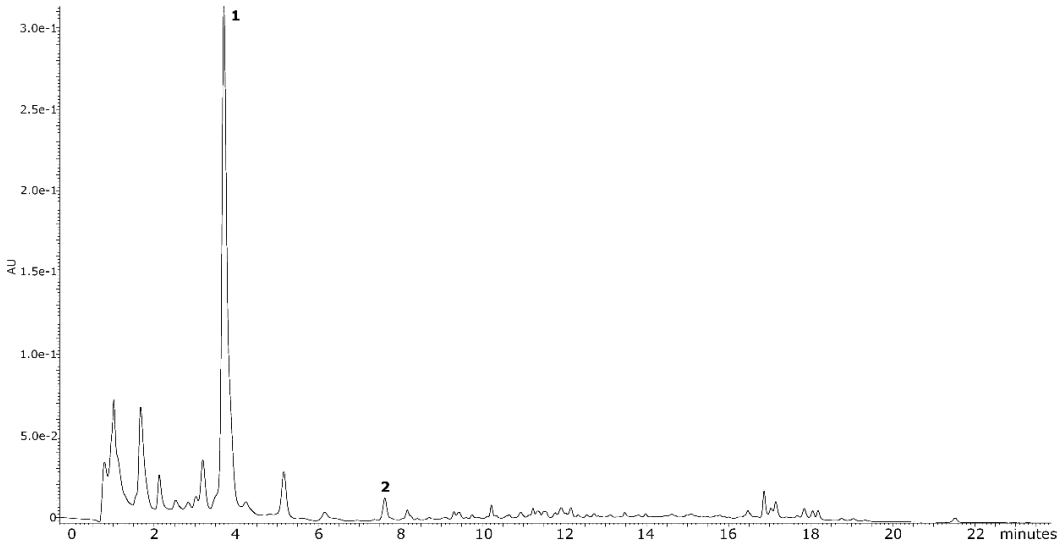

Figure S5. UPLC chromatogram of upscaled IPE (extract B) at 254 nm. For peaks identification see Table S4.

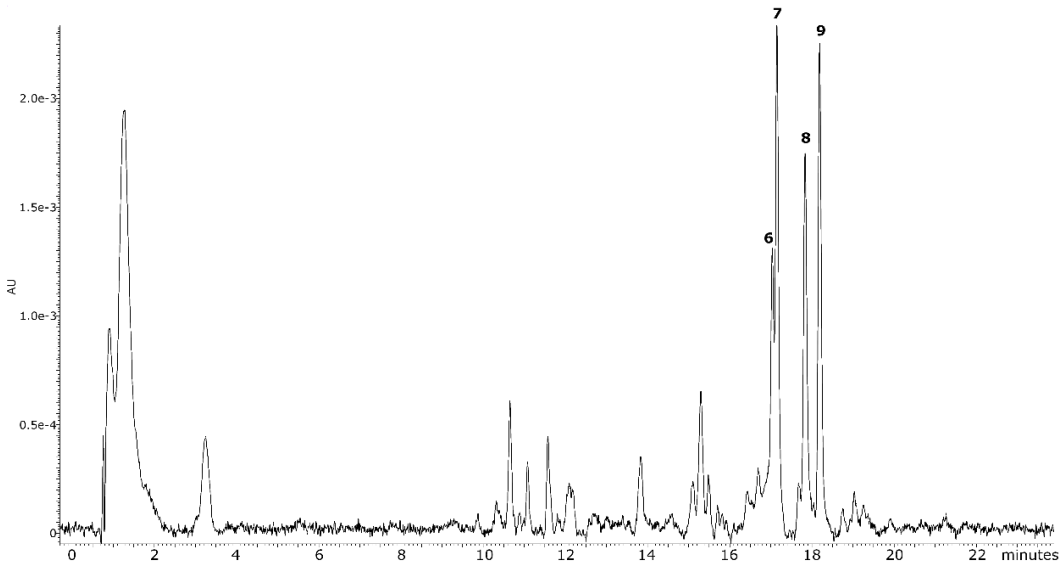

Figure S6. UPLC chromatogram of lab scale IPE (extract A) at 350 nm. For peaks identification see Table S4.

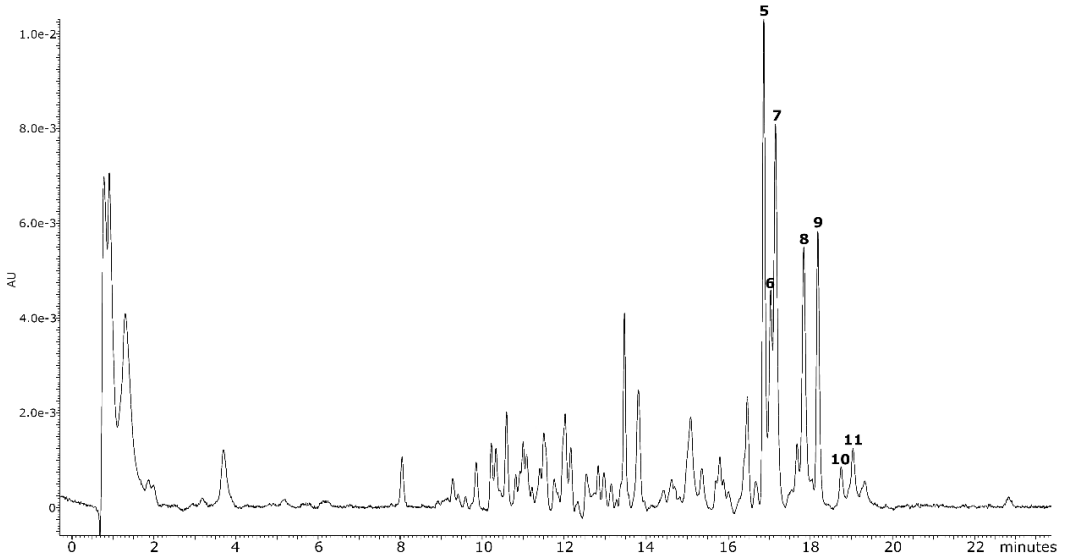

Figure S7. UPLC chromatogram of upscaled IPE (extract B) at 350 nm. For peaks identification see Table S4.

Genotoxicity screening assay

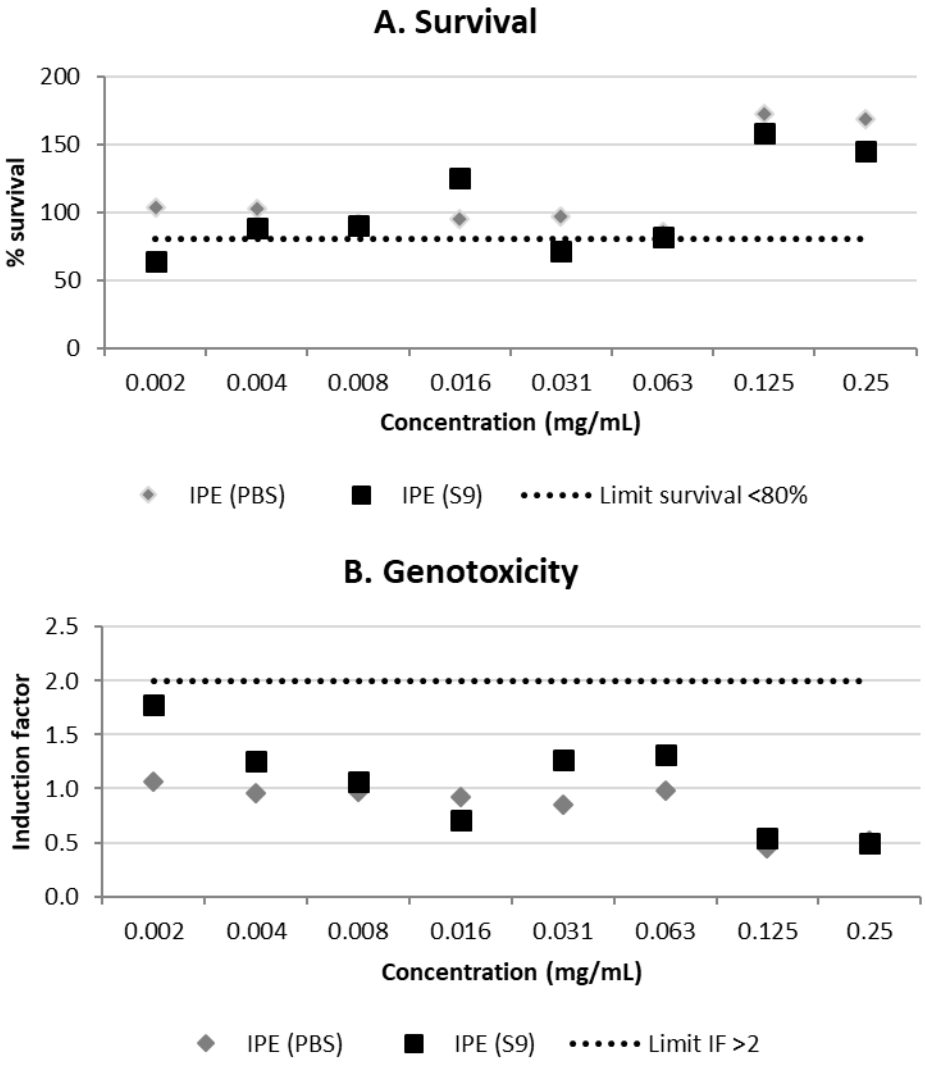

Figure S8. Results from SOS/umu test with (black) o without S9 (grey) activation. A) Bacterial survival is shown as percentage. Concentrations are considered non-toxic if survival is > than 80%. B) Genotoxicity. A compound is considered genotoxic if the induction factor is ≥2 at non-toxic concentrations for the bacteria in any of the conditions tested.

3.2.2

INFLUENCE OF THE EXTRACTION CONDITIONS ON THE CARBOHYDRATE AND PHENOLIC COMPOSITION OF FUNCTIONAL PECTIN FROM PERSIMMON WASTE STREAMS.

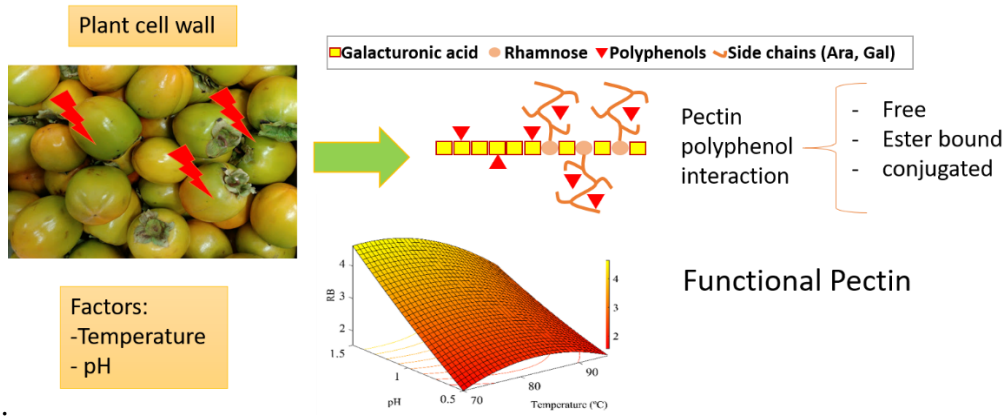

.

This section is an adapted version of the following published research article:

Mendez, D. A., Fabra, M. J., Odriozola-Serrano, I., Martín-Belloso, O., Salvia-Trujillo, L., López-Rubio, A., & Martínez-Abad, A. (2021). Influence of the extraction conditions on the carbohydrate and phenolic composition of functional pectin from persimmon waste streams. *Food Hydrocolloids*, 107066.

---

1 Abstract

Persimmon fruit (*Diospyros kaki Thunb.*) production suffers great losses (15-20%) due to the inefficient overripening process. In order to valorise this waste, a compositional characterization of different fruit stages of the residues was done, and immature fruit was selected due to its high pectin and very high polyphenol content. A 3-level full factorial design was carried out to study the effect of temperature (70-95 °C) and low pH (0.5-1.5), on yield, degree of esterification, carbohydrate constituents, phenolic content and antioxidant capacity of the extracted pectin, and a complete polyphenol profile (UPLC-MS/MS) was performed on selected extracts. All responses could be accurately adjusted to the models (R^2>80; lack of fit). Pectin yield, phenolic compounds and antioxidant activity ranged from 1.4 to 4.5%, 53.3 ±2.27 to 111.7 ±9.74 mg GAE/g pectin and 0.29 ±0.01 to 2.77 ±0.04 TEAC (Trolox µmol/mg pectin), respectively. A strong pectin-polyphenol interaction was found, which significantly enhanced acid resistance of both the pectin and polyphenol constituents, with optimum yield and polyphenol content at pH 1 and 95 °C. These new pectin-based ingredients might have a great potential as functional foods or natural food ingredients enhancing the quality and shelf-life.

2 Introduction

The future of food and agriculture faces a number of uncertainties that raise significant concerns about its performance and sustainability. While food demand is expected to increase anywhere between 59% to 98% by 2050 (Berbel & Posadillo, 2018), more than 1.3 billion tonnes of food are wasted every year, which is around 1/3 of the world's production (FAO, 2016). With a global aim towards sustainability, it is necessary to drive a change and look for different ways to valorise by-products or residues from the food chain with potential to become new ingredients improving the quality and/or preservation of foods (Carocho et al., 2018)

Persimmon (*Diospyros kaki Thunb.*) is a fruit tree originating from China, with a global production of 4.3 million tons in 2019 (FAOSTAT, 2021). Over the last decade, Spain has become the second global producer and the first exporter owing to the "*Rojo Brillante*"

variety with registered designation of origin in the Valencian province (FAOSTAT, 2021; Martínez-Las Heras et al., 2016). This especially resistant and high quality variety must be subjected to an overripening process with 1-methylcyclopropene and ethylene for 18–24 h cto reduce its astringency before consumption. Although great efforts have been carried out in post-harvesting techniques and storage conditions to improve the quality and minimize losses, immature untreated fruits are severely affected by small physiological changes causing a poor CO_2 diffusion, which results in a low anaerobic respiration rate, reducing acetaldehyde accumulation which in turn causes a decrease in its interactions with soluble tannins, these being responsible for astringency and rejection (Munera et al., 2019). The seasonal production and this inefficient overripening result in huge amounts of discarded fruit (about 15-20% of the fruit harvested) (Munera et al., 2019), representing ~ 9500 Tn/ year in the Valencian region only (data provided by the second grade cooperative ANECOOP).

Apart from free sugars, persimmon contains significant amounts of pectin and very high contents in polyphenols. Pectin is a family of polysaccharides built with several structural elements, where the most studied and highly identified are the homogalacturonan (HG) and type I rhamnogalacturonan (RG-I). HG, known as the smooth region, is constituted by galacturonic acid (GalA) units which can be naturally methylesterified at the C-6 carboxyl group (Prasanna et al., 2007). The degree of methylesterification governs much of the properties in pectin, depending on which pectins are able to form gels with high amounts of soluble solids and/or the presence of divalent cations (Wai et al., 2010) and constitute a valuable texturizing ingredient used in foods, such as dairy products, juices, sauces, marmalades, and even meat products or cheese (Adetunji et al., 2017; Virk & Sogi, 2004). Polyphenols are widely recognized for their health benefits as antioxidants, among other bioactivities (antimicrobial, prebiotic, etc) (Hamauzu, 2018; Pérez-Burillo et al., 2018).

In fact, several works have been focused on their extraction and characterization from persimmon (Butt et al., 2015; Hamauzu & Suwannachot, 2019), since its antioxidant activity has been reported to be significantly higher than other antioxidant-rich fruits like apple, grape or tomato (X. N. Chen et al., 2008). Furthermore, these polyphenols have been reported to be linked to pectin moieties, reducing both astringency and firmness during the

ripening process (Mamet et al., 2018; Taira et al., 1997). This unique characteristic offers a great potential for the valorisation of functional pectins as new functional food ingredients with all benefits from the polyphenols adding up to the intrinsic properties of pectin.

Some authors have previously reported on the extraction of pectin from persimmon peel, (Jiang et al., 2020; Nguyễn & Savage, 2013). Nevertheless, little information is available on how the extraction conditions influence the structural and functional properties of persimmon pectin, and especially, about how polyphenol compounds can interact with it (Mamet et al., 2018; Taira et al., 1997) . To the best of our knowledge, there is no existing literature on how pectin extraction can modify these pectin polyphenol interactions and the physicochemical, structural and functional properties of persimmon pectin from discarded fruits.

This work presents a compositional analysis of persimmon discarded fruits of varying ripeness and, following response surface methodologies and a detailed polyphenolic profile, thoroughly investigates the effect of pH and temperature on the compositional, structural and functional properties of these potential new functional pectin ingredients.

3 Materials and methods

3.1 Material

Persimmon (*Diospyros kaki* Thunb) "Rojo brillante-Ribera del Xuquer" fruits in three ripeness stages (commercial immaturity -CI-, commercial mature non treated -CM- and commercial mature treated with 1-methylcyclopropene and ethylene -CMT) were kindly supplied by Anecoop S. Coop. during the autumn season of 2019 in Spain. The fruits were processed removing the calix and peduncle, cut into pieces of around 0.5 - 2.5 cm and stored in protective bags at -20 °C until their evaluation. Citrus (CP) and apple (AP) pectin (Sigma-Aldrich) were used for comparative purposes, as they are typical pectin sources of wide industrial use and well defined structure and properties. Folin-Ciocalteu's reagent, Sodium bicarbonate, Hydrochloric acid (37% (*v/v)*), β-carotene (≥97%), linoleic acid (≥99%), Tween® 40, Butylated hydroxytoluene (BHT) (≥99%), Trolox (97% purity), gallic acid

(≥98.0% purity), phenol red (ACS grade), sodium hydroxide (pharma grade) and $ABTS^{+\cdot}$ (HPLC grade) were supplied by Sigma-Aldrich (Stenheim, Germany). Acetone (99%) was from WVR chemicals. N-hexane (>95% purity) and ethanol (96% (v/v), USP grade) were purchased from Panreac Applichem (Darmstadt, Germany)

3.2 Proximate analysis

Persimmon fruits in all the ripeness stages were firstly characterized. Moisture was determined according to the approved method 935.29, (AOAC, 1996). Protein determination was carried out by the Dumas combustion method (N conversion factor 5.35, (Fujihara, Kasuga, & Aoyagi, 2001) according to ISO/TS, 16634–2 (2016). Lipid content was quantified by lipid extraction with a Soxhlet apparatus according to Somashekar et al., (2001). Ash content was determined according to the standard TAPPI T211 om-07. Carbohydrates were estimated as the sum of all monosaccharide components (section 2.8). All the analyses were done in triplicate.

3.3 Experimental design

The effect of temperature and pH on the chemical and structural properties of pectin extracted from immature persimmon fruit (CI) was studied through a 3-level full factorial design (3^2) with 4 centred points. The solid-liquid ratio was fixed at 1:20 for a balanced extraction yield and solvent use according to results on pectin extraction from persimmon peel and other fruits (Campbell, 2006; Dranca & Oroian, 2018; Jiang et al., 2020; Petkowicz et al., 2017; Prakash Maran et al., 2014; Rodsamran & Sothornvit, 2019a). Although time is usually an important factor for pectin extraction, the difference in extraction yield between 30 or 90 min using HCl as acidic solvent was not significant in persimmon fruit (e.g., 30 and 90 min extraction at 95 °C, pH 1.5, yielded 4.28 ±0.15 wt% and 4.34 ±0.09% pectin, respectively). Individual and interactive effects of process variables (temperature (X_1) and pH (X_2) over pectin extracts were evaluated (Table 1).

Analysis of variance (ANOVA) following by means comparison using Tukey's multiple comparison test, quality of fit (coefficient of determination (R^2), adjusted coefficient of

determination (adj-R^2)), were attained using the software Minitab, version 15 (Minitab Inc., Philadelphia, U.S.A.). Differences were considered significant at $p \leq 0.05$.

3.4 Extractions

Frozen persimmon was weighed, and the suitable amount of water was added taking into account the initial moisture content of the fruit. The pH was adjusted with 1 M HCl and solutions were heated under magnetic stirring on a hotplate during 30 min. After that, the pectin-based solution was filtered with a muslin cloth followed by vacuum filtration using Whatman filter paper No. 4 at 60 °C. Pectin in solution was coagulated by adding 2 volumes of ethanol and the mixture was left overnight in the freezer. The coagulated pectin was centrifuged (23450 g for 20 min) and washed three times with 96% (v/v) ethanol and two times with acetone to remove less polar compounds and small molecules. The wet pectin was left to dry at 60 °C in a hot air oven until constant weight, ground and stored in a desiccator chamber (0% RH) until further use. Pectin yield (Y(%)) was calculated from the following equation:

$$Y(\%) = \frac{m_0}{m} \times 100$$

where m_0 (g) is the weight of dried pectin and m (g) is the weight of dried persimmon powder.

Table 1. 3-level full factorial design, factors: temperature (X_1) and pH (X_2), and experimental values for yield and chemical properties (degree of esterification -DE%-, β-Carotene/linoleic acid bleaching antioxidant activity -%AA- and Trolox Equivalent Antioxidant Capacity -TEAC-) (on a dry weight basis).

run	X_1 (°C)	X_2 (pH)	Yield (%)	mg GAE/g pectin	DE (%)	%AA	TEAC (µmol Trolox/mg pectin)
1	70	1	1.76	83.14(2.54)	67.29(0.26)	27.57 (3.21)	1.74 (0.08)
2	82.5	0.5	3.98	61.36(1.32)	54.5(0.44)	17.87 (2.74)	1.04 (0.05)
3	95	0.5	4.02	53.26(2.27)	44.05(2.42)	4.42 (7)	0.29 (0.01)
4	82.5	1.5	2.49	111.71(9.74)	71.42(0.45)	28.41 (4.22)	2.4 (0.05)
5	70	1.5	1.37	103.41(0.76)	74.24(0.74)	25.95 (9.94)	2.65 (0.08)
6	82.5	1	3.46	100.28(0.74)	67.48(0.82)	25.15 (1.84)	2.21 (0.09)
7	82.5	1	3.54	100.21(0.62)	66.72(0.43)	29.74 (0.81)	2.72 (0.06)
8	95	1.5	4.32	101.96(1.78)	70.06(0.63)	45.87 (7.91)	2.36 (0.12)
9	82.5	1	3.44	100.11(0.5)	66.44(0.49)	29.55 (5.35)	2.77 (0.04)
10	82.5	1	3.39	100.07(0.92)	67.21(1.96)	29.39 (4.73)	2.65 (0.06)
11	95	1	4.50	79.48(0.78)	62.91(1.7)	14.91 (4.87)	1.52 (0.06)
12	82.5	1	3.65	98.67(1.87)	67.5(1.16)	27.94 (3.4)	2.66 (0.12)
13	70	0.5	2.18	65.85(0.82)	41.94(0.14)	27.21 (3.34)	1.16 (0.03)
AP			-	N.D.	78.57(3.47)	N.D.	N.D.
CP			-	N.D.	58.25(0.62)	N.D.	N.D.

Values in brackets correspond to standard deviation.

3.5 Esterification degree

Degree of esterification (DE) of the extracted pectin was measured according to the method described by Méndez et al., (2021). Pectin samples of 0.05 g were weighed and wetted with 0.5 mL of ethanol (96% (v/v)) and dissolved in 10 mL of a 10% (w/v) sodium chloride solution overnight under magnetic stirring. Two drops of phenol red were added to the dissolved pectin as indicator and the solution was titrated with 0.1 M NaOH (V1). Then, 25 mL of 0.25 M NaOH was added and mixed vigorously to de-esterify pectin and left at room

temperature for 30 min. Next, a volume of 25 mL at 0.25 M HCl to neutralize NaOH was added and titrated again with 0.1 M NaOH until colour change (V2). Calculations were performed according to equation (Eq. 1), in triplicate and compared to citrus and apple pectin as references.

$$DE = \frac{V2}{V2 + V1} \times 100 \quad \text{(Eq. 1)}$$

3.6 FTIR

FTIR measurements were recorded in transmission mode in a controlled chamber at 21 °C and dry air in order to avoid humidity and CO_2 using a Cary 630 FTIR spectrometer (Agilent, USA). The spectra were taken at 4 cm^{-1} resolution in a wavelength range of 400–4000 cm^{-1} and averaging a minimum of 32 scans. Spectra acquired were processed using Origin pro 2019 software (OriginLab Corporation, Northampton, MA, USA).

3.7 Monosaccharide composition

The sugar composition of the extracts was determined after acidic methanolysis as previously described (Martínez-Abad et al., 2018). Freeze-dried samples (1 mg) were incubated with 1 mL of 2 M HCl in dry methanol for 5 h at 100 °C. Samples were then neutralized with pyridine, dried under a stream of air, and further hydrolyzed with 2 M TFA at 120 °C for 1 h. The samples were again dried under a stream of air and re-suspended in milliQ, filtered and injected. The monosaccharides were analyzed using high performance anion exchange chromatography with pulsed amperometric detection (HPAEC-PAD) with a ICS-3000 system (Dionex) equipped with a CarboPac PA1 column (4 × 250 mm, Dionex). Control samples of known concentrations of mixtures of glucose (Glc), fucose (Fuc), rhamnose (Rha), galactose (Gal), arabinose (Ara), xylose (Xyl), mannose (Man), galacturonic acid (GalA) and glucuronic acid (GlcA) were used for calibration (Merck, Germany). Due the high lability of fructose (Fru) during methanolysis, the free Fru and Glc were measured spectrophotometrically using a sucrose, D-fructose and D-glucose (K-SUFRG) Assay Kit (Megazyme, Bray, Ireland), according to the manufacturer's instructions. All measurements were carried out in triplicate.

3.8 Total phenolic content (TPC)

The phenolic compounds from the pulp fruit were first extracted according to Pellegrini et al., (2017) from the freeze-dried material and measured with an spectrophotometric method (Singleton et al., 1999). In the case of pectin extracts, 0.2 mL of the pectin solutions in distilled water (5 mg/mL) were mixed with 1 mL of 10% Folin-Ciocalteu's reagent and 0.8 mL 7.5% $NaHCO_3$. The samples were thereafter incubated at 50 °C for 10 min and the absorbance was measured at 750 nm. Gallic acid was used for calibration and the content of phenolic compounds in the enriched-pectin extracts and phenolic extracts from pulp fruit was expressed in terms of gallic acid equivalents (mg GAE/g pectin). Assays were performed in triplicate.

3.9 Phenolic profile

A complete phenolic profile of immature persimmon fruit (CI) and selected pectin extracts obtained after less severe (pH 1.5, 70 °C, run 5 and pH 1.5, 82 °C, run 4), averagely severe (pH 1, 90 °C, run 11) or extreme acid conditions (pH 0.5, 82 °C, run 2) was performed according to (Mattila & Kumpulainen, 2002). The free phenolic fraction was recovered after liquid-liquid extraction. 0.5 g of sample were dissolved in 7 mL of solution A (85 mL of methanol + 15 mL of acetic acid at 10% (v/v) + BHT at 0.2% (w/v)), sonicated for 30 min, and further diluted in distilled water to 17 mL. Then, the pH was adjusted to 2.0 and 15 mL of solution B (50 mL of diethyl ether + 50 mL of ethyl acetate) were added. After gentle shaking, the organic phase was separated and dried overnight at room temperature. The aqueous solution was further diluted with distilled water (12 mL), and 10 mL of 10 M NaOH was added. Alkaline-hydrolysis was performed under anaerobic conditions by stirring the mixture overnight at room temperature. Monomer aglycone phenolics were then recovered by the same procedure using solution B in order to obtain the alkaline fraction, corresponding to esterified phenolics. The aqueous phase was then acidified with HCl (2.5 mL) and heated (85 °C) for 30 min. The mixture was cooled down to room temperature and processed in the same way using solution B to obtain the acid fraction, corresponding to conjugated phenolics. The detection and quantification of the individual phenolic compounds was performed by UPLC-MS/MS on an AcQuity Ultra-Performance™ liquid

chromatography/tandem mass spectrometry equipment (Waters, USA) with a flow rate of 0.3 mL/min and the injection volume 2.5 μL The UPLC-MS/MS detection conditions are previously described elsewhere (Yuste et al., 2018). The quantification of the individual phenolic compounds was determined by comparison with calibration curves of commercial standards. Due to lack of commercial standards of all the individual phenolic compounds, some of these compounds were tentatively quantified by using the calibration curve of another phenolic compound with a similar structure.

3.10 Trolox Equivalent Antioxidant Capacity (TEAC).

The Trolox Equivalent Antioxidant Capacity (TEAC) was only determined in the pectin-enriched extracts using a modification of the original TEAC method (Re et al., 1999). Samples were dissolved in distilled water for 12 hours and analysed for $ABTS^{+\cdot}$ (2,2-azinobis (3-4ethylbenzothiazoline)-6-sulfonic acid) radical scavenging activity. The $ABTS^{+\cdot}$ solution with an initial absorbance at 734 nm of 0.70 ±0.08 was freshly prepared, 20 μL of the enriched-pectin extract solution were added to 230 μL of the $ABTS^{+\cdot}$ solution and the absorbance was registered after 6 min. Trolox (6-hydroxy-2,5,7,8-tetramethylchroman-2-carboxylic acid) solutions were used as a standard for calibration. The TEAC of the enriched-pectin extracts was determined by comparing the corresponding percentage of absorbance reduction at 6 min with the Trolox concentration-response curve. All the determinations were carried out, at least six times using a CLARIOstar (BMG LABTECH, Germany) spectrophotometer with water as blank.

3.11 β- Carotene/linoleic acid bleaching

The antioxidant activity of the enriched-pectin extracts was determined according to the β-carotene bleaching method described by Fontes-Candia, Erboz, Martínez-Abad, López-Rubio, & Martínez-Sanz, (2019) with some modifications. Briefly, 4 mL β-carotene solution (20 mg in 10 mL chloroform), 50 mg linoleic acid and 400 mg Tween 40 were transferred to a round-bottomed flask. The mixture was then dried with air flow during 5 min to remove chloroform. Then, 100 mL of oxygenated distilled water was slowly added and vigorously stirred resulting in a stable emulsion. 10 μL of the pectin solutions (2 mg/mL

in PBS) were added to 250 mL aliquots of the β-carotene/linoleic acid emulsion and the absorbance was measured (Abs^0) at 470 nm using a microplate spectrophotometer CLARIOstar (BMG LABTECH, Germany). Microtiter plates were incubated in the dark at 45 °C and the absorbance of each sample measured again after 120 min (Abs^{120}). PBS and tert-Butyl hydroxytoluene (BHT) (2 mg/mL) were analogously used as blank and positive control, respectively. All samples were assayed in triplicate. The antioxidant activity (AA) was expressed as the percentage of inhibition relative to the degradation rate (DR) using the following equation:

$$DR=\ln(Abs^0/\ Abs^{120})\text{x } 1/120 \text{ min}$$

$$AA\%=\left[(DR_{control}-DR_{sample})/DR_{control}\right]\text{x}100 \quad \text{(Eq. 2)}$$

4 Results and discussion

4.1 Proximate analysis and sugar composition at different maturity stages

The proximate composition of the persimmon fruit at the three ripeness stages is shown in Table 2. Moisture content was significantly different (82.42 ±0.5%, 79.45 ±0.12% and 78.39 ±0.41% for CI, CM and CMT persimmon fruits) depending on the ripeness of the fruit, which is in agreement with previous literature (Butt et al., 2015; J. Chen et al., 2016). Changes in moisture content often represent the humidity loss during storage, which can affect the polysaccharide composition (Tsuchida et al., 2004). The ripeness stage did not significantly alter the overall carbohydrate, protein, ashes or fat content, these values being also similar to those reported for persimmon fruit by other authors (Butt et al., 2015; Yaqub et al., 2016). However, a significant change was noticed in the carbohydrate composition of the different samples, highly affected by the physiological and chemical changes due to the climacteric nature of the persimmon fruit, and related to ripening (Taira et al., 1997). As expected, a positive correlation was observed between ripeness and increased fructose and glucose content (Table 2), typical for astringent persimmon species and the "Rojo Brillante" variety (Novillo et al., 2016). The amount of GalA content, which is the main pectin constituent for persimmon, was significantly higher in CI fresh fruits than in CMT samples,

showing not significant differences between CMT and CM persimmon samples, the latter being in agreement with values reported for different persimmon cultivars at full-ripeness stage (0.69-2.39 g pectin/ 100 g fresh weight) (J. Chen et al., 2016). Persimmon fruit had a higher pectin content than other fruits, such as cherry, tomato, passion fruit or peach, although still lower than typical pectin sources, such as lemon or apple, or other alternative sources, such as watermelon or mango (Méndez et al., 2021; Prasanna et al., 2007). The decreasing pectin content with ripening is mainly caused by collective action of several pectin-degrading enzymes (Posé et al., 2019). Likewise, the significant reduction in the xylose content for the ripest fruits suggests further depolymerization of hemicellulose polysaccharides (Han et al., 2015). Also, a reduced moisture content in CM and CMT fruits may promote the reduction of some neutral sugars present in pectin, such as Ara and Gal (Tsuchida et al., 2004). Considering the results of the different stages and its composition, the preferred ripeness stage for pectin extraction was the CI stage, due to its significantly higher pectin and polyphenol content (Table 2).

4.2 Characterization of pectin extracts

Second order polynomial equations including linear, interactive and quadratic terms were employed to generate mathematical models to evaluate the relationship between process variables and responses (cf. Table 3, Eq. 3-14). Different responses were selected according to the potential functionality they may confer to the pectin extracted. Yield (%) is related to the extraction efficiency while DE is related to thickening, gelling and rheological properties. The main monosaccharide constituents (GalA, Gal, Ara, Rha and Xyl (µg/mg)) were analysed as a means to describe compositional changes in pectin, which in turn may govern their mechanical and functional properties, as well as the presence of hemicellulose impurities (Table 3). More important, the polyphenol content and antioxidant capacity were also introduced in the model, as a means to evaluate the potential of these pectins as functional ingredients.

Table 2. Chemical composition of persimmon fruit at different ripeness stages commercial immaturity (CI), commercial mature non treated (CM), commercial mature treated with 1-methyl cyclopropane and ethylene (CMT).

Fruit composition (dry wt. %)	CI	CM	CMT
Ash	3.63 (0.58)[a]	2.42 (0.47)[ab]	2.70 (0.6) [ab]
Lipids	3.64 (0.94)[a]	2.8 (0.43)[a]	3.4 (0.59)[a]
Protein	3.45 (0.01)[a]	3.6 (0.01)[a]	3.53 (0.02)[a]
Total polyphenol content (mg GAE/g)	25.91 (2.28) [a]	17.13 (0.94) [b]	1.97 (0.04)[c]
Carbohydrates[*]	78.95 (8.5)[a]	75.82(8.8)[a]	88.94(7.9)[a]
of which (µg/mg dry basis)			
GalA[**]	60.64 (13.56)[a]	44.12 (2.76)[a,b]	37.35 (3.33)[b]
Gal[**]	9.16 (0.95)[a]	6.09 (0.48)[b]	5.74 (0.24)[b]
Ara[**]	10.15 (1.79)[a]	6.35 (0.08)[b]	6.61 (0.35)[b]
Xyl[**]	36.37 (8.44)[a]	6.40 (0.05)[b]	5.42 (0.42)[b]
Glu[***]	385.25 (0.40)[b]	387.60 (0.42)[b]	451.09 (12.60)[a]
Fru[***]	288.00 (7.99)[b]	307.67 (13.20)[b]	383.00 (12.08)[a]

[*] as the sum of all detected monosaccharide constituents.
[**] Monosaccharide composition determined by HPAEC-PAD.
[***] Measured with D-fructose and D-glucose (K-SUFRG) Assay Kit.
Means of each characteristic followed by different letters in the same row are significantly different ($p \leq 0.05$). Moisture content of fresh samples was 82.42 ±0.5%, 79.45 ±0.12% and 78.39 ±0.41% for CI, CM and CMT persimmon fruits Values in brackets correspond to standard deviation.

Table 3. Polynomial equations generated and statistical results for responses evaluated depending on (X_1) temperature and (X_2) pH.

Polynomial equations		R^2	R^2-adj
$Y(\%)=15.08+ 0.390X_1 -2.64X_2$	(Eq. 3)	94.88	91.22
$-0.00202X_1^2 +0.0444X_1X_2 -0.844X_2^2$			
$DE(\%)=-151.9 + 3.99X_1+91.92X_2$	(Eq. 4)	94.89	91.23
$-0.0232X_1^2 -0.252X_1X_2 -23.04X_2^2$			
Carbohydrate composition			
$GalA\ (\mu g/mg)=1459+ 16.3X_1 - 751X_2$	(Eq. 5)	87.25	78.15
$+0.093\ X_1^2-8\ X_2^2+ 5.99\ X_1X_2$			
$Ara\ (\mu g/mg)= -325.8+7.43\ X_1 +69.6X_2$	(Eq. 6)	91.90	86.11
$-0,0417X_1^2 -0.906X_1X_2 +13.47\ X_2^2$			
$Xyl\ (\mu g/mg)=-18.7+1.03X_1 -31.9X_2$	(Eq. 7)	74.20	55.77
$-0.00910X_1^2 + 0.438X_1X_2 -3.51\ X_2^2$			
$Rha\ (\mu g/mg)= -27.6 + 2.10X_1 - 51.2X_2$	(Eq. 8)	80.90	67.26
$-7.09\ X_1^2 + 0.754X_1X_2 -7.09X_2^2$			
$Gal\ (\mu g/mg) = -303 + 10.98X_1 -38.7X_2$	(Eq. 9)	81.29	67.93
$-0.0776\ X_1^2 +1.278X_1X_2 + 0.0024\ X_2^2$			
$RL= 105.3 -3.08\ X_1+ 32.2\ X_2 - 0.0257\ X_1^2 +10.08$	(Eq. 10)	85.35	74.88
$X_2^2 -0.765\ X_1X_2$			
$RB= -23 +0.553\ X_1+ 7.03\ X_2 - 0.00314\ X_1^2 +0.4$	(Eq. 11)	78.57	63.26
$X_2^2 -0.068\ X_1X_2$			
Antioxidant capacity			
$TPC\ (mg\ GAE/g\ pectin)=-451+ 12.21X_1 +64.7\ X_2$	(Eq. 12)	96.60	94.18
$- 0.0782X_1^2 - 27.9\ X_2^2+ + 0.446\ X_1X_2$			
$TEAC\ (\mu Mol\ trolox/mg) = -21.58 + 0.541\ X_1+ 3.41$	(Eq. 13)	89.27	81.61
$X_2 - 0.0035\ X_1^2 - 1.859\ X_2^2 + 0.0236\ X_1X_2$			
$AA\% = 63 + 0.58\ X_1 -120.3X_2 - 0.0151\ X_1^2 - 1.9$	(Eq. 14)	86.00	76.00
$X_2^2 + 1.708\ X_1X_2$			

Abbreviations: Yield (Y), degree of esterification (DE, galacturonic acid (GalA), Arabinose (Ara), Xylose (Xyl), Rhamnose (Rha), Galactose (Gal), ratio linearity (RL), Ratio branching (RB), Total phenolic content (TPC), Trolox Equivalent Antioxidant Capacity (TEAC), β- Carotene/linoleic acid bleaching antioxidant activity (AA%)

4.2.1 Yield

The yield values of the enriched-pectin extracts were properly fitted (R^2 94.88; Table 3), indicating a good reliability for the experimental predictions. To investigate the effect of pH and temperature on the yield, the response surface plots were also obtained for the pectin enriched extracts (Figure 1a). In general, the response surface plot illustrates that the highest yield was obtained for extractions performed at the highest temperature ($p<0.05$) and pH 1.0, which correspond to the average conditions for pectin extraction from other fruits (Denman & Morris, 2015). At high temperatures and under extreme acidic conditions (pH 0.5), yields decreased, most probably due to hydrolytic depolymerisation resulting in the loss of this low molecular weight pectin after washing (see Figure 1a). It should be noted that the maximum yield values in this work (4.5% dry weight, Table 1) corresponds to 75% of all pectin being extracted from the fruit, which evidences high extraction efficiency. These values are slightly higher than those previously reported by other authors for freeze-dried persimmon (Nguyễn & Savage, 2013). Most often, the strong hydrogen bonds generated during the freeze-drying process much detrimentally affect the extraction yield (Pettolino et al., 2012), suggesting higher yields might be achieved with fresh residues.

Even though the aim of this work was to obtain higher added-value functional pectin and lower yields compared to traditional pectin sources were expected, due to the higher pectin content in both dried citrus peel (20-30%) and dried apple pulp (15-20%, compared to persimmon fruit, (Lara-Espinoza et al., 2018), the extraction time in this work was significantly lower compared to traditional pectin extraction. Similar short extraction times also resulted in lower yields for orange (2.95%, (Ognyanov & Kussovski, 2013)) or melon peel (2.87%, (Raji, Khodaiyan, Rezaei, Kiani, & Hosseini, 2017)), pointing out the relative cost-efficiency of this process.

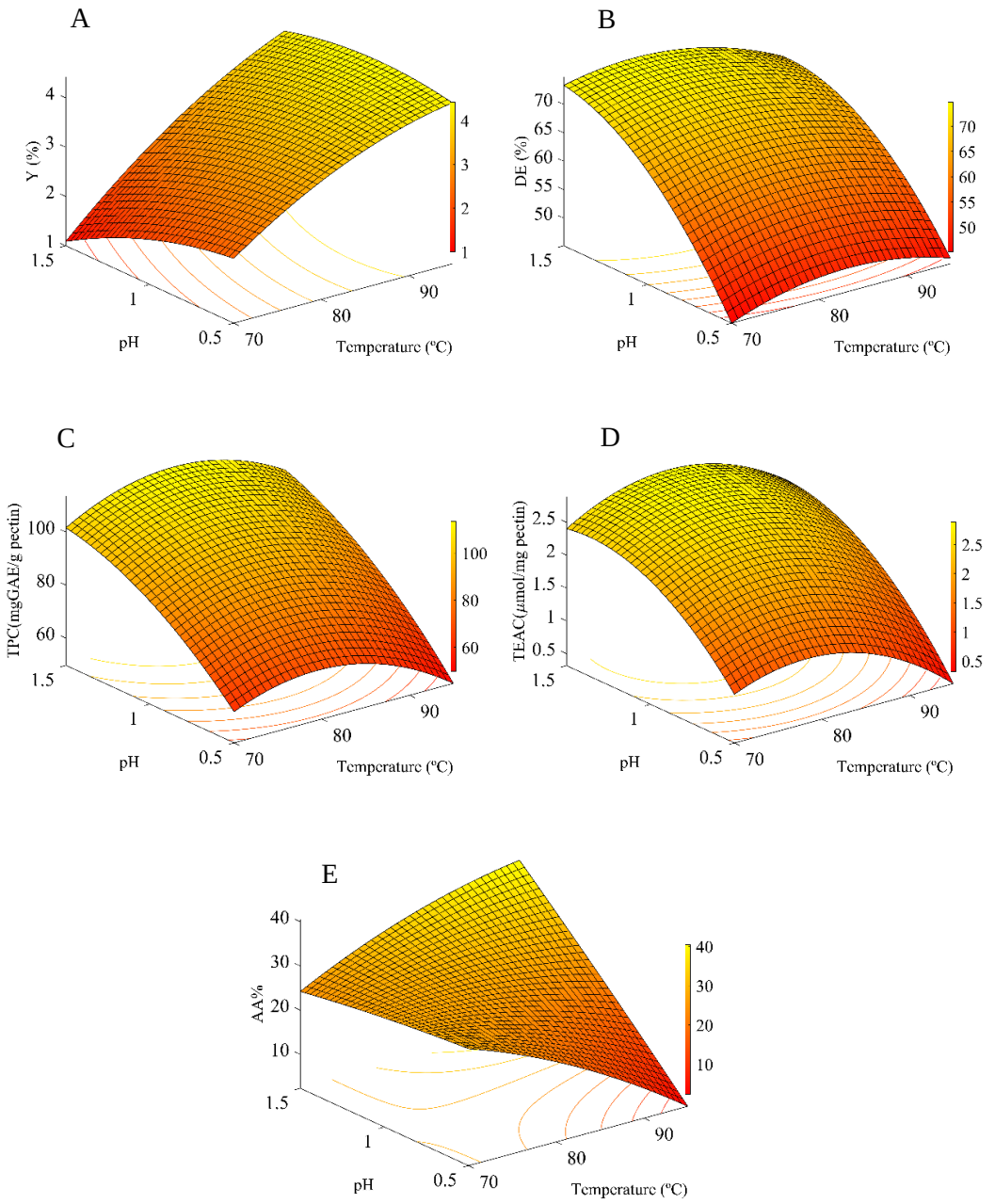

Figure 1. Surface response for pectin (A) yield extraction (Y(%)), (B) degree of esterification (DE(%)), (C) total phenolic content (mg GAE/mg sample), (D) TEAC, and (E) AA% β- Carotene/linoleic acid bleaching from persimmon fruit pectin rich extracts with temperature and pH as main factors.

4.2.2 Pectin esterification

The degree of esterification in pectin much governs the rheological properties and gelling behaviour. High methoxyl pectin (HM; DE > 50%) can form gels at a high sugar content, whilst low methoxyl pectin (LM) form gels at a lower sugar content in the presence of divalent cations (Lara-Espinoza et al., 2018; Wai et al., 2010). The degree of pectin esterification in the present work properly fitted to the polynomial model (R^2 94.89; Table 3, Equation 4). The obtained response surface plot, shown in Figure 1b, revealed that changes in the DE values of enriched pectin extracts were mainly influenced by pH ($p<0.05$), while the correlation between Y and DE is also illustrated in Figure S1 (in the Supplementary Material). Interestingly, the usual decrease in DE under severe acidic conditions is only patent at pH 0.5, while no significant decrease is observed at pH 1 or pH 1.5 (Jafari et al., 2017). The higher acid stability of pectin esterification in persimmon samples might be associated with the high abundance of pectin-polyphenol complexes, as commented below, which has interesting implications towards the potential application as functional bioactive pectin (Denman & Morris, 2015; Wai et al., 2010). The highest yields attained at pH 1 and high temperature also show a high DE (Table 1). These DE values are somewhat higher compared to pectin extracts from other pectin sources (Aina et al., 2012), but in line with reference AP or CP (see Table 1)

4.2.3 Sugar constituents

A quantitative sugar analysis was carried out in order to elucidate the composition of the pectin extracts (Table 4) and understand how it is affected by process parameters (pH and temperature). To get an overall perspective on the structural features of the pectin extracts, different sugar ratios were also calculated for each extraction condition, giving valuable information on the degree of arabinogalactan branching (RB), the linearity (RL), the severity of the extraction (RS) or the contribution of RG-I, HG and their relative ratio (Alba et al., 2018; Denman & Morris, 2015) (Table 5). The main sugar constituents in persimmon pectin extracts were GalA, Fuc, Rha, Ara, Gal and Xyl, which is in accordance with previous works carried out with persimmon peel (Jiang et al., 2020). Man, Glc and Fru were not detected or only present in trace amounts (≤0.5 μm/mg). The lack of free sugars in the

extracts indicates a successful separation of pectin from the very abundant free sugar fraction and other potential low molecular weight compounds not bound to the polysaccharide (Houben et al., 2011). The different degree of aggressiveness in the extractions results in a wide range of compositional characteristics and both the abundance of the different pectin constituents as well as the degree of branching and linearity, were analyzed as responses and properly fitted to the polynomial model (R^2 >75% except for Xyl), enabling a reliable prediction of the pectin traits based on specific extraction conditions (Table 3, Equation 7).

According to the definitions of the international scientific expert committee on Food Additives (JECFA) administered jointly by the Food and Agriculture Organization of the United Nations (FAO) and the World Health Organization (WHO), GalA is recognized as an indicator of the purity of pectin and HG is related to the quality of pectin which is associated to its intrinsic properties and functionality (Alba et al., 2018; Müller-Maatsch et al., 2016). Both values for persimmon pectin produced under all tested conditions are in line with reference citrus and apple pectin (see Table 4 and Table 5), except for the less severe (70 °C, pH 1.5, run 5), while extreme conditions (pH 0.5) resulted in purer HG fractions (62.7-63.4% compared to 45.7% and 54.3% for AP and CP, respectively) at the expense of yield, highest at pH 1 and 95 °C (run 11). Again, it is notable that only extreme acidic conditions are able to significantly degrade the pectin backbone (e.g. reduction in Rha and GalA; Table 5, Fig 3a and 3b) (Denman & Morris, 2015; Kulkarni & Vijayanand, 2010). Extracted pectin under optimum conditions maximizing yield result in a theoretical 4.42% yield, 79.4 mg GAE/g at pH 0.93 and 95 °C, very much as run 11, and would thus generate a pectin complying with current standards for its use as texture modifier in the food industry, which would add up to its bioactive functionalities commented below.

Table 4. Experimental values for neutral sugar (rhamnose (Rha), arabinose (Ara), galactose (Gal) and xylose (Xyl)) and galacturonic acid (GalA) composition of pectins extracted according to the experimental design.

Runs	Rha (µg/mg)	Ara (µg/mg)	Gal (µg/mg)	Xyl (µg/mg)	GalA (µg/mg)
1	19.19(1.46)^{bc}	4.01(0.48)^{fg}	36.59(2.72)^{e}	3.31(0.32)^{e}	501.51(4.03)^{d}
2	20.68(4.31)^{b}	0(0)^{g}	42.85(1.89)^{d}	6.86(0.26)^{bc}	654.9(5.64)^{a}
3	8.64(0.38)^{d}	0(0)^{g}	12.39(0.74)^{fg}	0(0)^{f}	635.98(5.21)^{a}
4	19.71(0.67)^{bc}	23.78(0.71)^{b}	46.04(1.64)^{cd}	3.45(0.25)^{e}	409.98(15.25)^{h}
5	13.92(9.12)^{cd}	32.11(15.18)^{a}	42.03(4.56)^{d}	0(0)^{f}	210.15(23.16)^{i}
6	18.65(5.3)^{bc}	11.09(3.32)^{de}	55.43(1.97)^{a}	4.51(0.04)^{cde}	450.59(13.45)^{f}
7	19.21(5.86)^{bc}	15.16(1.78)^{cde}	55.75(2.63)^{a}	4.57(0.26)^{cde}	460.4(25.5)^{ef}
8	13.88(6.1)^{cd}	9.47(0.04)^{ef}	34.56(0.97)^{e}	3.06(0.14)^{e}	422.68(1.25)^{gh}
9	23.56(3.4)^{ab}	12.6(2.36)^{cde}	54.39(0.18)^{a}	4.5(0.11)^{cde}	452.58(7.72)^{f}
10	21.76(0.22)^{ab}	13.25(3.07)^{cde}	55.48(2.33)^{a}	7.56(5.31)^{b}	461.35(13.29)^{ef}
11	18.86(0.49)^{bc}	0(0)^{g}	43.47(4.27)^{d}	5.91(0.21)^{bcd}	596.44(20.1)^{b}
12	20.79(1.34)^{b}	13.96(0.23)^{cde}	53.1(1.98)^{ab}	4.37(0.16)^{de}	444.49(14.16)^{fg}
13	27.54(0.49)^{a}	0(0)^{g}	51.82(4.16)^{ab}	7.89(1.02)^{b}	573.22(17.82)^{bc}
AP	24.19(0.96)^{ab}	18.47(0.58)^{bcd}	49.44(1.68)^{bc}	16.02(0.85)^{a}	481.97(17.89)^{de}
CP	22.27(0.53)^{ab}	19.46(0.71)^{bc}	35.18(1.59)^{e}	3.56(0.12)^{e}	565.91(22.27)^{c}

Means of each characteristic followed by different letters in the same column (a–f) are significantly different (Fisher $p \leq 0.05$).
*Traces or cero values were found for Glucose, fructose, mannose, fucose and glucuronic acid, Values in brackets correspond to standard deviation.

Ara and Gal are the main neutral sugar constituents found in RG-I, in the form of arabinan, galactan or arabinogalactan (AGI) side chains. Their higher acid lability, especially of arabinofuranosyl residues, is patent in the results and reflected in the model, as temperature, pH and their interaction have a very significant effect on their presence (Table 3, Figure 3c and 3d). In fact, Ara was neither detected in pectin obtained at pH 0.5 (Denman & Morris, 2015; Morris et al., 2010) nor at high temperature and pH 1.0 (Table 4). Gal was the most abundant neutral sugar found in the pectin extracts, ranging between 12.9 and 55.7 µg/mg (see Table 4), in agreement with previously reported values for persimmon peel (Jiang et al., 2020) or other pectin sources (Müller-Maatsch et al., 2016; Yang et al., 2018). The reduction of Gal, although not as affected as Ara (Table 4; Figure 3c), further adds up to the

significant effects of temperature and pH on the degree of branching (RB) and linearity (RL) of pectin (Table 5, Figure 3e and 3f). On the other hand, less severe extraction conditions result in high RB at the expense in HG purity (Table 5 and Figure S4). The good fitting of the degree of RL, and relative high purity of the pectin extracted evidence the possibility of producing pectin with desired structural features, which in turn govern the functional (texturizing, prebiotic, etc.) properties of the final product. Interestingly, conditions with highest yields and relatively high purity result in slightly higher branching degree compared to reference pectin (AP and CP), while RL values are more similar to apple pectin, citrus pectin being more linear. This is probably explained by the inherent higher Rha to Gal ratio in citrus pectin, pointing towards a lower arabinogalactan contribution in RG-I.

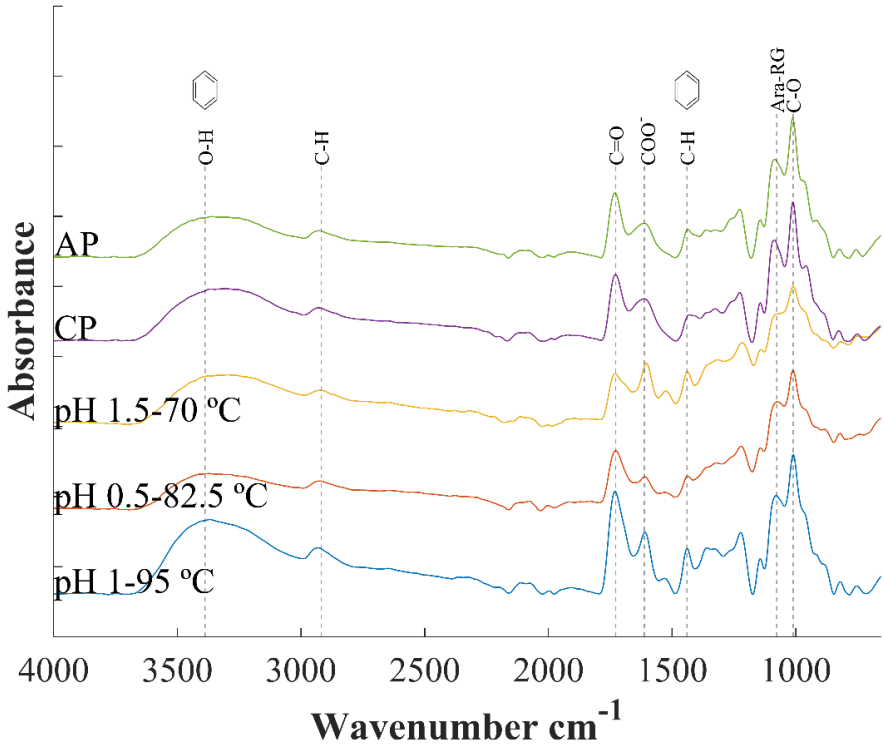

Figure 2. FT-IR spectra comparing harshest, medium and softer pectin extractions conditions from persimmon "Rojo brillante", apple pectin (AP) and citrus pectin (CP).

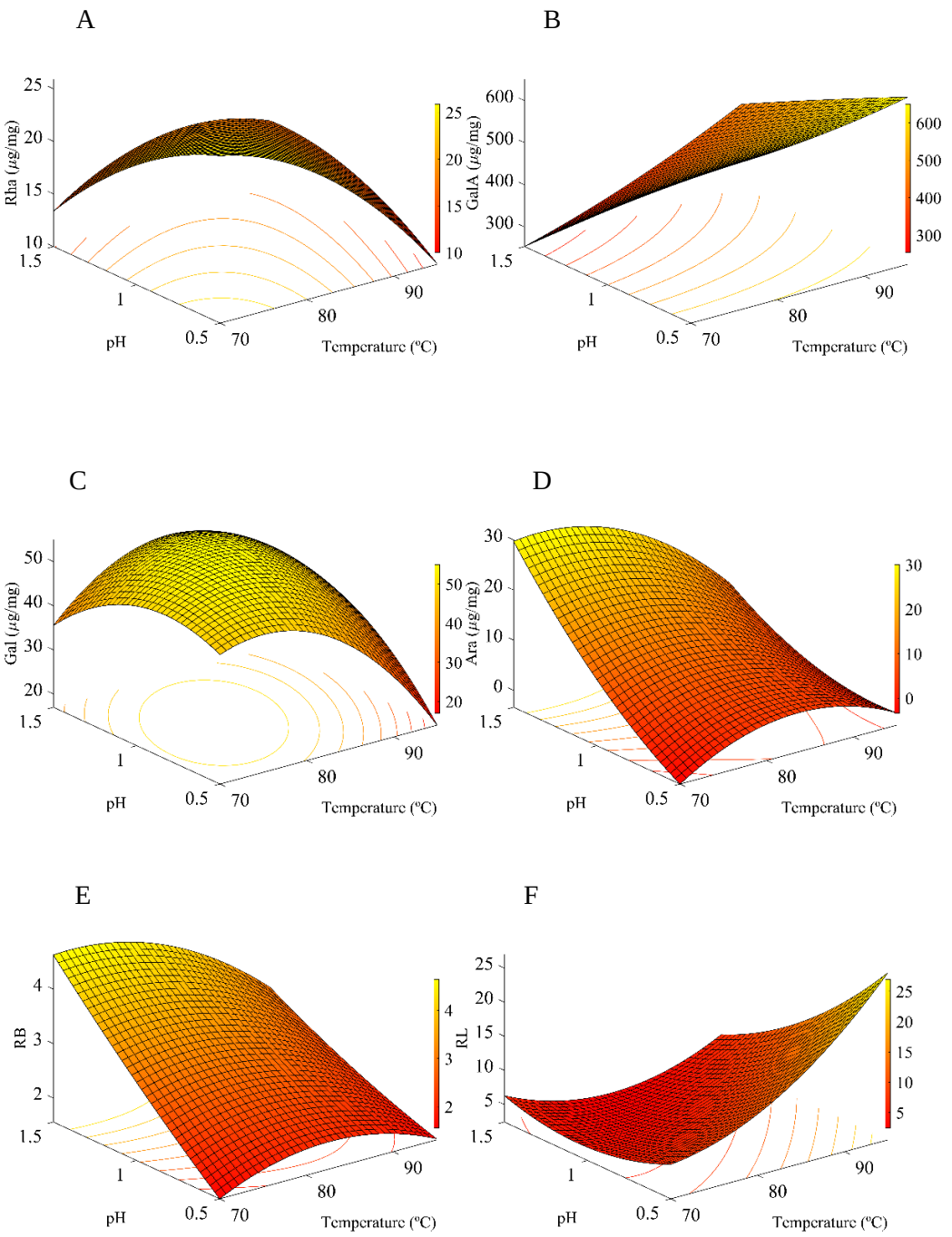

Figure 3. Surface response for (A) Rha, (B) GalA, (C) Gal and (D) Ara content from persimmon pectin. (E) RB and (F) RL as ratios for linearity and branching respectively with temperature and pH as main factors.

Table 5. Composition ratios based on the neutral sugars and galacturonic acid content for each enriched-pectin extract.

Run	Branching (RB)[a]	Linearity (RL)[b]	Severity of extraction (RS)[c]	HG %[d]	RG-I %[e]	HG:RG-I
1	2.12	7.95	124.98	48.2	4.1	11.77
2	2.07	9.30	-	63.4	4.3	14.6
3	1.43	30.24	-	62.7	1.2	49.9
4	3.54	4.41	17.24	39.0	7.0	5.5
5	5.32	2.39	6.54	19.6	7.4	2.6
6	3.57	5.02	40.64	43.1	6.6	6.4
7	3.69	4.86	30.38	44.1	7.1	6.1
8	3.17	6.93	44.63	40.8	4.4	9.2
9	2.84	4.76	35.91	42.9	6.7	6.3
10	3.16	5.10	34.83	43.9	6.9	6.3
11	2.31	8.74	-	57.7	4.3	13.1
12	3.23	5.06	31.84	42.3	6.7	6.2
13	1.88	6.57	-	54.5	5.2	10.4
AP	2.81	4.39	26.09	45.7	6.8	6.6
CP	2.45	6.98	29.09	54.3	5.5	9.8

[a] RB A larger value is indicative of larger average size of the branching side chains. (Gal+Ara/Rha).
[b]RL A larger value suggest of more linear/less branched pectins. (GalA/(Xyl+Rha+Ara+Gal).
[c]RS larger value or not determined value is indicative of more severe extraction conditions and loss of arabinofuranoside (Araf) residues. (GalA/Ara).
[d] (GalA-Rha).
[e] (2Rha+Ara+Gal).

4.2.4 TPC content and phenolic profile of persimmon pectin

The visual appearance of the pectin extracts is shown in Figure S6, where a dark brown coloration is evidenced most likely due to the presence of polyphenols. During pectin extraction, the sequential ethanol and acetone washings to precipitate pectin were expected to remove the major part of polyphenols from pectin extracts (Mamet et al., 2018; Taira et al., 1997). Nevertheless, the detection of high amounts of polyphenols on the pectin extracts suggests the existence of pectin-polyphenol interactions. The TPC of the pectin enriched

extracts was therefore analysed and could also be properly fitted (R^2 96.6) using the polynomial model described by Equation 12 (Table 3). The effect of pH and temperature on the TPC can also clearly be observed in the response surface plot (Figure 1c). As expected, TPC decreased with decreasing pH, while temperature mostly affected TPC if extreme acid pH was used for extraction. Specifically, the TPC ranged between 53.26 and 111.71 mg GAE/g pectin, pointing out the very high polyphenol content of persimmon. In fact, extraction conditions with high pectin yields also showed higher TPC values (e.g. yield 4.32% and 101.96 ±1.78 mg GAE/g pectin, Table 1) than those reported for other pectin sources with high TPC values and antioxidant activity (Hosseini et al., 2020; Rodsamran & Sothornvit, 2019b; Sanchez-Aldana et al., 2013).

Although the TPC value is a good indicator for overall phenolic content and potential beneficial effects as food ingredients, TPC values usually overestimate the real phenolic content, as the Folin reagent readily reacts with other components, such as ascorbic acid, soluble protein, aromatic amines, sulfur dioxide, organic acids, and Fe (II) (Prior et al., 2005)

The identification of specific phenolic compounds and their interaction with other constituents is therefore a better approach to describe the potential bioactive effects of the extracts and their stability upon processing, storage or bioavailability after digestion. In order to identify the specific phenolic compounds present, their potential type of interaction, and relate compositional changes in the phenolic profile to the different extraction treatments, a quantification of conjugated, esterified and free phenolic compounds of the initial raw material (CI) and 3 representative pectin extracts after extreme, averagely severe and less severe extraction conditions was performed. Although the release of phenolics upon alkali or acid treatment is not a direct evidence of their covalent bonding, this approach serves for a rapid estimation of putatively esterified or conjugated phenolic compounds (Dvořáková et al., 2008; Krygier et al., 1982; Mattila & Kumpulainen, 2002; Russell et al., 2009). Results on the main individual phenolic compounds present in persimmon fruit and in the pectin extracts are summarized in Table 6. For detailed extended information of all phenolic compounds identified and analysed in these and one additional pectin extract refer to Table S1 (supplementary material).

Table 6. Concentration (mg/kg sample standard deviation) of individual phenolic compounds in lyophilized persimmon fruit (CI) and persimmon fruit extracts at less severe (L, run 5), averagely severe (M, run 11), extreme acidic conditions (H, run 2).

	Free Phenolics				Alkali fraction				Acid fraction			
Phenolic compounds	CI	M (run 11)	H (run 2)	L (run 5)	CI	M (run 11)	H (run 2)	L (run 5)	CI	M (run 11)	H (run 2)	L (run 5)
Benzoic acids												
Vanillin	22.9(1.55)	123(29.7)	157(3.6)	126(8)	14.6(17.9)	31.4(5.5)	35.8(0.3)	19.5(5.2)	21.8(1.6)	30.6(0.9)	18.3(1.21)	16(0.11)
Gallic acid	161(25.2)	1560(190)	781(128)	1618(158)	9646(25.2)	258(205)	27(2.3)	3874(1955)	762(57.4)	484(16)	41.3(30.3)	1072(143)
Gallic acid glucoside	298(34.3)	n.d.	n.d.	n.d.	1.57(0.04)	n.d.	n.d.	n.d.	n.d.	n.d.	n.d.	n.d.
Protocatechuic acid	n.d.	192(49.7)	75.8(8.7)	69.4(24.7)	211(39.1)	22.8(9.6)	21.9(9.2)	561(268)	44.5(7.2)	184(7.0)	68(15.3)	126(26.5)
Protocatechuic acid glucoside	4.8(1.3)	n.d.	n.d.	n.d.	n.d.	n.d.	n.d.	n.d.	n.d.	n.d.	n.d.	n.d.
Vanillic acid	n.d.	n.d.	n.d.	n.d.	11(0.2)	n.d.	n.d.	26.2(0)	15.7(1.6)	n.d.	n.d.	n.d.
Vanillic acid glucoside	278(43.4)	n.d.	n.d.	n.d.	19(0.4)	4.2(0.7)	2.8(1.4)	n.d.	4.5(2.4)	n.d.	n.d.	27.9(14.9)
Total Benzoic acids*	4.3(0.86)	n.d.	n.d.	n.d.	6.7(1.2)	19.3(8.9)	17.3(3.8)	21.7(2.6)	3.4(0.2)	n.d.	n.d.	2.76(0.84)
Hydroxycinnamic acids*	2.6(0.17)	n.d.	n.d.	n.d.	68.7(6.7)	9.7(2.2)	4.7(0.2)	31.9(3.4)	10.41(1.1)	n.d.	n.d.	n.d.
Total Phenolic acids	772	1874	1013	1814	9978	346	110	4534	862	698	128	1245
Flavan-3-ols												
Epigallocatechin	15.5(3.19)	n.d.	n.d.	n.d.	3.3(0.1)	n.d.	n.d.	4.7(0.2)	n.d.	n.d.	n.d.	n.d.
Epigallocatechin gallate	1.8(0.76	n.d.	n.d.	n.d.	n.d.	n.d.	n.d.	n.d.	n.d.	n.d.	n.d.	n.d.
Other Falvan-3-ols *	29.1(3.77)	n.d.	n.d.	n.d.	3.1(0.5)	n.d.	n.d.	32.8(18.1)	n.d.	n.d.	n.d.	11.03(3.53)
Total Flavan-3-ols	46.4(7.72)	n.d.	n.d.	n.d.	6.3(0.6)	n.d.	n.d.	37.5(18.3)	n.d.	n.d.	n.d.	11.03(3.53)
Flavonol												
Quercetin[a]	18.9(0.68)	3.8(1.7)	n.d.	n.d.	10.5(2.2)	n.d.	n.d.	14.6(8.2)	2.2(0.4)	n.d.	n.d.	1.39(0.47)
Other Flavonol*	73.4(20.71)	10.4(6.1)	n.d.	n.d.	11.5(4.1)	n.d.	1.2(0.1)	20.3(13.8)	1.7(0.3)	n.d.	n.d.	7.05(1.18)
Total Flavonol	92.3(21.39)	14.2(6.1)	n.d.	n.d.	22.1(6.2)	n.d.	1.2(0.1)	34.9(13.8)	3.9(0.3)	n.d.	n.d.	8.44(1.18)
Total Flavanone*	1.6(0.38)	n.d.	n.d.	n.d.	0.4(0.0)	n.d.	n.d.	0.2(0.2)	n.d.	n.d.	n.d.	n.d.
TOTAL PHENOLICS	970	1889	1013	1814	10011	346	111	4607	866	698	128	1264

* Not included phenolic compounds can be consulted in supplementary material Table S1. Values in brackets correspond to standard deviation.

For persimmon fruit, the sum of all identified phenolic compounds (as the sum of free phenolics, alkali fraction and acid fraction) was 11847 mg/kg (Table 6). In agreement with the present results, Senica et al., (2016) and Lucas-González et al., (2017) reported a concentration of total phenolic between 10000 to 17500 mg/kg in different cultivars of persimmon flours. To the best of our knowledge, analysis of the polyphenolic profile in persimmon fruit pectin extracts has not been reported. Phenolic acids, and specifically gallic acid, account by far for the highest part (11613 mg/kg), followed by flavonols (120 mg/kg), flavan-3-ols (112 mg/kg), and minor amounts of flavanones (2.03 mg/kg). In agreement with our results, Fu et al. (2016) reported that phenolic acids, flavan-3-ols and flavonols are the most abundant phenolic group detected in persimmon fruits(Fu et al., 2016) . The abundant gallic acid contents in the immature fruit (CI) was mainly found in the alkali fraction (9646 mg/kg), pointing towards ester bonding to pectin constituents. Protocatechic acid and p-coumaric acid were also found in significant amounts as esters while the glucosides of gallic acid and vanillic acid, quercetin and its derivatives, and epigallocatechin gallate were found as non-covalently bound in the free fraction. A small fraction of most phenolics found as esters in the alkaline fraction could also be detected in the acid extracted fraction.

Although the range of relatively severe acid treatments (pH 0.5-1.5) at high temperatures could be expected to degrade most phenolic compounds, a significant amount is retained in the pectin extracts after acid treatment, coagulation and washing. In fact, at less severe (L) conditions, >7500mg/kg identified phenolics were found in the pectin extracts (as the sum of identified free phenolics, or in the alkali and acid fractions), whereas lower but still very significant quantities (2933 mg/kg and 1252 mg/kg) were identified at averagely severe (M) and extreme acidic conditions (H), respectively (Table 6). The presence of strong pectin-polyphenol interactions via ester and glycosidic linkages has already been suggested and associated to the ripening process, where the formation of complexes between soluble tannins and pectin is concomitant to the partial de-polymerization of pectin, resulting in fruits with decreased astringency and firmness through ripening (Mamet et al., 2018; Taira et al., 1997). The use of increasingly severe acidic conditions and increase temperature results, however, in the cleavage of these bonds (and loss of the free polyphenols) or their

degradation (Saura-Calixto & Pérez-Jiménez, 2018; Zhang & Mu, 2011) together with the pectin backbone (as commented before). Interestingly, significant amount of "free" phenolics were also detected in all pectin extracts, the proportion of which increases with extraction severity. As an example, averagely severe conditions (M) display a very significant reduction in esterified phenolics, while non-covalently bound, "free" phenolics significantly increase compared to less severe conditions (L). This might be explained by the formation of electrostatic and hydrogen bonding between pectin constituents and tannins. This interaction would then be broken when applying the liquid-liquid extraction procedure to extract free phenolics. (Bermúdez-Oria et al., 2019).

In agreement with the model for TPC, pH is the determinant factor for polyphenol recovery (Fig 1c), with gallic acid as the main constituent in all extractions, but the detailed profile provides further unreported insights on qualitative aspects. The glucoside forms of phenolic compounds were not detected in the pectin extracts, most probably as a result of the acid treatment (Tsao, 2010) Flavan-3-ols and flavanones were only detected at pH>1 and in minor amounts as compared to the starting material. Although it is generally accepted that flavan-3-ols are stable in acidic pH environments (Guyot et al., 1995), extremely low pH conditions might enhance losses of these phenolic compounds or facilitate the conversion of the trans-configured form into the cis-isomers. (Li, Taylor, Ferruzzi, & Mauer, 2012) suggested that the cis-configured catechins such as epigallocatechin gallate, epicatechin gallate and epicatechin could be easily transformed to the trans-configured catechins such as gallocatechin gallate and catechin gallate as isomerization products produced under high temperatures.

On the other hand, an increase in the presence of protocatechic acid, vanillin, quercetin and myricetin is observed. In all cases, the increase might be the result of the enrichment in a polyphenol rich pectin, especially at less severe extraction conditions. The partial degradation of gallic acid (3,4,5-trihydroxybenzoic acid) into protocatechic acid (3,4-dihydroxybenzoic acid) or trans-esterification to yield vanillin are also plausible. However, knowledge of the mechanism involved in degradation of hydroxybenzoic acids is rather limited, particularly with regard to fruits and vegetables. The results demonstrate the high

relative resistance of polyphenols to pectin acid extraction and shows that the susceptibility of plant phenolic compounds to extraction conditions depends on the phenol structure.

4.2.5 Antioxidant capacity (TEAC, β- Carotene/linoleic acid bleaching)

To confirm the antioxidant properties of the functional persimmon pectins and investigate how it is affected by the extraction parameters, the $ABTS^{+\cdot}$ radical scavenging and the β-carotene/linoleic acid bleaching assay were carried out on all pectin extracts. TEAC and AA% values could also be modelled with a good adjustment (R^2 89.3 and 86.0 respectively; Table 3, Eq. 13 and 14). TEAC values varied between 0.29 – 2.77 µmol trolox/mg between samples and was significantly affected by the two factors ($p<0.05$). Although previous reports attribute some antioxidant capacity to pectins, related to the GalA content (Hu et al., 2016; Sun et al., 2020), it is the TPC content which significantly affects the antioxidant activity (Jiang et al., 2020). The antioxidant capacity based on TEAC values was highly correlated with TPC values (Figure 1c and 1d), and very low pH ($p=0.001$) and high temperatures ($p=0.001$) adversely affected the antioxidant activity.

AA% values for the natural pectin extracts based on the β-carotene/linoleic acid bleaching assay showed very good results compared to the artificial BHT positive control (79.21%), with values ranging between 4.42 and 45.86%. Interestingly, unlike for TPC and TEAC, extraction temperature also had a very significant impact ($p<0.05$) on AA%. Higher AA% capacity was achieved when severe acid or temperature conditions were not combined (e.g. pH 1.5 and 95 °C or pH 0.5 and 70 °C; Figure 1e). Commercial pectins (AP, CP) showed no detectable antioxidant activity, which is probably ascribed to the lower quantities of polyphenols in the raw cultivars (Wikiera et al., 2021) and purification steps used at industrial scale contributing to eliminate proteins and polyphenols (Venkatanagaraju et al., 2020). Differences between results from both ABTS and β-carotene/linoleic acid bleaching methods are expected due to their very different approach of measuring antioxidant activity. Different compounds or conjugated polyphenols could, for example, not readily interact with ABTS and nevertheless prevent beta-carotene bleaching. In fact, some authors suggested that the antioxidant activity of pectin-polyphenolic complexes was significantly higher than that reported for free-polyphenols, based on a “protective effect” (Mercado-

Mercado et al., 2020) , which could be related to with the quantities reached of conjugated and esterified polyphenols of some of the functional pectins. The reduced solubility and different supramolecular conformation of pectin in the more hydrophobic β-carotene/linoleic acid bleaching method might also play a role in the differences found. The results point out the great potential to be used as bioactive ingredients due their relatively high TPC and antioxidant capacity. Although enriched-pectin extracts could have a high concentration of non-extractable polyphenols which probably affect some physicochemical properties of the neat pectin extracts, the benefit associated to the non-extractable polyphenols in health-promoting properties (Yaqub et al., 2016), like gastrointestinal health and cardiovascular risk reduction, substantially expands the scope of potential applications.

4.2.6 Fourier transformed infrared analysis.

Differences in the composition and molecular organization of the pectin enriched extracts derived from the different treatment aggressive could also be qualitatively examined by FTIR. Figure 2 displays the spectra of two different enriched pectin extracts obtained at two different pH. The spectra of commercial AP and CP samples were also included for comparative purposes. The vibrational band located at 1722 cm^{-1} is usually assigned to esterified carbonyl groups C=O and the peak centred at 1612 cm^{-1} is related to free carboxylic groups COO^- (Edison & Sethuraman, 2013; Pasandide et al., 2018), the ratio of which is usually used for DE measurement. The band at 1722 cm^{-1} was more intense in enriched pectin extracts from persimmon than in AP and CP samples, indicating a higher esterification degree. Furthermore, the vibrational band around 1438 cm^{-1} suggests the presence of aliphatic or aromatic (C-H) plane deformation vibrations of methyl, methylene and methoxy groups (Edison & Sethuraman, 2013; Grassino et al., 2016). The band observed at 1011 cm^{-1} is ascribed to glycosidic linkages (C-O) and is typical for backbone vibrations of pectin samples (Košťálova et al., 2013). In addition, the band at 1077 cm^{-1} could be attributed of neutral arabinose-based glycans, possibly from RG (Košťálova et al., 2013).

It is worth noting that when the extraction severity was higher, the intensity of the peak corresponding to glycosidic linkages (1011 cm^{-1}) increased, confirming higher pectin

content at the expense of decreased phenolics. Although, the peak at 1722 cm^{-1} (esterified carboxyl group) was more prominent for the sample obtained at pH 1 and 95 °C, further lowering the pH to 0.5 produced the decrease of this specific band, along with a decrease in the intensity of the bands located at 1438 and 3362 cm^{-1} and associated to the presence of aromatic compounds and -OH groups, respectively (Bulut & Özacar, 2009; Edison & Sethuraman, 2013), which would confirm the partial degradation of pectin and polyphenols under the harshest acidic conditions.

5 Conclusions

The potential use of discarded persimmon fruit as a source for a functional pectin-polyphenol based ingredient was studied. Immature non-treated rejected fruits were selected due to their higher pectin and polyphenol content. A full factorial design could accurately model how extraction temperature and pH affected process efficiency, as well as the composition and functional properties of pectin. Persimmon pectin was comparable in terms of composition, purity and esterification degree but was found to be more acid resistant compared to reference pectin or other alternative pectin sources. The presence of strong pectin-polyphenol interactions also enabled a high acid resistance of the very abundant polyphenolic fraction, with gallic acid as the main constituent. Only extreme acid conditions (pH 0.5) were able to degrade both the pectin structure and polyphenolic profile, and only the combination of both low pH and temperature produced a decrease in antioxidant activity. Averagely severe conditions (pH 1) produced the highest pectin and polyphenol yields, with abundant non-covalent interaction, while less severe conditions (pH 1.5) produced a pectin with intact pectin-polyphenol ester and O-glycosyl bonds (indirectly inferred by the released polyphenols after alkali or acid treatment). The very high TPC and antioxidant activity together with their acid resistance points out the great potential of persimmon waste as a potential source of functional food pectin based ingredients enhancing the quality and shelf-life of foods. The potential enhanced bioavailability of the pectin-polyphenol complexes and their health benefits is the subject of future investigations.

6 Acknowledgements

This work was funded by grant RTI-2018-094268-B-C21 and RTI2018-094268-B-C22 (MCIU, AEI; FEDER, UE). Mendez D. A. is supported by the Ministry of Science Technology and Innovation of the Colombian Government (783-2017). A. Martinez-Abad is recipient of JdC (IJDC-2017-31255) contract from the Spanish Ministry of Economy, Industry and Competitiveness.

7 References

Adetunji, L. R., Adekunle, A., Orsat, V., & Raghavan, V. (2017). Advances in the pectin production process using novel extraction techniques: A review. *Food Hydrocolloids*, *62*, 239–250. https://doi.org/10.1016/j.foodhyd.2016.08.015

Aina, V. O., Barau, M. M., Mamman, O. A., Zakari, A., Haruna, H., Hauwa Umar, M. S., & Abba, Y. B. (2012). Extraction and Characterization of Pectin from Peels of Lemon (Citrus limon), Grape Fruit (Citrus paradisi) and Sweet Orange (Citrus sinensis). *British Journal of Pharmacology and Toxicology*, *3*(6), 259–262.

Alba, K., Bingham, R. J., Gunning, P. A., Wilde, P. J., & Kontogiorgos, V. (2018). Pectin Conformation in Solution [Research-article]. *Journal of Physical Chemistry B*, *122*(29), 7286–7294. https://doi.org/10.1021/acs.jpcb.8b04790

AOAC. (1996). *Official Methods of Analysis* (16th ed.). Maryland: AOAC International.

Berbel, J., & Posadillo, A. (2018). Review and Analysis of Alternatives for the Valorisation of Agro-Industrial Olive Oil By-Products. *Sustainability*, *10*(1), 237. https://doi.org/10.3390/su10010237

Bermúdez-Oria, A., Rodríguez-Gutiérrez, G., Fernández-Prior, Á., Vioque, B., & Fernández-Bolaños, J. (2019). Strawberry dietary fiber functionalized with phenolic antioxidants from olives. Interactions between polysaccharides and phenolic

compounds. *Food Chemistry*, *280*, 310–320. https://doi.org/10.1016/j.foodchem.2018.12.057

Bulut, E., & Özacar, M. (2009). Rapid, facile synthesis of silver nanostructure using hydrolyzable tannin. *Industrial and Engineering Chemistry Research*, *48*(12), 5686–5690. https://doi.org/10.1021/ie801779f

Butt, M. S., Sultan, M. T., Aziz, M., Naz, A., Ahmed, W., Kumar, N., & Imran, M. (2015). Persimmon (diospyros kaki) fruit: Hidden phytochemicals and health claims. *EXCLI Journal*, *14*, 542–561. https://doi.org/10.17179/excli2015-159

Campbell, M. (2006). *Extraction of Pectin From Watermelon Rind*. Oklahoma State University.

Carocho, M., Morales, P., & Ferreira, I. C. F. R. (2018). Antioxidants: Reviewing the chemistry, food applications, legislation and role as preservatives. *Trends in Food Science & Technology*, *71*, 107–120. https://doi.org/10.1016/j.tifs.2017.11.008

Chen, J., Du, J., Ge, Z., Zhu, W., Nie, R., & Li, C. (2016). Comparison of sensory and compositions of five selected persimmon cultivars (Diospyros kaki L.) and correlations between chemical components and processing characteristics. *Journal of Food Science and Technology*, *53*(3), 1597–1607. https://doi.org/10.1007/s13197-015-2102-y

Chen, X. N., Fan, J. F., Yue, X., Wu, X. R., & Li, L. T. (2008). Radical scavenging activity and phenolic compounds in persimmon (Diospyros kaki L. cv. Mopan). *Journal of Food Science*, *73*(1), C24–C28. https://doi.org/10.1111/j.1750-3841.2007.00587.x

Denman, L. J., & Morris, G. A. (2015). An experimental design approach to the chemical characterisation of pectin polysaccharides extracted from Cucumis melo Inodorus. *Carbohydrate Polymers*, *117*, 364–369. https://doi.org/10.1016/j.carbpol.2014.09.081

Dranca, F., & Oroian, M. (2018). Extraction, purification and characterization of pectin from alternative sources with potential technological applications. *Food Research International*, *113*(February), 327–350. https://doi.org/10.1016/j.foodres.2018.06.065

Dvořáková, M., Guido, L. F., Dostálek, P., Skulilová, Z., Moreira, M. M., & Barros, A. A. (2008). Antioxidant Properties of Free, Soluble Ester and Insoluble-Bound Phenolic Compounds in Different Barley Varieties and Corresponding Malts. In *J. Inst. Brew* (Vol. 114, Issue 1).

Edison, T. J. I., & Sethuraman, M. G. (2013). Biogenic robust synthesis of silver nanoparticles using Punica granatum peel and its application as a green catalyst for the reduction of an anthropogenic pollutant 4-nitrophenol. *Spectrochimica Acta - Part A: Molecular and Biomolecular Spectroscopy*, *104*, 262–264. https://doi.org/10.1016/j.saa.2012.11.084

FAO. (2016). *Food wastage: Key facts and figures*. http://www.fao.org/news/story/pt/item/196402/icode/

FAOSTAT. (2021). *CROPS*. http://www.fao.org/faostat/en/#data/QC/visualize

Fontes-Candia, C., Erboz, E., Martínez-Abad, A., López-Rubio, A., & Martínez-Sanz, M. (2019). Superabsorbent food packaging bioactive cellulose-based aerogels from Arundo donax waste biomass. *Food Hydrocolloids*, *96*, 151–160. https://doi.org/10.1016/j.foodhyd.2019.05.011

Fu, L., Lu, W. Q., & Zhou, X. M. (2016). Phenolic Compounds and In Vitro Antibacterial and Antioxidant Activities of Three Tropic Fruits: Persimmon, Guava, and Sweetsop. *BioMed Research International*, *2016*. https://doi.org/10.1155/2016/4287461

Fujihara, S., Kasuga, A., & Aoyagi, Y. (2001). Nitrogen-to-Protein Conversion Factors for Common Vegetables in Japan. *Journal of Food Science*, *66*(3), 412–415. https://doi.org/10.1111/j.1365-2621.2001.tb16119.x

Grassino, A. N., Halambek, J., Djaković, S., Rimac Brnčić, S., Dent, M., & Grabarić, Z. (2016). Utilization of tomato peel waste from canning factory as a potential source for pectin production and application as tin corrosion inhibitor. *Food Hydrocolloids*, *52*, 265–274. https://doi.org/10.1016/j.foodhyd.2015.06.020

Guyot, S., Cheynier, V., Souquet, J.-M., & Moutounet, M. (1995). Influence of pH on the Enzymatic Oxidation of (+)-Catechin in Model Systems. *Journal of Agricultural and Food Chemistry*, *43*(9), 2458–2462. https://doi.org/10.1021/jf00057a027

Hamauzu, Y. (2018). Non-extractable Polyphenols in Fruit: Distribution, Changes, and Potential Health Effects. In *Food Chemistry, Function and Analysis* (Vols. 2018-Janua, Issue 5, pp. 284–306). Royal Society of Chemistry. https://doi.org/10.1039/9781788013208-00284

Hamauzu, Y., & Suwannachot, J. (2019). Non-extractable polyphenols and in vitro bile acid-binding capacity of dried persimmon (Diospyros kaki)fruit. *Food Chemistry*, *293*, 127–133. https://doi.org/10.1016/j.foodchem.2019.04.092

Han, Y., Zhu, Q., Zhang, Z., Meng, K., Hou, Y., Ban, Q., Suo, J., & Rao, J. (2015). *Analysis of Xyloglucan Endotransglycosylase/ Hydrolase (XTH) Genes and Diverse Roles of Isoenzymes during Persimmon Fruit Development and Postharvest Softening*. https://doi.org/10.1371/journal.pone.0123668

Hosseini, S., Parastouei, K., & Khodaiyan, F. (2020). Simultaneous extraction optimization and characterization of pectin and phenolics from sour cherry pomace. *International Journal of Biological Macromolecules*, *158*, 911–921. https://doi.org/10.1016/j.ijbiomac.2020.04.241

Houben, K., Jolie, R. P., Fraeye, I., Van Loey, A. M., & Hendrickx, M. E. (2011). Comparative study of the cell wall composition of broccoli, carrot, and tomato: Structural characterization of the extractable pectins and hemicelluloses. *Carbohydrate Research*, *346*(9), 1105–1111. https://doi.org/10.1016/j.carres.2011.04.014

Hu, S., Yin, J., Nie, S., Wang, J., Phillips, G. O., Xie, M., & Cui, S. W. (2016). In vitro evaluation of the antioxidant activities of carbohydrates. *Bioactive Carbohydrates and Dietary Fibre*, *7*(2), 19–27. https://doi.org/10.1016/j.bcdf.2016.04.001

Jafari, F., Khodaiyan, F., Kiani, H., & Hosseini, S. S. (2017). Pectin from carrot pomace: Optimization of extraction and physicochemical properties. *Carbohydrate Polymers*, *157*, 1315–1322. https://doi.org/10.1016/j.carbpol.2016.11.013

Jiang, Y., Xu, Y., Li, F., Li, D., & Huang, Q. (2020). Pectin extracted from persimmon peel: A physicochemical characterization and emulsifying properties evaluation. *Food Hydrocolloids*, *101*(September 2019), 105561. https://doi.org/10.1016/j.foodhyd.2019.105561

Košťálova, Z., Hromádková, Z., Ebringerová, A., Polovka, M., Michaelsen, T. E., & Paulsen, B. S. (2013). Polysaccharides from the Styrian oil-pumpkin with antioxidant and complement-fixing activity. *Industrial Crops and Products*, *41*(1), 127–133. https://doi.org/10.1016/j.indcrop.2012.04.029

Krygier, K., Sosulski, F., & Hogge, L. (1982). Free, Esterified, and Insoluble-Bound Phenolic Acids. 1. Extraction and Purification Procedure. *Journal of Agricultural and Food Chemistry*, *30*(2), 330–334. https://doi.org/10.1021/jf00110a028

Kulkarni, S. G., & Vijayanand, P. (2010). Effect of extraction conditions on the quality characteristics of pectin from passion fruit peel (Passiflora edulis f. flavicarpa L.). *LWT - Food Science and Technology*, *43*(7), 1026–1031. https://doi.org/10.1016/j.lwt.2009.11.006

Lara-Espinoza, C., Carvajal-Millán, E., Balandrán-Quintana, R., López-Franco, Y., & Rascón-Chu, A. (2018). Pectin and pectin-based composite materials: Beyond food texture. In *Molecules* (Vol. 23, Issue 4, p. 942). MDPI AG. https://doi.org/10.3390/molecules23040942

Li, N., Taylor, L. S., Ferruzzi, M. G., & Mauer, L. J. (2012). Kinetic study of catechin stability: Effects of ph, concentration, and temperature. *Journal of Agricultural and Food Chemistry*, *60*(51), 12531–12539. https://doi.org/10.1021/jf304116s

Lucas-González, R., Viuda-Martos, M., Pérez-Álvarez, J. Á., & Fernández-López, J. (2017). Evaluation of Particle Size Influence on Proximate Composition, Physicochemical, Techno-Functional and Physio-Functional Properties of Flours Obtained from Persimmon (Diospyros kaki Trumb.) Coproducts. *Plant Foods for Human Nutrition*, *72*(1), 67–73. https://doi.org/10.1007/s11130-016-0592-z

Mamet, T., Ge, Z. zhen, Zhang, Y., & Li, C. mei. (2018). Interactions between highly galloylated persimmon tannins and pectins. *International Journal of Biological Macromolecules*, *106*(2018), 410–417. https://doi.org/10.1016/j.ijbiomac.2017.08.039

Martínez-Abad, A., Giummarella, N., Lawoko, M., & Vilaplana, F. (2018). Differences in extractability under subcritical water reveal interconnected hemicellulose and lignin recalcitrance in birch hardwoods. *Green Chemistry*, *20*(11), 2534–2546. https://doi.org/10.1039/c8gc00385h

Martínez-Las Heras, R., Amigo-Sánchez, J. C., Heredia, A., Castelló, M. L., & Andrés, A. (2016). Influence of preharvest treatments to reduce the seasonality of persimmon production on color, texture and antioxidant properties during storage. *CYTA - Journal of Food*, *14*(2), 333–339. https://doi.org/10.1080/19476337.2015.1113204

Mattila, P., & Kumpulainen, J. (2002). Determination of free and total phenolic acids in plant-derived foods by HPLC with diode-array detection. *Journal of Agricultural and Food Chemistry*, *50*(13), 3660–3667. https://doi.org/10.1021/jf020028p

Méndez, D. A., Fabra, M. J., Gómez-Mascaraque, L., López-Rubio, A., & Martinez-Abad, A. (2021). Modelling the Extraction of Pectin towards the Valorisation of Watermelon Rind Waste. *Foods*, *10*(4), 738. https://doi.org/10.3390/foods10040738

Mercado-Mercado, G., de la Rosa, L. A., & Alvarez-Parrilla, E. (2020). Effect of pectin on the interactions among phenolic compounds determined by antioxidant capacity. *Journal of Molecular Structure*, *1199*, 126967. https://doi.org/10.1016/j.molstruc.2019.126967

Morris, G. A., Ralet, M. C., Bonnin, E., Thibault, J. F., & Harding, S. E. (2010). Physical characterisation of the rhamnogalacturonan and homogalacturonan fractions of sugar beet (Beta vulgaris) pectin. *Carbohydrate Polymers*, *82*(4), 1161–1167. https://doi.org/10.1016/j.carbpol.2010.06.049

Müller-Maatsch, J., Bencivenni, M., Caligiani, A., Tedeschi, T., Bruggeman, G., Bosch, M., Petrusan, J., van Droogenbroeck, B., Elst, K., & Sforza, S. (2016). Pectin content and composition from different food waste streams. *Food Chemistry*, *201*, 37–45. https://doi.org/10.1016/j.foodchem.2016.01.012

Munera, S., Aleixos, N., Besada, C., Gómez-Sanchis, J., Salvador, A., Cubero, S., Talens, P., & Blasco, J. (2019). Discrimination of astringent and deastringed hard 'Rojo Brillante' persimmon fruit using a sensory threshold by means of hyperspectral imaging. *Journal of Food Engineering*, *263*, 173–180. https://doi.org/10.1016/j.jfoodeng.2019.06.008

Nguyễn, H. V., & Savage, G. P. (2013). The effects of temperature and pH on the extraction of oxalate and pectin from green kiwifruit (Actinidia deliciosa L.), golden kiwifruit (Actinidia chinensis L.), kiwiberry (Actinidia arguta) and persimmon (Diospyros kaki). *International Journal of Food Science & Technology*, *48*(4), 794–800. https://doi.org/10.1111/ijfs.12029

Novillo, P., Salvador, A., Crisosto, C., & Besada, C. (2016). Influence of persimmon astringency type on physico-chemical changes from the green stage to commercial harvest. *Scientia Horticulturae*, *206*, 7–14. https://doi.org/10.1016/j.scienta.2016.04.030

Ognyanov, M., & Kussovski, V. (2013). Isolation , characterization and modification of citrus pectins Isolation. *J. BioSci. Biotech*, *1*(October), 223–233.

Pasandide, B., Khodaiyan, F., Mousavi, Z., & Hosseini, S. S. (2018). Pectin extraction from citron peel: optimization by Box–Behnken response surface design. *Food Science and Biotechnology*, *27*(4), 997–1005. https://doi.org/10.1007/s10068-018-0365-6

Pellegrini, M., Lucas-Gonzalez, R., Fernández-López, J., Ricci, A., Pérez-Álvarez, J. A., Sterzo, C. Lo, & Viuda-Martos, M. (2017). Bioaccessibility of polyphenolic compounds of six quinoa seeds during in vitro gastrointestinal digestion. *Journal of Functional Foods*, *38*, 77–88. https://doi.org/10.1016/j.jff.2017.08.042

Pérez-Burillo, S., Oliveras, M. J., Quesada, J., Rufián-Henares, J. A., & Pastoriza, S. (2018). Relationship between composition and bioactivity of persimmon and kiwifruit. In *Food Research International* (Vol. 105, pp. 461–472). Elsevier Ltd. https://doi.org/10.1016/j.foodres.2017.11.022

Petkowicz, C. L. O., Vriesmann, L. C., & Williams, P. A. (2017). Pectins from food waste: Extraction, characterization and properties of watermelon rind pectin. *Food Hydrocolloids*, *65*, 57–67. https://doi.org/10.1016/j.foodhyd.2016.10.040

Pettolino, F. A., Walsh, C., Fincher, G. B., & Bacic, A. (2012). Determining the polysaccharide composition of plant cell walls. *Nature Protocols*, *7*(9), 1590–1607. https://doi.org/10.1038/nprot.2012.081

Posé, S., Paniagua, C., Matas, A. J., Gunning, A. P., Morris, V. J., Quesada, M. A., & Mercado, J. A. (2019). A nanostructural view of the cell wall disassembly process during fruit ripening and postharvest storage by atomic force microscopy. *Trends in Food Science & Technology*, *87*(August 2017), 47–58. https://doi.org/10.1016/j.tifs.2018.02.011

Prakash Maran, J., Sivakumar, V., Thirugnanasambandham, K., & Sridhar, R. (2014). Microwave assisted extraction of pectin from waste Citrullus lanatus fruit rinds.

Carbohydrate Polymers, *101*(1), 786–791. https://doi.org/10.1016/j.carbpol.2013.09.062

Prasanna, V., Prabha, T. N., & Tharanathan, R. N. (2007). Fruit ripening phenomena-an overview. *Critical Reviews in Food Science and Nutrition*, *47*(1), 1–19. https://doi.org/10.1080/10408390600976841

Prior, R. L., Wu, X., & Schaich, K. (2005). Standardized methods for the determination of antioxidant capacity and phenolics in foods and dietary supplements. *Journal of Agricultural and Food Chemistry*, *53*(10), 4290–4302. https://doi.org/10.1021/jf0502698

Raji, Z., Khodaiyan, F., Rezaei, K., Kiani, H., & Hosseini, S. S. (2017). Extraction optimization and physicochemical properties of pectin from melon peel. *International Journal of Biological Macromolecules*, *98*, 709–716. https://doi.org/10.1016/j.ijbiomac.2017.01.146

Re, R., Pellegrini, N., Proteggente, a., Pannala, a., Yang, M., & Rice-Evans, C. (1999). Antioxidant Activity Applying an Improved Abts Radical Cation Decolorization Assay. *Free Radical Biology and Medicine*, *26*(9), 1231–1237. https://doi.org/10.1016/S0891-5849(98)00315-3

Rodsamran, P., & Sothornvit, R. (2019a). Microwave heating extraction of pectin from lime peel: Characterization and properties compared with the conventional heating method. *Food Chemistry*, *278*(November 2018), 364–372. https://doi.org/10.1016/j.foodchem.2018.11.067

Rodsamran, P., & Sothornvit, R. (2019b). Preparation and characterization of pectin fraction from pineapple peel as a natural plasticizer and material for biopolymer film. *Food and Bioproducts Processing*, *118*, 198–206. https://doi.org/10.1016/j.fbp.2019.09.010

Russell, W. R., Labat, A., Scobbie, L., Duncan, G. J., & Duthie, G. G. (2009). Phenolic acid content of fruits commonly consumed and locally produced in Scotland. *Food Chemistry*, *115*(1), 100–104. https://doi.org/10.1016/j.foodchem.2008.11.086

Sanchez-Aldana, D., Noe Aguilar, C., Nevarez-Moorillon, G. V., & Contreras Esquivel, J. C. (2013). Comparative extraction of pectic and polyphenols from Mexican lime pomace and bagasse. *American Journal of Agricultural and Biological Science*, *8*(4), 309–322. https://doi.org/10.3844/ajabssp.2013.309.322

Saura-Calixto, F., & Pérez-Jiménez, J. (2018). *Non-extractable Polyphenols and Carotenoids* (F. Saura-Calixto & J. Pérez-Jiménez, Eds.). Royal Society of Chemistry. https://doi.org/10.1039/9781788013208

Senica, M., Veberic, R., Grabnar, J. J., Stampar, F., & Jakopic, J. (2016). Selected chemical compounds in firm and mellow persimmon fruit before and after the drying process. *Journal of the Science of Food and Agriculture*, *96*(9), 3140–3147. https://doi.org/10.1002/jsfa.7492

Singleton, V. L., Orthofer, R., & Lamuela-Raventós, R. M. (1999). Analysis of total phenols and other oxidation substrates and antioxidants by means of folin-ciocalteu reagent. *Methods in Enzymology*, *299*, 152–178. https://doi.org/10.1016/S0076-6879(99)99017-1

Somashekar, D., Venkateshwaran, G., Srividya, C., Krishnanand, Sambaiah, K., & Lokesh, B. R. (2001). Efficacy of extraction methods for lipid and fatty acid composition from fungal cultures. *World Journal of Microbiology and Biotechnology*, *17*(3), 317–320. https://doi.org/10.1023/A:1016792311744

Sun, D., Chen, X., & Zhu, C. (2020). Physicochemical properties and antioxidant activity of pectin from hawthorn wine pomace: A comparison of different extraction methods. *International Journal of Biological Macromolecules*, *158*, 1239–1247. https://doi.org/10.1016/j.ijbiomac.2020.05.052

Taira, S., Ono, M., & Matsumoto, N. (1997). Reduction of persimmon astringency by complex formation between pectin and tannins. *Postharvest Biology and Technology*, *12*(3), 265–271. https://doi.org/10.1016/S0925-5214(97)00064-1

Tsao, R. (2010). Chemistry and biochemistry of dietary polyphenols. *Nutrients*, *2*(12), 1231–1246. https://doi.org/10.3390/nu2121231

Tsuchida, Y., Sakurai, N., Morinaga, K., Koshita, Y., & Asakura, T. (2004). Effects of water loss of "Fuyu" persimmon fruit on molecular weights of mesocarp cell wall polysaccharides and fruit softening. *Journal of the Japanese Society for Horticultural Science*, *73*(5), 460–468. https://doi.org/10.2503/jjshs.73.460

Venkatanagaraju, E., Bharathi, N., Hema Sindhuja, R., Roy Chowdhury, R., & Sreelekha, Y. (2020). Extraction and Purification of Pectin from Agro-Industrial Wastes. In *Pectins - Extraction, Purification, Characterization and Applications*. IntechOpen. https://doi.org/10.5772/intechopen.85585

Virk, B. S., & Sogi, D. S. (2004). Extraction and characterization of pectin from apple (Malus Pumila. Cv Amri) peel waste. *International Journal of Food Properties*, *7*(3), 693–703. https://doi.org/10.1081/JFP-200033095

Wai, W. W., Alkarkhi, A. F. M., & Easa, A. M. (2010). Effect of extraction conditions on yield and degree of esterification of durian rind pectin: An experimental design. *Food and Bioproducts Processing*, *88*(2–3), 209–214. https://doi.org/10.1016/J.FBP.2010.01.010

Wikiera, A., Grabacka, M., Byczyński, Ł., Stodolak, B., & Mika, M. (2021). Enzymatically Extracted Apple Pectin Possesses Antioxidant and Antitumor Activity. *Molecules (Basel, Switzerland)*, *26*(5). https://doi.org/10.3390/molecules26051434

Yang, J. S., Mu, T. H., & Ma, M. M. (2018). Extraction, structure, and emulsifying properties of pectin from potato pulp. *Food Chemistry*, *244*(October 2017), 197–205. https://doi.org/10.1016/j.foodchem.2017.10.059

Yaqub, S., Farooq, U., Shafi, A., Akram, K., Murtaza, M. A., Kausar, T., & Siddique, F. (2016). Chemistry and Functionality of Bioactive Compounds Present in Persimmon. *Journal of Chemistry*, *2016*, 1–13. https://doi.org/10.1155/2016/3424025

Yuste, S., Macià, A., Ludwig, I. A., Romero, M.-P., Fernández-Castillejo, S., Catalán, Ú., Motilva, M.-J., & Rubió, L. (2018). Validation of Dried Blood Spot Cards to Determine Apple Phenolic Metabolites in Human Blood and Plasma After an Acute Intake of Red-Fleshed Apple Snack. *Molecular Nutrition and Food Research*, *62*(23). https://doi.org/10.1002/mnfr.201800623

Zhang, C., & Mu, T. (2011). Optimisation of pectin extraction from sweet potato (Ipomoea batatas, Convolvulaceae) residues with disodium phosphate solution by response surface method. *International Journal of Food Science & Technology*, *46*(11), 2274–2280. https://doi.org/10.1111/j.1365-2621.2011.02746.x

8 Supplementary material

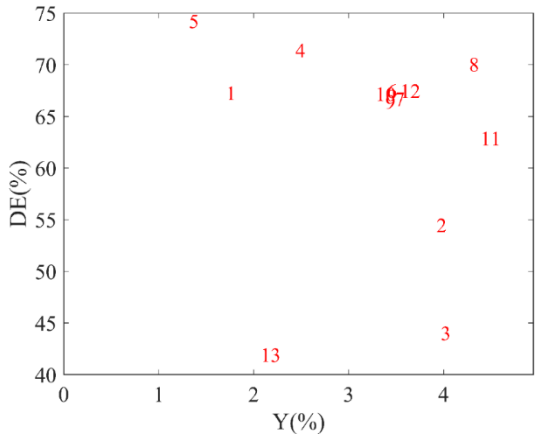

Figure S1. The inter-relationship between of yield and degree of esterification (DE) for pectins extracted from Persimmon. Numbers represent the treatment described in Table 1.

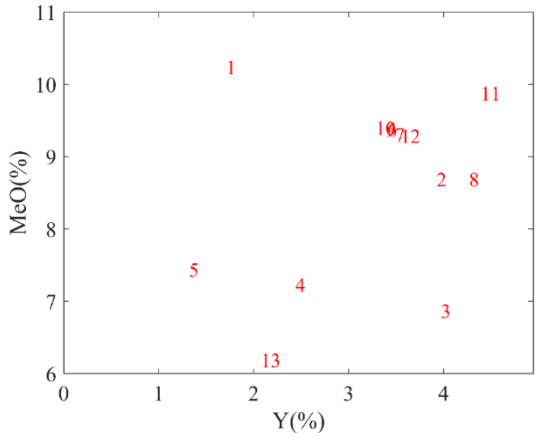

Figure S2. The inter-relationship between of yield and methoxyl content (MeO%) for pectins extracted from Persimmon. Numbers represent the treatment described in Table 1.

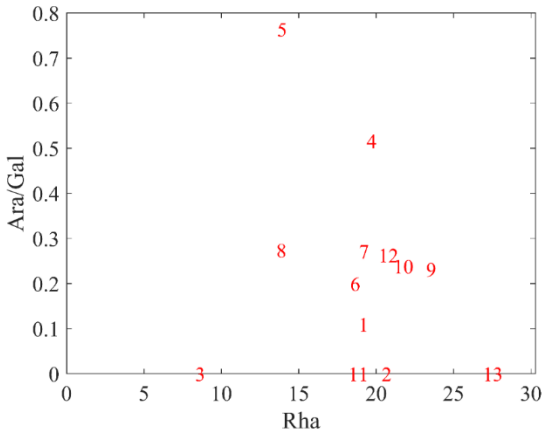

Figure S3. The inter-relationship between Rha and Ara/Gal rate for pectins extracted from Persimmon. Numbers represent the treatment described in Table 1.

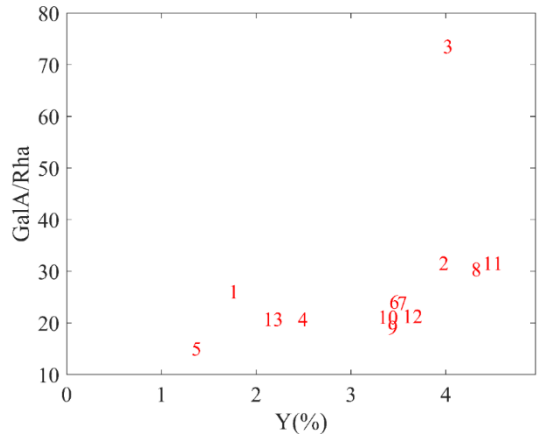

Figure S4. The inter-relationship between yield and GalA/Rha for pectin extracted from Persimmon. Numbers represent the treatment described in Table 1.

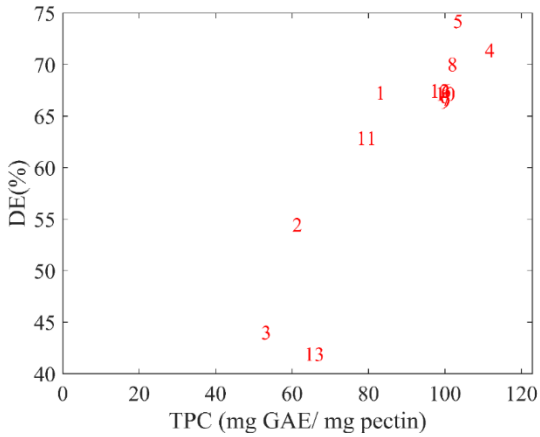

Figure S5. The inter-relationship between of degree of esterification (DE) and TPC (mg GAE/mg) for pectins extracted from Persimmon. Numbers represent the treatment described in Table 1.

Figure S6. Visual appearance of dry pectin enriched extracts from persimmon.

Table S1. Concentration (mg/kg sample) of individual phenolic compounds in lyophilized persimmon fruit (CI) and persimmon fruit extracts at less severe (L, run 5), averagely severe (M, run 11), extreme acidic conditions (H, run 2).

	Free Phenolics				Alkali fraction				Acid fraction			
Phenolic compounds	CI	M (11)	H (2)	L (5)	CI	M (11)	H (2)	L (5)	CI	M (11)	H (2)	L (5)
Benzoic acids												
p-hydroxybenzoic acid	2.86(0.8)	n.d.	n.d.	n.d.	6.26(0.9)	13.3(4.1)	11.3(3.7)	15.9(1.1)	1.16(0.1)	n.d.	n.d.	2.22(0.1)
Hydroxybenzoic acid	n.d.	n.d.	n.d.	n.d.	0.45(0.4)	6.06(4.9)	6.05(0.1)	2.94(0.7)	2.23(0.1)	n.d.	n.d.	0.54(0.7)
Vanillin	22.9(1.6)	123(29.7)	157(3.67)	126(8)	14.6(17.9)	31.4(5.6)	35.8(0.3)	19.5(5.2)	21.8(1.6)	30.6(0.9)	18.3(1.2)	16.0(0.1)
Gallic acid	161(25.2)	1560(190)	781(128)	1618(158)	9646(25.2)	258(205)	27.0(2.3)	3874(1955)	762(57.4)	484(16.0)	41.3(30.3)	1072(143)
Gallic acid glucoside	298(34.3)	n.d.	n.d.	n.d.	1.57(0.04)	n.d.	n.d.	n.d.	n.d.	n.d.	n.d.	n.d.
Protocatechuic acid	n.d.	192(49.7)	75.8(8.8)	69.4(24.7)	211(39.1)	22.8(9.6)	21.9(9.2)	561(268)	44.5(7.3)	184(7.0)	68.0(15.3)	126(26.5)
Protocatechuic acid glucoside	4.80(1.3)	n.d.	n.d.	n.d.	n.d.	n.d.	n.d.	n.d.	n.d.	n.d.	n.d.	n.d.
Hydroxytyrosol	0.46(0.0)	n.d.	n.d.	n.d.	n.d.	n.d.	n.d.	n.d.	n.d.	n.d.	n.d.	n.d.
Hydroxytyrosol glucoside	1.01(0.07)	n.d.	n.d.	n.d.	n.d.	n.d.	n.d.	n.d.	n.d.	n.d.	n.d.	n.d.
Vanillic acid	n.d.	n.d.	n.d.	n.d.	11.0(0.2)	n.d.	n.d.	26.2(0.0)	15.7(1.6)	n.d.	n.d.	n.d.
Vanillic acid glucoside	278(43.4)	n.d.	n.d.	n.d.	19.0(0.5)	4.29(0.7)	2.83(1.4)	n.d.	4.53(2.4)	n.d.	n.d.	27.9(14.9)
Syringic acid	n.d.	n.d.	n.d.	n.d.	n.d.	n.d.	n.d.	2.94(0.9)	n.d.	n.d.	n.d.	n.d.
Hydroxycinnamic acids												
p-coumaric acid	0.79(0.06)	n.d.	n.d.	n.d.	49.0(5.2)	8.32(1.8)	4.70(0.3)	25.8(3.06)	2.37(0.4)	n.d.	n.d.	n.d.
Coumaric acid glucoside	1.45(0.00)	n.d.	n.d.	n.d.	n.d.	n.d.	n.d.	n.d.	n.d.	n.d.	n.d.	n.d.

Caffeic acid	n.d.	n.d.	n.d.	n.d.	4.38(0.1)	n.d.	n.d.	1.37(0.01)	0.31(0.1)	n.d.	n.d.	n.d.
Caffeic acid acetylglucuoside glucoside	0.38(0.1)	n.d.	n.d.	n.d.	n.d.	n.d.	n.d.	n.d.	n.d.	n.d.	n.d.	n.d.
Ferulic acid	n.d.	n.d.	n.d.	n.d.	12.4(1.2)	0.82(0.3)	n.d.	1.12(0.2)	6.73(0.6)	n.d.	n.d.	n.d.
Isoferulic acid	n.d.	n.d.	n.d.	n.d.	2.81(0.1)	0.65(0.2)	n.d.	0.43(0.01	1.00(0.02)	n.d.	n.d.	n.d.
Ferulic acid glucoside	n.d.	n.d.	n.d.	n.d.	0.14(0.0)	n.d.	n.d.	n.d.	n.d.	n.d.	n.d.	n.d.
Sinapic acid	n.d.	n.d.	n.d.	n.d.	n.d.	n.d.	n.d.	3.24(0.2)	n.d.	n.d.	n.d.	n.d.
Total Phenolic acids	772	1874	1013	1814	9978	346	110	4534	862	698	128	1245
Falvan-3-ols												
Epicatechin	n.d.	n.d.	n.d.	n.d.	1.26(0.2)	n.d.	n.d.	n.d.	n.d.	n.d.	n.d.	4.08(0.4)
Catechin glucoside	1.49(0.5)	n.d.	n.d.	n.d.	n.d.	n.d.	n.d.	n.d.	n.d.	n.d.	n.d.	n.d.
Epicatechin glucoside	2.56(0.3)	n.d.	n.d.	n.d.	n.d.	n.d.	n.d.	n.d.	n.d.	n.d.	n.d.	n.d.
Epigallocatechin	15.5(3.2)	n.d.	n.d.	n.d.	3.33(0.1)	n.d.	n.d.	4.75(0.2)	n.d.	n.d.	n.d.	n.d.
Epicatechin gallate	4.97(0.9)	n.d.	n.d.	n.d.	n.d.	n.d.	n.d.	n.d.	n.d.	n.d.	n.d.	n.d.
Gallocatechin gallate	n.d.	n.d.	n.d.	n.d.	1.79(0.3)	n.d.	n.d.	32.8(18.1)	n.d.	n.d.	n.d.	4.27(1.6)
Epigallocatechin gallate	1.87(0.8)	n.d.	n.d.	n.d.	n.d.	n.d.	n.d.	n.d.	n.d.	n.d.	n.d.	n.d.
Dimer	19.3(1.8)	n.d.	n.d.	n.d.	n.d.	n.d.	n.d.	n.d.	n.d.	n.d.	n.d.	2.68(1.5)
Trimer	0.79(0.2)	n.d.	n.d.	n.d.	n.d.	n.d.	n.d.	n.d.	n.d.	n.d.	n.d.	n.d.
Total Flavan-3-ols	103.5	n.d.	n.d.	n.d.	8.36	n.d.	n.d.	37.6	n.d.	n.d.	n.d.	11.0
Flavonol												
Quercetin	n.d.	3.88(1.8)	n.d.	n.d.	0.27(0.1)	n.d.	n.d.	14.6(8.2)	1.93(0.3)	n.d.	n.d.	1.39(0.5)
Quercetin glucoside	18.9(0.7)	n.d.	n.d.	n.d.	10.3(2.1)	n.d.	n.d.	n.d.	0.30(0.04)	n.d.	n.d.	n.d.
Other quercetin derivatives	27.9(8.6)	n.d.	n.d.	n.d.	n.d.	0.6(0.14)	1.2(0.1)	n.d.	n.d.	n.d.	n.d.	2.59(0.9)
Kaempferol glucoside	28.1(10.6)	n.d.	n.d.	n.d.	8.83(3.6)	n.d.	n.d.	n.d.	n.d.	n.d.	n.d.	n.d.

Other Kaempferol derivatives	4.64(0.6)	n.d.	n.d.	n.d.	n.d.	n.d.	n.d.	n.d.	n.d.	n.d.	n.d.	n.d.
Myricetin	n.d.	10.4(6.1)	n.d.	n.d.	n.d.	n.d.	n.d.	20.3(13.8)	1.70(0.3)	n.d.	n.d.	4.46(0.3)
Myricetin glucoside	12.8(0.8)	n.d.	n.d.	n.d.	2.68(0.4)	n.d.	n.d.	n.d.	n.d.	n.d.	n.d.	n.d.
Total Flavonol	92.4	14.3	n.d.	n.d.	23.7	0.61	1.26	34.9	3.93	n.d.	n.d.	8.44
Flavanone												
Naringenin	n.d.	n.d.	n.d.	n.d.	n.d.	n.d.	n.d.	0.15(0.2)	n.d.	n.d.	n.d.	n.d.
Naringenin glucoside	0.43(0.2)	n.d.	n.d.	n.d.	0.26(0.1)	n.d.	n.d.	n.d.	n.d.	n.d.	n.d.	n.d.
Eriodictyol	n.d.	n.d.	n.d.	n.d.	n.d.	n.d.	n.d.	n.d.	n.d.	n.d.	n.d.	n.d.
Eriodictyol glucoside	1.18(0.2)	n.d.	n.d.	n.d.	0.16(0.1)	n.d.	n.d.	n.d.	n.d.	n.d.	n.d.	n.d.
Total Flavanone	1.61	n.d	n.d.	n.d.	0.42	n.d.	n.d.	0.15	n.d.	n.d.	n.d.	n.d.
TOTAL PHENOLICS	970	1889	1013	1814	10011	346	111	4607	866	698	128	1264

n.d.: not detected. Values in brackets correspond to standard deviation

3.2.3

SUSTAINABLE BIOACTIVE PECTIN-BASED FILMS TO IMPROVE FRUIT SAFETY VIA A CIRCULAR ECONOMY APPROACH

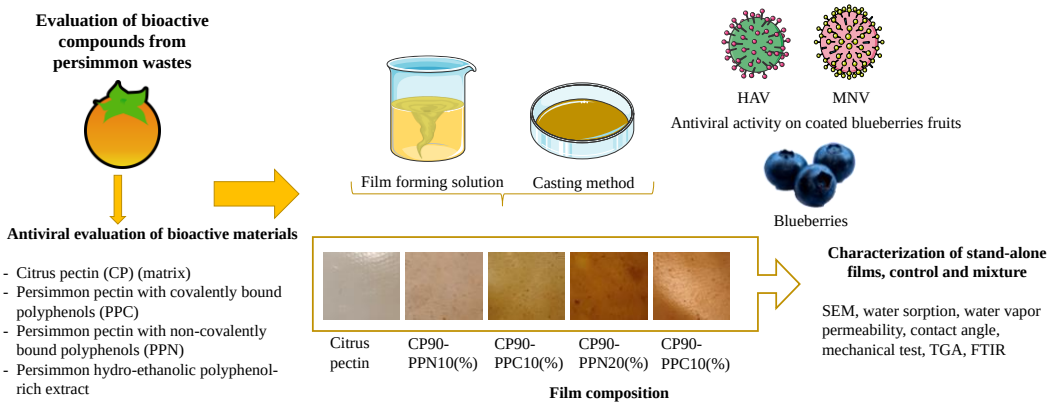

This section is an adapted version of the following submitted research article:

Méndez, D. A., Falcó, I., Martínez-Abad A., López-Rubio, A., Fabra, M. J. Sustainable bioactive pectin-based films to improve fruit safety via a circular economy approach. Food hydrocolloids. (submitted).

1 Abstract

This work reports on the valorisation of persimmon (*Diospyros kaki Thunb.*) for the development of food-grade antiviral coatings against major viral foodborne pathogens, human noroviruses (NoVs) and hepatitis A virus (HAV). Initially, the antiviral activity of polyphenol-rich pectin extracts with abundant non-covalent interactions (PPN), pectin extracts enriched with intact pectin-polyphenol ester and O-glycosyl bonds (PPC) and hydro-ethanolic polyphenol-rich extracts (EPE) was compared. Higher viral reductions were found for the pectin extracts rich in polyphenols, mainly in those containing covalent pectin-polyphenol interactions. This specific extract was mixed with commercial citrus pectin (CP) to develop active edible films. Dry films were analysed in terms of their optical, morphological, mechanical and barrier properties. Addition of the bioactive pectin persimmon extract resulted in more coloured films with lower transparency. The presence of covalently-linked polyphenols gave rise to stiffer films, with lower sorption capacity and more hydrophobic nature. The infectivity of MNV and HAV on fresh blueberries after the coating treatments was reduced by approximately 4.28 and 2.38 log, respectively, after overnight incubation, as compared to the controls, when 10% PCC was incorporated into the film. Higher amounts of PPC did not significantly improve the antiviral activity and a complete inactivation for both viruses was observed after 4 days of storage at 25 ºC. This paper highlights the potential of persimmon discards as a cheap source of food-grade antiviral coatings with improved physicochemical properties as compared to commercial citrus pectin.

2 Introduction

In the last decade, there has been an increased interest in the preservation of both the environment and the health of consumers. Thus, a great deal of emphasis has been placed on the use of natural and biological products and food consumption habits. For instance, bioprotection has emerged as an important natural strategy for sustainable postharvest management of perishable produce. In particular, biopolymer applications to preserve vegetables freshness and quality of fruits (edible coatings) have emerged as a prospective

approach. Both polyphenol-rich extracts and biopolymers are currently being explored as important natural preservatives for preventing bacterial and fungal spoilage in fruits following harvest(Cenobio-Galindo et al., 2019; Gaikwad et al., 2019). In this sense, recent studies have reported that the application of polyphenol-rich extracts (e.g. green tea extract) incorporated within edible coatings is a highly effective strategy for the preservation of berries quality following harvest and offer substantial protection not only against fungal decay but also antiviral activity (Moreno et al., 2020). In this regard, antiviral edible films and coatings are a promising area to explore due to the risk of disease transmission by food contaminated with enteric viruses. In fact, foodborne viral outbreaks are a growing concern for food safety authorities. A wide variety of viruses may be transmitted by food, nevertheless, the most frequently reported viruses are human noroviruses. Presence of human enteric viruses can occur in food which has been directly contaminated with faecal material or contaminated water. The main foodstuffs involved in foodborne infections are mollusc bivalves, vegetables and salads and berries which have been contaminated during their production or along the supply chain by improper handling after their preparation.

An inexpensive source for biopolymer production could be the use of food industry wastes which can be upcycled for extracting biopolymers or bioactive molecules (Awasthi et al., 2021; Esparza et al., 2020; Mendez et al., 2021; Méndez, Fabra, Gómez-Mascaraque, et al., 2021).

Persimmon (*Diospyros kaki Thunb*) fruits are considered a valuable functional produce. Their nutritional and medicinal benefits have been attributed to their high content in various nutrients and phytochemicals such as carbohydrates (e.g. pectin), vitamins, proanthocyanidins, phenolic acids, tannins, dietary fibre and carotenoids (Bordiga et al., 2018; Conesa et al., 2019; Mendez et al., 2021). However, around 15-20% of the fruit harvested is wasted (Munera et al., 2019), mainly due to factors associated with storage, ripening processes, fruit disease and stringent quality standard demands, thereby resulting in a huge amount of discarded fruits. Therefore, there is a need to develop holistic approaches for the management and utilization of persimmon wastes, since they can be a source of high-value compounds with different industrial applications. In particular, their high pectin and polyphenols content makes them ideal for the extraction of bioactive pectin

extracts (polyphenol-rich pectin) and hydro-ethanolic polyphenol extracts (Mendez et al., 2021; Méndez, Fabra, Falcó, et al., 2021), the extraction of which has been previously optimized for further applications in food-related industries. Interestingly, it was found that the polyphenol functional pectin extract extracted under severe conditions (pH 1 at 95 ºC during 30 minutes) produced the highest pectin and polyphenol yields, with abundant non-covalent interactions, while applying less severe extraction conditions (pH 1.5 at 70 ºC during 30 minutes) produced a pectin with intact pectin-polyphenol ester and O-glycosyl bonds (Mendez et al., 2021). Pectin-polyphenol complexes are formed mainly through cooperative hydrogen bonds and hydrophobic interactions and play an important role in the regulation of the phenolic resource, for instance having better health promoting benefits than free-polyphenols since these bound polyphenols reach the colon where they are released and fermented by bacteria into absorbable metabolites (Liu et al., 2017; Tomas, 2022). However, only a minor part of the existing literature on polyphenols addresses the great importance of the formation of non-extractable polyphenols (bound polyphenols) by interaction with polysaccharides (in this case pectin) (Bermúdez-Oria et al., 2021; Mendez et al., 2021; Siemińska-Kuczer et al., 2022).

In the light of the above, and based on the findings of the research group, it was hypothesized that bioactive pectins extracts may have higher antiviral activity than hydro-ethanolic polyphenol extracts with the additional advantage that they may present film-forming capacity due to the presence of pectin. Therefore, the main goals of this study were first to assess the effect of several chemical forms of polyphenols (isolated in an extract, non-covalently- bound to pectin and covalently-bound to pectin) on the antiviral properties of the extracts and, later on to investigate the film-forming capacity of the bioactive pectin extracts and to evaluate the antiviral efficacy of the developed coatings when applied to blueberries at room temperature.

3 Materials and methods

3.1 Extraction of bioactive pectins and hydro-ethanolic polyphenolic enriched extracts

Following the 3-level full factorial design carried out to optimize the extraction process of polyphenol-rich pectin extracts from persimmon fruit (*Diospyros kaki Thunb*.) (Mendez et al., 2021), two different conditions were selected for this work: i) where the yield and polyphenol content were the highest (79.48 ±0.78 mg gallic acid equivalent -GAE-/g pectin) , with abundant non-covalent interactions (PPN) (95 ºC pH 1.0 and 30 min) and ii) where the yield was high, leaving intact pectin-polyphenol ester and O-glycosyl bonds (PPC) (70 ºC pH 1.5 and 30 min), (103.41 ±0.76 mg GAE/g pectin). Similarly, hydro-ethanolic polyphenol-rich extracts (EPE) were obtained following the full central composite design carried out to optimize ethanolic heat extraction process in terms of total polyphenol content (26 ±0.58 mg GAE/g extract) and antioxidant activity from persimmon fruit (Méndez, Fabra, Falcó, et al., 2021). Briefly, the ethanolic heat extraction was carried out at 60 °C for 1 h using a solid:liquid ratio of 83.3 g L^{-1} and a mixture of 75:25 ethanol:water solution. The extract was subsequently filtered with a muslin cloth, freeze-dried and stored in a desiccator with silica gel until subsequent characterization**.**

Citrus pectin (CP), obtained from Sigma-Aldrich was used for comparative purposes. The degree of esterification (DE) of CP was˜59%, as reported by Mendez et al., (2022).

3.2 Antiviral capacity-virus propagation and cell lines.

Murine norovirus (MNV-1), used as a human norovirus surrogate, was propagated and assayed in RAW 264.7 cells, both kindly provided by Prof. H. W. Virgin (Washington University School of Medicine, USA). Hepatitis A virus (HAV) (strain HM-175/18f) was purchased from ATCC (VR-1402), and was propagated and assayed in confluent FRhK-4 cells (kindly provided by Prof. A. Bosch, University of Barcelona, Spain). Semi-purified MNV and HAV viruses were harvested at 2 days and 12 days after infection, respectively, by three freeze-thaw cycles of infected cells followed by centrifugation at 660 × g for 30

min to remove cell debris. Infectious viruses were enumerated by determining the 50% tissue culture infectious dose ($TCID_{50}$) with eight wells per dilution and 20 µL of inoculum per well using the Spearman-Karber method (Pintó et al., 1994).

Extracts and pectins (EPE, PPN, PPC and CP) were dissolved in PBS at 10 mg/mL concentration. To reach a final concentration of 5 mg/mL, each solution was incubated in an equal volume of MNV and HAV suspensions (*ca.* 5-6 log $TCID_{50}$ mL, respectively) for 16 h (overnight, ON) at 25 and 37 °C in a final extract concentration of 2.5 mg/mL. Samples were then ten-fold diluted in Dulbecco's Modified Eagle's Medium (DMED) supplemented with 10% fetal calf serum (FCS) and infectivity was determined by $TCID_{50}$. Ten-fold dilutions of treated and untreated virus suspensions were inoculated into confluent cell monolayers in 96-well plates. Virus suspensions untreated in PBS under the same experimental conditions were used as a positive control. Each treatment was done in triplicate. Virus decay titer was calculated as log10 (Nx/N0), where N0 is the infectious virus titer for untreated samples and Nx is the infectious virus titer for extracts treated samples (Falcó et al., 2018).

3.3 Preparation and characterization of stand-alone films

Four different coating formulations were obtained using both persimmon pectin (PPC and PPN) by the solvent casting method: two with PPN and two with PPC, mixed with commercial citrus pectin (CP) at two different ratios, 90:10 and 80:20 (CP-PPC or PPN ratio). Control films only with CP were also prepared for comparative purposes.

To this end, 0.5 g pectin (CP, PPN or PPC) were dissolved overnight in 50 mL of distilled water using a magnetic stirrer at a controlled temperature of 30 ºC until they were completely dissolved. Then, solutions were mixed at different ratios and the mixture was homogeneously spread over a Teflon plate of 15 cm in diameter and left to dry in an oven at 30 ºC for 48 h. These conditions were established after previous experiments to ensure that homogeneous and continuous films without cracks and/or pinholes were obtained. Control films with CP were also prepared for comparative purposes. It is interesting to note that neither pure PPC nor PPN films could be properly obtained (without cracks) and thus,

neat polyphenol functional pectin films were not characterized. Dry films could be peeled intact from the casting surface. The obtained films were removed from the plates and equilibrated for four days in a desiccator at 23 ºC and 53% relative humidity (RH) using an oversaturated solution of $Mg(NO_3)_2$. Film thickness was measured in quintuplicate using a hand-held digital micrometer (Palmer-Comecta, Spain, 0.001 mm), and the average value was used to determine the physicochemical properties.

Samples' nomenclature was “Cx-PPx’ where ‘x’ refers to the pectin percentage in the mixture, “C” indicates citrus pectin and PP the persimmon pectin either N or C type.

3.3.1 Morphology characterization

The microstructural analysis of the cross-sections of the dried films was carried out using Scanning Electron Microscopy (SEM) (Hitachi S-4800) at an accelerating voltage of 10 kV and a working distance of 8–12 mm. Small pieces of the pectin-based films were sputtered with a gold–palladium mixture under vacuum before their morphology was examined.

3.3.2 Optical properties of bioactive films

The transparency of the films was determined through the surface reflectance spectra in a spectrocolorimeter CM26d (Minolta Co., Tokyo, Japan), with a 12 diameter illuminated sample area. Measurements were taken in triplicate for each sample using white and black backgrounds.

Film transparency was evaluated through the internal transmittance (Ti) (0–1, theoretical range) by applying the Kubelka-Munk theory for multiple scattering to the reflection data. Moreover, CIE-L_{ab}* h_{ab}* C_{ab}* coordinates were obtained from the reflectance of an infinitely thick layer of material.

3.3.3 Mechanical properties

Tensile tests were carried out at ambient conditions of typically 23 (±1) °C and 54 (±2)% RH on a universal test Machine (Instron, USA), according to ASTM standard method D882.10 (ASTM D 882-02, 2002). Pre-conditioned samples were mounted in the film-

extension grips of the testing machine and stretched at 50 mm min^{-1} until breaking. The tensile strength (TS), elastic modulus (E), and elongation at break (EAB) of the films were determined from the stress-strain curves, estimated from force-distance data obtained for the different films (1 cm wide and 8 cm long). At least eight replicates were obtained per formulation.

3.3.4 Water vapour and oxygen permeability

Direct permeability to water vapour (WVP) was determined from the slope of the weight gain versus time curves at 23 °C, using the (ASTM-E96/E96M, 2016) gravimetric method. For each type of sample, tests were done in triplicate and water vapour permeability was carried out at 0–75% relative humidity gradient. The films were sandwiched between the aluminium top (open O-ring) and bottom (deposit for silica gel) parts of Payne permeability cups (3.5 cm diameter, Elcometer SPRL, Hermelle /s Argenteau, Belgium). A Viton rubber O-ring was placed between the film and bottom part of the cell to enhance sealability. Permeability cups containing silica were subsequently placed in equilibrated cabinet at 75 % RH using an oversaturated solution of sodium chloride salt.

3.3.5 Water contact angle measurements

The surface hydrophobicity as the wettability of fungal-based films were measured in a DSA25 equipment (Kruss) equipped with image analysis AD4021 software at ambient conditions. A water droplet (~3µL) was deposited on the film surface with a precision syringe. Contact angle values were obtained by analysing the shape of the distilled water drop after it had been placed over the film for 2 s. Five replicates were analysed per film formulation.

3.3.6 Water uptake

The water absorption behaviour of the films was determined. The samples were dried prior to testing at 60 °C to constant weight. They were then placed in a 75% RH equilibrated cabinet with a supersaturated sodium chloride salt solution and gravimetric measurements were performed until constant weight. For each type of sample, the tests were carried out in

triplicate. The water absorption content was calculated as a percentage of weight gained with respect to the initial weight of the sample.

3.4 Antiviral test on berries

Locally purchased blueberries were exposed to UV for 15 min in a laminar flow hood to reduce the microbial load. Then, they were inoculated by spotting 50 µL of MNV or HAV suspensions (about ca. 5-6 log $TCID_{50}$/mL) and dried under continuously circulating laminar flow hood for 45 min before the application of the coatings. Blueberries were coated by dipping in the coating solution for 2 min, let them dry for 20 min and then stored at 25 ºC during 16 hours and 4 days. On each sampling day, individual treated and untreated blueberries were placed in a tube containing 5 mL of DMEM supplemented with 10% FCS and shaken for 2 min at 180 rpm to release viral particles from the surface. Finally, blueberries were removed from the tube and serial dilutions were performed from the resultant virus suspension. Each treatment was carried out in triplicate. Positive controls were uncoated blueberries and coated berries with commercial citrus pectin (CP), and samples coded CP90-PPN10, CP90-PPC10, CP80-PPN20 and CP80-PPC20 were tested with their respective coating forming solution. The decay of MNV and HAV titers was calculated as described above.

3.5 Statistical analysis

All statistical analysis was performed using the statistical software Statgraphics Centurion XVI® (Manugistics Inc.; Rockville, MD, USA). Statistically significant differences were determined by using one-way analyses of variance (ANOVA) and Tukey-test was used to determine statistically significant differences among means (p-value < 0.05).

4 Results

4.1 Antiviral activity of bioactive pectins

In the first part of this work, the antiviral activity of polyphenol-rich pectin extracts (PPC and PPN) were evaluated and compared with the hydro-ethanolic polyphenol extract (EPE)

and commercial citrus pectin (CP). The main phenolic compound identified in the EPE extracts was the hydrolysable tannin gallic acid and others such as naringin, hesperidin or naringenin were also present, as it has been recently reported (Méndez, Fabra, Falcó, et al., 2021). Regarding the polyphenol-rich pectin extracts, the extraction conditions significantly affected the amount and type of polypohenols. PPN obtained under severe conditions displayed a very significant reduction in esterified phenolics, while non-covalently bound ("free" phenolics) significantly increased compared to those obtained under less severe conditions (PPC). Furthermore, flavan-3-ols and flavanones were only detected in PPC and not in PPN (Méndez et al., 2022).

Table 1 shows the effect of each extract against MNV and HAV at two different temperatures. Overall, polyphenol-rich pectin (PPC and PPN) exhibited the most effective antiviral activity at both temperatures, thus confirming that the presence of polyphenol-polysaccharide complexes had a positive effect on the antimicrobial properties, being even accentuated in those containing covalent pectin-polyphenol interactions. Higher reductions were reported for MNV and HAV after overnight (ON) incubation at 37 ºC, with MNV titers decreasing under detection limits and 2.20 log $TCID_{50}$/mL for PPC and PPN, respectively. HAV titers were completely reduced under detectable limits for both PPC and PPN after ON incubation at 37 ºC. Statistically significant reductions ($p < 0.05$) on MNV infectivity were observed for PPC at both temperatures, while no differences ($p > 0.05$) between PPN and PPC were reported on HAV neither at 37 ºC nor at 25 ºC.

Therefore, considering that polyphenol-rich pectin extracts had better antiviral properties, PPC and PPN were used to develop edible films and coatings for food preservation, with the additional advantage that the presence of pectin confers them in relation to film-forming capacity.

Table 1. Reduction of murine norovirus (MNV) and hepatitis A virus (HAV) titers (log $TCID_{50}$/mL) on bioactive pectins and hydro-ethanolic polyphenol persimmon extract at different temperatures.

	MNV			
Sample*	37 ºC		25 ºC	
	Log $TCID_{50}$ · mL^{-1}	**R**	**Log $TCID_{50}$ · mL^{-1}**	**R**
Control	6.65(0.13)^{a}	-	6.62(0.47)^{a}	
CP	6.28(0.14)^{b}	0.37	5.57(0.13)^{bc}	1.04
EPE	6.55(0.25)^{ab}	0.1	6.57(0.13)^{a}	0.04
PPC	<1.15 ^{d}	>5.50	3.16(0.07)^{d}	3.46
PPN	4.45(0.12)^{c}	2.2	4.87(0.56)^{c}	1.75
	HAV			
Sample*	37 ºC		25 ºC	
	Log $TCID_{50}$ · mL^{-1}	**R**	**Log $TCID_{50}$ · mL^{-1}**	**R**
Control	4.99(0.44)^{a}		5.24(0.26)^{a}	-
CP	5.28(0.52)^{a}	-0.29	4.70(0.33)^{a}	0.54
EPE	5.32(0.13)^{a}	-0.33	4.95(0.45)^{a}	0.29
PPC	< 1.15 ^{b}	>3.84	3.41(0.19)^{b}	1.83
PPN	< 1.15 ^{b}	>3.84	4.03(0.38)a^{b}	1.21

Different superscripts within a column indicate significant differences among formulations ($p < 0.05$). Data reported are mean values and standard deviation (in parentheses).
(*) CP: citrus pectin, EPE: hydro-ethanolic polyphenolic enriched extracts; PPC: polyphenol functional pectin with intact pectin-polyphenol ester and O-glycosyl bonds, PPN: polyphenol functional pectin with abundant non-covalent interaction.

4.2 Properties of stand-alone pectin-based films

With the aim of developing antiviral edible coatings, PPC and PPN were used as biopolymer coatings and mixed with a commercial citrus pectin at different ratios, justified by their higher antiviral properties but lower extraction yields (Mendez et al., 2021) when compared to commercial pectin sources. Then, the physicochemical characterization of the developed films and the antiviral efficiency when applied as coatings onto blueberries were evaluated.

The morphology of the films was analysed by SEM and representative micrograph images of the pectin-based films after one week storage at 23 ºC and 53% RH are shown in Figure 1. As observed, commercial citrus pectin films (Figure 1A) exhibited a smooth and homogeneous appearance with no brittle areas or bubbles, evidencing the formation of a

compact arrangement of pectin chains. The incorporation of persimmon pectin extracts provided a slightly rougher structure, being more accentuated as the PPN or PPC concentration increased (Figures 1D and 1E). Interestingly, blending PPN or PPC with CP gave rise to a substantially different microstructure, probably ascribed to differences in the extracted pectin structure and also to the different polyphenol-pectin interactions in both extracts. The presence of more polar compounds (phenolic acids, and specifically gallic acid) found in a higher amount in functional pectins extracted under less severe conditions (PPN) could be interacting with CP matrix through OH bond, producing a less heterogeneous cross-section than those containing PPN. In contrast, a coarse aspect can be distinguished when PPC was mixed with commercial citrus pectin, where PPC appeared randomly distributed throughout the film cross-section (Figures 1C and 1E), fact which will have a positive impact on the physicochemical properties of the film as it will be shown below.

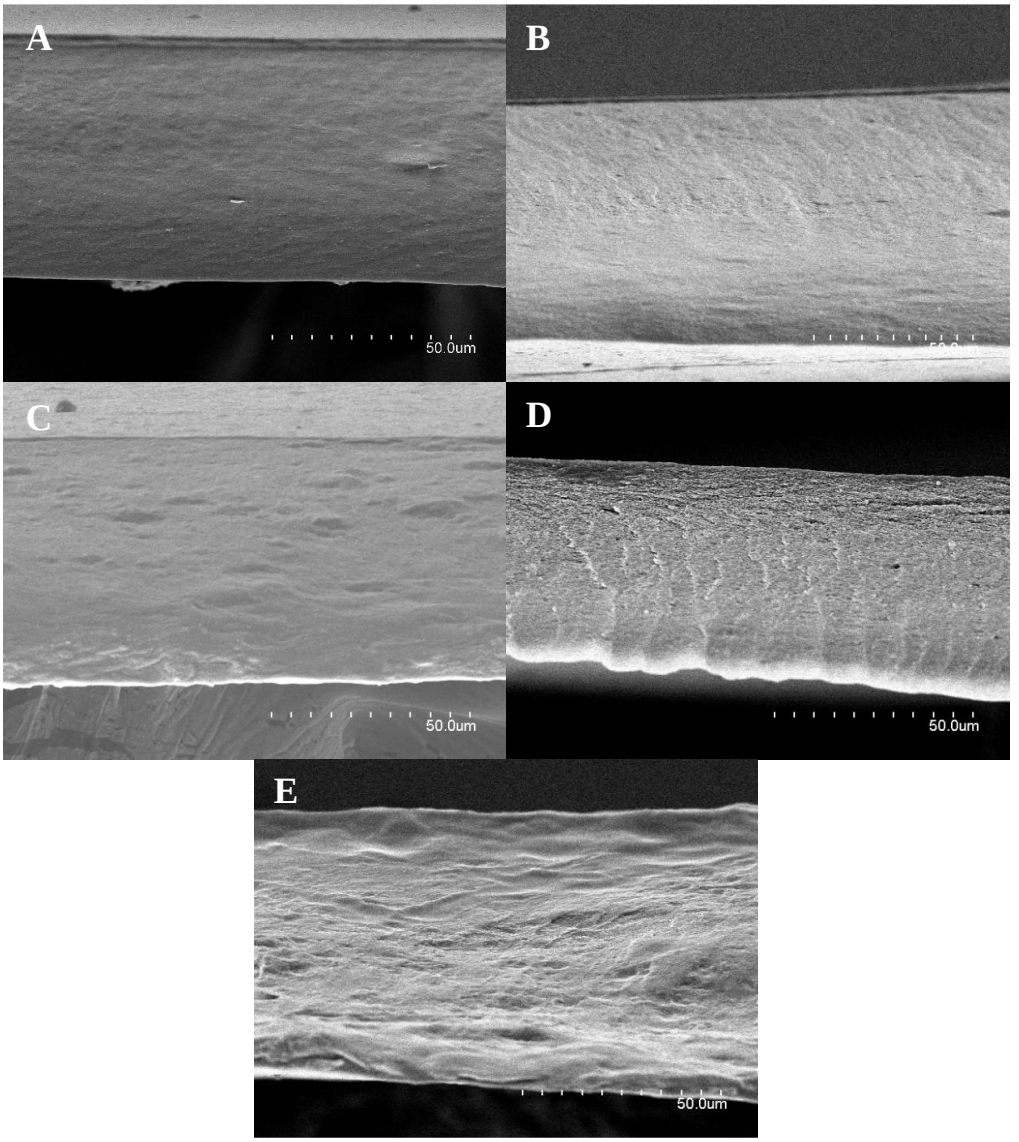

Figure 1. Cross-section images of the developed films. (A) CP, (B) CP90-PPN10, (C) CP90-PPC10, (D) CP80-PPN20, (E) CP80-PPC20.

Figure 2 shows the spectra distribution curves of internal transmittance (T_i), used as transparency indicator, of the developed films. An increase in the Ti values is ascribed to an increase in transparency. As observed, those prepared with pure commercial pectin (CP) were the most transparent. In contrast the presence of polyphenol-rich pectin significantly reduced the transparency of the films, showing lower Ti values in all the wavelength

considered. This was expected not only because of the more heterogenous internal structure, ascribed to the presence of different compounds with different refractive indices which provoked light dispersion, but also due to the light selective absorption of polyphenol compounds at low wavelengths which, moreover, are the main responsible of the brownish colour of the films.

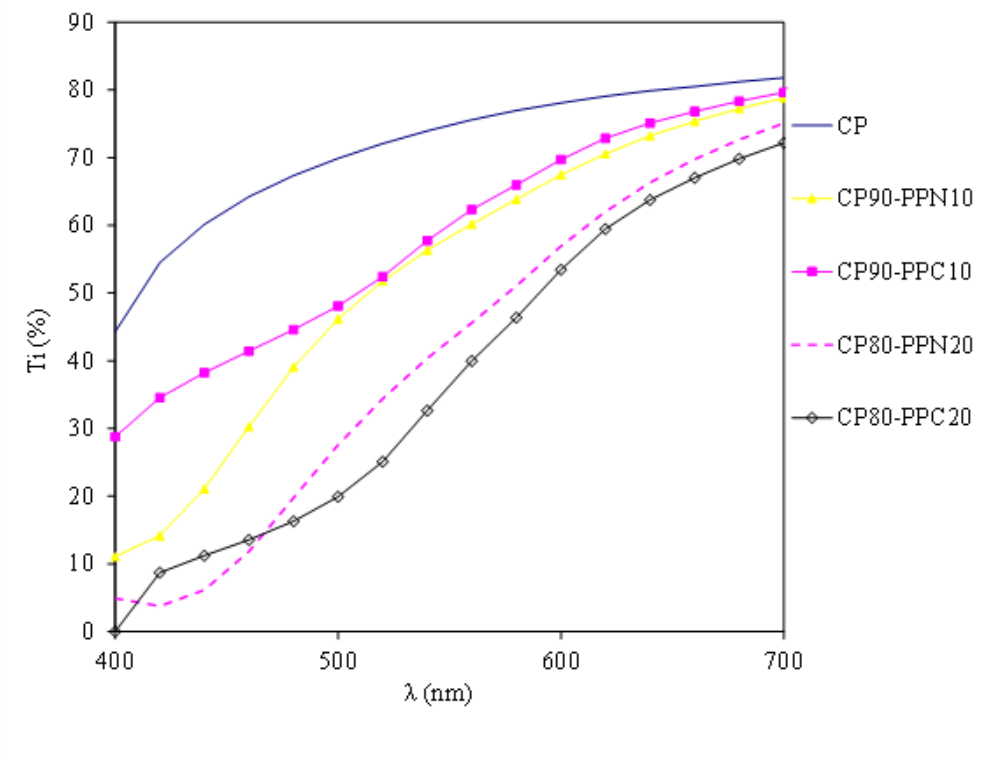

Figure 2. Spectral distribution of internal transmittance (Ti) of the developed pectin-based films.

Table 2 summarizes the optical parameters (Lightness -L*-, hue -h^*_{ab}- and Chroma -C^*_{ab}-) and the total colour differences (ΔE) obtained from the reflectance spectra of an infinite thickness film. As clearly observed, films containing polyphenol-rich pectin extracts were darker (lower L*) with a saturated brownish colour (higher C* and lower h*), which was similar to those previously reported in other biopolymer matrices (Falcó et al., 2019; Moreno et al., 2020; Orqueda et al., 2022; Zhang et al., 2021). These differences were

clearly evidenced by the increase of ΔE values in films prepared with the polyphenol-containing persimmon pectin, being accentuated as the PPN and PPC content increased.

Table 2. Colour parameters of the developed stand-alone pectin-based films.

Films	L*	C^*_{ab}	h^*_{ab}	ΔE
CP	60.21(0.08)^a	19.05(0.09)^c	76.75(0.06)^a	-
CP90-PPN10	54.46(0.18)^b	28.31(0.18)^a	75(0.42)^a	11.01(0.13)^a
CP90-PPC10	47.37(0.42)^c	22.03(0.56)^b	61.19(0.36)^c	14.2(0.13)^b
CP90-PPN20	35.13(0.37)^e	20.02(0.38)^c	54(1.41)^b	26.37(0.24)^c
CP90-PPC20	37.31(0.13)^d	20.3(0.49)^c	49.46(0.53)^d	24.74(0.01)^d

Different superscripts within a column indicate significant differences among formulations ($p < 0.05$). Data reported are mean values and standard deviation (in parentheses). L* lightness, C^*_{ab} Chroma, h^*_{ab} hue. ΔE Total colour differences with respect to the control film (CP).

The performance properties of the films were also characterized to assess their potential as food coatings. The mechanical properties were measured by means of tensile testing and the most representative parameters (E, TS and EAB) obtained from the stress-strain curves are gathered in Table 3. The first clear observation is that, for the films containing polyphenol-rich pectin extracts, the ones with covalently-bound polyphenols (PPC) were stiffer (higher E values) and more resistant to break (higher TS values) than their counterparts prepared with PPN. This can be correlated with the established interactions between polyphenolic compounds and pectin via ester and glyosidic linkages (Mendez et al., 2021). In fact, an increase in E and TS values was observed as the PPC amount increased in the pectin-based film Falcó et al., (2019) reported similar results for carrageenan films containing green tea extract who also attributed this behaviour (higher E and TS values and lower EAB values) to the existing polyphenol-polysaccharide interactions. Curiously, no significant differences were observed for EAB values.

With regards to water vapour permeability (WVP) values of the pectin-based films, shown in Table 3, they ranged between 1.4 and 2.1×10^{-13} Kg-/Pa-s-m, which agree with those from previous studies in which pectin-based films were obtained (Aguirre-Joya et al., 2018; Bernhardt et al., 2017; Rodsamran & Sothornvit, 2019).

Table 3. Mechanical parameters (E: elastic modulus, TS: tensile strength, EAB: elongation at break), water vapour permeability (WVP), water vapour sorption ($w_{e)}$ and contact angle (**θ**) of the stand-alone coatings.

Stand-alone coatings (films)*	E (MPa)	TS (MPa)	EAB (%)	w_e (g water/100 g sample)	θ (°)	WVP (Kg-/Pa-s-m) x10^{-13}
CP	4793(437)^{b}	62.61(11.83)^{b}	2.08(0.34)^{a}	18.41(1)^{a}	80.71(0.46)^{b}	2.12(0.33)^{a}
CP90-PPN10	4850(219)^{ab}	43.33(12.86)^{b}	1.25(0.57)^{a}	17.98(0.64)^{ab}	71.8(0.99)^{c}	1.41(0.26)^{a}
CP90-PPC10	5493(274)^{ab}	67.4(24.9)^{ab}	1.80(0.75)^{a}	14.06(0.31)^{d}	89.56(1.02)^{a}	2.00(0.08)^{a}
CP80-PPN20	4888(305)^{b}	82.14(19.24)^{ab}	2.48(0.69)^{a}	16.69(0.67)^{ab}	64.25(1.65)^{d}	1.63(0.05)^{a}
CP80-PPC20	6484(1047)^{a}	94.27(10.39)^{a}	2.40(0.26)^{a}	15.29(0.86)^{c}	90.07(0.77)^{a}	1.59(0.37)^{a}

Different superscripts within a column indicate significant differences among formulations ($p < 0.05$). Data reported are mean values and standard deviation (in parentheses). (*) CP: citrus pectin; PPC: polyphenol functional pectin with intact pectin-polyphenol ester and O-glycosyl bonds, PPN: polyphenol functional pectin with abundant non-covalent interaction.

However, higher permeability values were previously reported for persimmon-derived pectin-based films (Matheus et al., 2021). The results evidence no major differences between samples, regardless of the presence of polyphenol compounds.

The water sorption capacity was also measured through gravimetrical tests and the results are summarized in Table 3. The presence and type of polyphenols seemed to have a notable effect as the films produced from PPC presented lower values when compared with those obtained with pure commercial pectin or mixtures with PPN. This is mostly explained by the chemical nature of the phenolic compounds and, specifically, by their polarity. The greatest reduction was seen when less polar phenolic compounds (such as flavonoids) present in the covalently bound pectin extracts (PPC sample) were incorporated in the films, in comparison with those obtained under severe extraction conditions, which rendered more polar phenolic acids (Mendez et al., 2021). Furthermore, the presence of pectin-polyphenol

ester and O-glycosyl bonds in the PPC sample, reduced the amount of free OH- groups thus increasing the hydrophobicity of the film.

The wettability properties of the developed pectin-based films were also determined by direct measurement of contact angles of a water drop deposited on the upper surface of samples and the results are also gathered in Table 3. Interestingly, the presence of PPC had a positive impact on the hydrophobicity of the films (increased θ values). In contrast, PPN addition provoked a significant decrease of the contact angle values, suggesting the more hydrophilic character of these films. This might be related to the differences in the chemical structure and polyphenol-pectin interactions. The presence of more polar compounds (phenolic acids, and specifically gallic acid) found in a higher amount in persimmon pectins extracted under less severe conditions (PPN), made the surface of the film more hydrophilic. In contrast, the less polar covalently-bound polyphenols (i.e. flavonoids aglycones) and the presence of pectin-polyphenol ester and O-glycosyl bonds found in a greater amount in PPC samples increased the hydrophobicity of the films and thus, higher contact angle values were found in the CP-PPN mixtures.

4.3 Challenge tests

Challenge tests on coated blueberries were carried out under conditions of *in vivo* storage, mimicking realistic scenarios of fresh fruit handing. To this end, each film-forming dispersion was used to treat fresh blueberries artificially inoculated with MNV and HAV and stored at room temperature (ON and during 4 days). Interestingly, as observed in **Table 4**, the infectivity of MNV and HAV in fresh blueberries after CP-coating treatment was reduced by 3.07 and 1.63 logs, respectively, after ON storage at 25 ºC. However, the efficacy of the coatings containing pectin persimmon extract was not significantly improved, except in those containing the lower amount of PPC or PPN. The slightly higher antiviral activity in those containing 10% PPC agreed with the *in-vitro* results (see Table 1) and can be related to the presence of covalent pectin-polyphenol complexes. Surprisingly, despite of having higher PPC and PPN content, lower reductions were reported in coated blueberries. In fact, MNV and HAV titers were not significantly ($p < 0.05$) reduced for CP80-PPC20 or CP80-PPN20 coatings when compared to the commercial citrus pectin

coating. It should be noted that a complete inactivation for both viruses was observed after 4 days storage at 25 ºC, even in those treated with pure CP. Although the antiviral effects of bioactive polysaccharides have been mainly ascribed to the sulphated ones (Falcó et al., 2019; Guo et al., 2022), some pectins have been reported to exert antiviral activity. For instance, Chen et al., (2019) demonstrated that pectin from *Saussurea laniceps* petals showed antiviral activity against hepatitis B virus. Similarly, de Godoi et al., (2019) reported the antiviral activity of pectin isolated from *Inga ssp.* fruits against the herpes simplex virus type 1 (HSC-1) and the poliovirus (PV). The antiviral effect of *Houttuynia cordata* polysaccharide extract (a pectin-like acidic polysaccharide) on MNV was also evaluated by Cheng et al., (2019) . Furthermore, hesperidin is the predominant flavonoid in citrus fruits with potential antiviral activity and thus, hesperidin-rich citrus pectin has also shown antiviral activity (Meneguzzo et al., 2020).

Furthermore, the differences between the *in-vitro* and *in-vivo* assays can be ascribed to the fact that *in-vitro* assays in commercial growth media pose no limit for the growth of control uninfected cells. This promotes the observation of differences in the antiviral efficacy. On the contrary, the lack of a favourable environment (moisture, etc) in the coating may hinder viral viability at longer incubation times even in control coatings.

Table 4. Reduction murine norovirus (MNV) and hepatitis A virus (HAV) titers (log TCID50/mL) on blueberry surfaces after treatment coatings at room temperature and different times.

Sample*	**MNV**			
	16 h (ON)		4 days	
	Log $TCID_{50} \cdot mL^{-1}$	**R**	**Log $TCID_{50} \cdot mL^{-1}$**	**R**
Fruit control	5.49(0.19) [a]	1.07	4.74(0.19)[b]	1.82 [a]
CP	3.49(0.26) [b]	3.07	< 1.15	> 5.41 [b]
CP90-PPN10	2.74(0.73)[bc]	3.82	< 1.15	> 5.41 [b]
CP90-PPC10	2.28(0.14)[c]	4.28	< 1.15	> 5.41 [b]
CP80-PPN20	3.45(0.22)[b]	3.11	< 1.15	> 5.41 [b]
CP80-PPC20	3.37(0.07)[b]	3.19	< 1.15	> 5.41 [b]

Sample*	**HAV**			
	16 h (ON)		4 days	
	Log $TCID_{50} \cdot mL^{-1}$	**R**	**Log $TCID_{50} \cdot mL^{-1}$**	**R**
Fruit control	4.95(0.13)[a]	0.04	4.99(0.19)	0.00 [a]
CP	3.37(0.19)[bc]	1.63	< 1.15	> 3.84 [b]
CP90-PPN10	2.66(0.63)[c]	2.33	< 1.15	> 3.84 [b]
CP90-PPC10	2.62(0.07)[c]	2.38	< 1.15	> 3.84 [b]
CP80-PPN20	3.66(0.40)[b]	1.33	< 1.15	> 3.84 [b]
CP80-PPC20	3.41(0.26)[bc]	1.58	< 1.15	> 3.84 [b]

Different superscripts within a column indicate significant differences among formulations ($p < 0.05$). Data reported are mean values and standard deviation (in parentheses).
(*) Coatings: CP: citrus pectin; PPC: polyphenol functional pectin with intact pectin-polyphenol ester and O-glycosyl bonds, PPN: polyphenol functional pectin with abundant non-covalent interaction.

5 Conclusions

In this work, the potential use of functional polyphenol-rich pectin extracts (PPC and PPN) and hydro-ethanolic polyphenol extracts (EPE) obtained from discarded persimmon fruits has been evaluated to develop antiviral edible coatings. Initially, the *in-vitro* assays showed that polyphenol-rich pectin exhibited the most effective antiviral activity, evidencing that the presence of polyphenol-polysaccharide complexes had a positive effect on the antiviral properties, being accentuated in those containing covalent pectin-polyphenol interactions (PPC). Therefore, PPC and PPN were used as biopolymer coatings and mixed with commercial citrus pectin at two different ratios (90-10 and 80-20, CP: persimmon pectin ratio). Addition of persimmon pectin gave rise to more coloured films with lower

transparency and, the presence of covalently-linked polyphenols (PPC) produced stiffer films, with lower sorption capacity and more hydrophobic nature. The developed functional films revealed a notable antiviral activity against MNV and the HAV when applied onto blueberries. Adding 10% of PPC or PPN enhanced the antiviral activity after ON incubation at room temperature, although a complete inactivation for both viruses was observed after 4 days storage at 25 ºC, even in those coated with pure CP. These functional edible coatings could be an alternative to reduce or eliminate human enteric viruses since they effectively reduce MNV and HAV titers in artificially contaminated blueberries.

6 Acknowledgements

Grant RTI-2018-094268-B-C22 funded by MCIN/AEI/10.13039/501100011033 and by "ERDF A way of making Europe". This work was also funded by the grant INNVAL10-19-009 - CA8250 from Agència Valenciana d´Innovació (AVI). D.A. Méndez. is supported by the Administrative Department of Science, Technology and Innovation (Colciencias) of the Colombian Government (783-2017). This research is part of the CSIC program for the Spanish Recovery, Transformation and Resilience Plan funded by the Recovery and Resilience Facility of the European Union, established by the Regulation (EU) 2020/2094. Interdisciplinary Platform for Sustainable Plastics towards a Circular Economy+. PTI-SusPlast+ is also acknowledged for financial support.

7 References

Aguirre-Joya, J. A., Pastrana-Castro, L., Nieto-Oropeza, D., Ventura-Sobrevilla, J., Rojas-Molina, R., & Aguilar, C. N. (2018). The physicochemical, antifungal and antioxidant properties of a mixed polyphenol based bioactive film. *Heliyon*, *4*(12), e00942. https://doi.org/10.1016/J.HELIYON.2018.E00942

ASTM D 882-02. (2002). Standard Test Method for Tensile Properties of Thin Plastic Sheeting, ASTM International. In *Www.Astm.Org*. https://doi.org/10.1520/D0882-18

ASTM-E96/E96M. (2016). *Standard Test Methods for Water Vapor Transmission of materials, West Conshohocken*. *October*, 14p.

Awasthi, M. K., Ferreira, J. A., Sirohi, R., Sarsaiya, S., Khoshnevisan, B., Baladi, S., Sindhu, R., Binod, P., Pandey, A., Juneja, A., Kumar, D., Zhang, Z., & Taherzadeh, M. J. (2021). A critical review on the development stage of biorefinery systems towards the management of apple processing-derived waste. *Renewable and Sustainable Energy Reviews*, *143*, 110972. https://doi.org/10.1016/J.RSER.2021.110972

Bermúdez-Oria, A., Rodríguez-Juan, E., Rodríguez-Gutiérrez, G., Fernández-Prior, Á., & Fernández-Bolaños, J. (2021). Effect of the Olive Oil Extraction Process on the Formation of Complex Pectin-Polyphenols and Their Antioxidant and Antiproliferative Activities. *Antioxidants (Basel, Switzerland)*, *10*(12). https://doi.org/10.3390/ANTIOX10121858

Bernhardt, D. C., Pérez, C. D., Fissore, E. N., De'Nobili, M. D., & Rojas, A. M. (2017). Pectin-based composite film: Effect of corn husk fiber concentration on their properties. *Carbohydrate Polymers*, *164*, 13–22. https://doi.org/10.1016/J.CARBPOL.2017.01.031

Bordiga, atteo, Travaglia, F., Giuffrida, D., Mangraviti, D., Rigano, F., Mondello, L., Arlorio, M., & Coïsson, J. D. (2018). Characterization of peel and pulp proanthocyanidins and carotenoids during ripening in persimmon "Kaki Tipo" cv, cultivated in Italy. *Food Research International*, *120*(November 2018), 800–809. https://doi.org/10.1016/j.foodres.2018.11.041

Cenobio-Galindo, A. de J., Pimentel-González, D. J., del Razo-Rodríguez, O. E., Medina-Pérez, G., Carrillo-Inungaray, M. L., Reyes-Munguía, A., & Campos-Montiel, R. G. (2019). Antioxidant and antibacterial activities of a starch film with bioextracts microencapsulated from cactus fruits (Opuntia oligacantha). *Food Science and Biotechnology*, *28*(5), 1553. https://doi.org/10.1007/S10068-019-00586-9

Chen, W., Zhu, X., Ma, J., Zhang, M., & Wu, H. (2019). Structural Elucidation of a Novel Pectin-Polysaccharide from the Petal of Saussurea laniceps and the Mechanism of its

Anti-HBV Activity. *Carbohydrate Polymers*, *223*, 115077. https://doi.org/10.1016/J.CARBPOL.2019.115077

Cheng, D., Sun, L., Zou, S., Chen, J., Mao, H., Zhang, Y., Liao, N., & Zhang, R. (2019). Antiviral Effects of Houttuynia cordata Polysaccharide Extract on Murine Norovirus-1 (MNV-1)—A Human Norovirus Surrogate. *Molecules*, *24*(9). https://doi.org/10.3390/MOLECULES24091835

Conesa, C., Laguarda, N., Pedro, M., & Lucía, F. (2019). Evaluation of Persimmon (Diospyros kaki Thunb . cv . Rojo Brillante) Industrial Residue as a Source for Value Added Products. *Waste and Biomass Valorization*, *0*(0), 0. https://doi.org/10.1007/s12649-019-00621-0

de Godoi, A. M., Faccin-Galhardi, L. C., Rechenchoski, D. Z., Arruda, T. B. M. G., Cunha, A. P., de Almeida, R. R., Rodrigues, F. E. A., Ricardo, N. M. P. S., Nozawa, C., & Linhares, R. E. C. (2019). Structural characterization and antiviral activity of pectin isolated from Inga spp. *International Journal of Biological Macromolecules*, *139*, 925–931. https://doi.org/10.1016/J.IJBIOMAC.2019.07.212

Esparza, I., Jiménez-Moreno, N., Bimbela, F., Ancín-Azpilicueta, C., & Gandía, L. M. (2020). Fruit and vegetable waste management: Conventional and emerging approaches. *Journal of Environmental Management*, *265*, 110510. https://doi.org/10.1016/j.jenvman.2020.110510

Falcó, I., Randazzo, W., Gómez-Mascaraque, L. G., Aznar, R., López-Rubio, A., & Sánchez, G. (2018). Fostering the antiviral activity of green tea extract for sanitizing purposes through controlled storage conditions. *Food Control*, *84*. https://doi.org/10.1016/j.foodcont.2017.08.037

Falcó, I., Randazzo, W., Sánchez, G., López-Rubio, A., & Fabra, M. J. (2019). On the use of carrageenan matrices for the development of antiviral edible coatings of interest in berries. *Food Hydrocolloids*, *92*, 74–85. https://doi.org/10.1016/j.foodhyd.2019.01.039

Gaikwad, K. K., Singh, S., & Lee, Y. S. (2019). Antimicrobial and improved barrier properties of natural phenolic compound-coated polymeric films for active packaging applications. *Journal of Coatings Technology and Research*, *16*(1), 147–157. https://doi.org/10.1007/S11998-018-0109-9/FIGURES/7

Guo, Q., Huang, X., Kang, J., Ding, H., Liu, Y., Wang, N., & Cui, S. W. (2022). Immunomodulatory and antivirus activities of bioactive polysaccharides and structure-function relationship. *Bioactive Carbohydrates and Dietary Fibre*, *27*, 100301. https://doi.org/10.1016/J.BCDF.2021.100301

Liu, D., Martinez-Sanz, M., Lopez-Sanchez, P., Gilbert, E. P., & Gidley, M. J. (2017). Adsorption behaviour of polyphenols on cellulose is affected by processing history. *Food Hydrocolloids*, *63*, 496–507. https://doi.org/10.1016/J.FOODHYD.2016.09.012

Matheus, J. R. V., de Assis, R. M., Correia, T. R., da Costa Marques, M. R., Leite, M. C. A. M., Pelissari, F. M., Miyahira, R. F., & Fai, A. E. C. (2021). Biodegradable and Edible Film Based on Persimmon (Diospyros kaki L.) Used as a Lid for Minimally Processed Vegetables Packaging. *Food and Bioprocess Technology*, *14*(4), 765–779. https://doi.org/10.1007/S11947-021-02595-1/FIGURES/6

Méndez, D. A., Fabra, M. J., Falcó, I., Sánchez, G., Aranaz, P., Vettorazzi, A., Ribas-Agustí, A., González-Navarro, C. J., Castellari, M., Martínez-Abad, A., & López-Rubio, A. (2021). Bioactive extracts from persimmon waste: influence of extraction conditions and ripeness. *Food & Function*, *12*(16), 7428–7439. https://doi.org/10.1039/D1FO00457C

Méndez, D. A., Fabra, M. J., Gómez-Mascaraque, L., López-Rubio, A., & Martinez-Abad, A. (2021). Modelling the Extraction of Pectin towards the Valorisation of Watermelon Rind Waste. *Foods*, *10*(4), 738. https://doi.org/10.3390/foods10040738

Méndez, D. A., Fabra, M. J., Odriozola-Serrano, I., Martín-Belloso, O., Salvia-Trujillo, L., López-Rubio, A., & Martínez-Abad, A. (2022). Influence of the extraction conditions on the carbohydrate and phenolic composition of functional pectin from persimmon

waste streams. *Food Hydrocolloids*, *123*, 107066. https://doi.org/10.1016/j.foodhyd.2021.107066

Meneguzzo, F., Ciriminna, R., Zabini, F., & Pagliaro, M. (2020). Review of Evidence Available on Hesperidin-Rich Products as Potential Tools against COVID-19 and Hydrodynamic Cavitation-Based Extraction as a Method of Increasing Their Production. *Processes 2020, Vol. 8, Page 549*, *8*(5), 549. https://doi.org/10.3390/PR8050549

Moreno, M. A., Vallejo, A. M., Ballester, A. R., Zampini, C., Isla, M. I., López-Rubio, A., & Fabra, M. J. (2020). Antifungal edible coatings containing Argentinian propolis extract and their application in raspberries. *Food Hydrocolloids*, *107*, 105973. https://doi.org/10.1016/J.FOODHYD.2020.105973

Munera, S., Aleixos, N., Besada, C., Gómez-Sanchis, J., Salvador, A., Cubero, S., Talens, P., & Blasco, J. (2019). Discrimination of astringent and deastringed hard 'Rojo Brillante' persimmon fruit using a sensory threshold by means of hyperspectral imaging. *Journal of Food Engineering*, *263*, 173–180. https://doi.org/10.1016/j.jfoodeng.2019.06.008

Orqueda, M. E., Méndez, D. A., Martínez-Abad, A., Zampini, C., Torres, S., Isla, M. I., López-Rubio, A., & Fabra, M. J. (2022). Feasibility of active biobased films produced using red chilto wastes to improve the protection of fresh salmon fillets via a circular economy approach. *Food Hydrocolloids*, *133*, 107888. https://doi.org/10.1016/J.FOODHYD.2022.107888

Pintó, R. M., Diez, J. M., & Bosch, A. (1994). Use of the colonic carcinoma cell line CaCo-2 for in vivo amplification and detection of enteric viruses. *Journal of Medical Virology*, *44*(3), 310–315. https://doi.org/10.1002/jmv.1890440317

Rodsamran, P., & Sothornvit, R. (2019). Preparation and characterization of pectin fraction from pineapple peel as a natural plasticizer and material for biopolymer film. *Food and Bioproducts Processing*, *118*, 198–206. https://doi.org/10.1016/j.fbp.2019.09.010

Siemińska-Kuczer, A., Szymańska-Chargot, M., & Zdunek, A. (2022). Recent advances in interactions between polyphenols and plant cell wall polysaccharides as studied using an adsorption technique. *Food Chemistry*, *373*, 131487. https://doi.org/10.1016/J.FOODCHEM.2021.131487

Tomas, M. (2022). Effect of dietary fiber addition on the content and in vitro bioaccessibility of antioxidants in red raspberry puree. *Food Chemistry*, *375*. https://doi.org/10.1016/J.FOODCHEM.2021.131897

Zhang, W., Jiang, H., Rhim, J. W., Cao, J., & Jiang, W. (2021). Tea polyphenols (TP): a promising natural additive for the manufacture of multifunctional active food packaging films. *Https://Doi.Org/10.1080/10408398.2021.1946007*. https://doi.org/10.1080/10408398.2021.1946007

IV. GENERAL DISCUSSION

General discussions of the results

4.1 Valorisation of watermelon rind pectin

This chapter focused on the valorisation of pectin from watermelon rinds, covering the composition and structural features, optimization of the extraction conditions and exploration of potential applications. In this sense, the application of the pectin material as an emulsifier at high oil concentrations was compared and evaluated. On the other hand, enzymatic modification of pectin obtained under optimum conditions was investigated to improve the gelation capacity. Finally, the pectin material with the best gelation properties was transformed into aerogels to study its properties and potential application as drug carriers.

The first work of this chapter included an initial characterisation of the watermelon rind waste and a Box-Behnken experimental design to evaluate the effect of temperature, time and pH on yield, composition and structure of pectin. Watermelon rind waste showed pectin contents (~30%) similar to conventional pectin-rich sources and pectin yields of around ~13% were achieved by the conventional heat acid method, again in line with conventional sources. The inherent recalcitrance of pectin in the cell wall, non-precipitated pectic material or degradation, might be some of the reasons for not recovering all pectin from the biowaste. The broad range of extraction conditions led to pectin with a wide range of esterification degrees, molar mass and compositional or structural characteristics, all of which were accurately fitted to the polynomial models and experimentally validated. This pointed out the reliability of the models to predict and design extraction processes triggering specific compositional traits depending on the pectin requirements, offering the possibility of producing novel customised pectin ingredients with a broader potential application scope depending on the targeted structure. According to the severity of extraction, the harshest conditions generated purer homogalacturonan fractions at the expense of yield (higher hydrolysis effect), while milder extraction conditions (pH≥2) produced highly branched entangled pectin structures and lower yields, which was expected due to the lower hydrolytic effect to extract the pectin from the plant matrix. However, the different

extraction conditions only yielded pectin with a high esterification degree. The work did not only expand the knowledge towards the optimization of pectin extraction from watermelon rind, setting the basis for the preparation of specific pectin structures for subsequent works, but also revealed very interesting differential traits in the composition and structure, when compared to commercial pectin sources such as apple (AP) and citrus pectin (CP). The two main differential characteristics were the abundance of arabinogalactan side chain contribution and the strong protein-pectin interaction. Optimum conditions favouring yield (95 ºC, 90 min and pH 1.36) led to more linear pectins with similar molecular mass as commercial AP or CP, but with significantly higher branching degree and a small protein contents recalcitrant to the strong acidic conditions.

Owed to the interesting compositional and structural features elucidated in this first work, the second work of this chapter explored the functionality of the pectin extracted from watermelon rind as an emulsifier, evaluating the different factors that influence the emulsification process and stability. Thus, they were jointly analysed with typical commercial pectins (AP and CP) to understand the underlying mechanisms and compare them. The results showed that characteristics typically ascribed to a better emulsion capacity, such as the degree of esterification, were less influential than factors such as high molecular weight. For instance, AP used in this study and having a degree of esterification of 78%, led to certain phase separation, being the initial emulsification ability only based on its capacity to increase the viscosity of the emulsion (as it had the higher MW) without a noticeable interaction in the interphase. In other words, this pectin did not affect oil droplet size, but slowed down oil droplet movement by providing viscosity to the continuous aqueous phase. Thus, it was concluded that AP worked as a stabilizer rather than as an emulsifier. On the contrary, CP, having the lowest degree of esterification (and thus, a more balanced amphiphilic character), greatest homogalacturonan content and greatest linearity and flexibility, was capable to have a better interaction and absorption in the oil-in-water interface.

However, the relatively short branch chains of this pectin did not provide the required steric hindrance and repulsion among droplets to avoid oil droplet coalescence during emulsion storage. In contrast, WRP exhibited excellent emulsification capacity, being able to

incorporate 60% (v/v) oil in the emulsions, providing long-term stability and avoiding coalescence with a densely packaged oil-pectin structure and a mayonnaise-like texture. The emulsification mechanism, in this case, was explained by a combination of its protein content (the proteins acting as surface active materials) and the steric repulsions between droplets caused by the very long side chains of this RG-I enriched pectin. Despite the good emulsifying properties attributed to the presence of protein, neither high protein concentration nor the presence of proteins guarantees excellent emulsifying properties since both the protein accessibility and its chemical interaction with the branched neutral sugars are responsible for their emulsifying capacity. All these results indicate the potential of WRP for food and pharma applications, not only because of its outstanding emulsification properties but also derived from the biological implications of their increased RG-I content, all of which has attracted the attention of several companies and has prompted recently granted projects and industrial collaboration on both research lines.

To explore other potential applications for WRP, such as typical thickening/gelling technological application of pectin, the third work includes the development of new modified pectins through enzymatic treatment. Two pectin types with different branching degree (OP and OPA), obtained according to the mathematical models developed in the first work, were used, and the effect of different carbohydrate active enzymes, proteases and their combination in the structural, rheological and gelling properties was studied. The six different treatments included de-esterification (pectin methyl esterase, -PME-), de-branching of arabinan (arabinanase -EAR-) and galactan (galactanase -EGA-) side chains, their combinations (PME+EAR, PME+EGA) and removal of protein (protease and pepsine -PP-). The compositional analyses indicated that the de-esterification and its combination with de-branching enzymes (galactanase and arabinanase) had the most significant impact on the pectin structure, greatly reducing the degree of esterification of both pectin extracts and significantly modifying the linearity and branching ratios. Furthermore, the proteolytic enzymes hydrolysed the protein moieties linked to the arabinogalactan part of pectin, which resulted in a significant increase in the linearity in both pectin samples. This effect was more patent in the less branched pectin samples, in which arabinogalactan-protein fragments were

removed in equal amounts. These structural changes had a significant impact on the rheology and gelling properties of the pectin.

The presence of highly branched pectin components contributed to the formation of chain entanglements and, consequently, to a higher pseudoplastic character of the pectin solution. Pectin solutions treated only with PME were more viscous and more shear-thinning than their untreated counterparts due to the removal of the lower molecular weight fraction of neutral sugar side chains and also to the higher amount of non-esterified groups which may form hydrogen bonds with the carboxyl free groups and neutral sugar side chains. Regarding the pectin hydrogels formed with $CaCl_2$, the presence of long branched side chains and high methyl esterified galacturonic acid chains prevent the adequate formation of an egg-box structure, promoting the formation of weaker hydrogels. In contrast, de-esterification of the original pectin enabled intermolecular association giving rise to stronger hydrogels with the formation of ordered and densely packed structures with the Ca^{+2} cations. Interestingly, after de-esterifying and de-branching the galacturonic side chains, the presence of smaller arabinogalactan side chains in the pectin extracts acted as reinforcement agents, inducing the formation of more densely packed networks and stronger hydrogels, similar to benchmark low methoxyl citrus pectin gels. Enzymes acting on neutral sugar side chains (EAR and EGA) alone were not capable of effectively de-branching the pectin structure, decreased the electrostatic interaction and resulted in a decrease of the gel strength.

Understanding the gelation mechanism of WRP hydrogels and nanostructure, depending on their composition and pectin primary structure, will open the possibility of designing hydrogels with specific properties for targeted applications, such as carrier systems for the controlled release of bioactive compounds. To finalize the study on watermelon pectin in this thesis with a more advanced, specific application, one of the samples with better rheological and gelling behaviour was selected to study pectin as aerogel precursor for drug delivery applications and it was compared with three commercial citrus pectin samples with different physicochemical properties. The pectin aerogel particles obtained presented high surface areas and low-density values, thus making them attractive vehicles for delivery applications. The bead shape formation and thus, the resulting aerogel structure was highly affected by the molecular weight, degree of branching and purity of pectin. The shrinkage

phenomenon could be reduced with linear and purer pectin. The drug loading efficiency was shown to depend on pectin matrix structure and properties (specific surface area and density), being higher at lower pectin concentration. This was ascribed to the higher availability of the carboxyl groups capable to interact with calcium cations to form the so-called egg-box junctions, increasing the hydrophobic zones, where vanillin molecules can penetrate and deposit. Specifically, WRP was able to incorporate much more vanillin than the citrus pectin aerogels, explained by the lower HG content (61%) and greater protein content, as aromatic compounds such as vanillin are prone to interact with proteins. Regarding the drug release, it was governed not only by the chemical affinity between pectin and vanillin but also by the solvent diffusion towards the inner part of the aerogels. In fact, the formation of a compacted structure during aerogel formation contributed to decrease the release kinetics of vanillin. A slower release, especially in the initial phase was observed for the samples with smaller average pore sizes (e.g WRP), probably due to the limited solvent diffusion towards the inner part of the aerogels.

4.2 Valorisation of persimmon functional extracts

Valorisation of biomass waste from rejected persimmon fruits significantly depends on the potential for exploitation of added-value compounds, high yields, and the final technological or bioactive functionalities. This chapter investigated the potential valorisation of persimmon biomass waste through the extraction of bioactive compounds and pectin-rich extracts and the evaluation of their functional properties.

The first work included the analysis of the influence of two different fruit maturity stages (mature and immature) on the available polyphenol content. Then, the effects of extraction parameters (temperature, solid:liquid ratio and ethanol:water ratio) that could influence the antioxidant and total phenolic content of bioactive extracts was investigated by means of a central composite design (CCD). The ripeness degree of the fruits was seen to affect, not only the extract composition (greater in phenolic compounds in those obtained from immature fruits), but also the determining factors for extraction. Specifically, in mature fruits, increased phenolic content extraction and antioxidant capacity was seen upon temperature increase, while in the case of immature persimmons, the solvent composition

was the most relevant factor affecting polyphenol extraction. The overall extraction yields for the different extraction conditions and raw materials (both immature and mature persimmons) ranged between 50 g/100 g dry weight and 75 g/100 g dry weight, including polyphenols and sucrose, both major constituents in the rejected fruits. Coefficients of determination for the total phenolic content (TPC) model (R^2 = 93–96%) and ABTS antioxidant activity (R^2 of 94.61%) exhibited a high accuracy, pointing out that the models were highly reliable.

The best extraction conditions in terms of phenolic content and antioxidant capacity (from immature persimmon fruits) were adapted for semi-industrial scale production and both extracts characterized. The main phenolic compound in both extracts was gallic acid, a hydrolysable tannin, which was more abundant in the up-scaled process from immature fruit than in the one produced in laboratory conditions. Other phenolic compounds such as naringin, hesperidin or naringenin were only present in the industrially up-scaled extract, along with other phenolic compounds previously described to have diverse bioactive properties. Regarding the functional activity, it demonstrated a good antiviral capacity, with a significant reduction in the titers of hepatitis A virus and murine norovirus. Likewise, it was able to reduce the cellular ageing and fat content without affecting the development of *C. elegans* model organism. Although further studies are needed to investigate the antioxidant effect of the extract on *C. elegans*, as well as to confirm the anti-obesity and anti-ageing activities of persimmon extracts in superior mammalian models, these preliminary data suggest an interesting potential application for the prevention of obesity and age-related diseases.

Results from the first work indicated a substantial part of the polyphenol contents was actually bound to pectin, which determined different solubility depending on the alcohol used for extraction at laboratory or industrial scale. The interest to study this potentially functional pectin motivated the second part of this chapter. This included a preliminary analysis of the composition of three maturity stages of persimmon fruit, to elucidate the best option to obtain high extraction yields of pectin-rich bioactive extracts. Among the three maturity stages, the immature non-treated rejected fruits were selected due to their higher pectin content, which decreased with ripening mainly caused by the collective action of

several pectin-degrading enzymes. The polyphenol content was also reduced during ripening (25.9±2.3, 17.1±1.0 and 2.0 ±0.0 mg GAE/g pectin for immature, mature, and induced mature stages respectively), also attributed to the interaction of pectin and tannins during maturity. Focusing on this raw material, the influence of different extraction parameters on the yields and composition of both pectin and polyphenol fractions was analysed, with an insight on polyphenol-pectin interaction. For this purpose, a 3-level full factorial design was applied with temperature and pH as the process variables and yields, sugar (pectin) composition and structural features, polyphenol contents and antioxidant activity as the response factors. The full polyphenol profile and type of pectin-polyphenol interaction were also analysed for several key extraction conditions. The full factorial design could accurately model how extraction temperature and pH affected process efficiency, as well as the composition and functional properties of the persimmon pectin. Aside from significantly lower yields, persimmon pectin was comparable to other conventional sources in terms of composition, purity and degree of esterification. Interestingly, this pectin was found to be more acid resistant compared to reference pectin or other alternative pectin sources. The presence of strong pectin-polyphenol interactions also enabled an outstanding high acid resistance of the very abundant polyphenol fraction, with gallic acid as the main constituent. Only extreme acid conditions (pH 0.5) were able to degrade both the pectin structure and polyphenol profile, and only the combination of both very low pH and high temperature produced a decrease in antioxidant activity. Relatively severe conditions (pH 1) produced the highest pectin and polyphenol yields, with abundant non-covalent interaction, while less severe conditions (pH 1.5) produced pectin with intact pectin-polyphenol ester and O-glycosyl bonds (indirectly inferred by the released polyphenols after alkali or acid treatment). The results showed a full polyphenol profile of these persimmon fruits, but more important, they opened up the possibility of developing novel functional pectin ingredients with increased bioactive properties and acid resistance, depending on type of pectin-polyphenol interaction.

Finally, a practical application for these functional pectin and polyphenol extracts was explored with the preparation of antiviral edible coatings for the preservation of blueberries. First, in vitro antiviral assays against hepatitis A virus, and murine norovirus were

performed, showing high antiviral efficiency of all polyphenol and functional pectin samples. A higher and long-lasting efficiency was found for functional pectin with covalently-bound polyphenols, compared to pectin-polyphenol mixtures or to the crude polyphenol extracts. For the preparation of edible coatings, citrus pectin was used as a cheaper, benchmark film-forming material and was mixed with functional pectin obtained at two different extraction conditions (high and low conjugated polyphenols), again showing a practical prove of the high efficiency of these novel functional pectin ingredients. Regarding the physicochemical properties of stand-alone coatings (films), the addition of the bioactive pectin persimmon extract resulted in more coloured films with lower transparency. The presence of covalently-linked polyphenols gave rise to stiffer films, with lower sorption capacity and more hydrophobic nature. These results have prompted further studies and projects, now in progress, on the bioavailability and bioactivity of these functional pectin, compared to other polyphenol-rich ingredients.

V. CONCLUSIONS

Conclusions

- Watermelon rind is a yet neglected by-product of one of the most cultivated fruit crops worldwide. Pectin in watermelon rind is available in similar amounts and is equally extractable compared to typical pectin sources. Moreover, the yield, composition and structural features which, in turn, will influence their potential applications, could be accurately modelled.

- WRP showed markedly different compositional and structural features compared to citrus and apple pectin, with longer galactan side chain contribution and significant protein content, recalcitrant to strong acidic extraction. Extraction factors such as pH and temperature play a key role in the final pectin structure, modifying the degree of branching, and under harsher conditions, degrading the structure and affecting yield.

- WRP was proven to be an excellent emulsifier, demonstrating superior performance than commercial pectin. Furthermore, the emulsion system with WRP was capable to retain high amounts of sunflower oil (>60%), avoiding coalescence and flocculation. This was explained by its protein moieties and the high entanglement with arabinogalactan, resulting in a high steric repulsion and favourable oil-in-water emulsion.

- Among different carbohydrate active enzymes, PME had the highest impact over the suprastructure, rheology and gelling properties of WRP, acting synergistically with arabinanases and galactanases to effectively remove neutral sugar chains. Long side chains promoted the gel strength in pectin with a high degree of esterification. In pectin with low degree of esterification, small arabinogalactan side chains acted as a reinforcement, inducing the formation of more densely packed networks and stronger hydrogels than their less-branched counterparts. These results open up the possibility to apply different enzymatic modifications according to the desired technological applications.

- Bio-based aerogels with great adsorption capacity and fast release could be produced by enzymatically modifying WRP. Factors such as molecular weight, degree of branching and purity, affected viscosity, bead shape formation and ultimately the aerogel structure. Likewise, the shrinkage could be reduced with linear and purer pectins. Impregnated aerogels showed a hydrophilic character and fast vanillin release. The formation of a compacted structure during aerogel formation contributed to decrease the release kinetics of vanillin.

- A huge amount of unripen persimmon fruits accumulate as they are found inadequate for further ripening treatment or consumption. These unripen fruits contain huge amounts of tannins, mostly covalently bound to pectin components.

- High temperature conditions enhance the extraction of polyphenols, mainly influenced by solvent composition. A semi-industrially scaled-up polyphenol-rich extract showed an effective antiviral efficiency against murine norovirus and hepatitis A virus. Likewise, it was able to reduce the cellular ageing and fat content without affecting the development of *C. elegans* model organism.

- A very strong pectin-polyphenol interaction, both electrostatic and covalent, allowed for the recovery of functional pectin-polyphenol complexes, even under extreme acidic extraction conditions and subsequent ethanol-acetone washes. The type of pectin-polyphenol interactions and pectin composition depended on the severity of the extraction conditions.

- These functional pectin extracts showed high antiviral efficiency, probably enhanced by the higher stability of the polyphenols as pectin complexes. A successful potential application was explored as edible coatings on blueberries. The bio-functional properties of these novel pectin ingredients pose interesting opportunities and further research on the bioavailability and specific health effects.

VI. ANNEXES

Annex A: List of publications included in this thesis

Food Hydrocolloids 135 (2023) 108119

Contents lists available at ScienceDirect

Food Hydrocolloids

journal homepage: www.elsevier.com/locate/foodhyd

Tailoring structural, rheological and gelling properties of watermelon rind pectin by enzymatic treatments

D.A. Méndez [a,b], A. Martínez-Abad [a,c], M. Martínez-Sanz [c,d], A. López-Rubio [a,c], M.J. Fabra [a,c,*]

[a] Food Safety and Preservation Department, Institute of Agrochemistry and Food Technology (IATA-CSIC), Valencia, Spain
[b] Grupo de investigación Bioecono, Facultad de ciencias económicas y administrativas, Universidad del Tolima, Tolima, Colombia
[c] Interdisciplinary Platform for Sustainable Plastics towards a Circular Economy- Spanish National Research Council (SusPlast-CSIC), Madrid, Spain
[d] Instituto de Investigación en Ciencias de la Alimentación, CIAL (CSIC-UAM, CEI UAM + CSIC), Nicolás Cabrera, 9, 28049, Madrid, Spain

ARTICLE INFO

Keywords:
Scattering
Enzymes
SAXS
Rheology
Gelation

ABSTRACT

In this work, pectin extracts from watermelon rind (WRP) were enzymatically treated to evaluate their potential for preparing hydrogels with the addition of $CaCl_2$. Based on a previous work, two different conditions were selected to obtain WRP extracts according to the 1) highest yield (OP) or 2) highest yield without negatively affecting the branching and native structure of pectin (OPA). Firstly, both WRP extracts were enzymatically modified using different treatments (de-esterification and/or de-branching of galacturonic and arabinose side chains, and deproteinization), and their impact on the esterification degree, monosaccharide composition and changes on their structural properties (linearity and branching degree) were analysed. Then, the effect of the structural properties of the resulting pectin on the rheological behaviour and nanostructure of the hydrogels was investigated. The presence of long branched side chains and high methyl-esterified galacturonic acid chains promoted the formation of weaker hydrogels whereas de-esterification of the original pectin enabled intermolecular association giving rise to stronger hydrogels with the formation of ordered and densely packed structures (as deduced from SAXS results). However, the presence of small arabinogalactans side chains in the de-branched and de-esterified pectin extracts acted as reinforcement agents, inducing the formation of more densely packed networks and stronger hydrogels than their less-branched counterpart. These results demonstrated the impact of the pectin structure on the hydrogel-forming capacity.

Author statement

D.A. Méndez: Methodology, Investigation, Formal analysis, Writing - original draft. A Martínez-Abad: Conceptualization, Methodology, Writing - review & editing. M. Martínez-Sanz: Methodology, Supervision, formal analysis, writing-review & editing. A. López-Rubio: Conceptualization, Methodology, Funding acquisition, Project administration, Writing- Review & Editing. M.J. Fabra: Conceptualization, Methodology, Supervision, Writing - review & editing.

1. Introduction

Pectin is a family of complex heteropolysaccharides consisting of homogalacturonan (HG), rhamnogalacturonan I (RG-I) and rhamnogalacturonan II (RG-II). HG is a linear chain of 1,4 – linked α-D- galacturonic acid (GalA) residues, which can be methoxylated at C-6 and/or acetylated on the O-2 and/or O-3 position. The degree and distribution of methoxylation are important parameters for their gelling properties (Ngouémazong et al., 2012; Voragen, Coenen, Verhoef, & Schols, 2009). HG is often referred to as the pectin smooth region, whereas RG-I is called the hairy region since its backbone can be abundantly substituted by neutral sugars like arabinose and galactose forming arabinan, galactan and arabinogalactans on the side chains, predominantly attached to the O-4 position of rhamnose (Lara-Espinoza, Carvajal-Millán, Balandrán-Quintana, López-Franco, & Rascón-Chu, 2018). In contrast, RG-II is composed of a HG backbone, which is branched with chains at C-2 and C-3. These side chains include arabinose, fucose, galactose, rhamnose, glucuronic acid, galacturonic acid, xylose, apiose and fucose units.

The worldwide application of pectin in the food industry as gelling, thickening, and stabiliser agents (Schols & Voragen, 2003a) together with the global aim towards sustainability, has prompted the interest in

* Corresponding author. Food Safety and Preservation Department, Institute of Agrochemistry and Food Technology (IATA-CSIC), Valencia, Spain.
E-mail address: mjfabra@iata.csic.es (M.J. Fabra).

https://doi.org/10.1016/j.foodhyd.2022.108119
Received 2 May 2022; Received in revised form 16 August 2022; Accepted 2 September 2022
Available online 13 September 2022

Food Hydrocolloids 123 (2022) 107066

Contents lists available at ScienceDirect

Food Hydrocolloids

journal homepage: www.elsevier.com/locate/foodhyd

Influence of the extraction conditions on the carbohydrate and phenolic composition of functional pectin from persimmon waste streams

D.A. Méndez [a], M.J. Fabra [a,b], I. Odriozola-Serrano [c], O. Martín-Belloso [c], L. Salvia-Trujillo [c], A. López-Rubio [a,b], A. Martínez-Abad [a,b,*]

[a] Food Safety and Preservation Department, Institute of Agrochemistry and Food Technology (IATA-CSIC), Valencia, Spain
[b] Interdisciplinary Platform for Sustainable Plastics Towards a Circular Economy- Spanish National Research Council (SusPlast-CSIC), Madrid, Spain
[c] Food Technology Department, University of Lleida – Agrotecnio-CERCA Center, Av. Alcalde Rovira Roure 191, 25198, Lleida, Spain

ARTICLE INFO

Keywords:
Pectin extracts
Diospyros kaki
Polyphenols
Carbohydrate analysis
Surface response
Waste valorization

ABSTRACT

Persimmon fruit (*Diospyros kaki Thunb.*) production suffers great losses (15–20%) due to the inefficient over-ripening process. In order to valorise this waste, a compositional characterization of different fruit stages of the residues was done, and immature fruit was selected due to its high pectin and very high polyphenol content. A 3-level full factorial design was carried out to study the effect of temperature (70–95 °C) and low pH (0.5–1.5), on yield, degree of esterification, carbohydrate constituents, phenolic content and antioxidant capacity of the extracted pectin, and a complete polyphenol profile (UPLC-MS/MS) was performed on selected extracts. All responses could be accurately adjusted to the models ($R^2 > 80$; lack of fit). Pectin yield, phenolic compounds and antioxidant activity ranged from 1.4 to 4.5%, 53.3 ± 2.27 to 111.7 ± 9.74 mg GAE/g pectin and 0.29 ± 0.01 to 2.77 ± 0.04 TEAC (Trolox μmol/mg pectin), respectively. A strong pectin-polyphenol interaction was found, which significantly enhanced acid resistance of both the pectin and polyphenol constituents, with optimum yield and polyphenol content at pH 1 and 95 °C. These new pectin-based ingredients might have a great potential as functional foods or natural food ingredients enhancing the quality and shelf-life.

1. Introduction

The future of food and agriculture faces a number of uncertainties that raise significant concerns about its performance and sustainability. While food demand is expected to increase anywhere between 59% and 98% by 2050 (Berbel & Posadillo, 2018), more than 1.3 billion tonnes of food are wasted every year, which is around 1/3 of the world's production (FAO., 2016). With a global aim towards sustainability, it is necessary to drive a change and look for different ways to valorise by-products or residues from the food chain with potential to become new ingredients improving the quality and/or preservation of foods (Carocho, Morales, & Ferreira, 2018).

Persimmon (*Diospyros kaki Thunb.*) is a fruit tree originating from China, with a global production of 4.3 million tons in 2019 (FAOSTAT, 2021). Over the last decade, Spain has become the second global producer and the first exporter owing to the "*Rojo Brillante*" variety with registered designation of origin in the Valencian province (FAOSTAT, 2021; Martínez-Las Heras, Amigo-Sánchez, Heredia, Castelló, & Andrés, 2016). This especially resistant and high quality variety must be subjected to an overripening process with 1-methylcyclopropene and ethylene for 18–24 h to reduce its astringency before consumption. Although great efforts have been carried out in post-harvesting techniques and storage conditions to improve the quality and minimize losses, immature untreated fruits are severely affected by small physiological changes causing a poor CO_2 diffusion, which results in a low anaerobic respiration rate, reducing acetaldehyde accumulation which in turn causes a decrease in its interactions with soluble tannins, these being responsible for astringency and rejection (Munera et al., 2019). The seasonal production and this inefficient overripening result in huge amounts of discarded fruit (about 15–20% of the fruit harvested) (Munera et al., 2019), representing ~ 9500 Tn/year in the Valencian region only (data provided by the second grade cooperative ANECOOP).

Apart from free sugars, persimmon contains significant amounts of pectin and very high contents in polyphenols. Pectin is a family of polysaccharides built with several structural elements, where the most studied and highly identified are the homogalacturonan (HG) and type I

* Corresponding author. Food Safety and Preservation Department, Institute of Agrochemistry and Food Technology (IATA-CSIC), Valencia, Spain.
E-mail address: conaba@iata.csic.es (A. Martínez-Abad).

https://doi.org/10.1016/j.foodhyd.2021.107066
Received 1 May 2021; Received in revised form 22 June 2021; Accepted 25 July 2021
Available online 28 July 2021

Food Hydrocolloids 120 (2021) 106957

Contents lists available at ScienceDirect

Food Hydrocolloids

journal homepage: www.elsevier.com/locate/foodhyd

Understanding the different emulsification mechanisms of pectin: Comparison between watermelon rind and two commercial pectin sources

D.A. Mendez [a], M.J. Fabra [a,b], A. Martínez-Abad [a,b], M. Martínez-Sanz [b,c], M. Gorria [a], A. López-Rubio [a,b,*]

[a] Food Safety and Preservation Department, Institute of Agrochemistry and Food Technology (IATA-CSIC), Valencia, Spain
[b] Interdisciplinary Platform for Sustainable Plastics Towards a Circular Economy- Spanish National Research Council (SusPlast-CSIC), Madrid, Spain
[c] Instituto de Investigación en Ciencias de La Alimentación, CIAL (CSIC-UAM), Nicolás Cabrera, 9, 28049, Madrid, Spain

ARTICLE INFO

Keywords:
Stability
Microstructure
SAXS
Emulsion
Rheology
Spreadability

ABSTRACT

In this work, an advanced approach combining small angle X-ray scattering (SAXS) experiments, rheology and confocal laser scanning microscopy was used to explain the different emulsification mechanisms of three pectin sources (pectin extracted from watermelon rind -WRP- and commercial citrus -CP- and apple pectin -AP). Very interestingly, three different emulsification mechanisms were identified, related to the structure and composition of the pectin extracts. WRP had significantly greater emulsifying capacity than commercial CP and AP. This enhanced emulsification ability was mainly ascribed to a combination of its relatively high protein content (mainly acting as the surface-active material), combined with the presence of longer sugar side chains in pectin, further contributing to stabilizing the oil droplets in the emulsions. All these structural features resulted in a reduction in the mean droplet size as the concentration increased, thus, hindering flocculation and coalescence during the short-term storage conditions at 4 °C. In contrast, AP had the lowest emulsification capacity, which was only related to its viscosifying effect (provided by its greater Mw), while CP, having the greatest homogalacturonan content, greatest linearity and a more balanced hydrophilic/hydrophobic character (reflected in the degree of esterification), was able to form a better adsorbed layer at the o/w interphase, although it could not avoid flocculation and creaming at low pectin concentration during refrigerated storage.

1. Introduction

Pectin is a natural complex heteropolysaccharide extracted from plant cell walls, which can be currently found in multiple food, cosmetic, pharmaceutical and nutraceutical products, contributing to relevant technological and functional attributes, like fiber enrichment or rheology control (Ciriminna, Chavarría-Hernández, Inés Rodríguez Hernández, & Pagliaro, 2015). It is a complex mixture of blocks of homogalacturonan (HG), the so-called "smooth region" and rhamnogalacturonan I (RG-I) and II (RG-II), constituting the "hairy regions" and having a greater degree of chemical complexity. The backbone of pectin is mainly composed of D-galacturonic acid (GalA) units connected by α-1,4-glucoside bonds which can be naturally methylesterified at the C-6 carboxyl group (Prasanna, Prabha, & Tharanathan, 2007; Henk A.; Schols, Visser, & Voragen, 2009; Henk A.; Schols & Voragen, 2003; Voragen, Coenen, Verhoef, & Schols, 2009). While commercial pectin are classified according to their methoxyl content and gel-forming rate (Ciriminna et al., 2017), the structural complexity of these polysaccharides, which depend on a number of factors like source or extraction conditions, define their properties, thus making it a very versatile natural polymer (Denman & Morris, 2015; Dranca & Oroian, 2018; Méndez, Fabra, Gómez-Mascaraque, López-Rubio, & Martínez-Abad, 2021).

Although most commercial pectin are extracted with mineral acids from citrus peels or apple pomace (waste materials from juice industries), other fruit waste materials have been investigated for pectin extraction, like banana peels (Oliveira et al., 2016), grape pomace (Minjares-Fuentes et al., 2014) or watermelon rinds (Campbell, 2006). Specifically, this last waste material can be envisaged as a highly promising pectin source, not only because of the economic importance of the crop, being the second world's largest fruit in terms of volume with around 100 million tons produced in 2019 (FAOSTAT, 2021) and constituting the rind about one third of the fruit, but also because of the good pectin yields obtained (Jiang, Shang, He, & Dan, 2012; Lee &

* Corresponding author. Food Safety and Preservation Department, Institute of Agrochemistry and Food Technology (IATA-CSIC), Valencia, Spain.
E-mail address: amparo.lopez@iata.csic.es (A. López-Rubio).

https://doi.org/10.1016/j.foodhyd.2021.106957
Received 17 April 2021; Received in revised form 18 May 2021; Accepted 11 June 2021
Available online 19 June 2021
0268-005X/

foods

MDPI

Article

Modelling the Extraction of Pectin towards the Valorisation of Watermelon Rind Waste

Daniel Alexander Méndez [1], María José Fabra [1,2], Laura Gómez-Mascaraque [3], Amparo López-Rubio [1,2] and Antonio Martinez-Abad [1,2,*]

[1] Food Safety and Preservation Department, Institute of Agrochemistry and Food Technology (IATA-CSIC), 46980 Valencia, Spain; daamendezre@iata.csic.es (D.A.M.); mjfabra@iata.csic.es (M.J.F.); amparo.lopez@iata.csic.es (A.L.-R.)

[2] Interdisciplinary Platform for Sustainable Plastics towards a Circular Economy—Spanish National Research Council (SusPlast-CSIC), 28006 Madrid, Spain

[3] Department of Food Chemistry & Technology, Teagasc Food Research Centre, Moorepark, Fermoy, Co., P61 C996 Cork, Ireland; laura.mascaraque@teagasc.ie

* Correspondence: conaba@iata.csic.es; Tel.: +34-96390-0022; Fax: +34-96363-6301

Abstract: Watermelon is the second largest fruit crop worldwide, with great potential to valorise its rind waste. An experimental design was used to model how extraction parameters (temperature, pH, and time) impact on the efficiency of the process, purity, esterification degree, monosaccharide composition and molar mass of watermelon rind pectin (WRP), with an insight on changes in their structural properties (linearity, branching degree and extraction severity). The models for all responses were accurately fitted (R^2 > 90%, lack of fit $p \geq 0.05$) and experimentally validated. At optimum yield conditions, WRP yield (13.4%), purity (540 µg/g galacturonic acid) and molar mass (106.1 kDa) were comparable to traditional pectin sources but showed a higher branching degree with longer galactan side chains and a higher protein interaction. Harsher conditions (pH 1) generated purer homogalacturonan fractions with average molar masses (80 kDa) at the expense of yield, while mild extraction conditions (pH ≥ 2) produced highly branched entangled pectin structures. This study underlines novel compositional features in WRP and the possibility of producing novel customized pectin ingredients with a wider potential application scope depending on the targeted structure.

Keywords: pectin composition; Box–Behnken design; *Citrullus lanatus*; carbohydrate analysis; valorisation

Citation: Méndez, D.A.; Fabra, M.J.; Gómez-Mascaraque, L.; López-Rubio, A.; Martinez-Abad, A. Modelling the Extraction of Pectin towards the Valorisation of Watermelon Rind Waste. *Foods* **2021**, *10*, 738. https://doi.org/10.3390/foods10040738

Academic Editors: Zlatina Genisheva

Received: 4 March 2021
Accepted: 24 March 2021
Published: 31 March 2021

1. Introduction

Around 60% of the total food waste is attributed to agricultural, post-harvesting, processing or distribution, causing significant losses for producers as well as food security and environmental concerns [1]. Watermelon (*Citrullus lanatus*) is a fruit with a great economic importance, being the second world's largest fruit crop, with a global production of approximately 103 million tonnes in 2018 [2]. Watermelon rind (WR), which constitutes approximately 30% of the whole fruit, is most often dumped arbitrarily into the environment, raising environmental concerns [3]. The valorisation of this waste is limited due the lack of knowledge on possible conversion strategies of potential valuable compounds [4,5].

Pectin is a complex cell wall polysaccharide from plant sources, consisting mainly of homogalacturonan (HG), rhamnogalacturonan-I (RG-I) and minor rhamnogalacturonan-II (RG-II) and xylogalacturonan (XGA) regions. HG is a homopolymer consisting of α-(1–4)-linked-D-galacturonic acid units (GalA), which can be naturally methylesterified at the C-6 carboxyl group [4]. The degree of esterification (DE) governs much of the properties in pectin, where high methoxy (HM) pectin (DE 50–80%) form gels at low pH (2.5–3.5) or in the presence of high amounts of soluble solids such as sucrose (55%) and low methoxy (LM) pectin (DE < 50%) can form gels in the presence of divalent cations, and is also more resistant to a wider range of pH than HM pectin [6]. Rhamnogalacturonan-I (RGI) is generally

Food & Function

ROYAL SOCIETY OF CHEMISTRY

PAPER

View Article Online
View Journal

Cite this: DOI: 10.1039/d1fo00457c

Bioactive extracts from persimmon waste: influence of extraction conditions and ripeness†

Daniel Alexander Méndez,[a] María José Fabra,[a,b] Irene Falcó,[a] Gloria Sánchez,[a] Paula Aranaz,[c,d] Ariane Vettorazzi,[c] Albert Ribas-Agustí,[f] Carlos Javier González-Navarro,[c] Massimo Castellari,[f] Antonio Martínez-Abad[a,b] and Amparo López-Rubio[*a,b]

In this work, a bioactive persimmon extract was produced from discarded fruits. A central composite design was used to evaluate the effect of different extraction parameters and ripeness stages of persimmon fruits on the total phenolic content and antioxidant activity of the resulting extracts. Significantly greater phenolic contents were obtained from immature persimmon (IP) fruits. The optimum IP extract with the conditions set by the experimental design was industrially up-scaled and its composition and functional properties were evaluated and compared with those obtained under lab-scale conditions. Both extracts contained significant protein (>20%) and phenolic contents (~11–27 mg GA/g dry extract) and displayed significant antiviral activity against murine norovirus and hepatitis A virus. Moreover, the extract showed no toxicity and significantly reduced the fat content and the cellular ageing of *Caenorhabditis elegans* (*C. elegans*) without affecting the worm development. These effects were mediated by down-regulation of fat-7, suggesting an anti-lipogenic activity of this extract.

Received 12th February 2021,
Accepted 1st June 2021
DOI: 10.1039/d1fo00457c
rsc.li/food-function

1. Introduction

According to the Food and Agriculture Organization (FAO), around 14 percent of the food produced worldwide every year is lost from the post-harvest stage to the retail stage and, of this, fruits and vegetables have the second highest wastage rate of the different commodity groups after roots and tubers.[1] The reduction of food loss and waste is an important target of the Sustainable Development Goals (SDGs), relating to food security, nutrition and environmental sustainability.

To date, most agro-industrial wastes have been extensively used as a source of fuel, animal feed or organic fertilisers.[2] However, there is growing interest in the valorisation of agro-industrial by-products and wastes as abundant, cheap and renewable sources of high added value molecules with specific functional properties.[3,4]

Persimmon (*Diospyros kaki* Thunb.) fruits are rich in various nutrients and phytochemicals, including carbohydrates, vitamins, proanthocyanidins, flavonoid oligomers, tannins, phenolic acids, dietary fibre and carotenoids, which significantly contribute to their taste, colour, and nutritional and medicinal value.[5] Although China is by far the larger producer, a significant amount of persimmon is also produced in Spain, being the main exporter of the fruit, particularly in Europe.[6] Currently, the seasonality and overproduction, together with problems associated with storage, ripening processes, fruit disease and stringent standard demands in terms of fruit appearance, give rise to huge amounts of discarded fruits at different stages of ripeness, which are estimated to be around 5–20% of the fruit harvested.[7] In this sense, and given the existing evidence related to the beneficial functional attributes derived from phytochemicals (and more specifically polyphenols) present in the persimmon fruits,[6,8] a plausible strategy for their valorisation can be obtaining polyphenol-rich extracts from the discarded fruits. It is also well known that composition changes with fruit ripeness and, thus, exploring these functional attributes in different stages of development can also be helpful to determine the best ripening stage if aiming at this type of valorisation.

Although a few research studies have focused on obtaining purified tannins from persimmon pulp,[9,10] from an appli-

[a]Food Safety and Preservation Department, Institute of Agrochemistry and Food Technology (IATA-CSIC), Valencia, Spain. E-mail: amparo.lopez@iata.csic.es
[b]Interdisciplinary Platform for Sustainable Plastics towards a Circular Economy-Spanish National Research Council (SusPlast-CSIC), Madrid, Spain
[c]Center for Nutrition Research, University of Navarra, Pamplona, Spain
[d]Navarra Institute for Health Research (IdiSNA), Pamplona, Spain
[e]Department of Pharmacology and Toxicology, Universidad de Navarra, Pamplona, Spain
[f]Institute of Agriculture and Food Research and Technology, Food Industries, Finca Camps i Armet, Monells, Spain

†Electronic supplementary information (ESI) available. See DOI: 10.1039/d1fo00457c

Annex B: List of additional publications

foods

MDPI

Article

Electrosprayed Agar Nanocapsules as Edible Carriers of Bioactive Compounds

Barbara Tomadoni [1], María José Fabra [2,3], Daniel Alexander Méndez [2,4], Antonio Martínez-Abad [2,3] and Amparo López-Rubio [2,3,*]

[1] Grupo de Materiales Compuestos Termoplásticos (CoMP), Instituto de Investigaciones en Ciencia y Tecnología de Materiales (INTEMA), Universidad Nacional de Mar del Plata (UNMdP) y Consejo Nacional de Investigaciones Científicas y Técnicas (CONICET), Av. Colón 10850, Mar del Plata 7600, Argentina; btomadoni@gmail.com

[2] Packaging Group, Food Safety and Preservation Department, Institute of Agrochemistry and Food Technology (IATA-CSIC), Catedrático Agustín Escardino Benlloch 7, 46980 Paterna, Spain; mjfabra@iata.csic.es (M.J.F.); daamendezre@iata.csic.es (D.A.M.); conaba@iata.csic.es (A.M.-A.)

[3] Interdisciplinary Platform for Sustainable Plastics towards a Circular Economy-Spanish National Research Council (SusPlast-CSIC), 26006 Madrid, Spain

[4] Grupo de Investigación Bioecono, Facultad de Ciencias Económicas y Administrativas, Universidad del Tolima, Tolima 730006299, Colombia

* Correspondence: amparo.lopez@iata.csic.es

Abstract: Electrosprayed agar nanocapsules were developed using an acetic acid solution as solvent. The role of solution properties (viscosity, surface tension, and conductivity) in the formation of agar particles was assessed, together with the effect of both agar and acetic acid concentrations on the size and morphology of the resulting particles. Agar solutions with a concentration below 10% *w*/*v* were not suitable for electrospraying. Furthermore, the agar–acetic acid ratio was also critical for the formation of agar nanostructures (with an optimum ratio of 1:2). A decrease in particle size was also observed when decreasing agar concentration, with particle diameter values ranging between 50 and 400 nm. Moreover, the suitability of the electrosprayed agar nanocapsules as carriers for a model bioactive compound, chlorophyllin sodium copper salt (CHL), was also evaluated. The release profile of encapsulated CHL, with an estimated encapsulation efficiency of around 40%, was carried out in food simulants with different hydrophilicity (10% *v*/*v* and 50% *v*/*v* ethanol). While the release of the bioactive was negligible in the hydrophilic food simulant, an initial burst release followed by a slower sustained release was observed when the capsules were immersed in 50% ethanol solution. The results open up a broad range of possibilities that deserve further exploration related to the use of these edible polysaccharide-based nanocapsules.

Keywords: agar; nanocapsules; electrospraying; chlorophyllin

Citation: Tomadoni, B.; Fabra, M.J.; Méndez, D.A.; Martínez-Abad, A.; López-Rubio, A. Electrosprayed Agar Nanocapsules as Edible Carriers of Bioactive Compounds. *Foods* **2022**, *11*, 2093. https://doi.org/10.3390/foods11142093

Academic Editors: Moshe Rosenberg and I Hong Wu

Received: 16 May 2022
Accepted: 12 July 2022
Published: 14 July 2022

Publisher's Note: MDPI stays neutral with regard to jurisdictional claims in published maps and institutional affiliations.

1. Introduction

The incorporation of bioactive compounds to food products with the aim of extending their shelf-life or improving their nutritional quality is of high interest for the food industry [1]. Antioxidants, antimicrobials, probiotics, pigments, and flavoring agents are typically present in food products in small amounts, but are often highly active [2]. These active compounds are usually difficult to process and store, since they can impart strange aromas, are prone to rapid degradation, and can interact with other compounds in the food matrix, leading to a loss in the quality of functional assets. For example, phenolic compounds that are used as natural antioxidants for their health benefits can decrease their bioavailability after binding with carbohydrates and proteins present in the food matrix [3]. Natural pigments are also affected by other components naturally occurring in foods, especially after processing steps that damage the structure of the product, releasing

Food Hydrocolloids 133 (2022) 107888

Contents lists available at ScienceDirect

Food Hydrocolloids

journal homepage: www.elsevier.com/locate/foodhyd

Feasibility of active biobased films produced using red chilto wastes to improve the protection of fresh salmon fillets via a circular economy approach

María Eugenia Orqueda [a,b], Daniel A. Méndez [c,e], Antonio Martínez-Abad [b,c,d], Catiana Zampini [a,b], Sebastian Torres [a,b], María Inés Isla [a,b], Amparo López-Rubio [b,c,d], María José Fabra [b,c,d,*]

[a] Laboratorio de Investigación de Productos Naturales (LIPRON), Instituto de Bioprospección y Fisiología Vegetal (INBIOFIV-CONICET-UNT), Facultad de Ciencias Naturales e Instituto Miguel Lillo, Universidad Nacional de Tucuman, San Lorenzo, 1469, San Miguel de Tucuman, Tucumán, Argentina
[b] Biolatex Network for Sustainable Use of Ibero-American Vegetable Biomass Resources in Cosmetics (Biolatex CYTED), Tucuman, Argentina
[c] Instituto de Agroquímica y Tecnología de Alimentos (IATA-CSIC) Avda, Agustín Escardino 7, Paterna, Valencia, Spain
[d] Interdisciplinary Platform for Sustainable Plastics Towards a Circular Economy- Spanish National Research Council (SusPlast-CSIC), Madrid, Spain
[e] Grupo de Investigación Bioecono, Facultad de Ciencias Económicas y Administrativas, Universidad Del Tolima, Tolima, Colombia

ARTICLE INFO

Keywords:
Active films
Valorization
Fish preservation
Polyphenol extracts
Pectin
Solanum betaceum

ABSTRACT

By-products of a native fruit of the Argentina northwest have been valorized for the extraction of both pectin and bioactive extracts with the aim of developing antioxidant films with potential application as food packaging materials. Initially, the composition and antioxidant properties of polyphenol-rich, anthocyanin-rich, and pectin extracts obtained from the seed and peel of *Solanum betaceum* (chilto) red fruits were characterized. Based on their higher antioxidant properties, peel extracts were selected as active compounds and incorporated in a film-forming matrix based on the pectin extract. Dry films were evaluated concerning their morphological, optical, thermal, mechanical, and water barrier properties. The developed antioxidant films were directly applied on salmon fillets, effectively improving their shelf-life and reducing lipid and protein oxidation during 10 days of storage at 4 °C. It was also found that the films containing peel-polyphenolic extract were the most promising, in agreement with their better barrier properties.

1. Introduction

The high consumers' demand for safe and healthier food, together with the increased awareness of the negative environmental impact of non-biodegradable packaging, has encouraged scientists to develop novel alternatives to plastic packaging which can help increasing products shelf-life through the use of natural compounds. In fact, there is a growing interest in the food industry to develop sustainable packaging materials (i.e., biodegradable coatings and films) to improve the food quality and shelf-life and to prevent food waste. However, biobased plastics do not fulfill the high-performance standards required to protect food products against contamination or the loss of food quality. Moreover, most of the starting raw materials are vegetable resources whose primary use is as food sources. Therefore, there is an increasing need to implement new strategies for agricultural waste management in a circular biobased economy for the extraction of biopolymers. The development of biodegradable films based on agro-industrial plant products and by-products is an excellent opportunity to add value to these residues and reduce waste accumulation leading to positive impacts on the environment (Zhong, Godwin, Jin, & Xiao, 2020). Furthermore, agro-industrial waste is a source of bioactive compounds (i.e., polyphenols) that can serve as functional or active compounds in the biodegradable food package. The development of biobased films derived from biological resources and food waste offers a great opportunity since their biodegradability and environmental compatibility are ensured.

Biobased packaging materials with active properties can prolong shelf-life or enhance safety, improving the stability of oxidation-sensitive foodstuff or retarding the microbial growth in food products while maintaining or even enhancing the quality of the product (Falcó,

* Corresponding author. Instituto de Agroquímica y Tecnología de Alimentos (IATA-CSIC), Avda Agustín Escardino 7, 46980 Paterna, Valencia, Spain.
E-mail address: mjfabra@iata.csic.es (M.J. Fabra).

https://doi.org/10.1016/j.foodhyd.2022.107888
Received 27 April 2022; Received in revised form 2 June 2022; Accepted 16 June 2022
Available online 22 June 2022

Polímeros naturales obtenidos de residuos agroindustriales y sus potenciales aplicaciones

Autores: Hylenne Bojorges, Daniel Alexander Mendez, Zaida Pérez-Bassart, María José Fabra, Antonio Martínez-Abad, Amparo López-Rubio*

Food Safety and Preservation Department, IATA-CSIC, Avda. Agustín Escardino 7, 46980 Paterna, Valencia, Spain.

Interdisciplinary Platform for Sustainable Plastics towards a Circular Economy- Spanish National Research Council (SusPlast-CSIC), Madrid, Spain.

*amparo.lopez@iata.csic.es

Resumen

En el contexto de la economía circular, en el que se busca un aprovechamiento integral de los recursos, la valorización de residuos generados en actividades agroindustriales para la obtención de materiales es un área de creciente interés. En concreto, la obtención de biopolímeros a partir de residuos es una opción muy atractiva, ya que permitiría, por un lado, abaratar el coste de materiales necesarios para que puedan competir con los plásticos convencionales, sobre todo en aplicaciones de menor coste añadido (como es el área del envasado alimentario) y, por otro lado, valorizar macromoléculas presentes en dichos residuos con potenciales aplicaciones en distintas áreas. En este artículo mostramos el potencial de diferentes residuos agroindustriales, concretamente los residuos del cultivo de setas, corteza de sandía y de algas marrones para la obtención de biopolímeros de interés industrial.

Palabras clave: pectinas, fucoidanos, beta-glucanos, alginatos, laminarina.

Abstract

In the context of circular economy, in which an integral exploitation of resources is sought, the valorisation of agro industrially generated residues for obtaining materials is an area of increased interest. Specifically, the extraction of biopolymers from residues is a very attractive option as it would allow, on one hand, to lower the price of materials needed to compete with conventional plastics, especially in low added-value applications (like in the case of food packaging) and, on the other hand, to valorise macromolecules present in these residues with potential applications in different areas. In this dissemination paper, we will show the potential of various residues, concretely residues from mushroom cultivation, watermelon rinds and residues from brown algae for obtaining biopolymers with industrial interest.

Keywords: pectins, fucoidans, beta-glucans, alginates, laminarin.


El conocimiento es de todos
Minciencias
GOBIERNO DE ESPAÑA
MINISTERIO DE CIENCIA E INNOVACIÓN
CSIC
Consejo Superior de Investigaciones Científicas